Identification and characterization of *Dothistroma septosporum* effectors

A thesis presented in partial fulfilment of the requirements for the degree of Doctor of Philosophy (PhD) in Genetics

Yanan Guo

2015

Abstract

Dothistroma septosporum is the main causal agent of Dothistroma needle blight of pines. However little is known about mechanisms of pine resistance against *D. septosporum*, or whether there is any classical gene-for-gene resistance involved. The molecular basis of how fungal effector proteins can trigger plant host resistance in a gene-for-gene manner was determined partly by work with the model fungus *Cladosporium fulvum* and its tomato host. Comparative genome analysis of *C. fulvum* and *D. septosporum* genomes identified nine putative effector genes (*DsAvr4*, *DsEcp2-1*, *DsEcp2-2*, *DsEcp2-3*, *DsEcp4*, *DsEcp5*, *DsEcp6*, *DsEcp13* and *DsEcp14*) in *D. septosporum* that are homologous to well-characterized *C. fulvum* effector genes. Other effector candidates were identified as small cysteine rich proteins that are highly expressed *in planta*, including *DsHdp1* which is a hydrophobin gene and *Ds69335* which belongs to the sperm-coating protein-like extracellular protein SCP/Tpx-1/Ag5/PR-1/Sc7 (SCP/TAPS) superfamily.

Transcriptome analysis showed that, except for *DsEcp2-1* and *DsEcp6*, the *in planta* expression of *D. septosporum* effectors was low. Targeted gene replacement of *DsAvr4*, *DsEcp2-1*, *DsEcp6* and *DsHdp1* caused no observed changes in fungal physiology *in vitro* compared to wild type (WT) and also showed that *DsAvr4*, *DsEcp6* and *DsHdp1* are not virulence factors when infecting *Pinus radiata*. However deletion of *DsEcp2-1* caused larger lesions compared to WT, suggesting that DsEcp2-1 may act to suppress a host target which is involved in necrosis induction during the biotrophic infection stage.

A domain swap experiment in this study showed that swapping the region between cysteine residues C6 (Cys102) to C7 (Cys114), which contains the chitin binding domain, caused loss of resistance (R) protein Cf-4 recognition of DsAvr4 (with CbAvr4) and gain of Cf-4 recognition of CbAv4 (with DsAvr4 or CfAvr4). Further experiments carried out in Wageningen University showed that a Pro residue located in the chitin binding domain in DsAvr4 is important for Cf-4 recognition, and may have a role in DsAvr4 stability. In this study, effector candidates DsEcp2-1 and DsEcp2-3 were able to trigger a non-host necrotic response in *N. tabacum* suggesting possible interaction with a *N. tabacum* protein. Polymorphism analysis showed that *DsEcp4* and *DsEcp5* have internal stop codons and encode pseudogenes in all the *D. septosporum* strains tested,

except for *DsEcp4* in strains from Guatemala and Columbia in which a functional gene is predicted. DsEcp4 and DsEcp5 are the only *D. septosporum* effectors tested that showed evidence of positive selection. Those results lead to the suggestion that R proteins that recognise DsEcp4 and DsEcp5 may be present in pine species. *DsEcp13* appears to be absent from ten *D. septosporum* strains, suggesting that DsEcp13 is not important for virulence and can also be deleted to avoid an R protein mediated defence response such as a hypersensitive response. Infiltration of DsAvr4, DsEcp2-1 and DsEcp6 *P. pastoris* expression culture filtrates triggered necrosis in *P. radiata* needles suggesting that R proteins that directly or indirectly recognise those effectors may also be present in *P. radiata*.

The finding that *D. septosporum* has homologues of *C. fulvum* effectors allowed the first study of molecular pathogen-host interactions in this pathosystem. Targeted gene replacement studies identified genes that may have a virulence function and resistance against these effectors may be durable in the field. The pine needle infiltration assay provides a basic screening method to identify pine genotypes that carry resistance proteins and future work in this area is expected to impact on breeding strategies in the forest industry.

Acknowledgements

I would like to gratefully thank my supervisor Dr Rosie Bradshaw for her continuous encouragement, guidance and support during the course of my PhD. Thanks for your kindness and patience when I have questions. You are a great supervisor and I could not have imagined having a better advisor and mentor for my PhD study. I would also like to express my gratitude to my co-supervisors Dr Rebecca Ganley and Dr Kee Sohn for their valuable advice and support.

To my lab colleagues, thanks for Carol for her technical support and advice, you are always there to help whenever I knock on your door. Thanks for Pranav for his willingness to listen and sharing his knowledge with me. Thanks for Kabir, Yanfei, Kutay, Simren and Lukas for technical assistance and advice. It is a pleasure to work with all of you.

Most important I would like to thank my parents, although it is far from home, you have always been so supportive, encouraging and understanding over the duration of my studies. To my loving husband Xiaoxiao, thanks for believing in me, without your support I would not have achieved my goals.

Finally I would like to thank Scion for providing me with a fellowship for three and half years to pursue my PhD studies in New Zealand. Thanks to Massey University for providing six month financial support at the end of my PhD and travel fund.

Table of contents

List of Figures

List of Tables

Abbreviations

Abbreviation	Meaning
Avr	avirulence protein
CC:	coiled-coil domain
ChBD	chitin-binding domain
Cys	cysteine residue
Dnase	deoxyribonuclease
dNTP	deoxynucleotide triphosphate
Ecp	extra cellular protein
eLRR	extracellular LRR
G	gram
HR	Hypersensitive response
IPTG	isopropyl-β-d-thiogalactoside
kb	kilobase pair
L	litre
LRR	leucine-rich repeat domain
M	molar
Mb	megabase
ml	milliliter
mM	millimolar
NBS	nucleotide-binding site
ng	nanogram
NLP	necrosis and ethylene-inducing like protein
NLS	nuclear localization signal
ORF	open reading frame
PAMPs	pathogen-associated molecular patterns
PCD	programed cell death
PCR	polymerase chain reaction
PEST	Pro-Glu-Ser-Thr domain
PRRs	plant PAMP-recognition receptors
PTI	PAMP triggered immunity
qPCR	real-time PCR
R protein	resistant protein
RGAs	Rprotein analogs
RLKs	receptor-like kinase proteins
RLPs	receptor like protein
RNA	ribonucleic acid
RNase	ribonuclease
ROS	reactive oxygen species
rpm	revolutions per minute
SDS	sodium dodecyl sulfate
SSCP	small secreted cysteine rich protein
T3SS	bacterial type III secretion system
TIR:	toll-interleukin 1 receptors
TM	transmembrane domain
UV	ultraviolet
WRKY	DNA binding domain
WT	wild type
X-Gal	5- bromo-4-chloro-3-indolyl-β-D-galactopyranoside
µg	microgram
µl	microlitre
µM	micromolar

Chapter 1. Introduction

1.1 *Dothistroma septosporum*: A foliar pathogen that causes Dothistroma needle blight in *Pinus* spp.

1.1.1 Dothistroma needle blight

Dothistroma needle blight (DNB), caused by *Dothistroma septosporum,* is one of the most important foliar diseases of *Pinus* species. DNB has caused huge economic losses in Southern hemisphere commercial pine plantations for decades (Bulman et al., 2013). Since the 1990s, increased outbreaks of DNB have been observed in the Northern hemisphere (Watt et al., 2011). Climate change and planting of susceptible pine species are contributing factors to this increased incidence (Watt et al., 2009; Welsh et al., 2014).

The disease is characterized by the appearance of yellow spots on the needle surface, then early lesions circling the pine needles which develop into 1-3 mm red colored necrotic bands. Later, black fruiting bodies appear on the red bands that led to release of spores. Regions around the red bands normally die which leads to premature defoliation, and sometimes death of the infected pine trees (Figure 1.1) (Bradshaw, 2004; Gibson, 1972). Studies showed that host defense responses to the invading pathogen contribute to the DNB symptoms. For example, a phytoalexin benzoic acid, produced by the host to inhibit *D. septosporum,* is also toxic to the plant (Franich et al., 1986).

During infection, a non-host selective toxin dothistromin is produced by *D. septosporum*. Artificial injection of dothistromin into the pine needles produced DNB lesion-like symptoms (Shain and Franich, 1981). Dothistomin shows a similar structure to the aflatoxin precursor versicolorin B in *Aspergillus* species. By using aflatoxin genes as hybridization probes, genomic clones containing putative dothistromin genes were found in *D. septosporum* (Bradshaw et al., 2002; Bradshaw and Zhang, 2006; Zhang et al., 2007). The availability of the *D. septosporum* genome sequence enabled rapid identification of the remaining dothistromin genes, which are dispersed over chromosome 12 in six loci (de Wit et al., 2012). Dothistromin-deficient strains produced by deletion of dothistromin biosynthesis genes are able to infect *P. radiata,* but cause

decreased mesophyll colonization, smaller lesion size and fewer spores compared to wild type (WT), indicating dothistromin as a virulence factor during infection (Kabir et al., 2015).

Figure 1.1 Dothistroma needle blight symptoms

(http://www.nzffa.org.nz/farm-forestry-model/the-essentials/forest-health-pests-and-diseases/diseases/Needle-diseases/Dothistroma/dothistroma-needle-blight/)

Left: Necrotic lesions and fruiting bodies (black spots) on *Pinus radiata* needles infected with *Dothistroma septosporum*. Right: Needle death and premature defoliation caused by Dothistroma needle blight in the lower part of a *P. radiata* tree.

1.1.2 Causal organisms *Dothistroma septosporum* and *Dothistroma pini*

Two distinct phylogenetic lineages were identified for *Dothistroma* isolates based on a comparison of DNA sequences, leading to the splitting of one species into two: *D. septosporum* and *D. pini* (Barnes et al., *2004*). Both *D. septosporum* and *D. pini* can cause DNB on *Pinus* species. *D. septosporum* has a worldwide distribution. *D. pini* was first found in the north-central United States but more recently has been identified in other countries including Ukraine, France, Russia, Switzerland, Slovenia and Hungary (Barnes et al., 2011; Fabre et al., 2012; Fabre et al., 2010; Piou and Ioos, 2014; Piškur et al., 2013; Queloz et al., 2014). The sexual form of *D. septosporum* used to be called *Mycosphaerella pini* before the recent 'one fungus - one name' nomenclature revision; no sexual form has been identified for *D. pini* so far. Mating-type specific primers were used to screen global collections of *D. septosporum* and *D. pini* isolates, which are heterothallic. For *D. pini*, both mating types MAT1 and MAT2 were seen in the USA and Switzerland, the rest of the countries have only MAT2. For *D. septosporum*, both

MAT1 and MAT2 were identified in all Northern hemisphere populations, while in the Southern hemisphere, Kenya and South Africa are the only countries known to have isolates of both mating types; the rest of the countries have only MAT2 (Barnes et al., 2014; Groenewald et al., 2007).

1.1.3 *Dothistroma septosporum* is a hemibiotrophic fungus

A recent study showed that *D. septosporum* has a hemibiotrophic life cycle when infecting *Pinus* species (Kabir et al., 2015). The life cycle was divided into four stages. In stage one, single or multiple germ tubes germinated from fungal spores to form an extensive network of hyphae over the needle surface. In stage two, fungal hyphae grew into the stomatal chambers. Stages one and two were characterized as a symptomless biotrophic phase since no direct penetration of the epidermis was seen and the pathogen has a low fungal biomass. In stage three, hyphae invaded and colonized intercellular spaces, and early lesions started to appear on infected needles. In stage four, early lesions extended to circle the whole needle and mature with fruiting bodies that erupt through the epidermis and release spores. Stages three and four were characterized as necrotrophic phases since mesophyll cells started to disintegrate along with tissue collapse, and there was a significant increase in fungal biomass and toxin accumulation (Kabir et al., 2015).

1.2 Plant Immunity

1.2.1 Plant Immunity system

1.2.1.1 A two layered innate immune system

Plants have a two layered innate immune system for defence against living organisms. Jones and Dangl (2006) presented a zigzag model for plant-pathogen interactions (Figure 1.2) (Jones and Dangl, 2006). The primary layer of defence is achieved through recognition of pathogen-associated molecular patterns (PAMPs) by plant PAMP-recognition receptors (PRRs), which are localized in extracellular spaces. Two types of PRRs have been identified: receptor-like kinase proteins (RLKs) and receptor like proteins (RLPs). Both types of receptor proteins contain an extracellular domain which is responsible for PAMP recognition. RLKs contain an extra kinase domain that

is responsible for downstream signaling pathway activation (van Loon et al., 2006; Wang et al., 2014).

The first layer of defence inhibits microbes spreading at an early stage by activation of PAMP triggered immunity (PTI). Typical PTI responses include cell wall alterations, induction of defence related proteins and production of reactive oxygen species (ROS) (van Loon et al., 2006). One well characterized PTI system in *Magnaporthe oryzae* involves recognition of fungal cell wall chitin by rice PRR chitin oligosaccharide elicitor-binding proteins CEBiP and OsCERK1. Mutation of OsCERK1 led to a dramatic decrease in chitin induced defense responses in the host. Both these proteins contain extracellular LysM motifs that are responsible for chitin binding. OsCERK1 also contains a kinase domain that is responsible for downstream signaling. In the presence of fungal cell wall chitin, CEBiP and OsCERK1 form a hetero-oligomer which activates chitin triggered immunity in rice (Shimizu et al., 2010). Another elicitor of PTI is bacterial flagellin. A transmembrane leucine-rich repeat receptor kinase FLS2 in *Arabidopsis thaliana* recognizes bacterial flagellin flg22 and activates plant basal defenses (Chinchilla et al., 2006). Recognition of chitin and flg22 activates the same downstream mitogen-activated protein kinase pathway, which is important for plant basal defense (Rasmussen et al., 2012; Wan et al., 2004). Those findings suggested that recognition of different pathogen PAMPs by plant cell receptors can utilize a common downstream pathway to mediate basal-innate immunity (Wan et al., 2008).

To establish infection, pathogens secrete effectors to supress host PTI (the effectors will be discussed in detail in section 1.3). The second layer of defence is achieved through direct or indirect detection of effectors by host resistance (R) proteins. Recognition of effectors by R proteins activates effector-triggered immunity (ETI) that may leads to a hypersensitive defence (HR) response (de Wit, 2007). To avoid ETI, pathogens can either mutate the effector or evolve new effectors. This results in selective pressure on host R proteins to recognize newly acquired or mutated effectors, resulting in ETI again (Thomma et al., 2011).

Figure 1.2 Arms race between pathogen and plant

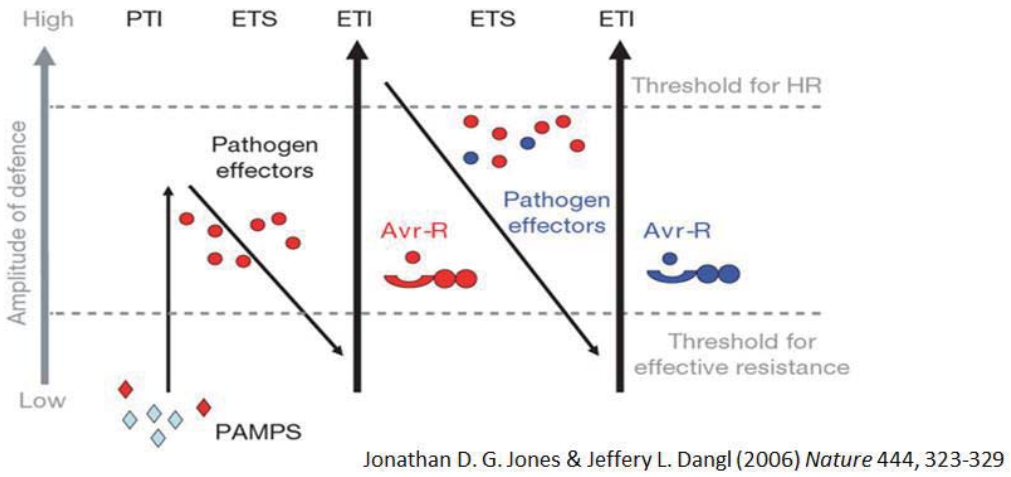

Zigzag model for arms race between pathogen and plant. Recognition of pathogen PAMPs triggers PAMP-triggered immunity in the plant (PTI). To allow infection, pathogens secrete effectors to overcome PTI. Plant resistance proteins recognize effectors and trigger effector-triggered immunity (ETI), leading to a hypersensitive response (HR). Pathogens can then mutate effectors or new effectors can evolve to overcome ETI. There is a constant arms race between plant and pathogen.

1.2.2 Resistance Protein

1.2.2.1 Molecular models of pathogen recognition

R proteins recognize effectors in a highly specific manner (Stergiopoulos and de Wit, 2009). There are three models of interactions between effectors and R proteins. The gene-for-gene model predicts that R proteins specifically recognize the corresponding effector directly from the pathogen (Flor, 1971) (Figure 1.3A). The guard model predicts that R proteins monitor the effector target which is normally involved in PTI (van der Hoorn and Kamoun, 2008). Any modification of the guardee by the effector will activate ETI in the host. The guard model allows a single R protein to recognize multiple effectors that interact with the same guardee (de Wit, 2007; Jones and Dangl, 2006). In the absence of R protein, the pathogen effectors are able to target the guardee and suppress PTI without triggering any ETI. In the guard model, the guardee is under opposing selection pressure: in the presence of R protein, the guardee is under selection pressure that favours interaction between guardee and pathogen effectors, but in the absence of R protein, the guardee is under selection pressure to avoid interaction with pathogen effectors. To relax evolutionary constraints on the guardee protein, plants can produce decoy proteins that are structurally similar to the guardee. The decoy is also

monitored by R proteins but, unlike the guardee, the decoy is not involved in PTI. The only function of the decoy is to compete with the guardee to bind the pathogen effectors. Interaction of effectors with the decoy does not supress PTI. In the presence of R protein, interaction between decoy and pathogen effector triggers HR. In the absence of R protein, interaction of pathogen effectors and the decoy does not contribute to pathogen fitness (van der Hoorn and Kamoun, 2008) (Figure 1.3B). The integrated decoy model predicts that a pair of R proteins act together. The decoy may be intergrated into the structure of an R protein. Binding of effector to the decoy leads to a direct recognition event, however the defence signalling is mediated through the second R protein (Wu et al., 2015). One example of an integrated decoy system is the R protein pair RRS1 and RPS4 from *Arabidopsis*. In the inactive state, RRS1 and RPS4 form a heterodimer through the toll-interleukin 1 receptors (TIR) domain. Binding of effector to RRS1 bait domain (DNA binding domain WRKY) induced a confirmation change and led to RPS4 homodimerization and downstream defence signaling (Cesari et al., 2014) (Figure 3C).

Figure 1.3 Models of plant pathogen recognition

(A) Gene-for-gene model

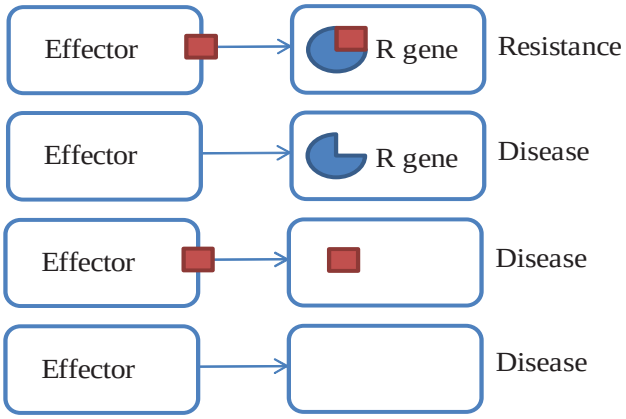

(B) Guard (decoy) Model

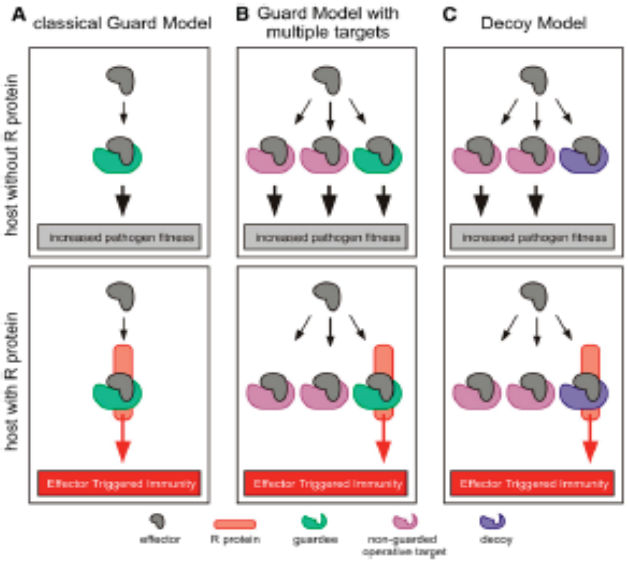

(van der Hoom and Kamoun, 2008) Plant cell

(C) Intergrated decoy model

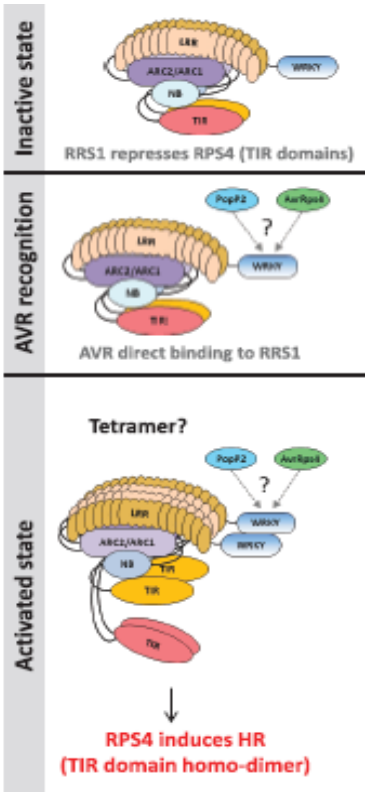

(Cesari et al., 2014) Frontiers in plant science

(A) The gene-for-gene model suggests direct interaction between R protein and effector. (B) the Guard model suggested an indirect interaction between R protein and effector. The effector interacts with the guarded protein and conformational change in the guardee triggers R protein mediated immunity. The decoy model is a further modification of the guard model as explained in the text. (C) The integrated decoy model suggests a pair of R proteins act together. Binding of effector to the decoy of first R protein triggers a conformational change in the second R protein and downstream defence signalling.

1.2.2.2 Structure and function of resistance proteins

The R proteins are characterized into eight classes according to their amino acid domains. The structure and classes of plant disease resistance genes are summarised in Table 1.1 (Sharma et al., 2014). Most classes of R proteins contain a C-terminus leucine-rich repeat (LRR) domain followed by a nucleotide-binding site (NBS).

Depending on the class, the N-terminus of the R proteins contain one or more domains including toll-interleukin 1 receptors (TIR), transmembrane domain (TM), coiled-coil domain (CC), kinase domain (KM), PEST (Pro-Glu-Ser-Thr) domain, endocytosis cell signalling domain (ESC), nuclear localization signal (NLS) and DNA binding domain (WRKY) (Sharma et al., 2014). Some different types of R proteins do not have an NBS-LRR domain. For example in maize, the resistance gene *Hm1* encodes a reductase that can inactivate the production of HC-toxin, a toxin produced by *Cochliobolus carbonum* to invade certain genotypes of maize. The Hm1 protein is classified as a detoxifying enzyme (Johal and Briggs, 1992).

Table 1.1 structure and classes of plant disease resistance genes

Class	Structure	R gene	Location	Plant
1	Toxin reductase	*Hm1*	Cytoplasm	Maize
2	NBS-LRR-CC	*RPM1, RPS2, I2*	Cytoplasm	*Arabidopsis* , Rice, Tomato
3	NBS-LRR-TIR	*N, L6, RPS5*	Cytoplasm	Tobacco, Flax
4	eLRR-TM	*Cf-2, Cf-4, Cf-9, FLS2*	Transmembrane	Tomato, *Arabidopsis*
5	eLRR-TM-KIN	*Xa21*	Transmembrane	Rice
6	eLRR-PEST-ECS	*Ve1, Ve2*	Transmembrane	Tomato
7	TM-CC	*RPWS*	Transmembrane	*Arabidopsis*
8	TIR-NBS-LRR-NLS-WRKY	*RRS1-R*	Cytoplasma	*Arabidopsis*

Structure of R protein: NBS: nucleotide-binding site; LRR: leucine-rich repeat domain; eLRR: extracellular LRR; CC: coiled-coil domain; TIR: toll-interleukin 1 receptors; TM: transmembrane domain; KIN: kinase domain; PEST: Pro-Glu-Ser-Thr domain; ECS: endocytosis cell signalling domain; NLS: nuclear localization signal; WRKY: DNA binding domain.

R gene: example of R gene with the corresponding structure.

Location: Location of R protein in plant cell.

Plant: plant that carries the corresponding R genes.

The LRR domain contains various lengths of tandem repeats (LxxLxLxxNxL) and forms a horseshoe shape with five β-sheets surrounded by seven α-helixes. The C-terminus of the LRR contains hydrophobic, aliphatic residues that are involved in effector recognition (Bella et al., 2008; Glowacki et al., 2011). This is supported by sequence analysis of flax resistance L proteins that recognize different isoforms of the *M. lini* effector AvrL567. The LRR domains of isoforms L5, L6 and L7 showed high levels of sequence differences (Dodds et al., 2006; Ellis et al., 2007). Another role of the LRR domain is to act as an intramolecular regulator that inhibits the R protein activity in the absence of effectors. Truncation of potato R protein LRR domain resulted in increased HR (Bendahmane, 2003).

The plant R protein NBS domain has ATP hydrolysis activity and also acts as an R protein regulator. The ATP bound R protein is an active form and the ADP bound R protein is in rest form. Binding of effectors to the LRR domain results in a conformational change between LRR and NBS domains, allowing ATP/ADP nucleotide exchange in the NBS domain and activation of the R protein (Rairdan and Moffett, 2006). The ATP hydrolysis activity of the NBS domain allows the R protein to return to the resting form after activation (Tameling et al., 2002).

Domain swaps of flux rust L protein TIR domain changed effector specificity, suggesting a role of the TIR domain in effector recognition (Luck et al., 2000). However the most important role of the TIR domain is in R protein mediated signalling. In tobacco, binding of effectors to R protein N triggers self-oligomerisation of the protein and leads to downstream signalling. Deletion or point mutation of the TIR domain in N protein blocks HR induction although oligomerisation still occurs (Rafiqi et al., 2009). The CC domain has a helix-loop-helix structure and is thought to be involved in R protein mediated signalling pathway by interacting with downstream proteins. Most CC domains contain a consensus sequence EDIVD; mutations in this motif abolish interaction of the CC domain with NB-LRR domains and result in decreased HR (Glowacki et al., 2011).

1.2.2.3 Resistance proteins in *Pinus* spp.

Several resistance proteins against *Cronartium ribicola* which causes blister rust in *Pinus* spp. have been identified in the five-needle species, including resistance genes *Cr1* in *P. lambertiana* (sugar pine), *Cr2* in *P. monticola* (western white pine), *Cr3* in *P. strobiformis* (southwestern white pine) and *Cr4* in *P. flexilis* (limber pine) (Kinloch and Littlefield, 1977; Kinloch et al., 1999; Schoettle et al., 2014). Since *Cr1*, *Cr2* and *Cr3* react differently to *C. ribicola* from specific locations with known virulence, it is suggested that *Cr1*, *Cr2* and *Cr3* are not the alleles of the same gene and each resistance gene can recognize specific pathogen effectors (Kinloch and Dupper, 2002). *C. ribicola* virulence factors vCr1 and vCr2 are able to avoid Cr1 and Cr2 mediated HR response, indicating resistance conferred by Cr1 and Cr2 is not durable in the field. However no virulence factor that suppresses Cr3 resistance has been identified so far (Liu et al., 2004).

A PCR strategy was used to identify R protein analogs from western white pine using oligonucleotide primers based on conserved motifs in the NBS domain of R proteins. More than one hundred NBS sequences were identified and sequence analysis revealed 67 NBS-LRR sequences belonging to the TIR-NBS-LRR family, which shared significant identity to well characterized flax R protein L and tobacco R protein N (Liu and Ekramoddoullah, 2004). Sixty one NBS sequences belonged to the CC-NBS-LRR family; those sequences showed high variation in predicted amino acid sequences from 13-98% among themselves and 5-28% amino acid identity to the TIR-NBS-LRR proteins identified earlier (Liu and Ekramoddoullah, 2007). Amongst these identified R protein candidates, one TIR-NBS-LRR class R protein PmTNL1 was analysed further. *PmTNL1* showed a low level of expression in different tissues of healthy *P. monticola* seedlings. When infected by *C. ribicola*, the expression of *PmTNL1* was significantly up-regulated in needles and stems (Liu and Ekramoddoullah, 2011). The promoter of *PmTNL1* was fused with *GUS* gene and transferred into *A. thaliana* plant, in which up-regulation occurred during pathogen infection (Liu and Ekramoddoullah, 2011). Sequence analysis of the *PmTNL1* promoter identified motifs that are involved in regulation of gene expression in response to biotic and abiotic stress. However no *GUS* fusion expression was detected in response to abiotic stress (Liu and Ekramoddoullah, 2011).

1.3 Effectors

1.3.1 Functions of effectors

1.3.1.1 Apoplastic effectors

Biotrophic pathogens establish a long-term relationship with the host in which they require living plant tissue. Hemibiotrophic pathogens have an initial symptomless biotrophic phase followed by a necrotrophic phase that triggers cell death. For both biotrophic and hemibiotrophic pathogens, suppression of PTI is required for invasion. Effectors are proteins produced by pathogens that facilitate host invasion. According to their localization, effectors are classified into two groups: apoplastic effectors and cytoplasmic effectors. Apoplastic effectors are often small cysteine rich proteins that are secreted by fungal hyphae into extracellular spaces and remain outside of the plant cells (Giraldo and Valent, 2013; Oliveira-Garcia and Valent, 2015; Stotz et al., 2014).

One role of apoplastic effectors is inhibition of plant defense enzymes such as proteases and chitinases. For example Avr2 from the biotrophic fungus *Cladosporium fulvum* is able to inhibit the tomato cysteine protease Rcr3 which is required for basal-immune defence (Esse et al., 2008; Rooney, 2005). However Rcr3 is the guardee for tomato R protein Cf-2; interaction of Avr2 with Rcr3 causes conformational change which leads to activation of Cf-2 mediated host resistance (Dixon et al., 2000). Unrelated pathogen effectors can target the same host protease. *Phytophthora infestans* secretes two protease inhibitors EPIC1 and EPIC2B (Tian et al., 2007). Both EPIC1 and EPIC2B are able to bind to and modify Rcr3. However in this case, EPIC1 and EPIC2B are not recognized by Cf-2, and thus modification of Rcr3 by EPIC proteins does not trigger a Cf-2 mediated hypersensitive response in tomato (Song et al., 2009). EPIC2B can also target another cysteine protease Pip1(Tian et al., 2007).

Other apoplastic effectors target plant chitinases. Chitin is an important component of fungal cell walls, and attack by plant chitinases is an important plant defence response. The *C. fulvum* effector Avr4 contains a chitin-binding domain (ChBD) that is able to bind to chitin oligomers and protect fungal cell wall chitin against plant chitinases during infection (van den Burg et al., 2006; van den Burg et al., 2004; van den Burg et al., 2003). Avr4 is recognized by the tomato Cf-4 resistance protein. Another *C. fulvum* effector Ecp6 can also bind to chitin but, different from Avr4, Ecp6 binds to fungal cell wall chitin oligosaccharides that are released from invading hyphae in order to prevent chitin triggered immunity in the host (Bolton et al., 2008; de Jonge et al., 2011).

Other apoplastic effectors target reactive oxygen species (ROS), which are important for PTI defense against pathogens. The effector Pep1 of the biotrophic pathogen *Ustilago maydis* surrounds fungal hyphae in the apoplast and protects it from ROS. Deletion of *Pep1* results in accumulation of H_2O_2 in fungal cell walls and transcriptional induction of the secreted maize peroxidase POX12. *In vivo* co-expression of fluorescent labelled Pep1 and POX12 in *Nicotiana benthamiana* showed direct interaction of Pep1 with POX12. Pep1 suppresses PTI by inhibiting peroxidase POX12 activity (Hemetsberger et al., 2012).

1.3.1.2 Cytoplasmic effectors

Cytoplasmic effectors are translocated into the host cytoplasm to assist host invasion by the pathogen. For example pathogen effectors were shown to suppress PTI by inhibiting the ubiquitination process. Ubiquitination plays an important role in plant immunity, ubiquitination-mediated R protein degradation prevents over accumulation and activation of plant defense responses in the absence of pathogen (Cheng and Li, 2012; Li et al., 2014; Trujillo and Shirasu, 2010). Rice gene *APIP6* encodes an enzyme that is involved in ROS production upon activation of PTI. Pathogen *Magnaporthe oryza*e effector AvrPiz-t is delivered into rice sheath epidermal cells during infection and interacts with APIP6. AvrPiz-t is able to target APIP6 for degradation and suppress ROS production in PTI (Park et al., 2012).

R protein mediated recognition of effectors can lead to an HR response which involves rapid localized programmed cell death (PCD) that restricts pathogen growth (Glazebrook, 2005). Several cytoplasmic pathogen effectors are able to inhibit host PCD. For example Agrobacterium-mediated infiltration of the *Colletotrichum higginsianum* necrosis and ethylene-inducing like protein (NLP) causes PCD on *N. benthamiana* leaves. Co-infiltration of *C. higginsianum* effectors ChEC3, ChEC3a and ChEC5 with NLP lead to reduced cell death on *N. benthamiana* leaves compared to infiltration of NLP alone. Interestingly co-expression of ChEC3, ChEC3a and ChEC5 with INF1, a protein that is also able to cause PCD on *N. benthamiana* leaves did not affect the level of PCD (Kleemann et al., 2012). It was previously demonstrated that distinct signaling pathways mediate NLP- and INF1-induced cell death in *N. benthamiana* (Kanneganti et al., 2006). *C. higginsianum* effectors are predicted to interfere with NLP-specific signaling components and thereby prevent amplification of a cell death signal or its spreading from cell to cell (Kleemann et al., 2012).

Suppression of PCD is also seen with oomycete effectors. For example the *P. infestans* effector Avr3a suppresses PCD triggered by another effector INFI when the two are co-expressed in *N. benthamiana* (Bos et al., 2006). The mechanism of suppression involves binding of Avr3a to E3 ligase CMPG1, which prevents it from triggering PCD (Bos et al., 2010). The effector Avr1b from *Phytophthora sojae* is similarly able to suppress PCD triggered by the pro-apoptotic BAX protein in *N. benthamiana* (Dou et al., 2008). Avr3a and Avr1b are able to suppress PCD in distantly related plant species,

suggesting that they target components of the host PCD mechanism that are conserved across the plant kingdoms. Mutation results showed that for Avr3a and Avr1b, the C-terminal region is important for suppression of HR-based PCD (Abramovitch et al., 2003; Bos et al., 2006).

Cytoplasmic effectors are able to target components of defense response signaling pathways, such as salicylic acid (War et al., 2011). In maize a chorismate mutase ZmCm2 is involved in salicylic acid production. The maize pathogen *Ustilago maydis* gene *Cmu1* encodes a cytosolic chorismate mutase which is localized into cytoplasm and the nucleus of maize cells. Cmu1 is able to bind to ZmCm2 and shift the production of salicylic acid towards aromatic amino acids and inhibit activation of defense responses. Deletion of *Cmu1* led to a ten times increase in salicylic acid production (Djamei et al., 2011).

1.3.1.3 Necrotrophic effectors

Unlike biotrophic pathogens, necrotrophic pathogens colonize and kill host tissue and live on dead host cells. An inverse gene-for-gene model is proposed in which necrotrophic effectors induce cell death in host genotypes carrying the corresponding susceptibility proteins. The necrotrophic effectors were traditionally called host specific toxins (HST) and the susceptibility proteins are receptors that interact with HST (Fenton et al., 2009).

The best-studied necrotrophic effector is ToxA which is secreted by *Pyrenophora tritici-repentis.* ToxA is a known pathogenicity factor, as transformation of *ToxA* into nonpathogenic *P. tritici-repentis* results in disease on *ToxA* sensitive wheat plants. The arginyl-glycyl-aspartic acid (RGD) motif of ToxA interacts with a susceptibility receptor ToxABP1. This leads to internalization of ToxA into mesophyll cells and subsequent changes in expression of wheat genes involved in defense, such as BAK1 which is involved in ROS production. BAK1 expression is significantly increased in the presence of ToxA which led to ROS production and cell death. It is interesting that the susceptibility receptor ToxABP1 is present and expressed at the same level in both ToxA susceptible and non-susceptible wheat genotypes. The result suggests that apart from ToxABP1, other susceptibility receptors for ToxA may be present in susceptible wheat genotypes (Ciuffetti et al., 2010; Manning et al., 2007).

1.3.1.4 Other types of virulence factors

Small secreted proteins produced by pathogenic fungi have important roles in host-pathogen interactions (Stergiopoulos and de Wit, 2009; Wösten, 2001). Such small secreted proteins include tomatinase and hydrophobins. Those proteins can also target host proteins involved in defense during infection and are required to achieve full virulence of the pathogen. For example, the toxin α-tomatine is produced by tomato and forms a chemical barrier against pathogen invasion. *C. fulvum CfTom1* which encodes tomatinase detoxifies α-tomatine in the apoplast and allows invasion of the pathogen. Mutation of *CfTom1* leads to high sensitivity to α-tomatine *in vitro*. The mutant strain showed delayed disease progress and a reduced fungal biomass when infecting tomato plants (Ökmen et al., 2013). Hydrophobins show similar structures to common types of apoplastic effectors in that they are cysteine rich, small secreted proteins and produced only by filamentous fungi (Wessels, 1994). Some hydrophobins are virulence factors. Deletion of *Magnaporthe grisea* hydrophobin *MHP1* led to loss of viability in conidia and reduced host colonization compared to WT (Kim et al., 2005). A detailed discussion of hydrophobins is in Chapter 4.

1.3.2 Translocation of effectors

1.3.2.1 Bacterial type III secretion system

Bacterial type III secretion system (T3SS) is shown to be involved in bacterial effector translocation into host cells. A complex called an injectisome consists of more than twenty proteins and comprises a cytoplasmic component, the export apparatus, a needle and a translocator (Diepold and Wagner, 2014). The cytoplasmic component of T3SS contains T3SS associated chaperones which form homodimers with a large hydrophobic groove. The chaperone is able to recognize bacterial effector signal peptides. Interaction of chaperone with effector directs the chaperone-effector complex to the cytoplasmic component of the T3SS. An ATPase in the cytoplasmic component dissociates the chaperone-effector complex and partially unfolds the effector so it can fit through the narrow needle component. The SctW protein located in the cytoplasmic component is required to keep T3SS in a relaxed form before it contacts the host cell. Host cell contact by the needle tip sends a signal to the cytoplasmic component and two hydrophobic proteins are exported and form a pore at the host cell membrane followed by secretion of bacteria effectors (Galán et al., 2014).

1.3.2.2 Biotrophic interfacial complex

Some hemibiotrophic fungi develop specialized intracellular invasive hyphae (IH) which remain enclosed by a plant-derived extra-invasive hyphal membrane (EIHM) during host infection (Kankanala et al., 2007). Live cell imaging of the rice blast fungus *Magnaporthe oryzae* showed that apoplastic effectors are retained within the EIHM, while cytoplasmic effectors accumulate in a membrane rich structure called the biotrophic interfacial complex (BIC). However, how a cytoplasmic effector is transferred to the BIC is not clear. The BIC is initially located at the tip of IH than moves to the side of growing IH when the fungus continues to colonize the host cell (Khang et al., 2010). Exocyst complex, a conserved multisubunit protein complex involved in tethering secretory vesicles to the plasma membrane is involved in secretion of *M. oryzae* cytoplasmic effectors into host cells (Giraldo et al., 2013). Deletion of two membrane trafficking genes *EXO70* and *SEC5* of the exocyst complex showed significant accumulation of cytoplasmic effectors in BIC (Giraldo et al., 2013).

1.3.2.3 Endocytosis mediated entry

Two types of cytoplasmic effectors are identified in oomycetes: RXLR and crinkler effectors. RXLR-effectors show extensive sequence divergence, but have a conserved RXLR domain (Arginine, any aa, Leucine, Arginine) in the N-terminal followed by an less conserved acidic region ending with EER (Birch et al., 2008). Studies showed that the RXLR domain is involved in translocation of cytoplasmic effectors into host cells. In *P. infestans*, transformants carrying Avr3a with single or combined mutations in RXLR-EER motifs failed to trigger a cytoplasmic R protein mediated HR response, indicating that after Avr3a secretion from haustoria, RXLR-EER is involved in translocation of Avr3a to the inside of host cells (Whisson et al., 2007). GFP fused to RXLR-EER domains is shown to enter soybean root cells (Dou et al., *2008*). This also suggested that RXLR-EER mediated entry is a pathogen independent process. A domain swap experiment between the RXLR-EER domain of *P. sojae* effector Avr1b and erythrocyte targeting signals from three *Plasmodium* effectors showed that the erythrocyte targeting signals are able to translocate Avr1b into soybean cytoplasm, indicating that machinery of the hosts targeted by the effectors may be very ancient. Point mutation experiments showed that Arg at position 1 and the Leu residue at position 3 are essential for function of the motif (Dou et al., *2008*)

One possible mechanism for RXLR mediated translocation is that the RXLR motif can bind to phosphatidylinositol-3-phosphate (PI3P), a phospholipid that is abundant on the outer surface of plant cell plasma membranes. Binding of effector to PI3P leads to subsequent lipid-raft dependent uptake of effectors into host cytoplasm. Mutations of the RXLR-EER motif of a RXLR-EER-GFP fusion protein abolished the binding. Blocking of PI3P with excess biosensor proteins (GFP or mCherry fusion protein that binds to PIP3) abolished the RXLR-EER-GFP fusion entry into soybean root cells (Kale et al., 2010). However a study by Yaeno showed that a positively charged patch at the C-terminus but not the N-terminus RXLR-EER motif of *P. infestans* Avr3a interacts with PI3P (Yaeno et al., 2011). So the C-terminus ligand binding domain may also have a role in effector translocation into host cells. Alternatively it is possible that the effectors target cell membrane proteins other than PI3P for translocation, and the mechanism requires both C and N-terminal domains.

The second class of translocated oomycete effector is crinkler (CRN) effectors, which contain a conserved N-terminus LxLFLAK motif required for translocation of the effector into host cells. Experiments showed that the LxLFLAK domain enables translocation of the C-terminal half of Avr3a into host and to trigger cytoplasmic R protein R3a mediated immunity (Schornack et al., 2010).

1.4 Evolutionary arms race between tomato resistance proteins and *C. fulvum* effectors

There is a constant evolutionary arms race between effectors and R proteins. The pathogen is under pressure to escape detection, while the R protein is under pressure to recognize newly evolved effectors. Effectors that do not have critical roles in pathogenicity or that have functional homologues in the pathogen are normally mutated or lost in the field. R proteins that recognize effectors that are important for pathogen fitness are normally more durable in the field, because those effectors are less likely to mutate or be lost (van der Hoorn and Kamoun, 2008).

1.4.1 Tomato Cf resistance protein variation

Sequence exchange, tandem duplication of *Hcr* genes, unequal crossing over and random mutation followed by divergent selection at LRR locus result in variation in R protein sequences in tomato (Wulff et al., 2009). Hybridization of DNA gel blots using *Cf-9* and *Cf-2* tomato resistance genes as probes revealed that they belong to multigene families *Hcr9s* and *Hcr2* located at the short arm of chromosomes 1 and 6 respectively (Dixon et al., 1996; Jones et al., 1994). *Cf-9* gene resides at the *MILKY Way* (MW) locus along with four other paralogs of which *Cf-9B* is also a functional resistance gene. *Cf-4* and *Cf-4E* genes also reside at the *MW* locus (Figure 1.4) (Parniske et al., 1997). The tandemly duplicated gene structure of the Hcr9 locus allows multiple specificities at the same locus. Alignment of *Hcr9* genes identified regions of shared sequences within their protein-coding sequences, suggesting that *Hcr9* gene variation is generated by sequence exchange between paralogs through unequal crossing over or gene conversion (Parniske et al., 1997). Sequence analysis of *Hcr9* proteins revealed the β-sheet of LRR domain contains 7 regions with high amino acid variability, which contributes to effector recognition specificity. The high rate of nonsynonymous mutations suggested divergent selection in Hcr9 proteins (Parniske et al., 1997).

The Hcr2 Locus proteins have extreme intraspecific variation in LRR copy number (Caicedo and Schaal, 2004; Dixon et al., 1998). DNA gel blot of 16 individual *Solanue pimpinellifolium* using Cf-2 probe showed that different *S. pimpinellifolium* strains contain different Cf-2 copy numbers with various sizes. The size difference of Cf-2 is due to numbers of type A and type B LRR coding units. Nucleotide and amino acid alignment of Type A and Type B units of Cf-2 showed that although both types have a high level of similarity, similar types are not closely positioned within the same gene, indicating complex recombination events rather than tandem duplication is involved in generating different Cf-2 isoforms. High levels of DNA polymorphisms were also identified within the LRR domain in Cf-2. (Caicedo and Schaal, 2004).

Figure 1.4 Structural organization of *Hcr9* and *Hcr2* Locus derived from various *Lycopersicon* species

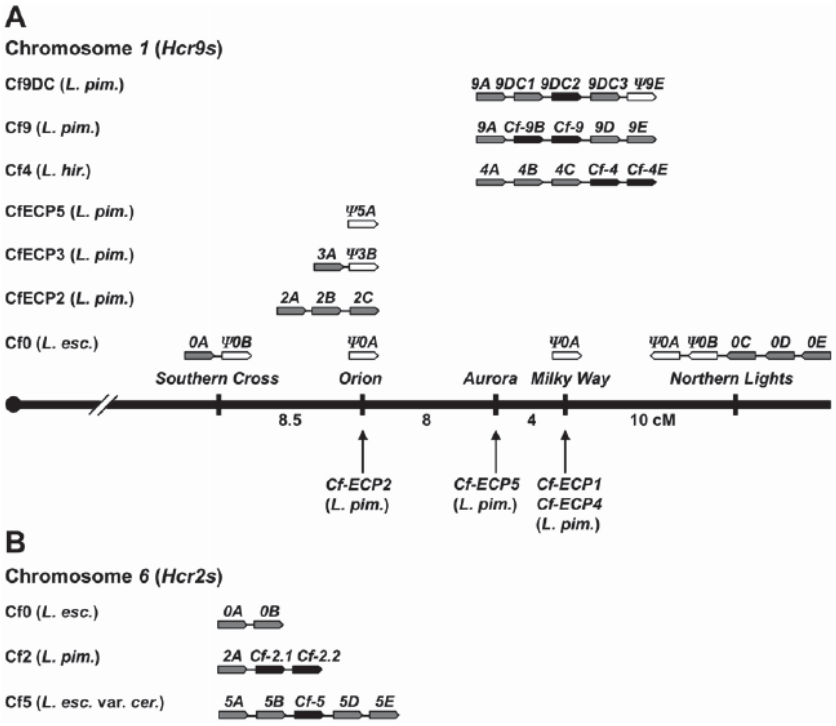

Wulff. *et al* (2009). Molecular Plant-Microbe Interactions *22*, 1191-1202

Organization of (A) *Hcr9* and (B) *Hcr2* gene clusters on chromosomes *1* and *6*, respectively. The orientation of *Hcr9* genes relative to each other and the centromere is indicated by arrowed boxes. Genetic distances are indicated in cM. *Hcr9* and *Hcr2* genes with known specificities are shown in black, while grey denotes no known function and white denotes nonfunctional gene. *Cf-ECP* map positions are indicated by black arrows at the bottom of the chromosome, but their identity as *Hcr9* genes has not been demonstrated.

1.4.2 Tomato guardee protein variation

The tomato and *C. fulvum* CfAvr2-Rcr3-Cf-2 interaction supports the guard model (Rooney, 2005). If a pathogen effector mutant is able to modify the guardee without detection by the guard, then the guard and guardee come under evolutionary pressure to regain recognition capacity or avoid modification by the effector. Sequence comparisons of Rcr3 and Pip1 from eight wild tomato strains suggested they are less conserved than other proteases tested. Rcr3 and Pip1 showed a high level of amino acid substitutions and the locations of the variant residues suggest diversifying selection at the substrate binding groove (Shabab et al., 2008).

1.4.3 *C. fulvum* effector variation

Stergiopoulos et al (2007) did a comprehensive analysis of allelic variation in *C. fulvum* effector genes from a global collection. They showed that *Ecp* genes of *C. fulvum* accumulated less polymorphisms than the *Avr* genes. Thirteen DNA polymorphisms involving twelve SNPs and one deletion were identified in *C. fulvum Ecp* genes. Unlike *Avr* genes, more polymorphisms were found in the non-protein coding regions of *Ecp* genes than in protein coding sequences. The lower level of polymorphisms in Ecps suggests that maintaining the Ecp protein sequences is favored by selection. However, only *C. fulvum* strains isolated from areas of commercially grown tomato were sampled. Commercial use of *Avr* matching R genes (but not *Ecp* matching R genes), which created evolutionary pressure for the selection of variation in the corresponding *Avr* genes, could also contribute to low level of polymorphism to *Ecp* genes.

DNA polymorphisms identified in *Avr2* and *Avr4* normally resulted in nonsynonymous changes and indicated positive diversifying selection. However different types of mutations were favoured by selection in *Avr4* and *Avr2*. Only one of nine mutations in *Avr4* resulted in a truncated Avr4 compared to 10 out of 12 mutations that resulted in truncated Avr2. Avr4E and Avr9 were lost from some *C. fulvum* strains, suggesting gene deletion as one mechanism to avoid Cf-mediated resistance in tomato. Only one nonsynonymous change was present in Avr9, and this was located in the signal peptide and not expected to significantly affect Avr9 avirulence in Cf-tomato (Stergiopoulos et al., 2007).

1.5 Hypothesis, aims and objectives

Little is known about *Pinus radiata* resistance against *D. septosporum*. It is well established that older *P. radiata* (>15 years old) develop resistance to *D. septosporum* (Bulman et al., 2013). However aged *P. radiata* cuttings are not useful for controlling *D. septosporum* (Bulman et al., 2013). Multivariate analysis of trials also showed that resistance to DNB has strong genetic correlations to stem diameter (Kennedy et al., 2014). However strong selection towards stem diameter compromises wood quality (Kennedy et al., 2014).

Recently effectors have been used to screen for plant germplasm that carries resistance proteins in other pathosystems. Identification of R proteins improved disease resistance breeding in the field. R proteins that recognize different allelic isoforms of effectors or target effectors that are required for pathogen full virulence will be more durable in the field (Vleeshouwers and Oliver, 2014). Understanding the biology of *D. septosporum* effectors will enable development of tools to screen for resistance in *P. radiata*. Eventually this could lead to knowledge of plant susceptibility and/or resistance genes that could be exploited in future breeding programmes. Classical work on how fungal effector proteins can trigger plant host resistance has been done with *C. fulvum* and its host tomato (de Wit et al., 2009). *D. septosporum* has been shown to be closely related to *C. fulvum* (de Wit et al., 2012). The intention of this study was to identify putative *C. fulvum* homologous effectors in *D. septosporum* and to understand the function of *D. septosporum* effectors during infection of *P. radiata*.

Hypothesis

Homologues of *C. fulvum* effectors are present in the *D. septosporum* genome.

D. septosporum effectors are virulence factors during infection of *P. radiata*.

Aim 1: **Identification of putative *C. fulvum* homologous effectors in *D. septosporum***

Objectives

a) Identification of putative *C. fulvum* homologous effector genes in *D. septosporum*

b) Annotation of putative *D. septosporum* effector genes

c) *In planta* transcriptome analysis of *D. septosporum* effector genes

Aim 2: Functional characterization of effectors in *D. septosporum*

a) Targeted gene replacement and cross genera complementation of selected *D. septosporum* effectors and a hydrophobin gene

b) Study the function of selected *D. septosporum* effectors and the hydrophobin gene

c) Identification of amino acid residues in DsAvr4 that are involved in Cf-4 recognition

Aim 3: Screening for necrosis-inducing activity of *D. septosporum* effectors in *P. radiata*

a) Heterologous expression of selected *D. septosporum* effector protein using *Pichia pastoris*

b) Screening for necrosis-inducing activity of selected *D. septosporum* effectors in *P. radiata*

Aim 4: Analysis of effector gene polymorphisms in a global population of *D. septosporum*

a) Determination of presence /absence of effectors in a global population of *D. septosporum*

b) Polymorphism analysis of effectors in a global population of *D. septosporum*

Chapter 2. Materials and Methods

2.1 Biological material

2.1.1 Fungal strains

The wild-type (WT) *Dothistroma septosporum* strains used for this study are listed in Table 2.1. The mutant *D. septosporum* strains used for this study are listed in Table 2.2.

Table 2.1 Wild-type *D. septosporum* strains

Continent	Strain Name	Country of Origin	Year of collection	Host
Asia	BHU1	Bhutan	2005	*P. radiata*
Oceania	NZE2	New Zealand	1965	*P. radiata*
	NZE10	New Zealand	2005	*P. radiata*
	AUST6	Australia	2003	*P. radiata*
North America	ORE12	USA	1983	*P. ponderosa*
	USA-MON8	USA	2006	*P. contorta v. latifolia*
	CAN3	Canada	1997	*P.contorta*
Africa	SAF1625	South Africa	1984	*P. radiata*
	SAF4	South Africa	2002	*P. radiata*
	KEN4	Kenya	2001	*P. radiata*
South America	GUA1	Guatemala	1983	*P. tecumumanii*
	GUA-N1	Guatemala	2012	*P. oocarpa*
	COL-N	Colombia	2011	*P. elliottii x taeda*
	COL-S	Colombia	2011	*P.kesiya*
	BRZ1	Brazil	1974	*P.pinaster*
	CHI17	Chile	2001	*P. radiata*
	ECU 13	Ecuador	2001	*P.radiata*
Europe	GRED1	Greece	2012	*P.burtia & P. nigra*
	ROM11	Romania	2007	-
	SLV1	Slovakia	2001	*P. sylvestris*
	POL4	Poland	2003	*P. nigra*
	CZE1	Czech Republic	2009	*P. nigra*
	ATRA4-2	Austria	2004	*P. sylvestris*
	Hun2-53	Hungary	2007	*P. nigra*
	ALP3	Germany	2001	*P. mugo*
	DPAR1	Denmark	2013	*P.aristata*
	FRA1	France	1970	*P. coulteri*
	SP2	Spain	2013	*P. sylvestris*
	UK402	England	2007	-
	SCO484	Scotland	2008	-
	FIN3.2	Finland	2011	*P. sylvestris*

D. septosporum strains used for this study are organized by continent. The date when the strains were collected and the pine hosts that the strains were isolated from are listed where known.

Table 2.2 Mutant *D. septosporum* strains

Knockout strains

Strain name	Plasmid transformed (Lab number)	Genotype	Reference	Alternative names in text
FJT20	R232	NZE7/*PToxA:sgfp , hph*	(Schwelm, 2007)	
FJT134	R337	NZE10/Δ*DsAvr4 : : hph*	This study	DsAvr4 KO T1
FJT135	R337	NZE10/Δ*DsAvr4 : : hph*	This study	DsAvr4 KO T2
FJT138	R338	NZE10/Δ*DsEcp6 : : hph*	This study	DsEcp6 KO T1
FJT141	R339	NZE10/Δ*DsEcp2-1: : hph*	This study	DsEcp2-1 KO T1
FJT142	R339	NZE10/Δ*DsEcp2-1: : hph*	This study	DsEcp2-1 KO T2
FJT145	R340	NZE10/Δ*DsHdp1: : hph*	This study	DsHdp1 KO T1
FJT146	R340	NZE10/Δ*DsHdp1: : hph*	This study	DsHdp1 KO T4

Complemented strains

Strain name	Plasmid transformed (Lab number)	Genotype	Reference	Alternative names in text	Copy number
FJT136	R347	FJT134/*DsAvr4 , phleo*	This study	DsAvr4 C4	1
FJT137	R347	FJT134/*DsAvr4 , phleo*	This study	DsAvr4 C2	2
FJT139	R348	FJT138/*DsEcp6 , phleo*	This study	DsEcp6 C2	1
FJT140	R348	FJT138/*DsEcp6 , phleo*	This study	DsEcp6C5	2
FJT143	R349	FJT141/*DsEcp2-1 , phleo*	This study	DsEcp2-1 C2	1
FJT144	R349	FJT141/*DsEcp2-1 , phleo*	This study	DsEcp2-1 C3	2
FJT147	R350	FJT145/*DsHdp1 , phleo*	This study	DsHdp1C4	1

sgfp: Green fluorescent protein gene

hph: Hygromycin resistance gene

phleo: Phleomycin resistance gene

Ds: *Dothistroma septosporum*

2.1.2 *Escherichia coli* strains

E. coli Top10 (F– *mcr*A Δ(*mrr-hsd*RMS-*mcr*BC) Θ80*lacZ*ΔM15 *lac*X74 *rec*A1 *ara*D139 Δ(*ara leu*) 7697 *gal*U *gal*K *rps*L (StrR) *end*A1 *nup*G and *E. coli* DB3.1™ (F– *gyr*A462 *end*A1 Δ(sr1-*rec*A) *mcr*B *mrr hsd*S20 (rB–, mB–) *sup*E44 *ara*-14 *gal*K2 *lac*Y1 *pro*A2 *rps*L20(SmR) *xyl*-5 λ– *leu mtl*1) (Life Technologies, Carlsbad, CA, USA) were used for propagation and maintenance of plasmids.

*E. coli ccd*B Survival™ 2 *T1R* (F- mcrA Δ(mrr-hsdRMS-mcrBC) Φ80lacZΔM15 ΔlacX74 recA1 araΔ139 Δ(ara-leu)7697 galU galK rpsL (StrR) endA1 nupG fhuA::IS2) (Life Technologies, Carlsbad, CA, USA) strain is resistant to the ccdB protein, which is normally toxic to *E. coli* cells *(Bernard and Couturier, 1992).* This strain was used for propagating Gateway® (Life Technologies, Carlsbad, CA, USA) destination and donor vectors that contain *ccdB* as a selection marker gene.

2.1.3 *Agrobacterium tumefaciens* strain

The *A. tumefaciens* GV3101 strain used for agro-infiltration in this study is a modified version of pathogenic *A. tumefaciens*. It has a C58 chromosome background but lacks the Ti plasmid. The GV3101 strain also contains a rifampicin selectable marker (Hellens et al., 2000; Holsters et al., 1980)

2.1.4 *Pichia pastoris* strain

The methylotrophic yeast *P. pastoris* GS115 strain (Life Technologies, CA, USA) was used for heterologous expression of *D. septosporum* effector proteins. The *P. pastoris* GS115 strain cannot synthesise histidine due to a mutation in the histidinol dehydrogenase gene (*his4*) and will only grow on plates supplemented with histidine.

2.1.5 Plant material

Less than 1 year old *Pinus radiata* seedlings raised from seeds with different levels of resistance to *D. septosporum* were used for shoot cuttings to make clonal seedlings at Scion (Rotorua, New Zealand). Sibling clones 3/1 and 3/2 are from a susceptible family. The clonal seedlings were kept in the Massey University greenhouse with natural light and two ventilating fans. Two weeks before the experiment, the cuttings were re-planted into 15 cm plastic pots using a standard potting mix (Daltons, New Zealand).

2.2 Growth and maintenance of cultures

2.2.1 Growth and maintenance of bacterial cultures

The *E. coli* cells were grown on LB agar plates or in LB broth (Appendix 1.1) (shaking at 180 rpm) with antibiotics as required at 37°C overnight. For short term storage, the LB agar plates were sealed with parafilm and stored at 4°C. For long-term storage, *E. coli* cells grown in LB broth were mixed with 50% (v/v) sterile glycerol to reach a final concentration of 15% (v/v) glycerol and stored at -80°C. The *Agrobacterium* cells were grown on LB agar plates or in LB broth (shaking at 150 rpm) with antibiotics as required at 30°C for 2 days. *Agrobacterium* cell cultures were stored the same as *E. coli* cell cultures.

2.2.2 Growth, maintenance and harvest of *D. septosporum* culture and mycelia

For *D. septosporum* spore generation, mycelia were cut from an actively growing colony and ground using a sterile plastic pestle in a microcentrifuge tube with 200 µl of sterile MilliQ water. Then 50 µl of mycelia mixture were spread on plates of dothistroma sporulation medium (DSM) or pine minimal salts medium (PMMG) agar (Appendix 1.1) plate. The plates were incubated at 22°C for 7 days and stored at 4°C.

To grow *D. septosporum* on solid medium (Dothistroma medium (DM) or potato dextrose agar (PDA)) (Appendix 1.1), 50 µl of 10^5 spores/ml generated as described above were spread on DM or PDA plates. The plates were incubated at 22°C for 10 days and stored at 4°C. Fresh sub-cultures were made every 6 months to maintain the *D. septosporum* strain. For long term storage, mycelia were cut from an actively growing colony, ground using a sterile plastic pestle in a microcentrifuge tube and stored in 200 µl of 20% (v/v) sterile glycerol at -80°C.

To grow *D. septosporum* in broth (DM, PD or PMMG), a 4 mm diameter plug of *D. septosporum* mycelium was cut from the edge of an actively growing colony with a sterile scalpel and ground using a sterile plastic pestle in 100 µl of sterile MilliQ water in a microcentrifuge tube. Then 25 µl of mycelia mixture were added to 25 ml of broth in a 125 ml flask. Flasks were incubated at 22°C for 10 days with shaking (180 rpm). The *D. septosporum* mycelia were harvested by filtration through a funnel covered with a sterile nappy liner (Johnson and Johnson). For genomic DNA extraction, the mycelia were collected in a 15 ml falcon tube, snapfrozen in liquid nitrogen; freeze dried overnight and stored at -20°C. For RNA extraction, the mycelia were collected and wrapped in foil paper, snap frozen in liquid nitrogen and stored at -80°C.

2.2.3 Growth and maintenance of *Pichia pastoris* cultures

The *P. pastoris* cells were grown on yeast extract peptone dextrose medium (YPD) (Appendix 1.7) agar plates at 30°C for 2 days. For short term storage, a single colony was picked with a sterile toothpick and transferred to a YPD agar slope in a screw-cap bottle. The yeast was grown at 30°C for 2 days and stored at 4°C. For long term storage, a single colony was picked by a sterile toothpick, transferred to 5 ml of YPD broth and grown at 30°C overnight. The *P. pastoris* cells were harvested by centrifugation at

15,862 g (Eppendorf 5415R) for 30 seconds and resuspended in YPD broth containing 15% (v/v) sterile glycerol. The cells were snapfrozen in liquid nitrogen and stored at -80°C.

2.3 DNA extraction, quantification and analysis

2.3.1 Genomic DNA isolation from *D. septosporum* by CTAB method

The hexadecyltrimethylammonium bromide (CTAB) DNA extraction method developed by Doyle and Doyle was used in this study (Doyle and Doyle, 1987). Freeze-dried mycelia (section 2.2.2) were ground to a fine powder using a sterile mortar and pestle with liquid nitrogen. Then 500 mg of ground sample was transferred into a sterile microcentrifuge tube containing 600 µl of 2% CTAB extraction buffer (Appendix 1.2). The sample was incubated at 37°C for 20 minutes with 2 µl of RNase A (100 mg/ml) (Sigma-Aldrich, St. Louis, Missouri, USA) and then at 65°C for 45 minutes with occasional inversion. After removal from the water bath, the sample was cooled to room temperature and 600 µl of chloroform was added. The sample was mixed by inversion and centrifuged at 15,862 g (Eppendorf 5415R) for 2 minutes. The upper aqueous phase was transferred to a new tube containing 600 µl of isopropanol, mixed and incubated on ice for 20 minutes. The mixture was centrifuged at 9279 g (Eppendorf 5415R) for 30 seconds to pellet the DNA. The supernant was discarded, 600 µl of 80% ethanol was used to wash the precipitated DNA pellet and centrifuged at 9279 (Eppendorf 5415R) for 1 minute. The ethanol washing step was repeated at least twice. Then the ethanol was decanted completely, and the sample was left to air dry. Finally the DNA was resuspended in 50 µl TE buffer (Appendix 1.2).

2.3.2 Isolation of plasmid DNA

Plasmid DNA was extracted from *E. coli* cultures (Section 2.2.1) using a High Pure Plasmid Isolation Kit (Roche Applied Science, Penzberg, Germany) or QIAprep Spin Miniprep Kit (Qiagen, Hilden, Germany) according to the manufacturer's instructions.

2.3.3 Nucleic acid quantification

Nucleic acid quantification of PCR product and plasmid DNA (not including genomic DNA) was done using a nanodrop® ND-1000 UV-Vis spectrophotometer and nanodrop® software version 3.1.0 (Nanodrop Technologies Inc, Wilmington) according to the manufacturer's instructions.

For genomic DNA samples, a Hoefer DyNA Quant 200 fluorometer (Amersham Biosciences) was used to determine the sample concentration since organic solvent used for gDNA extraction may interfere with nanodrop reading. 2 ml of fluorometer working buffer (Appendix 1.2) was used to zero the fluorometer, then 2 µl of standard DNA (100 µg/ml) was added to 2 ml of working buffer in the cuvette for calibration. To determine the sample DNA concentration, 2 µl of sample DNA was added to 2 ml of working buffer, and the concentration recorded by the fluorometer as ng/µl.

2.3.4 Agarose gel electrophoresis

An 0.4%-1% (w/v) agarose gel was prepared by melting agarose (Gold Bio, St Louis, USA) in 1x TBE buffer (Appendix 1.2) depending on the DNA sample molecular weight. 1x TBE buffer was added to the gel apparatus, the DNA sample was mixed with gel loading dye (Appendix 1.2) and loaded along with 1 kb plus DNA molecular weight ladder (Invitrogen, Carlsbad, CA, USA) on the gel. The electrophoresis was carried out at 40-80 volts (mini Sub-cell GT gel box, Bio-Rad, Hercules, CA, USA) until the dye moved to 2 cm from the end of the gel. Then the gel was stained with 1 µg/mL ethidium bromide (Appendix 1.2) for 15 minutes followed by rinsing in MilliQ water for 2 minutes. Finally the gel was visualized and photographed using a Gel- Doc™XR documentation system (Bio-Rad, Hercules, CA, USA) and Image Lab™ software.

2.3.5 Agarose gel purification of DNA

After gel electrophoresis, the selected DNA fragment was cut out from the gel using a sterile scalpel under long wave UV light (Alpha Innotech, Johannesburg, S.A) and transferred into a sterile microcentrifuge tube. The DNA was then recovered using a QIAquick gel extraction kit (Qiagen, Hilden, Germany) according to the manufacturer's instructions.

2.3.6 Restriction endonuclease digestion of DNA

For restriction endonuclease digestion of DNA, 1 unit of selected restriction endonuclease and appropriate digestion buffer was used to digest 1 µg of DNA in a microcentrifuge tube to a final volume of 20 µl to 50 µl according to the manufacturer's instruction. The temperature of incubation depended on the selected restriction endonuclease. The incubation time varied from 2 hours (plasmid, PCR product) to overnight (gDNA). To stop the digestion reaction, the digested DNA sample was incubated at 65°C for 15 minutes.

2.3.7 Ligation reaction

A 10 µl ligation mixture was prepared containing 1x ligation buffer, 1 µl of 3 U/µl T4 DNA ligase (Roche), vector and inserts. It was incubated at 4°C overnight. The ATP in the ligation buffer may degrade due to repeated freeze/thaw cycles. So fresh ATP was added to the ligation buffer as required to give a final concentration of 1 mM .

2.3.8 Vector construction

2.3.8.1 Vector construction by restriction endonuclease digestion and ligation

The vector and insert were digested as described in section 2.3.6. For vector construction, a 1:3 insert : vector molar ratio was used unless otherwise stated. The amount of insert DNA and vector used in ligation (section 2.3.7) was calculated using the following formula:

$$\frac{50 \text{ ng of vector} \times \text{kb size of insert}}{\text{kb size of vector}} \times \text{Molar ratio of } \frac{\text{Insert}}{\text{Vector}} = \text{ng of insert}$$

To make *D. septosporum DsAvr4*, *DsEcp2-1*, *DsEcp6* and *Dsdp1* complementation plasmids. The targeted genes with 1 kb of the 5' and 3' flanking regions were amplified using specific primers carrying restriction endonuclease digestion sites (Appendix 5.2 for primer sequences). The 1 kb 5' and 3' flanking regions were checked for the presence of upstream or downstream gene CDS; if another gene was present, the amplified regions were shortened to avoid them. The amplified target gene fragments and Phleomycin plasmid (Lab No. pR224) were digested with appropriate restriction enzymes and the target gene fragments ligated into the phleomycin vector by T4 ligase.

To make *P. pastoris* heterologous protein expression plasmids. cDNA of selected target genes were amplified using specific primers carrying restriction endonuclease digestion sites (Appendix 5.2 for primer sequences). The amplified cDNA target gene fragments were inserted into *P. pastoris* expression vectors by restriction digestion and ligation as described above.

2.3.8.2 Gateway three-fragment construction of gene replacement vector

For the Gateway system, there are two recombination steps involved. The first recombination, mediated by BP clonase, is between attB sites (insert) and attP (pDONR vector) sites. This will generate three entry vectors with different attL sites. The second recombination, mediated by LR clonase, is between attL (entry vectors) sites and attR (pDEST vector) sites. This will generate the final construct (Figure 2.1). For targeted gene replacement vector construction, 1 to 1.5 kb of the 5' or 3' flanking regions of the targeted gene, and a GFP-hygromycin resistance (hph) selectable marker, were amplified using PCR (section 2.4.2). Special primers were designed with the 22 to 25 bp attB sites at their 5'ends for BP recombination (see Appendix 5.1 for primer sequences). The 5'flanking insert had attB4 and attB1r sites, the GFP-hph insert had attB1 and attB2 sites and the 3'flanking insert had attB2r and attB3 sites. Three pDONR vectors were used, pDONR™ P4-P1R for 5' flanking insert, pDONR™ P2R-P3 for 3' flanking insert and pDONR™ 221 for GFP-hph insert.

The BP 5 µl recombination mixture contained 1 µl of BP Clonase™ II enzyme (Life Technologies, Carlsbad, CA, USA), 50 fmoles of each PCR products, 50 fmoles of pDONR vectors and TE buffer (Appendix 1.2). The reaction mixture was incubated at 25°C overnight. Then 1 µl of the Proteinase K solution (Appendix 1.2) was added to the reaction and incubated for 10 minutes at 37°C before transformation into *E. coli* competent cells by electroporation (section 2.3.9). The transformed *E. coli* colonies were screened as described in section 2.4.3. Plasmid was extracted as described in section 2.3.2.

The LR 5 µl recombination mixture contained 1 µl of LR Clonase® II Plus enzyme (Life Technologies, Carlsbad, CA, USA), 10 fmoles of each 5', 3' and GFP-hph entry vectors, 20 fmoles of pDEST™ R4-R3 vector and TE buffer. The reaction mixture incubated at 25°C overnight. Then 1 µl of proteinase K solution (Appendix 1.2) was

added to the reaction and incubated for 10 minutes at 37°C before transformation into *E. coli* competent cells by electroporation (section 2.3.9). The transformed *E. coli* colonies were screened as described in section 2.4.3. The final recombinant plasmid (Figure 2.1B) was then extracted from *E. coli* cells as described in section 2.3.2.

Figure 2.1 Construction of *D. septosporum* effector KO plasmid

(A) MultiSite Gateway three-fragment recombination reaction scheme

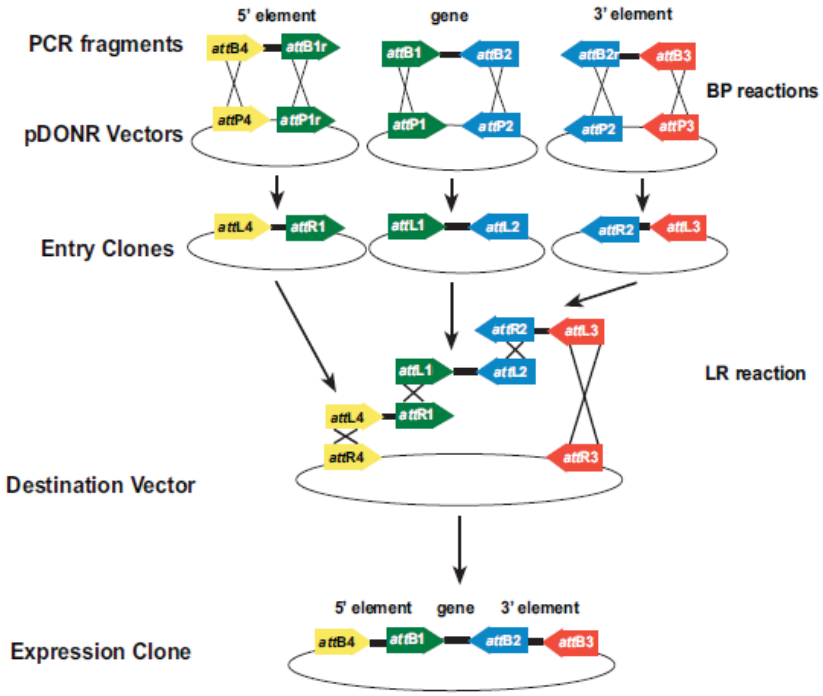

MultiSite Gateway® Three- Fragment Vector Construction Kit manual Catalog no. 12537-023 Version G, P 8, September 2008

(B) Schamatic diagram of *D. septosporum* effector KO plasmid

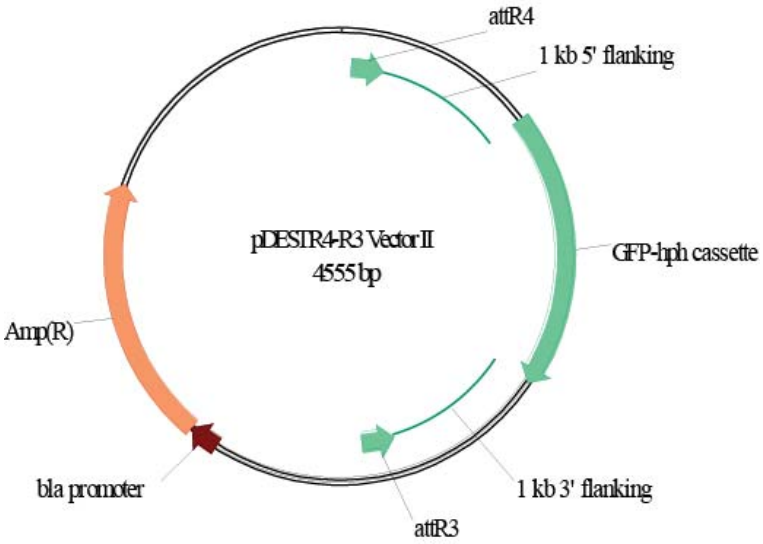

The KO plasmid contains a GFP-hph cassette which is flanked by 1 kb of 5' and 3' flanking regions of the targeted gene.

2.3.9 Transformation of *E. coli*

2.3.9.1 Making competent *E. coli* cells

A single Top 10 *E. coli* colony (section 2.1.2) was inoculated into 5 ml LB culture using a sterile loop. The LB culture was incubated at 37°C overnight with shaking (180 rpm). Then 50 µl of the above overnight LB culture was inoculated into 500 ml LB culture in a flask and incubated at 37°C with shaking (180 rpm) until the optical density of the LB broth showed the cells had reached mid-log phase (A_{600} 0.5-1.0). The cells were chilled on ice for 20 minutes, then harvested by centrifugation at 4025 g in a F21J-8x50y rotor (Thermo-Sorvall Waltham, Massachusetts, USA) for 10 minutes at 4°C. The supernatant was removed and cells were resuspended in 1 L ice cold sterile MilliQ water. The cells were harvested by centrifugation as before. The washing steps were repeated two times with 500 ml ice cold sterile MilliQ water and 20 ml ice cold sterile 10% glycerol respectively. Finally the cells were centrifuged and resuspended in 2 ml ice cold sterile 10% glycerol. Aliquots of 50 µl cells were transferred into fresh sterile microcentrifuge tubes, snap frozen in liquid nitrogen and stored at -80°C.

2.3.9.2 Transformation of *E. coli* by electroporation

Electroporation of *E. coli* was following the Dower method (Dower et al., 1988). 50 µl

of *E. coli* competent cells and 5 µl of ligation mixture were mixed in an ice cold 2 mm electroporation cuvette (Thermo fisher Scientific, MA, USA). The cuvette was placed in the Gene Pulser (Bio-Rad Hercules, CA, USA), which was set at a voltage of 2.5 kV for electroporation. After electroporation, 1 ml LB broth was immediately added to the cuvette. The cells were then transferred into a sterile microcentrifuge tube and incubated at 37°C for 1 hour. 50 µl to 100 µl of transformation culture was grown on an LB plate (section 2.2.1). If the vector had blue-white *lacZ* selection, 40 µl 2% X-gal and 40 µl 20% IPTG was added to each 25 ml LB plate.

2.3.10 DNA sequencing

Sequencing reactions were carried out at the Massey Genome service (Massey University Palmerston North) using an ABI PRISM® BigDye® Primer Cycle Sequencing Ready Reaction Kit in an ABI 3730 DNA Analyzer (Applied Biosystems, Foster City, CA). For plasmid sequencing, 300 ng of purified plasmid DNA and 3.2 pmol primer were mixed with sterile MilliQ water to a final volume of 15 µl. For PCR product sequencing, 2 ng / 100 bp PCR product and 3.2 pmol primer were mixed with sterile MilliQ water to a final volume of 15 µl. Ninety-six well plate PCR product sequencing was carried out at Macrogen (Macrogen, Seoul, Korea). 5 µl of 50 ng/µl PCR product was mixed with 5µl of 10 pmol primer and sent to Macrogen for sequencing using the EZ-Seq service. Sequence analysis was done using the National Center for Biotechnology Information (NCBI) BLAST programs (http://www.ncbi.nlm.nih.gov/blast/Blast.cgi) and Vector NTI 11.0 software (Informax, Invitrogen, Frederick, MD). The six-frame translation was done using the program six-pack translation Software (The European Molecular Biology Open Software Suite: http://www.bi.up.ac.za/cgi-bin/emboss.pl?_action=input&_app=sixpack).

2.4 Polymerase chain reaction

2.4.1 Standard PCR reactions

All PCR reactions were set up on ice, in a total volume of 25 µl, and were carried out in an Eppendorf Gradient Mastercycler® (Eppendorf, Hamburg, Germany). PCR primers were designed using clone manger (Sci-ED software) and synthesized by Integrated

DNA Technologies (Coralville, IA, USA) or Invitrogen (Life Technologies, Carlsbad, CA, USA). A schematic diagram of *DsAvr4* primers used for this study is given as an example for primer design (Appendix 2.1).

The 25 µl PCR mixture contained 1×PCR buffer, 0.05 mM of each dNTP; 1.5 mM $MgSO_4$, 0.4 µM of each primer and 0.02 unit *Taq* DNA polymerase enzyme (Life Technologies, Carlsbad, CA, USA). Finally DNA template was added (10 ng of plasmid DNA or 5 µg of gDNA). The PCR conditions were: an initialisation step of 94°C for 2 minutes; then 30 cycles of denaturation at 94°C for 30 seconds, annealing at 55°C to 58°C for 30 seconds and elongation at 72°C for 1 min/kb depending on product size; followed by 1 cycle of 72°C for 5 minutes. When required the PCR products were purified using a QIAquick PCR purification kit (Qiagen Hilden, Germany) according to manufacturer's instructions, and stored at 4°C**.**

2.4.2 *E. coli* and *A. tumefaciens* colony PCR

A sterile P2 pipette tip was used to pick cells from a single colony by gently touching the surface of a colony on a plate. The cells were transferred into a PCR tube containing 24 µl of PCR reaction mixture (as for standard PCR, section 2.4.1). The initial PCR step was 3 minutes at 96°C to release the cell components, the rest of the steps were the same as the standard PCR conditions (section 2.4.1).

2.4.3 *P. pastoris* colony PCR

A sterile P2 pipette tip was used to pick up cells as described in section 2.4.2. The cells were transferred into a microcentrifuge tube containing 10 µl of sterile MilliQ water and 5 µl of 5 unit/µl of lyticase solution (Sigma, MO, USA). The cell mixture was incubated at 30°C for 10 minutes and immersed in liquid nitrogen for 1 minute. After thawing on ice, the cell suspension was centrifuged at 2880 g (Eppendorf 5810) for 1 min. Then 1 µl of the cell supernatant fraction was used for a standard PCR reaction (section 2.4.1).

2.4.4 Overlapping PCR to construct DsAvr4 domain swap plasmids

Four gene fragments (*DsAvr4* WT, chimera C1-C4, chimera C4-C6 and chimera C6-C8,

sequences shown in Appendix 2.2) fused to Pr1a, a signal peptide that targets the mature protein into the extracellular space in *Nicotiana tabacum*, were synthesized by Integrated DNA Technology (IDT) gBlock ^{TM}. To insert the IDT synthesized fragments into a pDONR vector, PCR using WT or chimeric DNA templates and specific primers with gateway *attB* sites (section 2.4.1) were carried out (see Appendix 5.3 for primer sequences). The PCR products were inserted into gateway pDONR207 vectors using BP clonase (Invitrogen) as described in section 2.3.8.2. The pDONR207 vector plus inserts were transformed into TOP10 *E. coli* competent cells (section 2.3.9), and the positive colonies were selected by colony PCR (section 2.4.2). The inserted chimeric fragments were confirmed by sequencing (section 2.3.10).

The initial WT and chimeric fragments in pDONR207 vectors were used to create additional domain swaps. Part of the wild-type *DsAvr4* and part of a chimeric fragment were amplified from their respective clones in pDONR207 vectors by standard PCR (section 2.4.1). The PCR products were gel purified (section 2.3.5), then 50 ng of each purified PCR product was used in a standard PCR (section 2.4.1) with primers binding to the 5' of the first fragment and the 3' of the second fragment (Figure 2.2). The final PCR products were gel purified and inserted into a Gateway pK2WG7.0 vector (Invitrogen) using Invitrogen LR clonase as described in section 2.3.8.2.

Figure 2.2 Scheme for overlapping PCR used to swap domains between DsAvr4 and CbAvr4 proteins with an example of a chimeric protein in which the domain between C1-C2 has been exchanged.

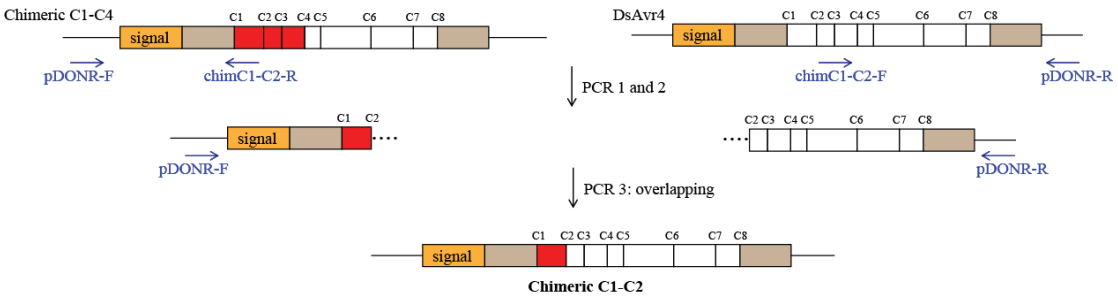

The WT *DsAvr4* and chimeric C1-C4 fragments were synthesized by IDT. The chimeric C1-C4 carries CbAvr4 (*Cercospora beticola*) sequences between cysteine residues C1 and C4 (red boxes) and *DsAvr4* sequences (white boxes). Firstly part of *DsAvr4* WT and part of Chimeric C1-C4 were amplified from respective clones in the pDONR207 vectors. An overlapping PCR was used to construct C1-C2 chimeric fragments.

2.5 Quantitative real time PCR (qPCR)

Appendix 5.4 for real-time PCR primer sequences

2.5.1 PCR conditions

All real-time PCR reactions were carried out using a LightCycler® 2.0 (Roche, Penzberg, Germany) and the data were analysed using RealQuant software. Three technical replicates were used for each strain. The quantitative real time PCR primers were designed using Beacon designer (Premier Biosoft) with the following parameters:

Primer parameter: Annealing Tm: 60°C±2°C

Primer length: 20-22 bp

Product size: 75-200 bp

A standard curve was made for each set of primers used in real-time PCR to calculate the PCR efficiency for that primer set. Six 5-fold serial dilutions of *D. septosporum* NZE10 gDNA or cDNA were used with 3 replicates for each dilution. The PCR efficiency was calculated as $10^{(-1/slope)}$.

The 10 µl PCR mixture contained 1×q•EvaGreen® qPCR master mix (Qarta Bio products, USA), 0.25 µM of each primer and 2 to 100 ng of DNA template. The PCR conditions were: 1 cycle of pre-incubation at 95°C for 15 minutes, 45 cycles of amplification (95°C for 15 seconds, 60°C for 15 seconds and 72°C for 30 seconds) and 1 cycle of cooling at 40°C for 10 seconds. The cycle threshold (Ct) value is used for real-time PCR analysis. The Ct value is defined as the cycle number at which the fluorescence signal crosses the threshold (background level). A Ct ≥ 35 cycles was not considered as positive PCR amplification. For melting curve analysis, the sample mixture was heated to 95°C for 5 seconds, cooled to 65°C for 10 sec and then re-heated to 95°C at the rate of 0.2°C/second with continuous measurement of fluorescence at 520 nm.

2.5.2 Gene expression analyses in gene replacement strains

RNA was extracted as described in section 2.6.1. cDNA was synthesized as described in section 2.6.3 and used in real time PCR as described in section 2.5.1. A constitutively expressed *D. septosporum* NZE10 wild type *β-tubulin* gene was used as a reference. The ratio between the target gene and the reference *β-tubulin* gene was calculated using

Ct values. The gene expression level in KO strain was normalized to WT strain (WT ratio = 1) (Pfaffl, 2001).

For example, to determine the expression of *DsAvr4* in *LaeA* KO strain using *β-tubulin* as the reference gene, the ratio between target gene and the reference gene was calculated using the formula:

$$\text{Ratio} = \frac{(E_{\text{target}})^{\Delta \text{Ct target } (control - sample)}}{(E_{\text{ref}})^{\Delta \text{Ct ref } (control - sample)}}$$

E_{target}: DsAvr4 primer efficiency; E_{ref}: β-tubulin primer efficiency

∆ Ct target (control-sample): Ct of *DsAvr4* in WT-Ct of *DsAvr4* in *LaeA* KO

∆ Ct ref (control-sample): Ct of *β-tubulin* in WT-Ct of *β-tubulin* in *LaeA* KO

2.5.3 Copy number determination in complemented strains

Genomic DNA was extracted as described in section 2.3.1 and 10 ng/µl gDNA was used in real time PCR as described in section 2.5.1. A single copy gene *DsAflR* verified by Southern hybridization was used as a reference gene. The ratio between the target gene and the reference *DsAflR* gene was calculated using Ct values (same formula as above). Any Ct value above 35 cycles was not considered as amplification. The results were normalized to WT strain (WT ratio = 1). A normalized ratio value ≤ 1.5 indicated a single copy of the target gene in the complemented strain (Zhu et al., 2014).

2.6 RNA extraction and manipulation

2.6.1 RNA extraction and DNase treatment

For transcriptome analysis, fresh whole needles or lesions were ground in liquid nitrogen. 100 mg of freshly grounded sample was used for RNA extraction. Three RNA extraction replications were done for each sample. RNA was extracted using a Spectrum™ plant total RNA kit (Sigma-Aldrich USA) according to the manufacturer's instructions. The RNA was first checked on a 1% formaldehyde denaturing gel (Section 2.6.2). For quality control, the RNA integrity was checked with a 2100 bioanalyser (Agilent USA) using an RNA 6000 nano kit (Agilent USA). The concentration of RNA was determined by the Qubit fluorometer (Invitrogen USA) using a Qubit® RNA assay

kit（Invitrogen). The DNA and protein contamination of RNA was checked with a Qubit fluorometer (Invitrogen) using Qubit® dsDNA HS assay kit and Qubit® Protein assay kit (Invitrogen）respectively.

TRIZOL (Invitrogen, Carlsbad, CA, USA) was used to extract RNA from fungal mycelia (Chomczynski and Sacchi, 1987). 0.5 g of snap frozen mycelia (section 2.2.2) were ground to a fine powder in a pre-cooled mortar using liquid nitrogen, then 5 ml of TRIZOL was added to the powder and mixed well. The sample was then transferred to an RNase-free falcon tube (BD Biosciences, USA) for centrifugation at 2880 g (Eppendorf 5810) for 5 min. The supernatant was transferred to a new falcon tube and 4 ml of phenol:chloroform:IAA (25:24:1) added. The sample was mixed by inverting the tube several times then centrifuged at 2880 g (Eppendorf 5810) for 5 min. The supernatant was transferred to a new falcon tube and 4 ml of Chloroform added, then mixed and centrifuged as before. The supernatant was again transferred and 0.5 volumes of isopropanol added. The sample was mixed thoroughly and incubated at -20 ºC for 25 minutes, then centrifuged at 2880 g (Eppendorf 5810) for 5 min. The supernatant was discarded and the pellet was washed with 70% ethanol for 3 times. The pellet was air-dried and resuspended in 50 µl of sterile DEPC-treated MilliQ water.

2.6.2 Formaldehyde gel electrophoresis

For RNA gel electrophoresis, all plastic equipment was treated with 2% H_2O_2 for 15-30 minutes to inactivate RNase, and then rinsed with MQ water. To make the 1.2% formaldehyde gel, 1.8 g of agarose was added to 110 ml of sterile DEPC-treated MilliQ water, then melted and cooled to 60 ºC in a water bath. 15 ml of 10 x MOPS buffer (Appendix 1.3) and 25 ml of 37% formaldehyde (Sigma, Louis, Germany) were quickly added to the agarose before pouring into the gel box. 5 µl of RNA was mixed with the RNA loading buffer (Appendix 1.3) and incubated at 65 ºC for 15 minutes to denature the RNA. The gel was run at 80 V using a mini Sub-cell GT gel box (Bio-Rad Hercules, CA, USA) for 45 minutes. Finally the gel was visualized and photographed using a Gel-Doc™XR documentation system (Bio-Rad, Hercules, CA, USA) and Image Lab™ software.

2.6.3 DNA removal and cDNA synthesis

To remove DNA contamination from RNA samples, the RNA was treated with Turbo DNase, (Life technologies, USA). The cDNA was synthesized using a qScript cDNA synthesis kit (Quanta Biosciences, MD, USA) according to the manufacturer's instructions.

2.7 Southern blotting and hybridization

2.7.1 DIG-labelling of the probes (PCR based)

A PCR based method was used to prepare DIG-labelled probes (see Appendix 5.5 for primer sequences). The PCR mixture was the same as described in section 2.4.1 except for the dNTPs. For DIG-labelling, the DIG-dNTPs mixture contains 0.05 mM each of dATP, dCTP, dGTP, 0.033 mM dTTP and 0.016 mM Digoxigenin-11-2'-deoxy-uridine-5'-triphosphate, alkali-labile (Roche, Penzberg, Germany).

2.7.2 Probe concentration determination

To determine the labelled probe concentration, six serial 5-fold dilutions of probe were made using sterile MilliQ water. Then 2 µl of each dilution was spotted on a Hybond-N^+ membrane (Amersham). The DNA was fixed to the membrane using a UV crosslinker Cex-800 (Ultra-Lum Inc). The hybridization and detection procedure was as described in sections 2.7.4 and 2.7.5. The probe concentration that gave a clear signal was selected for Southern hybridization.

2.7.3 Southern blot

Two µg of each of the restriction endonuclease digested genomic DNA samples were separated on a 0.8% agarose gel at 40 V overnight at 4°C (section 2.3.4 and 2.3.6). The gel was stained in ethidium bromide for 20 minutes, then visualized as described in section 2.3.4 with a ruler alongside. If the gel contained DNA fragments bigger than 5 kb, the gDNA was first depurinated with 0.25 M HCl (Appendix 1.4) for 15 minutes. Then the gel was incubated in denaturation buffer (Appendix 1.4) for 45 minutes followed by neutralization buffer (Appendix 1.4) for 1 hour. Finally the gel was

incubated in 20 x SSC solution (Appendix 1.4) for 20 minutes. To transfer DNA to a membrane, two layers of wet Whatman paper (Whatman, Maidstone, UK) were placed on top of a glass plate over a plastic box containing 20 x SSC buffer, with the edge of the Whatman paper touching the 20 x SSC buffer. The gel was placed upside down on the Whatman paper and membrane on top of the gel. Two pieces of Whatman paper pre wetted in 20 x SSC were placed on the membrane, all bubbles were excluded between each layer. Paper towels were laid on top of the blotting apparatus with a heavy weight and left at room temperature overnight. The membrane was washed in 2 x SSC for 1 minute and fixed under a UV crosslinker Cex-800 (Ultra-Lum Inc). The crosslinked membrane was allowed to air dry and was ready for hybridization.

2.7.4 Hybridization of DIG labelled probe

The membranes were prehybridised in DIG Easy Hyb solution (10 ml/100 cm^2 of membrane; Roche, Penzberg, Germany) at 42°C for 2 hours in a hybridization tube with rotation. The probe was denatured by incubation for 10 minutes in a boiling water bath and immediately chilled on ice. The denatured probe was added to the hybridization buffer and incubated at 42°C overnight with rotation. After overnight incubation, the membrane was washed 2 x 5 minutes in washing solution I (Appendix 1.4) at room temperature, then 2 x 15 minutes in washing solution II (Appendix 1.4) at 68°C. The hybridization buffer with probe was stored at –20°C. To re-use the probe, the mixture was heated at 68°C for 10 minutes and used directly after pre-hybridization.

2.7.5 Immunological detection

To detect the hybridising bands, the membrane was rinsed in buffer I (Appendix 1.4) then incubated in buffer II (buffer I + 1% skim milk) for 30 minutes. Anti-Digoxigenin-AP antibody (1:10000 dilution Roche, Penzberg, Germany) was added to buffer II and incubated for another 30 minutes. Then the membrane was washed 2×15 minutes in buffer I and equilibrated in buffer III (Appendix 1.4) for 5 minutes. The membrane was placed in an A4 copy-safe pocket and CSPD® ready-to-use chemiluminescence substrate (Roche, Penzberg, Germany) was added to the membrane directly. The membrane was incubated at 37°C for 10 minutes to activate the enzyme, then a x-ray film (Fuji film) was exposed to the membrane for 20 minutes to 1 hour.

Finally the x-ray film was developed using a 100 plus Automatic x-ray Processor (All Pro imaging).

2.7.6 Stripping the blot

To re-hybridise the membrane with another probe, the membrane was first washed in MilliQ water for 1 minute and incubated in stripping buffer (Appendix 1.4) at 37°C for 2 x 20 minutes.

2.8 Transformation of *D. septosporum*

2.8.1 Preparation of protoplasts

To grow *D. septosporum* mycelia, 100 µl of 1 x 10^6 spores/ml from a 7 days old culture were inoculated into 30 ml of DM broth in a 125 ml flask. The flask was incubated at 22°C for 7 days with shaking (180 rpm). The *D. septosporum* mycelia were harvested by filtration through a funnel covered with a sterile nappy liner (Johnson and Johnson). The mycelia were washed with sterile MilliQ water then OM buffer (Appendix 1.5) and transferred to a 125 ml conical flask. Then 30 ml of 10 mg/ml Glucanex® 200G (Novozymes) digestion buffer (Appendix 1.5) was added and the flask was incubated at 30°C overnight with shaking at 100 rpm. Protoplast formation was checked under a microscope the next day. Protoplasts were harvested at room temperature by filtering through a sterile nappy liner (Johnson and Johnson) and aliquoted in 5 ml volumes in 15 ml falcon tubes. Two ml of ST buffer (Appendix1.5) was carefully overlaid on top of the protoplast solution and centrifuged at 2880 g (Eppendorf 5810) for 5 min. A white layer of protoplasts formed between the glucanex solution and ST buffer. The protoplasts were removed using a yellow pipette tip and transferred to a new falcon tube. Five ml of STC buffer (Appendix 1.5) was added to the tube and centrifuged at 2880 g (Eppendorf 5810) for 5 min. The STC washing and centrifuge step was repeated 3 times. Finally protoplasts were resuspended in STC buffer to a concentration of 1.25 x 10^8 protoplasts/ml.

2.8.2 Transformation of *D. septosporum*

Protoplasts mediated transformation of *D. septosporum* was performed (Yelton et al., 1984). 5 µg of linearized or 10 µg of circular plasmid was mixed with 80 µl of protoplast suspension and 20 µl of 40% PEG solution (Appendix 1.5) in a microcentrifuge tube and kept on ice for 30 minutes. 900 µl of 40% PEG solution was added to the reaction and incubated at room temperature for 30 minutes. 100 µl of the reaction mixture was mixed with 5 ml of molten RG overlay (Appendix 1.5) kept at 50°C and poured over RG agar plates (Appendix 1.5). The plates were incubated overnight at 22°C. The next day 5 ml of molten 0.8% regeneration overlay, kept at 50°C, with antibiotic was poured over the RG agar plates to make a final concentration of 70 µg/ml hygromycin B (Roche Penzberg, Germany) for gene replacement plates or 7 µg/ml phleomycin (Apollo scientific Ltd, Stockpott, UK) for gene complementation plates. The plates were incubated at 22°C for 3-4 weeks. Undiluted protoplasts were spread on appropriate antibiotic plates as a negative control. Protoplasts transformed with pBC-Hygro (pR223) or pBC-Phleo (pR224) (Appendix 1.5) were spread on appropriate antibiotic plates as positive controls.

2.8.3 Screen for positive transformants

PCR was used to screen for positive colonies (section 2.4.1). Genomic DNA was extracted from colonies as described in section 2.3.1. For gene replacement screening, a pair of primers, of which one primer bound to the genome outside of either the 5' or 3' flanking region of the knockout construct and another primer bound to the GFP-hph cassette were used. For gene complementation screening, primers binding to the coding region of the target gene were used.

2.8.4 Purification of the positive candidates

Positive colonies confirmed by PCR may not be pure or stable. Some transformants only transiently express the selectable marker and use of 40% PEG for protoplast transformation fuses protoplasts and can result in heterokaryotic transformants containing untransformed as well as transformed nuclei. So the positive transformants need to be purified. For purification, two rounds of streaking on appropriate selective plates were done to obtain single spore isolates.

2.9 Phenotypic characterization and pathogenicity assay of *D. septosporum* mutants

2.9.1 Radial growth rate

Five mm diameter mycelia plugs were cut with a sterile cork borer from the edge of an actively growing colony and placed on DM plates. Three plugs were grown on each plate and 3 replicate plates were used for each strain. The plates were incubated at 22°C. Radial colony growth was measured along two axes perpendicular to one another at 1-week intervals for 3 weeks and growth rate calculated as mm/day over this period.

2.9.2 Sporulation assay

To assess sporulation, 50 µl spore suspension (1 x 10^5 spores/ml) were spread over PMMG plates, with 3 replicate plates for each strain. The plates were incubated at 22°C for 7 days. Two ml of sterile MilliQ water was added to each plate and incubated for 10 minutes at room temperature. Spores were collected using a sterile glass spreader. The spore concentration was quantified using a cytometer (Weber Scientific, Middlesex, England) and expressed as spores/ml.

2.9.3 Spore germination rate

To assess germination, spores were collected from 7 days old PMMG plates, resuspended in 1 ml of DSM broth and incubated at 22°C for 12 hours in a 2 ml microcentrifuge tube with shaking at 150 rpm, 3 replicates for each strain. A cytometer was used to count the number of total spores and germinated spores (spores showing visible germ tubes). The spore germination rate was calculated as % of germinated spores/ total spores.

2.9.4 Hydrophobicity assay

To compare the hydrophobicity of colony surfaces, 15 µl of an aqueous 0.2% bromophenol blue solution was placed on the surface of a fungal colony grown on a DM plate. The hydrophobicity was assessed as observing dye dispersal 10 min later.

2.9.5 Spore adhesion test

To assess spore adhesion, 10 µl of spores collected from 7 days old PMMG plates were placed on a cytometer and air dried at room temperature for 1 hour. The number of total spores was counted and the cytometer was washed by agitation under water for 10 min at 90 rpm and washed again with 1 ml of water using a pipette. The spores were counted again after washing. The spore adhesion was assessed as % of spores left on the cytometer after washing.

2.9.6 Pathogenicity assay

An artificial inoculation method was used for pathogenicity assay (Kabir et al., 2013). *D. septosporum* NZE10 spores (1 x10^6 spores/mL) from 7 days old PMMG plates were sprayed on 6 months old *Pinus radiata* clones using a multipurpose hand sprayer. Three replicate trees were used for each strain. The pine seedlings were covered using ventilated plastic bags and placed in a plastic container with two water misters to maintain high humidity under natural light conditions in a glasshouse. After 10–12 weeks all the needles were collected from each seedling. To assess needle blight symptoms, needles were categorized as un-infected (green) and infected (red bands). For each replicate, the percentage of needles showing infection symptoms was calculated as infected needles/total needles. The numbers of lesions per needle was calculated by total number of lesions/ number of infected needles. The lesion size was measured with a ruler and the lesion size was calculated as average lesion size/number of lesions. The data from mean and standard deviations of three replicate samples were used in a two tailed T-test of the significant difference between KO or complement strains to WT strains.

2.10 Agro-infiltration on *Nicotiana tabacum* Plants

2.10.1 Transformation of *A. tumefaciens*

2.10.1.1 Make chemically competent *A. tumefaciens* cells

A single *A. tumefaciens* GV3101 (section 2.1.3) colony was inoculated into 5 ml LB culture using a sterile loop. The LB culture was incubated at 30°C overnight with shaking (180 rpm). 50 µl of the above overnight LB culture was inoculated into 500 ml

LB broth in a flask and incubated at 30°C with shaking (180 rpm) until the OD reading indicated that the LB culture had reached mid-log phase, A_{600} 0.5-1.0. The cells were harvested by centrifugation at 4025 g in F21J-8x50y rotor (Thermo-Sorvall Waltham, Massachusetts, USA) for 10 minutes at 4°C. The supernatant was removed and cells were resuspended in 500 ml of ice cold sterile 0.1 M $CaCl_2$ solution. The cells were incubated on ice for 30 minutes and harvested by centrifugation as before. Finally the cells were resuspended in 2 ml ice cold sterile 0.1 M $CaCl_2$ solution with 10% (v/v) glycerol. Aliquots of 50 µl cells were transferred into a fresh sterile microcentrifuge tube, frozen in liquid nitrogen and stored at -80°C.

2.10.1.2 Transformation of *A. tumefaciens*

50 µl of *A. tumefaciens* chemical competent cells and 5 µl of ligation mixture or 50 ng of plasmid were mixed and incubated on ice for 30 minutes. The mixture was incubated in a 42°C water bath for 1 minute, then immediately chilled on ice for 5 min. 900 ml of LB was added to the mixture and incubated at 30°C for 2 hours. 100 µl of transformation culture was grown on LB plates with selective antibiotics (section 2.2.1) at 30°C for 2 days. The positive colony was screened as described in section 2.4.2.

2.10.2 Agro-infiltration on *Nicotiana tabacum* Plants

N. tabacum plants were obtained by growing from seeds (Tobacco Golden newt, Kings seeds New Zealand). A single colony of *A. tumefaciens* transformed with the appropriate plasmid was inoculated into 5 ml of LB broth with appropriate antibiotics and grown at 30°C overnight with shaking at 180 rpm. The next day 150 µl of the overnight culture was mixed with 4.64 ml LB broth, 100 µl of 100 mM acetosyringone (Sigma-Aldrich, St. Louis, Missouri, USA) solution, 100 µl of 0.5 M MES buffer (Appendix 1.6) and appropriate antibiotics. The mixture was grown at 30°C overnight with shaking at 180 rpm. When the OD_{600} reached 0.4 to 2, the cells were centrifuged at 2880 g (Eppendorf 5810) for 1 min and the pellet resuspended in 20 ml of MMA broth (Appendix 1.6) containing 1 ml/l acetosyringone (Sigma-Aldrich, St. Louis, Missouri, USA). The cells were grown at room temperature for 3 hours and the OD_{600} adjusted to 1.0 for agro-infiltration. The 2 month old *N. tabacum* plants were well watered before agro-infiltration to make sure most of the stomatal pores were open. The lower side of leaves was infiltrated with the 200 µl of *A. tumefaciens* culture using a 1ml syringe.

Positive and negative controls were included for each individual plant to avoid plant to plant variation. The infiltration assay was repeated at least twice for each construct. The plant was incubated in a GMO green house with natural light and a controlled temperature of 20℃ and, 7 days after infiltration, the plants were checked for the presence or absence of a necrosis response and photographed.

2.11 Heterologous production of *D. septosporum* effector protein by *P. pastoris*

2.11.1 Transformation of *P. pastoris*

2.11.1.1 Making competent *P. pastoris* cells

A single *P. pastoris* GS115 (section 2.1.4) colony was inoculated into 5 ml yeast extract peptone dextrose (YPD) (Appendix 1.7) broth using a sterile loop and grown at 30°C overnight with shaking (280 rpm). 0.5 ml of overnight culture was inoculated into 500 ml YPD broth and grown at 30°C with shaking (280 rpm) until the OD_{600} reached 1.3 to 1.5. The cells were harvested by centrifugation at 4025 g in a F21J-8x50y rotor (Thermo-Sorvall Waltham, Massachusetts, USA) for 5 minutes at 4°C. The supernatant was removed and cells were resuspended in 250 ml of ice cold sterile MilliQ water. The cells were harvested by centrifugation as before. The supernatant was discarded and the cells were resuspended in 20 ml ice cold 1 M sorbitol solution (Appendix 1.7). The cells were harvested by centrifugation as before, then the supernatant was removed and the cells were resuspended in 1 ml ice cold 1 M sorbitol.

2.11.1.2 Transformation of *P. pastoris*

5 µg of linearized plasmid was mixed with 80 µl of *P. pastoris* GS115 competent cells in an ice cold 2 mm electroporation cuvette (Thermo fisher Scientific, MA, USA). The cuvette was placed in the Gene Pulser (Bio-Rad Hercules, CA, USA), which was set at a voltage of 1.5 kV. 1 ml of 1 M sorbitol was immediately added to the cuvette after electroporation. The culture was transferred into a sterile microcentrifuge tube and grown at 30°C for 1 hour. The GS115 strain is a histidine auxotroph, the expression vector pPiC9xHis6 (Rooney, 2005) carries a functional histidinol dehydrogenase gene (*his4*) that can complement the GS115 mutation and allows selection of His+ colonies growing on histidine deficient media. 200 µl to 600 µl of transformation culture was

grown on each minimal dextrose-histidine (MD agar plate without histidine) plate (Appendix 1.7) at 30°C for 2 days.

2.11.2 Screen for positive transformants

A single colony growing on a histidine deficient plate was picked up using a sterile loop and resuspended in 10 µl of sterile MilliQ water. Five µl of lyticase (5 unit/µl) solution (Sigma-Aldrich, St. Louis, Missouri, USA) was added to the cell mixture to lyse the *P. pastoris* cells and incubated in a 30°C water bath for 10 minutes. The cell mixture was then immersed in liquid nitrogen for 1 minute. After thawing on ice, the cell culture was centrifuged at 2880 g (Eppendorf 5810) for 1 min to separate *P. pastoris* gDNA from cell debris. 1 µl of supernatant containing gDNA was used as a template in standard PCR (section 2.4.1). *P. pastoris* is capable of metabolizing methanol as its sole carbon source. *AOX1* encodes an alcohol oxidase which is involved in oxidation of methanol to formaldehyde (Ellis et al., 1985). The gene of interest encoding the *D. septosporum* effector was under the control of the *P. pastoris* alcohol oxidase *AOX1* promoter (Tschopp et al., 1987). The presence of *AOX1* sequence in the expression vector could lea,d to recombination at the WT *AOX1* locus in *P. pastori*s which will disrupt WT *AOX1* gene leading to a *P. pastori*s strain that cannot utilize methanol (Mut^S). The PCR-confirmed colonies were then tested for their ability to utilize methanol (Mut^+).

2.11.3 Expression of recombinant proteins in *P. pastoris* strain

Single colonies (His^+ and Mut^+) were inoculated into 25 ml of buffered glycerol-complex broth (BMGY) (Appendix 1.7) and grown at 30°C with shaking (280 rpm) until the OD_{600} reached 2 to 6 (approximate 16-18 hours). To induce protein expression, cells were harvested by centrifugation at 2880 g (Eppendorf 5810) for 5 minutes and resuspended in buffered methanol-complex (BMMY) broth (Appendix 1.7) to an OD_{600} of 1.0. The culture was grown at 30°C with shaking (280 rpm) for 3 days with 0.5% (v/v) methanol added every 24 hours. For collecting the secreted protein, the culture supernatant was collected by centrifugation at 2880 g (Eppendorf 5810) for 5 minutes and stored at -80°C until ready to assay.

2.12 Western blotting

2.12.1 SDS-polyacrylamide gel electrophoresis

A 15% SDS-polyacrylamide gel with 6% stacking gel was prepared in two falcon tubes as follows:

15% separating gel		6% stacking gel	
2.8 ml	MilliQ water	2.9 ml	MilliQ water
3 ml	40% Acrylamide	0.75 ml	40% Acrylamide
2 ml	1.5 M Tris pH8.8	1.25 ml	0.5 M Tris pH6.8
80 µl	10% SDS	50 µl	10% SDS
80 µl	10% APS*	50 µl	10% APS*
8 µl	TEMED*	5 µl	TEMED*

*Note: Ammonium Persulfate (APS) (Thermo fisher Scientific, MA, USA) and Tetramethylethylenediamine (TEMED) (Thermo fisher Scientific, MA, USA) were added just before setting up the gel

A mini-protean II electrophoresis cell system (Bio-Rad, Hercules, CA, USA) was used for SDS-polyacrylamide gel electrophoresis. The gel casting frame and gel box were assembled according to the manufacturer's instructions. Three ml of 15% separating gel was pipetted into the gap between the glass plates. One ml of isopropanol was added to ensure the top of the gel was horizontal. The gel was left to set for 20 minutes. The isopropanol was removed and 1.5 ml of 6% stacking gel was pipetted between the plates. The comb was inserted without air bubbles and the gel was allowed to set for 20 minutes. 15 µl of culture filtrate was mixed with 5x SDS gel loading dye (Appendix 1.8) and denatured in a boiling water bath for 5 minutes**.** The protein samples were loaded onto the gel along with pre-stained broad range protein standard (Bio-Rad, Hercules, CA, USA). The electrophoresis was carried out at 60-90 volts (Mini-PROTEAN II Electrophoresis Cell, Bio-Rad, Hercules, CA, USA) until the dye moved to 1 cm from the end of the gel. The gel was stained with Coomassie Brilliant Blue staining solution (Appendix 1.8) for 15 minutes and washed in destaining solution (Appendix 1.8) for 3-5 hours. Finally the gel was visualized and photographed using a Gel- Doc™XR documentation system (Bio-Rad, Hercules, CA, USA) and Image Lab™ software.

2.12.2 Western blot

The protein samples were separated on the SDS-polyacrylamide gel as described in section 2.12.1 without staining. To transfer the proteins to a membrane, the gel was

placed on top of 2 pieces of Whatman paper (Whatman, Maidstone, UK) pre-wetted in 1x blotting buffer (Appendix 1.8). A nitrocellulose membrane (Bio-Rad, Hercules, CA, USA) was placed on top of the gel and covered with 2 pieces of Whatman paper pre-wetted in 1x blotting buffer. All bubbles were excluded between each layer. The sandwich was placed in a transfer cassette (Hoffer TE22 mighty small transfer tank, Hoffer Holliston, USA) and proteins were transferred to membrane by electro-blotting at 200 mA for 2 hours.

2.12.3 Immunological detection

The membrane was first blocked in Tris-Tween 20 plus 3% skimmed milk (TBST + 3% milk) buffer (Appendix 1.8) for 1 hour at room temperature with gentle agitation. A His_6-FLAG-tag had been fused to the N-terminus of the *D. septosporum* effector (Appendix 2.3). Primary antibody raised in mouse against FLAG-tag was used to detect the *D. septosporum* effector proteins expressed by *P. pastoris*. Horseradish peroxidase conjugated secondary anti-mouse antibody raised in chicken was used to detect the primary antibody. Antibodies were obtained from Sigma-Aldrich (St. Louis, Missouri, USA). For detection the membrane was then incubated with TBST+ 3% milk buffer containing primary antibody (1:2000 dilution) for 2 hours at room temperature with gentle agitation. The membrane was washed 3 x 10 minutes in TBST buffer then incubated with TBST+ 3% milk buffer containing horseradish peroxidase conjugated secondary antibody (1:20,000 dilution Santa Cruz Biotechnology, USA) for 2 hours at room temperature with gentle agitation. The membrane was washed 3 x 10 minutes in TBST buffer. For signal development, the membrane was placed in an A4 copysafe pocket and Chemiluminescent Substrate (Supersignal west dura extended duration substrate, Thermo fisher Scientific, MA, USA) was added to the membrane directly according to the manufacturer's instructions. The membrane was incubated at room temperature for 5 minutes, and then it was exposed to x-ray film (Fuji film) for 1 to 10 minutes. Finally the x-ray film was developed using a 100 plus Automatic x-ray Processor (All Pro imaging).

2.12.4 Vacuum infiltration of *P. pastoris* expressed *D. septosporum* effector proteins on *P. radiata* needles.

Vacuum infiltration was used for *P. pastoris* culture filtrate on pine needles (Liu et al., 2009). Detached *P. radiata* needles were submerged in a 15 ml falcon tube containing 15 ml of *P. pastoris* culture filtrate. A hole on top of the falcon tube cap allowed vacuum infiltration. The falcon tube was placed into a vacuum jar and connected to the vacuum pump. The vacuum pump was turned on for 5 minutes and turned off. The switch of the vacuum jar was slowly released to allow infiltration of *P. pastoris* culture into the needles. The needles were patted dry with tissue and the bottom of the needle was placed inside a wet oasis with the rest of the needle exposed to the air in a plastic container for seven days for symptom development.

2.13 Transcriptome analysis

Three time points of early (fungal network on needle surface and penetration through stomata, 3 weeks post inoculation), mid (early lesions were collected twice at 7 and 8 weeks post inoculation) and late (mature lesions and fruiting bodies collected at 12 weeks post inoculation) were chosen for transcriptome analysis based on a microscope study of *D. septosporum* disease progression on *P. radiata* (Kabir et al., 2015). One *in vitro* sample (FM) was also included and prepared by inoculating 100 µl of 7 days old 1 x 10^6 spores/ml *D. septosporum* spores into 25 ml of DM broth in a 125 ml flask. The culture was grown and harvested as described in section 2.2.2.

RNA of two biological samples for each stage was extracted as described in section 2.6.1. Subsequent library preparation and sequencing was carried out by New Zealand Genomics Ltd. For each sample, a library was made with a unique 6 bp sequence tag. For RNA sequencing, all the libraries were pooled together. An Illumina MiSeq 150 base PE (3 consecutive flow cell runs) was carried out first to determine the ratio of fungal to plant reads for each sample. The result of MiSeq was used as guideline for pooling ratio of libraries for HiSeq to ensure the correct proportions of samples in the mix. An Illumina HiSeq100 base PE (1 lane) followed by 100 base SE (8 lanes) was carried out.

Bioinformatic analysis of the transcriptome was done by Associate Professor Murray Cox and Mr. Andre Sim at Massey University. Illumina Hiseq reads were mapped to the *D. septosporum* genome frozen gene catalog of coding sequences (3/July/2013 frozen gene catalog n=12558; http://genome.jgi-psf.org/Dotse1/) using the Burrows-Wheeler mapping algorithm implemented in Bowtie2 v.2.0.2 (Langmead et al., 2009). Gene expression was calculated as Reads Per Million per Kilobase (RPMK) values (Cox et al., 2010). Statistical significance, accounting for the variance between replicates, was calculated using Fisher's Exact Test as implemented in the R package DEGseq v. 1.14.0 (Wang et al., 2010). A correction for multiple testing was applied using the False Discovery Rate (FDR) approach (Storey and Tibshirani, 2003). The fold difference for each gene *i* was calculated from the raw read counts normalized by the total number of mapped reads as:

$$FD_i = \frac{\max(s_i^1, s_i^2)}{\min(s_i^1, s_i^2)}$$

where *s*1 and *s*2 are temporally adjacent samples (or an *in planta* sample versus an *in vitro* sample). Minimum fold differences are reported for genes with expression in one sample, but zero expression in the other.

Chapter 3. Putative *Cladosporium fulvum* homologous effectors in the New Zealand strain of *Dothistroma septosporum*

3.1 Introduction

The genome of the hemibiotrophic fungus *D. septosporum* (New Zealand strain NZE10) was sequenced by the Joint Genome Institute (USA) as part of the Dothideomycete Comparative Genomics Consortium (DCGC). The *D. septosporum* NZE10 sequence was assembled and annotated using standard JGI procedures. Since many of the *Dothideomycetes* are plant pathogens, a comparative approach to analysing these genomes provides important information in identifying key genes involved in disease development. Classic work with the biotrophic fungus *C. fulvum* and its tomato host identified the molecular basis of how fungal effector proteins can trigger plant host resistance (Thomma et al., *2005*). Homologues of the *C. fulvum avr4, ecp2* and *ecp6* effector genes were found in the genome of banana pathogen *Mycosphaerella fijiensis* (Stergiopoulos et al., *2010*), and their function as triggers of resistance was determined using a tomato system. A phylogenetic study showed that *D. septosporum* is even more closely related to *C. fulvum* than is *M. fijiensis* (de Wit et al., 2012), so the probability of finding functional effectors that might trigger a resistance response in pines is high.

To date, 15 *C. fulvum* effectors have been identified. Of these, 11 of them: CfAvr2, CfAvr4, CfAvr4E, CfAvr5, CfAvr9, CfEcp1, CfEcp2, CfEcp3, CfEcp4, CfEcp5 and CfEcp6 are able to trigger resistance-protein mediated HR in the tomato host through recognition by cognate R proteins (Bolton et al., 2008; de Wit et al., 2009; Joosten et al., 1994; Lauge et al., 2000; Lauge et al., 1997; Luderer et al., 2002; Mesarich et al., 2014; Ökmen et al., 2013; Stergiopoulos et al., 2012; van den Ackerveken et al., 1993; Vankan et al., 1991; Westerink et al., 2004; Yuan et al., 2002). Other *C. fulvum* effectors include CfEcp7, CfEcp13, CfEcp14 and CfTom (Bolton et al., 2008; Ökmen et al., 2013); for these no corresponding host R proteins have been identified so far.

The focus of the work described in this chapter was to identify and characterize putative effectors in the *D. septosporum* NZE10 genome that are homologous to characterized *C. fulvum* effectors.

3.2 Results

3.2.1 Search for putative *C. fulvum* homologous effectors in the *D. septosporum* NZE10 genome

Nine putative effectors were identified in *D. septosporum* using characterized *C. fulvum* effector protein sequences as queries in BlastP analysis against the *D. septosporum* NZE10 genome (http://genome.jgi.doe.gov/Dotse1/Dotse1.home.html). The *D. septosporum* effectors showed 36% to 72% amino acid sequence identify to the *C. fulvum* effectors (Table 3.1). A reciprocal BlastP analysis was performed using putative *D. septosporum* effector protein sequences as queries against the JGI fungal genome database (http://genome.jgi.doe.gov/pages/blast-query.jsf?db=fungi); all of the putative *D. septosporum* effectors showed reciprocal hits to the homologous *C. fulvum* effectors with expectation values ranging from $2E^{-104}$ to $7E^{-19}$ (Table 3.1).

Table 3.1 Characterization of putative effectors in the *D. septosporum* NZE10 genome

Name	JGI Protein ID	Length (aa)	Intron	No. of cys	Signal peptide cleavage site	BlastP best hit; E-value	aa% identity to *C. fulvum*
DsAvr4	36707	146	1	8	between aa 17 and 18: ALA-QP	***CfAvr4 (189855); $2E^{-36}$	51.0%
DsEcp2-1	158381	167	1	5	between aa 18 and 19: SLA-AV	CfEcp2-1 (197200); $9.09E^{-41}$	59.8%
DsEcp2-2**	23431	146	1	6	no signal peptide detected	CfEcp2-2 (193474); $1.21E^{-32}$	46.1%
DsEcp2-3	127671	310	1	5	between aa 18 and 19: GVA-TR	CfEcp2-3 (195482); $2.73E^{-102}$	52.7%
DsEcp4**	192200	123	1	6	between aa 19 and 20: AVA-DP	CfEcp4 (186834); $1E^{-36}$	51.4%
DsEcp5**	69490	147	-	7	between aa 23 and 24: IIA-ES	CfEcp5 (CAC01610)*; $7E^{-19}$	36.1%
DsEcp6	46236	228	1	9	between aa 17 and 18: VNG-FV	CfEcp6 (189398); $2E^{-104}$	65.9%
DsEcp13	90760	74	1	10	between aa 15 and 16: AKA-AV	CfEcp13 (188477); $2E^{-21}$	47.4%
DsEcp14	71428	209	1	12	between aa 19 and 20: AKA-SP	CfEcp14 (93467); $3.43E^{-70}$	72.2%

Note:

* *C. fulvum* Ecp5 was not predicted by JGI gene prediction tools, so the accession number is from NCBI Genbank.

**: Pseudogene with internal stop codon in coding region of the gene.

****Cf: Cladosporum fulvum*. Numbers in brackets are JGI protein identification numbers and NCBI Genbank (only Ecp5).

Signal peptide cleavage site was predicted using SignalP 4.0 (Petersen et al., 2011).

3.2.2 *In planta* transcriptome analysis of putative effectors in *D. septosporum*

An *in planta* transcriptome time-course assay of *D. septosporum* on clonal *P. radiata* seedlings was done (section 2.13). The clonal 3/1 and 3/2 susceptible seedlings were used to avoid host genotype effects. Three time points of early (fungal network on needle surface and penetration through stomata), mid (early lesions) and late (mature lesions and fruiting bodies) were chosen based on a microscope study of *D. septosporum* disease progression on *P. radiata* (Kabir et al., 2015). One *in vitro* sample (FM) was also included. The percentage of fungal reads mapped to the *D. septosporum* genome were 0.1%, 0.5%, 17.1% and 99.8% for early, mid, late and FM samples respectively. With the exception of *DsEcp2-1* and *DsEcp6*, the *in planta* expression of putative *D. septosporum* effectors was low (Table 3.2). Both *DsEcp2-1* and *DsEcp6* were highly up regulated by 31 fold and 104 fold respectively at the mid (early lesion) stage of disease progression compared to *in vitro* (FM). No expression was detected for *DsEcp4*. Even though their expression levels were low, *DsEcp5* and *DsEcp2-2* were expressed both *in vitro* and *in planta*. This suggests that truncated forms of DsEcp2-2 and DsEcp5 might be produced by *D. septosporum*. *DsEcp2-3* showed an 29 fold increase in mid infection stage compared to *in vitro* and *DsEcp13* showed an 11 fold increase in late infection stage compared to *in vitro*. However the functions of Ecp2-3 and Ecp13 are not known. It will be interesting to test whether DsEcp2-3 and DsEcp13 have roles during necrotrophic infection stages of *P. radiata*. Targeted gene knockouts could be used to test if DsEcp2-3 and DsEcp13 are virulence factors.

To data, all the *C. fulvum* effectors identified are small (less than 300 amino acid), cysteine rich (more than four cysteine residues), secreted (signal peptide) proteins that are highly expressed *in planta*. Using those parameters, more than one hundred secreted small cysteine rich proteins (SSCP) were identified in the *D. septosporum* NZE10 genome (de Wit et al., 2012). The expression of those candidate effector genes was analysed using transcriptome data. Two genes *Ds69335* and *DsHdp1* (JGI: 75009), which encode small secreted cysteine rich proteins, showed high *in planta* expression (Table 3.2). *Ds69335* was the 39th mostly highly up-regulated at early infection stage compared to *in vitro* (FM) (Bradshaw et al., 2015). *DsHdp1* encodes a class I hydrophobin. These two genes were selected for further analysis.

Table 3.2 *In planta* transcriptome analysis of putative *D. septosporum* effectors

JGI protein ID	Name	FM_RPMK	E_RPMK	M_RPMK	L_RPMK
36707	DsAvr4	1.09	0.00	13.82	2.13
158381	DsEcp2-1	1.31	7.74	243.56	17.91
23431	DsEcp2-2	29.84	14.17	50.02	18.32
127671	DsEcp2-3	1.43	2.09	41.18	6.83
69490	DsEcp5	8.35	7.14	8.4	25.28
46236	DsEcp6	47.05	5.86	606.34	171.38
90760	DsEcp13	5.37	2.21	34.47	58.69
71428	DsEcp14	3.17	0.00	9.18	5.66
69335	Ds69335*	425.93	1448.26	1012.5	553.55
75009	DsHdp1*	9234.4	455.07	6493.99	4861.6

FM: *In vitro* sample collected from 7 days old mycelium grown in DM broth

Early: fungal network on needle surface and penetration through stomata pore

Mid: early lesions

Late: late lesions and fruiting bodies

*: Two effector candidates which are small cysteine rich secreted proteins that are highly expressed *in planta*.

Two biological samples for each stage were used for *in planta* transcriptome analysis. Illumina Hiseq reads were mapped to the *D. septosporum* genome frozen gene catalog (gene coding sequences). Gene expression was calculated as Reads Per Million per Kilobase (RPMK) values (bioinformatic analysis of the transcriptome was done by Associate Professor Murray Cox and Mr. Andre Sim at Massey University). The expression of *D. septosporum* effectors was low *in planta*, except for *DsEcp2-1* and *DsEcp6* which were highly expressed at mid stage of infection *in planta*. *DsEcp4* was not expressed either *in vitro* or *in planta*. *DsEcp2-2* and *DsEcp5* which also encode pseudogenes with internal stop codons showed expression both *in vitr*o and *in planta*, however the expression level was low. This suggested that truncated forms of DsEcp2-2 and DsEcp5 might be produced. The two effector candidates *DsHdp1* and *Ds69335* are highly expressed *in planta*.

3.2.3 Core effectors identified in the *D. septosporum* NZE10 genome

CfAvr4, CfEcp2 and CfEcp6 homologues have been identified in other pathogenic species (de Jonge and Thomma, 2009; Marshall et al., 2010; Stergiopoulos et al., 2010). They are defined as core effectors that have conserved biological functions to facilitate the infection of various fungi on different host species (Stergiopoulos et al., 2010). These core effectors were identified in *D. septosporum* and the gene models of *DsEcp2-1* and *DsEcp6* were confirmed by cDNA sequencing. Due to low expression levels of *DsAvr4* and *DsEcp2-3 in vitro* and *in planta*, cDNA could not be amplified by PCR for those two genes. The EST data (short single-read transcript sequences) used for genome assembly and transcriptome analysis was used to predict the positions of introns for *DsAvr4*, *DsEcp2-1*, *DsEcp2-2*, *DsEcp2-3* and *DsEcp6*. The predicted translations of

DsAvr4, *DsEcp2-1*, *DsEcp2-2*, *DsEcp2-3* and *DsEcp6* are shown in Appendix figure 3.1.

3.2.3.1 *D. septosporum Avr4* (*DsAvr4*)

DsAvr4 has an open reading frame (ORF) of 498 nucleotides (nt) with one intron and encodes a protein of 146 amino acid residues with a 17 amino acid N-terminal signal peptide. Alignment of mature Avr4 amino acid sequences from Dothideomycete fungi showed that DsAvr4 has 8 conserved cysteine residues with the same positioning and spacing as seen in CfAvr4. In CfAvr4, 3 disulfide bonds (C1-5, C4-8 and C6-7) are required for protein stability. A chitin binding domain that contained all the conserved amino acid residues involved in chitin binding (Mesarich et al., 2015) was identified between cysteine residues C6 (Cys102) and C7 (Cys114) in DsAvr4 (Figure 3.1B).

Apart from DsAvr4, homologues of CfAvr4 have been identified in several other Dothideomycete fungi such as *Mycosphaerella fijiensis* (MfAvr4) that causes black leaf streak of banana, four *Cercospora* species (*C. apii* (CaAvr4), *C. beticola* (CbAvr4), *C. nicotianae* (CnAvr4) and *C. zeina* (CzAve4)) that cause leaf spot disease of celery, sugar beet, tobacco and maize respectively (de Wit et al., 2012; Stergiopoulos et al., 2010) and two *Septoria* species (*S. musiva* (SmAvr4) and *S. populicola* (SpAvr4)) that cause leaf spot and stem canker of poplar (Feau et al., 2010). DsAvr4 showed the highest (51%) amino acid identity to *C. fulvum* Avr4 (CfAvr4) compared to other Avr4 homologues (Figure 3.1B). A phylogenetic tree was constructed using predicted amino acid sequences of Avr4 homologues and showed that DsAvr4 clusters with CfAvr4 and MfAvr4 while *Septoria* and *Cercospora* Avr4s form a different clade (Figure 3.1A).

Figure 3.1 Phylogenetic analysis and amino acid alignment of Avr4 homologues from Dothideomycete fungi

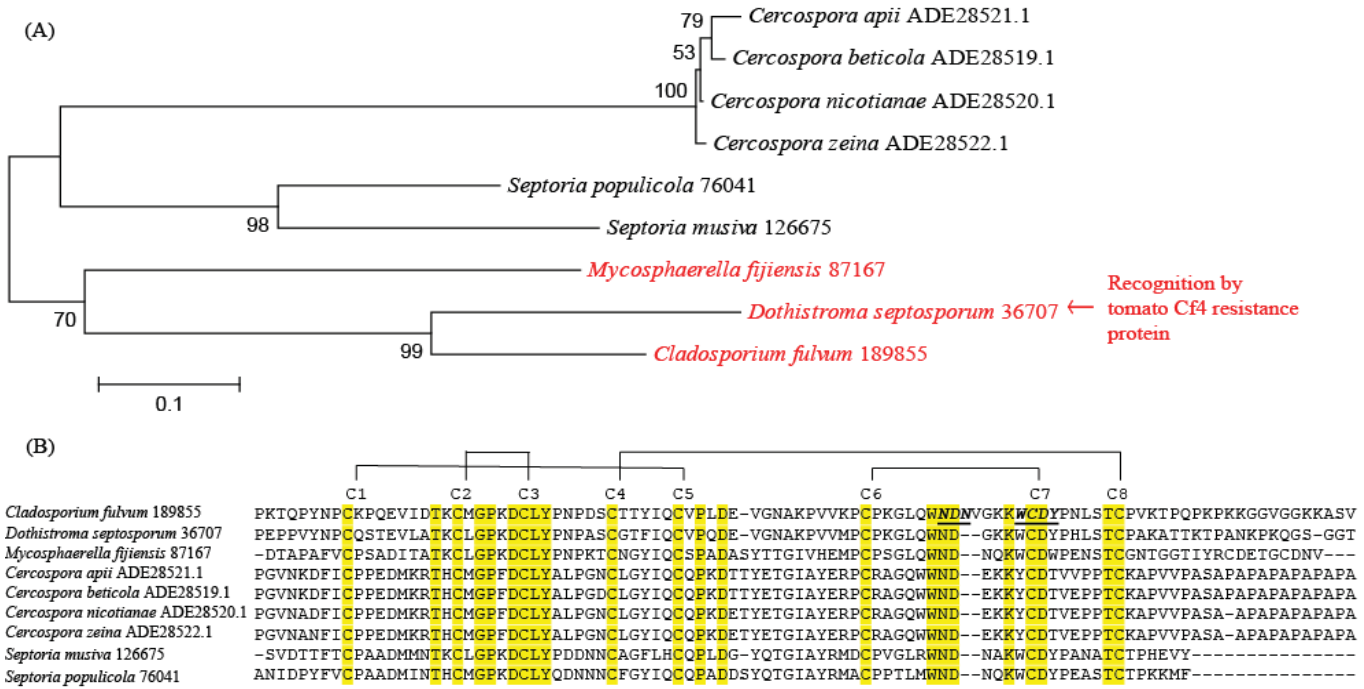

(A) A neighbor-joining tree of Avr4 homologues from Dothideomycete fungi. Bootstrap values are shown at the nodes as percentages. *C. fulvum* Avr4 (CfAvr4, JGI:189855), *M. fijiensis* Avr4 (MfAvr4, JGI:87167) and *D. septosporum* Avr4 (DsAvr4, JGI:36707) which are recognized by the tomato Cf4 resistance protein are clustered together, while the *Cercospora* spp. Avr4 proteins (NCBI: ADE28521.1, ADE28519.1, ADE28520.1 and ADE28522.1), which are not recognized by Cf4, form another cluster with *Septoria* spp. Avr4 (JGI: 76041 and 126675). (B) Amino acid alignment of the disulfide-bonded core region of mature Avr4 proteins from Dothideomycete fungi. Identical amino acids are highlighted in yellow and the eight conserved cysteine residues are indicated on top of the alignment. The positions of four disulfide bonds experimentally determined for CfAvr4 (van den Burg et al., 2001), but predicted for the other Avr4s, are indicated with black lines. Amino acid residues involved in chitin binding in CfAvr4 are indicated in underlined bold italic letters.

3.2.3.2 *D. septosporum Ecp6* (*DsEcp6*)

DsEcp6 has an ORF of 739 bp with one intron and encodes a protein of 227 amino acid residues that showed 65.9% amino acid identity to CfEcp6 (JGI: 189398) (Table 3.1). A neighbor-joining phylogenetic tree of Ecp6 homologues from fungi showed that DsEcp6 and CfEcp6 form a cluster with bootstrap value of 86% (Appendix figure 3.2A). CfEcp6 is predicted to have 5 N-glycosylation sites, however DsEcp6 is predicted to have only 4 N-glycosylation sites, 2 of which showed conserved positions as seen in CfEcp6 (Appendix figure 3.2B).

The crystal structure of CfEcp6 suggests that it has 3 extracellular lysin motifs (LysM) that all bind chitin (Sanchez-Vallet et al., 2013). Two other LysM effectors (Mg3LysM and Mg1LysM) have been identified in the wheat pathogen *Zymoseptoria tritici* which have three and one LysM motifs respectively. Both of these LysM effectors can bind chitin and protect fungal hyphae tips against host enzymes, but only Mg3LysM can inhibit chitin-triggered immunity in the host (Marshall et al., 2011). BlastP analysis revealed that DsEcp6 has three LysM motifs which showed a high percentage of amino acid identity of 68.2%, 60% and 77.3% to the corresponding CfEcp6 LysM motifs respectively (Figure 3.2B). A phylogenetic tree of LysM motifs from CfEcp6, DsEcp6 and two MgLysM effectors showed that LysM 1, 2 and 3 of DsEcp6 form three distinct clusters with the corresponding LysM 1, 2 and 3 of CfEcp6 and Mg3LysM (Figure 3.2C). Homology modelling of DsEcp6 using Phyre2 (Kelley and Sternberg, 2009) suggested that all LysM motifs of DsEcp6 showed a classic βααβ fold in which two α-helices are packed against one side of a two-stranded antiparallel β-sheet. DsEcp6 is predicted to contain three chitin binding sites, one in each of LysM motifs 1, 2 and 3 (Figure 3.2A).

Figure 3.2 Predicted DsEcp6 protein structure and Ecp6 LysM motifs alignment and phylogeny

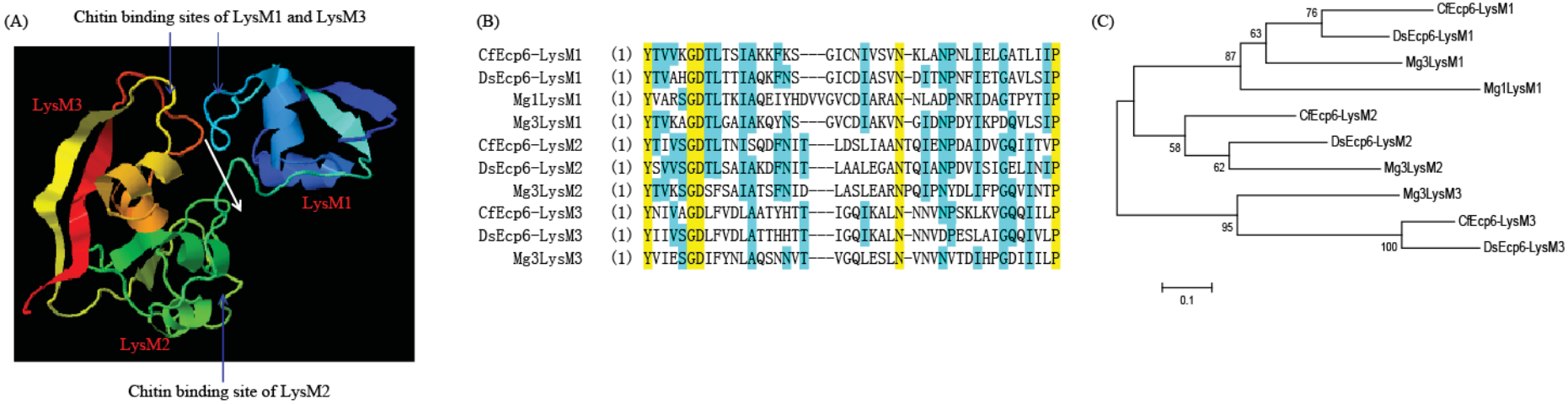

(A) 3D structure of DsEcp6 predicted using Phyre2 (Kelley and Sternberg, 2009). Three lysM motifs are labelled in blue (LysM1), green (LysM2) and yellow (LysM3). The twists and arrows indicate the positions of α helices and β sheets. The blue arrows indicate the predicted chitin binding sites in LysM1, 2 and 3. (B) Amino acid alignment of LysM domains from CfEcp6, DsEcp6 and two MgLysM effectors. Amino acid residue conservation is highlighted in yellow (100% conserved) or in blue (partially conserved). (C) A neighbor-joining tree of LysM motifs from CfEcp6, DsEcp6 and two MgLysM effectors. The bootstrap values are shown at the nodes as percentages. DsEcp6 LysM 1, 2 and 3 form 3 distinct clusters with the corresponding LysM 1, 2 and 3 of CfEcp6 and Mg3LysM.

3.2.3.3 *D. septosporum Ecp2* (*DsEcp2*)

Extracellular protein Ecp2 was first identified as a virulence factor in *C. fulvum* (Lauge et al., 1997). Genome annotation of *C. fulvum*, *M. fijiensis* (banana pathogen) and *Z. tritici* (wheat pathogen) revealed another two *Ecp2*-like genes named *Ecp2-2* and *Ecp2-3* in each genome (the original *Ecp2* was renamed *Ecp2-1*) (de Wit et al., 2012; Stergiopoulos et al., 2010). *CfEcp2-2* is a pseudogene (Stergiopoulos et al., 2012). Three *Ecp2* like genes *DsEcp2-1*, *DsEcp2-2* and *DsEcp2-3* were identified in the *D. septosporum* NZE10 genome. *DsEcp2-2* (JGI: 23431) is thought to be a pseudogene with one internal stop codon (Appendix figure 3.1). *D. septosporum* Ecp2-1, Ecp2-2 and Ecp2-3 showed predicted amino acid identities of 59.8%, 46.1% and 52.7% to CfEcp2-1, CfEcp2-2 and CfEcp2-3 respectively. *Ecp2-1*, *Ecp2-2* and *Ecp2-3* orthologues in *D. septosporum*, *C. fulvum* and *M. fijiensis* and *Ecp2-1* from *Z. tritici* each have an intron of approximate equivalent length in the same position (starts just after the third cysteine residue) (data not shown) (Stergiopoulos et al., 2010). The conserved intron suggests a common evolutionary origin for all these genes. A phylogenetic tree was made using Ecp2-1 Ecp2-2 and Ecp2-3 amino acid sequences. DsEcp2-1 appears to be more closely related to MfEcp2-1 than to CfEcp2-1. DsEcp2-2 and DsEcp2-3 form clusters with CfEcp2-2 and CfEcp2-3 respectively.

Figure 3.3 Phylogenetic analysis of Ecp2-1 Ecp2-2 and Ecp2-3 from fungi

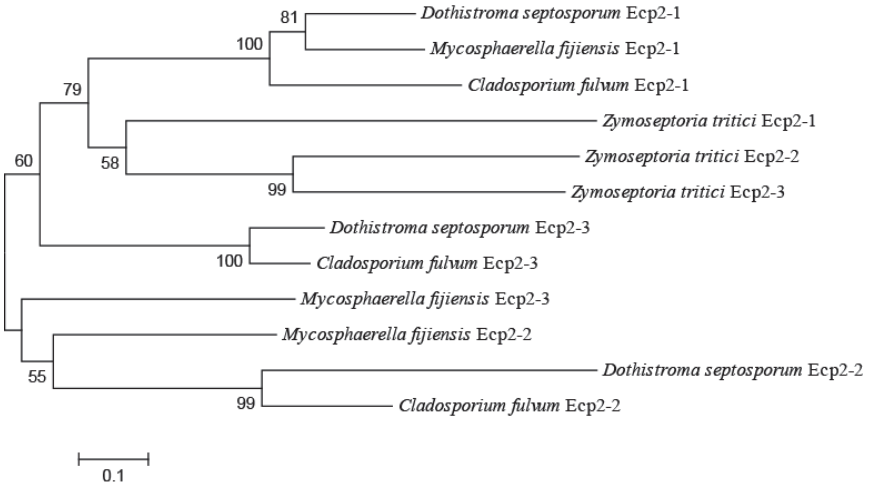

A neighbor-joining tree of Ecp2 from *C. fulvum* Ecp2-1 (CfEcp2-1, JGI: 197200), Ecp2-2 (JGI:193474), Ecp2-3 (JGI:195482), *M. fijiensis* Ecp2-1 (MfEcp2-1, JGI: 52972), Ecp2-2 (JGI:60658), Ecp2-3 (JGI:198160), *Z. tritici* Ecp2-1 (Mg Ecp2-1, JGI:104404), Ecp2-2 (JGI:107904), Ecp2-3 (JGI:111636) and *D. septosporum* Ecp2-1 (DsEcp2-1, JGI:158381) Ecp2-2 (JGI:71206), Ecp2-3 (JGI:99344). The bootstrap values are shown at the nodes as percentages. DsEcp2-1 is closely related to MfEcp2-1. DsEcp2-2 and DsEcp2-3 are closely related to CfEcp2-2 and CfEcp2-3 respectively.

3.2.4 Non-core effectors identified in the *D. septosporum* NZE10 genome

Based on their amino acid identity to the corresponding *C. fulvum* Ecp (extracellular protein) effectors, four other predicted *Ecp* genes were identified in *D. septosporum*: *DsEcp4*, *DsEcp5*, *DsEcp13* and *DsEcp14*. The cDNA sequences of those Ecp genes were confirmed using RNA-seq data as mentioned in section 3.2.3 due to low expression level both *in vitro* and *in planta*. Predicted translations of *DsEcp4*, *DsEcp5*, *DsEcp13* and *DsEcp14* are shown in Appendix figure 3.3. *DsEcp4* and *DsEcp5* are pseudogenes with 1 and 2 internal stop codons respectively (Figure 3.4A, B). *DsEcp13* has an ORF of 291 bp with 1 intron. Amino acid alignments showed that all 10 cysteine residues of DsEcp13 have conserved positions compared to those of CfEcp13 (Figure 3.4C).

DsEcp14 has an ORF of 688 bp with 1 intron. DsEcp14 showed very high amino acid identity of 72.2% to CfEcp14. Another two *Ecp14* genes were identified in *Z. tritici*; based on their amino acid identities to CfEcp14, these two proteins were named MgEcp14 and MgEcp14-2. MgEcp14 and MgEcp14-2 showed high amino acid identity to each other of 74.5% but low amino acid identity to DsEcp14 and CfEcp14 of about 28.8% to 34%. Amino acid alignments showed that 12 cysteine residues of CfEcp14, DsEcp14, MgEcp14 and MgEcp14-2 have conserved positions (Figure 3.4D). Both CfEcp13 and Ecp14 are able to trigger necrosis response in wild tomato species, but no corresponding resistance proteins were identified in the host (de Wit, personal communication).

Figure 3.4 Amino acid alignments of Ecp4, Ecp5, Ecp13 and Ecp14

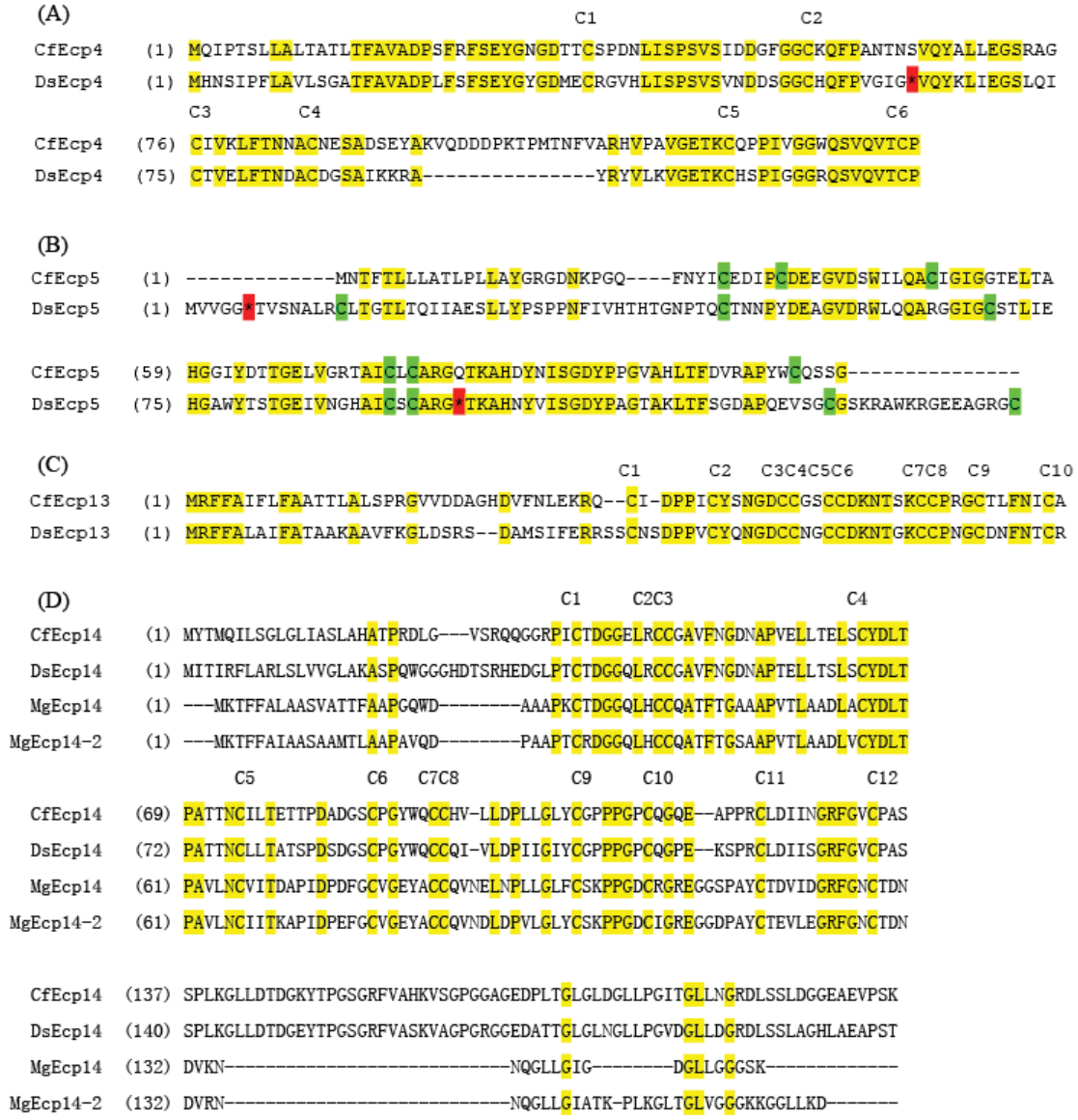

Conserved amino acids are highlighted in yellow. Conserved cysteine residues are written on top of the alignment. Internal stop codons are highlighted in red. (A) Amino acid alignment of DsEcp4 and CfEcp4. (B) Amino acid alignment of DsEcp5 and CfEcp5. Only three cysteine residues aligned in DsEcp5 and CfEcp5. The cysteine residues are highlighted in green. (C) Amino acid alignment of DsEcp13 and CfEcp13. (D) Amino acid alignment of DsEcp14, CfEcp14, MgEcp14 and MgEcp14-2.

From genome annotation and transcriptome data analysis, two highly expressed small cysteine rich secreted proteins *DsHdp1* and *Ds69335* were identified (section 3.2.2). *DsHdp1* has an ORF of 432 bp with two introns and is predicted to encode a protein of 109 amino acid residues. A hydrophobin-2 motif was identified in DsHdp1, which suggested that *DsHdp1* might be a hydrophobin gene (functional analysis of DsHdp1 is described in Chapter four). Ds69335 has an ORF of 894 bp with one intron and is

predicted to encode a protein of 280 amino acid residues. Blastp results showed that Ds69335 belongs to the SCP/TAPS (Sperm-Coating Protein/Tpx-1/Ag5/PR-1/Sc7) superfamily. The gene model of *DsHdp1* and *Ds569335* were confirmed by cDNA sequencing. The predicted translations of *DsHdp1* and *Ds569335* are shown in Appendix figure 3.3.

3.3 Discussion

3.3.1 Putative effectors identified in the *D. septosporum* NZE10 genome

In plant-pathogen interactions, there is a constant arms race between pathogen effectors and host resistance proteins; the pathogen is under selective pressure to avoid recognition by the host, leading to diversified effector sequences. However, effector orthologues were identified in the closely related pathogens *C. fulvum* and *D. septosporum* (de Wit et al., 2012). To date, *D. septosporum* was shown to carry the highest number of *C. fulvum* effector homologues of any other fungus. However several characterized *C. fulvum* effector genes, such as *Avr4E, Avr9* and *Avr5,* appear to be missing from the *D. septosporum* genome. At least two possibilities could cause the absence of those *C. fulvum* effectors from *D. septosporum*. First, some effectors show high host specificity (Ma, 2014). *C. fulvum* and *D. septosporum* have very different hosts, so the missing *C. fulvum* effector homologues might be host specific effectors that were lost in *D. septosporum*. Second, effectors which do not have an essential role in virulence can often be lost without significant impact on pathogen virulence (Dangl et al., 2013). For example some natural strains of *C. fulvum* were shown to have deletions of *Avr4E, Avr9* and *Avr5* (Stergiopoulos et al., 2007; van den Ackerveken et al., 1992; Westerink et al., 2004). However the presence of *C. fulvum* effectors was only searched in the New Zealand *D. septosporum* strain, it is possible that other *D. septosporum* strains from the global collection contain the missing *C. fulvum* effectors. More *D. septosporum* strains should be used to test the presence of *C. fulvum* effectors (The presence of *Avr2*, *Avr4E* and *Avr9* were tested in a Guatemala strain and the results are discussed in Chapter 6).

Two effector homologue pseudogenes, *DsEcp4* and *DsEcp5*, are present in *D. septosporum*. It is possible that R proteins that recognize DsEcp4 and DsEcp5 occur in pine species and that mutants of *DsEcp4* and *DsEcp5* have been selected for in the pathogen population. Pathogens can mutate or delete effectors to avoid R protein mediated HR in the host (Anderson et al., 2010). As mentioned above, it is likely that DsEcp4 and DsEcp5 are not key virulence factors when infecting pine. Thus an evolutionary arms race between *D. septosporum* and pine may have led to pseudogenization of *DsEcp4* and *DsEcp5* to avoid R protein mediated HR in pine.

3.3.2 *In planta* transcriptome analysis of putative *D. septosporum* effectors

DsEcp2-1 and *DsEcp6* are highly expressed *in planta* (Table 3.2). This result suggested that *DsEcp2-1* and *DsEcp6* may be required for virulence during infection of pine. Other studies showed that effectors are up-regulated *in planta* (Bolton et al., 2008; Marshall et al., 2011; Whisson et al., 2007). For example, *CfEcp2-1* is highly expressed *in planta* (van den Ackerveken et al., 1993). Deletion of *CfEcp2-1* led to reduced fungal biomass in infected tomato leaves, indicating that CfEcp2-1 is a virulence factor (Lauge et al., 1997). *CfEcp6* is also highly expressed *in planta* with highest expression at mid-infection stage on host. Silencing of *CfEcp6* led to significant reduction in leaf colonization on tomato plants (Bolton et al., 2008). Another two chitin binding effectors *Mg1LysM* and *Mg3LysM* from the hemibiotrophic fungus *Z. tritici* were also strongly transcriptionally up-regulated during the symptomless leaf infection stage. Deletion of *Mg1LysM* did not affect pathogen virulence, however, deletion of *Mg3LysM* led to significant reduction in leaf colonization and lesion formation on wheat plants, suggesting a role in virulence for this effector (Marshall et al., 2011).

Although *DsEcp2-1* and *DsEcp6* are highly expressed *in planta*, other *D. septosporum* putative effectors (*DsAvr4*, *DsEcp2-3*, *DsEcp13* and *DsEcp14*) are not. This could be due to the presence of R proteins in pine that recognize those effectors. To avoid R protein mediated HR, the evolutionary arms race between *D. septosporum* and pine may have led to silencing of those *D. septosporum* effector genes. In *Phytophthora sojae*, the effector Avr1c protein is recognized by soybean R protein Rps1c. Several *P. sojae* strains contain a single copy of the *Avr1c* gene, however no expression of the gene was

detected and those *P. sojae* strains do not trigger Rps1c mediated HR (Na et al., 2014). Another *P. sojae* effector, Avr3a, is recognized by R protein Rps3a. *P. sojae* strains with low levels of *Avr3a* expression do not trigger Rps3a mediated HR. The virulent *P. sojae* strain contains abundant levels of a 25 bp small RNA molecule which leads to transgenerational gene silencing of *Avr3a* (Qutob et al., 2013).

Transcriptome data was used to select new effector candidates in previous work. For example, examination of the transcriptome profiles using *M. oryzae* infected rice leaves revealed more than six thousand *in planta* expressed genes including 851 SSCPs in *M. oryzae*. Transient expression of selected up-regulated effector candidates in the host identified 5 effectors that trigger cell death in rice (Chen et al., 2013). Two highly expressed genes *Ds69335* and *DsHdp1* were selected on the basis of the *D. septosporum* transcriptome results for further analysis.

3.3.3 Identification of core putative effectors in the *D. septosporum* NZE10 genome

Phytopathogenic bacteria and oomycete secreted effectors can be identified on the basis of features specific to those groups of organisms. Phytopathogenic bacterial effector proteins are delivered into host cells through a bacterial type III secretion system (Alfano and Collmer, 2004) and oomycete effector proteins share a conserved RXLR-ERR motif (Birch et al., 2008). Fungal effectors are highly divergent and generally only facilitate virulence on specific hosts, however several core fungal effectors, such as Avr4, Ecp2 and Ecp6, have been identified that show conserved sequences and biological functions on un-related hosts (de Jonge and Thomma, 2009; Marshall et al., 2010; Stergiopoulos et al., 2010).

DsAvr4 could be a functional orthologue of CfAvr4. Amino acid alignment showed that DsAvr4 has conserved cysteine residue positions to CfAvr4. Moreover, like CfAvr4, a chitin binding domain was also predicted in DsAvr4. The CfAvr4 chitin binding domain was shown to bind to fungal cell wall chitin and protect the fungal invading hyphae from plant chitinase enzymes (van den Burg et al., 2006). Cysteine residues are important for CfAvr4 function. Six out of eight cysteine residues (except Cys2-Cys3) that form 3 disulfide bonds in CfAvr4 are required for protein stability. Natural isoforms of CfAvr4 that carry Cys to Tyr substitution led to either loss of virulence or

reduced virulence in the host (van den Burg et al., 2003). It has been demonstrated that DsAvr4, CfAvr4 and MfAvr4 are recognized by the tomato Cf4 resistance protein. Agrobacterium mediated infiltration of DsAvr4, CfAvr4 and MfAvr4 with Cf4 on *Nicotiana benthamiana* leaves led to Cf-4-mediated HR (de Wit et al., 2012; Stergiopoulos et al., 2010) while *C. apii* (CaAvr4) and *C. beticola* (CbAvr4) Avr4 failed to do so (Mesarich et al., *unpublished*). Together these data suggest that DsAvr4 could be a functional orthologue of CfAvr4.

DsEcp6 showed high amino acid identity and conserved tertiary protein structure to CfEcp6, suggesting that DsEcp6 could be a functional orthologue of CfEcp6. To date, Ecp6 has been found abundantly in other fungal species. More than 400 LysM containing proteins were identified from 56 fungal species (Akcapinar et al., 2015; de Jonge and Thomma, 2009). Those LysM motifs were classified into 5 groups, in which the largest group (group-1) of proteins contains only LysM motifs but no other characterized functional domains; CfEcp6 belongs to this group. 23% of group-1 proteins have a signal peptide for secretion. Multiple sequence alignment showed that in most fungal LysM motifs the first (N-terminal) 16 amino acid residues are more conserved than the ten amino acid residues towards the C-terminus of the motif (de Jonge and Thomma, 2009). The number of LysM motifs and the tertiary structure are important for Ecp6 function. For example, *Z. tritici* LysM effector Mg3LysM, which has a conserved number of LysM motifs and conserved structure to CfEcp6, is able to bind chitin and avoid chitin-triggered immunity, while *Z. tritici* Mg1LysM that has only 1 LysM motif is able to bind chitin but cannot avoid chitin triggered-immunity in the host (Marshall et al., 2011).

Ecp2-1 was identified in biotrophic (*C. fulvum*) and hemibiotrophic (*M. fijiensis, Z. tritici* and *D. septosporum*) fungi (de Wit et al., 2012; Stergiopoulos et al., 2010). Amino acid alignment and phylogenetic analysis showed that DsEcp2-1 is more closely related to MfEcp2-1 than to CfEcp2-1. It was expected that DsEcp2-1 would act like MfEcp2-1, however unlike MfEcp2-1 which can trigger necrosis on tomato plants in the absence of Cf-Ecp2 (R protein) (Stergiopoulos et al., 2010), DsEcp2-1 cannot trigger necrosis in the absence of Cf-Ecp2 in tomato plants (de Wit et al., 2012). Mutations in amino acid sequences could have arisen in DsEcp2-1 that abolished interaction with a host plant target.

In summary homologues of nine *C. fulvum* effector genes were present in the *D. septosporum* New Zealand genome. Three *D. septosporum* effector genes *DsEcp2-2*, *DsEcp4* and *DsEcp5* are pseudogenes that contain internal stop codons. Functional domains were identified in *D. septosporum* core effectors: DsAvr4 contains a chitin binding domain and DsEcp6 contains three LysM motifs which were shown to be involved in chitin binding in CfEcp6 (Sanchez-Vallet et al., 2013). Transcriptome analysis showed that, out of nine *D. septosporum* effectors, only *DsEcp2-1* and *DsEcp*6 are highly expressed *in planta,* suggesting that *DsEcp2-1* and *DsEcp6* may be functional orthologues of *CfEcp2-1* and *CfEcp6*. Two other effector candidates which are also cysteine rich small secreted proteins were shown to be highly expressed *in planta* using transcriptome data.

Chapter 4. Characterization of a highly-expressed hydrophobin gene in *D. septosporum*

4.1 Introduction

Small secreted proteins produced by pathogenic fungi have important roles in host-pathogen interactions (Stergiopoulos and de Wit, 2009; Wösten, 2001). One group of secreted fungal proteins are effectors which are shown to manipulate host physiology to allow infection (detailed discussion in Chapter 1 section 1.3). Another group of secreted proteins are hydrophobins which show similar structures to common types of apoplastic effectors in that they are cysteine rich small secreted proteins, and are produced only by filamentous fungi (Wessels, 1994). Like effectors, some hydrophobins are required by fungi for establishment of disease in the host (Hektor and Scholtmeijer, 2005; Wösten, 2001). The *D. septosporum* hydrophobin gene *Hdp1* was very highly expressed *in planta*, thus it was considered to be a possible virulence factor. The role of *D. septosporum* hydrophobins is discussed in this chapter

4.1.1 Class I and Class II hydrophobins

Based on solubility of the complex formed by hydrophobin monomers, hydrophobins are grouped into two classes (Wessels, 1994). Class I hydrophobins are more stable and only soluble in strong acid such as trifluoroacetic acid (de Vries et al., 1993), while class II hydrophobins are less stable and soluble in 60% ethanol or even in water (Russo et al., 1982). Phylogenetic studies revealed that class I hydrophobins are from Basidiomycetes and Ascomycetes while class II hydrophobins are only from Ascomycetes (Linder et al., 2005). Another important feature that differentiates class I and class II hydrophobins is the hydropathy patterns between cysteine residues (Cys) of the protein. Hydrophobins within the same class show high similarities in hydrophobicity plots, distinct from hydrophobins from the other class (Wessels, 1994). Both classes of hydrophobins have eight conserved cysteine residues. Cys2-Cys3 and Cys6-Cys7 are always close neighbors with no other amino acid residues in between. All eight Cys are involved in the formation of four disulfide bonds Cys1-Cys6, Cys2-Cys5, Cys3-Cys4 and Cys7-Cys8. Class I hydrophobins have a less conserved

amino acid sequence between cysteine residues within the class compared to class II hydrophobins (Sunde et al., 2008) .

4.1.2 Interfacial self-assembly of hydrophobins

Crystal structures of *Neurospora crassa* class I hydrophobin EAS (Kwan et al., 2006) and *Trichoderma reesei* class II hydrophobins HFBI and HFBII (Hakanpää et al., 2004; Hakanpää et al., 2006) revealed that class I and class II hydrophobins share a common core structure. Two β-hairpins located near the N-terminus and the C-terminus of the protein respectively interlock with each other by a disulfide bridge to form a β-barrel. The middle part of the protein forms an α-helix which is linked to the outside of the β-barrel by a disulfide bond. The core structure of the hydrophobin protein allows exposure of a big hydrophobic patch on the surface of the protein. Transmission electron microscopy images showed that class I hydrophobins form a compact membrane structure characterized by hydrophobic rodlets which are not seen in class II hydrophobins (Dempsey and Beever, 1979). Instead the class II hydrophobins form a striking honeycomb repeating structure (Sunde et al., 2008).

The unique structure of hydrophobin monomers allows the proteins to self-assemble to form an amphipathic rodlet layer at the hydrophobic/hydrophilic surfaces of hyphae or conidial cell walls (Sunde et al., 2008; Wösten, 2001; Wosten et al., 1994). Experiments using fluorescent dyes showed that the presence of an amphipathic surface led to a conformational change in class I hydrophobin SC3 from *Schizophyllum commune*. SC3 forms stacks of ordered β-sheet structure which leads to rodlet formation (Wang et al., 2005). The disulfide bonds are not involved in rodlet formation but have a role in preventing premature self-assembly of SC3 in the absence of a hydrophobic/hydrophilic surface (de Vocht et al., 2000; Sunde et al., 2008). Proteolysis assays combined with mass spectroscopy analyses suggested that the loop formed by amino acid residues between Cys3 and Cys4 is exposed in the soluble SC3. Adding a hydrophobic/hydrophilic interface leads to shielding of the Cys3-Cys4 loop by SC3, suggesting a role for this loop in self-assembly (Kwan et al., 2006; Sunde et al., 2008; Wang et al., 2004). The class II hydrophobin does not go through a conformation change when it self-assembles and does not exhibit any rodlet structure. Amino acid alignments showed that class II hydrophobin residues between Cys3-Cys4 are highly

conserved within the class. This region contains less hydrophobic amino acid residues compared to class I hydrophobins which leads to less force at the hydrophobic/hydrophilic interface, making it hard to fit the monomers together to form a compact rodlet structure (Niu et al., 2014). At present the mechanism of how class II hydrophobin self-assembles at the hydrophobic/hydrophilic interface is not clear.

4.1.3 Role of hydrophobins in filamentous fungi

As mentioned above, hydrophobins self-assemble into an amphipathic rodlet layer on spore and hyphae cell wall surfaces. One role of the amphipathic rodlet layer is to facilitate aerial hyphae production. Class I hydrophobin *SC3* from *S. commune* showed abundant expression at the aerial hyphae formation stage. WT *S. commune* grown in culture secretes class I hydrophobin SC3. The formation of a hydrophobin rodlet layer decreases water surface tension from 72 mJ m^{-2} to 30 mJ m^{-2}. Deletion of *SC3* results in a mutant strain that cannot lower culture water surface tension and produces less aerial hyphae (Wösten et al., 1999).

Apart from protecting aerial hyphae, the amphipathic rodlet layer formed by hydrophobins has been shown to mask pathogen-associated molecular patterns (PAMPS) such as chitin and β-(1,3)-glucan at the surface of the fungal spore cell wall to avoid recognition of PAMPs by the host. For example in *A. fumigatus*, deletion of *RodA* resulted in a mutant strain that triggered a faster host immune response compared to the WT (Dagenais et al., 2010). Some hydrophobins are pathogenicity factors. *Magnaporthe grisea* class I hydrophobin Mpg1 self-assembles to form an amphipathic rodlet layer on the rice leaf surface. Deletion of *MPG1* caused an 80% reduction in the number of disease lesions on infected rice seedlings (Kershaw et al., 1998).

Hydrophobins are also involved in spore adhesion and dispersal. The tomato pathogen *C. fulvum* produces multiple hydrophobins, the expression and localization of which are highly variable (Lacroix et al., 2008; Whiteford et al., 2004). Class I hydrophobin *CfHcf1* is constitutively expressed *in vitr*o and *in planta*, and is localized in conidia and aerial hyphae. Deletion of *CfHcf1* does not affect pathogenicity but reduces dispersal of conidia in water droplets compared to WT, suggesting a role of CfHcf1 in conidia dispersal (Whiteford and Spanu, 2001). Class II hydrophobin *CfHcf6* is highly

expressed in vegetative mycelia and down regulated at sporulation stage (Whiteford et al., 2004). It is localized at the surface of germinating conidia and growing hyphae. Unexpectedly, deletion of *CfHcf6* resulted in a mutant strain with enhanced adhesion on glass compared to the WT strain (Lacroix et al., 2008; Nielsen et al., 2001). It was proposed that deletion of *CfHcf6* caused a shift in organization of other secreted proteins that are involved in spore adhesion, resulting in increased adhesion ability (Lacroix et al., 2008).

Four hydrophobin genes were identified in the *D. septosporum* genome by Joint Genome Institute (JGI) automated gene predictions (de Wit et al., 2012). In order to determine if hydrophobin genes are virulence factors in *D. septosporum*, I characterized the hydrophobins from *D. septosporum*. The expression profile of *D. septosporum* hydrophobins was determined. Targeted gene knockout and complementation was then used to study the role of the highly expressed hydrophobin *DsHdp1* (JGI: 75009) in *D. septosporum*.

4.2 Results

(Confirmation of *D. septosporum* hydrophobin *DsHdp1* gene structure and construction of Δ*DsHdp1* plasmid was done by Panan Sitthirit, Massey University).

4.2.1 Characterization of *D. septosporum* hydrophobins

Four hydrophobin genes *DsHdp1* (JGI: 75009), *DsHdp2* (JGI: 67650). *DsHdp3* (JGI: 37242) and *DsHdp4* (JGI: 120918) identified in the *D. septosporum* genome were characterized. Translations of hydrophobin genes are shown in Appendix figure 3.3. All four hydrophobin genes contain two introns at similar positions in the C-terminus of their coding regions. Both *DsHdp1* and *DsHdp2* are predicted to encode proteins of 109 amino acid residues. *DsHdp4* encodes the smallest hydrophobin of 94 amino acid residues. *DsHdp*3 encodes the longest protein of 227 amino acid residues (Table 4.1). The N-terminus of DsHdp3 contained a glycine and asparagine rich region. All four hydrophobins contain a signal peptide at the N-terminus.

Table 4.1 Characterization of hydrophobins in the *D. septosporum* NZE10 genome

JGI protein ID	Name	Length	Amino acid	Signal peptide cleavage site	Intron	Class
Ds75009	Hdp1	433 bp	109 aa	between aa 22 and 23: IAG-EE	2	II
Ds67650	Hdp2	442 bp	109 aa	between aa 18 and 19: VAA-IP	2	I
Ds37242	Hdp3	792 bp	227 aa	between aa 18 and 19: VAA-MP	2	II
Ds120918	Hdp4	388 bp	94 aa	between aa 16 and 17: AAA-AP	2	II

Four hydrophobin genes were identified in the *D. septosporum* genome by JGI gene prediction (de Wit et al., 2012). The predicted N-terminal signal peptide cleavage sites are shown in the table. DsHdp1, DsHdp3 and DsHdp4 are class II hydrophobins. DsHdp2 is a class I hydrophobin.

Amino acid alignments and phylogenetic analysis were used to determine the classes of the four predicted *D. septosporum* hydrophobins. A phylogenetic tree constructed using *C. fulvum* and *D. septosporum* hydrophobin protein sequences showed that DsHdp1, DsHdp3 and DsHdp4 form a cluster with class II *C. fulvum* hydrophobins, while DsHdp2 forms a cluster with class I *C. fulvum* hydrophobins (Figure 4.1A) and these relationships are reflected in their amino acid identities (Figure 4.1B). Amino acid alignments showed that all four hydrophobins have eight conserved cysteine residues. *D. septosporum* hydrophobins showed typical class cysteine patterns and hydrophobicity between Cys residues. In general, the class I hydrophobins of *D. septosporum* and *C. fulvum* had a long stretch of 17 to 31 amino acids between the third (Cys3) and fourth (Cys4) cysteine residues (DsHdp2 has 23aa between Cys3 and Cys4), while the class II hydrophobins had only a short stretch of 11 amino acids in the equivalent position, as seen for other fungal hydrophobins (Mgbeahuruike et al., 2013) (Figure 4.2). Together these results suggested that DsHdp1, DsHdp3 and DsHdp4 encode class II hydrophobins whilst DsHdp2 encodes a class I hydrophobin.

Figure 4.1 Phylogenetic tree and amino acid identity of hydrophobin genes

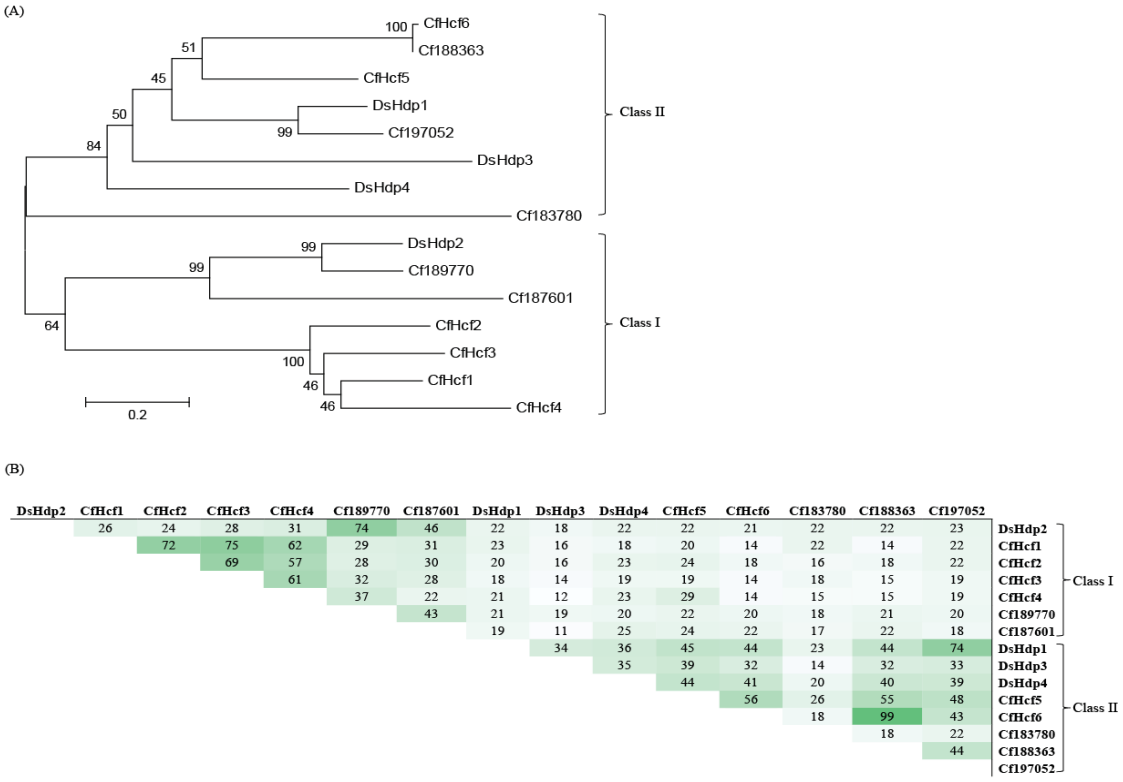

(A) A neighbor-joining tree of DsHdp and CfHcf hydrophobin proteins. The bootstrap values are shown at the nodes as percentages. The classes of all *C. fulvum* hydrophobin genes included in the analysis are known (de Wit et al., 2012), enabling classification of DsHdp1, DsHdp3 and DsHdp4 as class II hydrophobins and DsHdp2 as a class I hydrophobin. (B) Amino acid identity comparing predicted amino acid sequences from hydrophobin genes of *C. fulvum* and *D. septosporum*. The color trends indicate high (darker) to low (lighter) % amino acid identity. Hydrophobin genes show higher aa% identity to genes within the same class than genes from the other class.

Figure 4.2 Partial amino acid alignments of hydrophobin

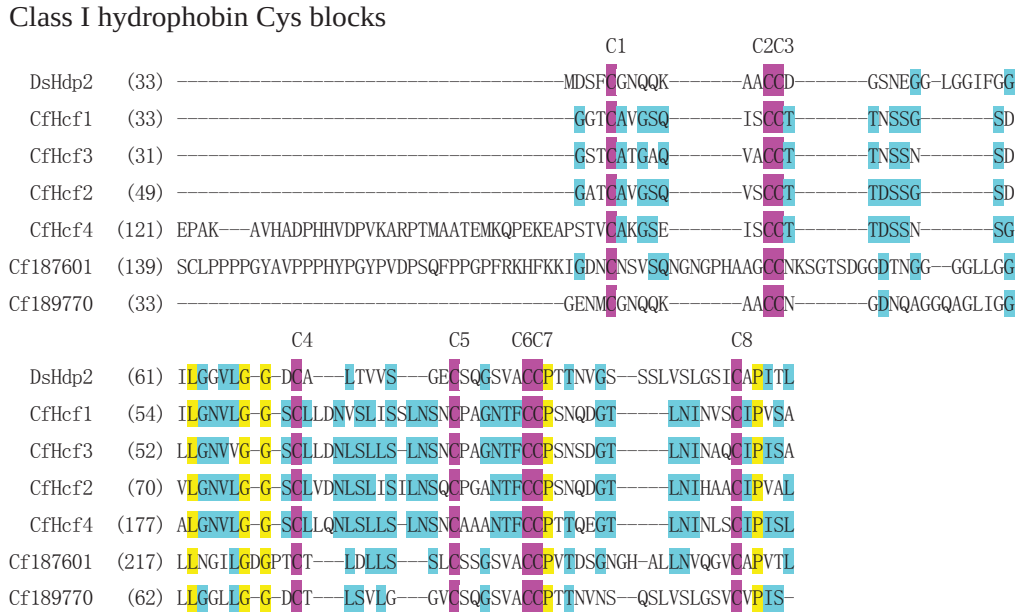

Partial amino acid alignment of Cys blocks of class I hydrophobin proteins DsHdp2 (JGI: 67650), CfHcf1 (JGI: 193176), CfHcf2 (JGI:184635), CfHcf3 (JGI:184193), CfHcf4 (JGI:189850), Cf187601 and Cf189770. Amino acid residue conservation is highlighted in yellow (100% conserved) or in blue (partially conserved). DsHdp2 shared eight conserved cysteine residues with *C. fulvum* class I hydrophobins as highlighted in pink.

Partial amino acid alignment of Cys blocks of class II hydrophobin proteins DsHdp1 (JGI: 75009), DsHdp3 (JGI: 37242), DsHdp4 (JGI: 120918), CfHcf-5 (JGI: 193013), CfHcf-6 (JGI: 193331), Cf197052, Cf188363 and Cf183780. Amino acid residue conservation is highlighted in yellow (100% conserved) or in blue (partially conserved).DsHdp1, DsHdp3 and DsHdp4 shared eight conserved cysteine residues with *C. fulvum* class II hydrophobins as highlighted in pink.

4.2.2 Expression profile of *D. septosporum* hydrophobins

Previous studies showed that the expression pattern of hydrophobin genes during infection correlated with their function (Nakari-Setälä et al., 1997). To predict the role of *D. septosporum* hydrophobins, the expression patterns of hydrophobin genes were analysed at three time points during infection of *P. radiata*. *DsHdp1* showed the highest expression level amongst all hydrophobin genes both *in vitro* and *in planta*. During disease progression, the expression of *DsHdp1* was highly up-regulated at initial lesion (mid) and late lesion/fruiting body formation (late) stages compared to the early stage. Although the expression of *DsHdp2* was low, it was up-regulated *in planta* compared to *in vitro*. *DsHdp3* showed very little expression *in vitro* or *in planta*. *DsHdp4* showed higher expression at early fungal network formation stage compared to later stages. When compared to *in vitro* expression, *DsHdp2* showed the lowest (7 fold) and *DsHdp4* showed the highest (262 fold) relative fold increase at early fungal network formation stage compared to *in vitro* respectively (Table 4.2).

Table 4.2 Transcriptome analysis of four *D. septosporum* hydrophobin genes

JGI protein ID	Name	FM	Early	Mid	Late
Ds75009	Hdp1	9234.40	455.07	6493.99	4861.60
Ds67650	Hdp2	5.06	35.46	31.29	25.74
Ds37242	Hdp3	0.05	0.00	0.00	0.78
Ds120918	Hdp4	0.47	123.29	39.56	3.05

FM: *In vitro* sample collected from 7 days old mycelium grown in DM broth

Early: fungal network on needle surface and penetration through stomatal pores

Mid: initial lesions

Late: mature sporulating lesions with fruiting bodies

Expression of *D. septosporum* hydrophobin genes *in vitro* and *in planta* calculated as Reads Per Million per Kilobase (RPMK) (for detailed description see Table 3.2).

4.2.3 Targeted gene replacement and complementation of *D. septosporum* hydrophobin *DsHdp1*

Because *DsHdp1* is highly expressed *in planta*, it was decided to study its function by targeted gene knockout and complementation. *ΔDsHdp1* strains were obtained by protoplast-mediated transformation (Materials and Methods section 2.8) and identified by screening hygromycin-resistant transformants, initially by PCR, and then by Southern hybridization as described in sections 2.4.1 and 2.7. Southern hybridization

revealed that two *⊿DsHdp1* strain candidates (DsHdp1-T1 FJT145, DsHdp1-T4 FJT146) had lost the WT *DsHdp1* gene fragment, and showed correct-sized *Hin*dIII or *Bcl*I digestion products, indicating successful targeted *DsHdp1* replacement. Another two putative *⊿DsHdp1* strains showed the expected correct-sized *Hin*dIII or *Bcl*I digestion products plus other nonspecific products suggesting that those strains had an additional ectopic integration of the KO construct (Figure 4.3).

Figure 4.3 Southern hybridization of targeted *DsHdp1* replacement candidates in *D. septosporum*

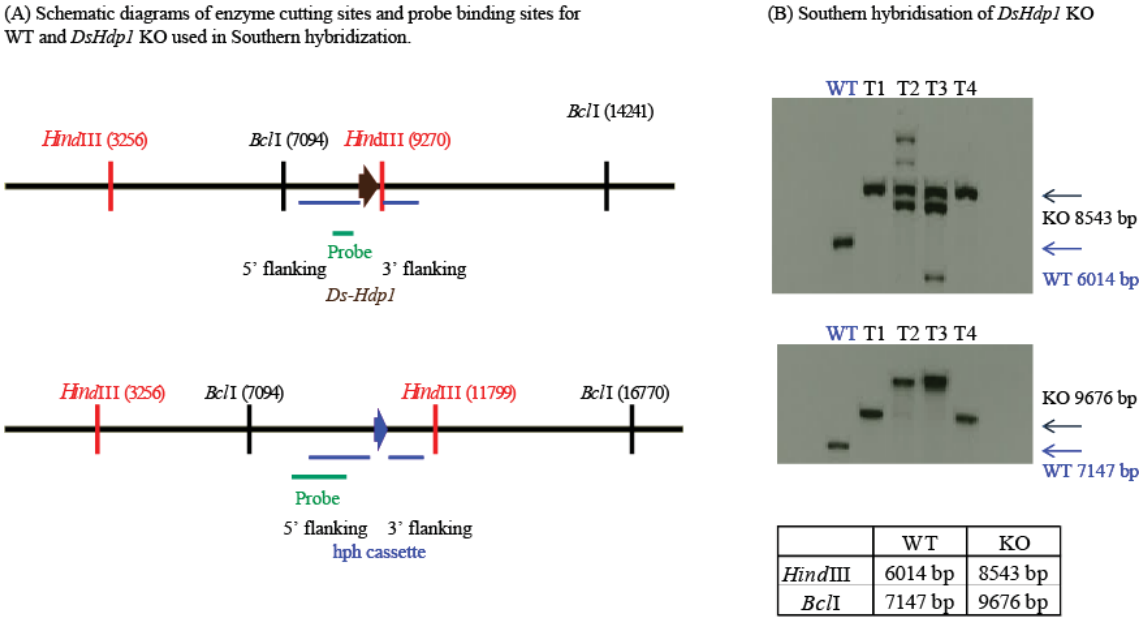

	WT	KO
*Hin*dIII	6014 bp	8543 bp
*Bcl*I	7147 bp	9676 bp

(A) Schematic diagrams of enzyme cutting sites and probe binding sites for WT and *DsHdp1* replacement loci used in Southern hybridization. The black and red vertical lines show enzyme cutting sites. The horizontal green lines show the probe binding sites. The horizontal blue lines show 5' and 3' flanking regions. The brown arrow shows WT *DsHdp1* coding region. The blue arrow shows the hygromycin replacement cassette in KO strain. (B) Southern hybridization showed that two *⊿DsHdp1* strains (DsHdp1-T1 FJT145, DsHdp1-T4 FJT146) lost the WT band and showed correct-sized restriction fragments according to the table shown below. The other two *⊿DsHdp1* strains (T2 and T3) showed extra nonspecific products suggesting that those two KO strains had ectopic insertions of the vector. The blue and black arrows indicate the expected positions of restriction fragments for WT and *⊿DsHdp* strains in Southern hybridization.

To confirm that mutant phenotypes are due to *DsHdp1* deletion but not to other non-specific effects of the transformation process, one *⊿DsHdp1* strain (*DsHdp1*-T1 FJT145 from Figure 4.3B) was selected for complementation by protoplast-mediated transformation as above. The complemented transformants were screened using

DsHdp1 gene specific primers (Materials and Methods section 2.4.1). Five *DsHdp1* complemented transformants showed expected sized PCR products on a gel and were selected for two rounds of purification on selective plates (Figure 4.4A). The copy numbers of intact *DsHdp1* in complemented strains were determined by qPCR (Materials and Methods section 2.5.3) using *DsAflR* as a single-copy reference gene. A normalized target/reference ratio of <1.5 indicated a copy number of one for the targeted *DsHdp1* gene (Weng et al., 2004). All four complemented strains of *DsHdp1* showed estimated copy numbers of one for *DsHdp1* (Figure 4.4B). The *⊿DsHdp1* (DsHdp1-T1 FJT145, DsHdp1-T2 FJT146) and complemented (DsHdp1-C4, FJT147) strains were renamed as shown in table 2.2.

Figure 4.4 PCR screening and copy determination of *DsHdp1* complementation strains

(A)

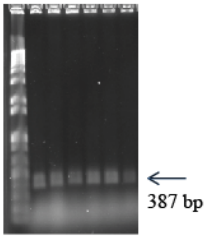

(B)

Targets	References	Mean Cp Target	Mean Cp References	Target/Ref	Average	Normalised	Copy number
WT-Hdp1	WT-AflR	22.09	20.76	0.75			
WT-Hdp1	WT-AflR	22.06	20.86	0.81	0.83	1.00	
WT-Hdp1	WT-AflR	21.88	20.91	0.94			
Hdp1-C3-Hdp1	Hdp1-C3-AflR	24.32	23.03	0.73			
Hdp1-C3-Hdp1	Hdp1-C3-AflR	24.40	23.12	0.73	0.70	0.84	1.00
Hdp1-C3-Hdp1	Hdp1-C3-AflR	24.58	23.11	0.64			
Hdp1-C4-Hdp1	Hdp1-C4-AflR	24.00	22.88	0.81			
Hdp1-C4-Hdp1	Hdp1-C4-AflR	23.97	22.88	0.83	0.83	1.00	1.00
Hdp1-C4-Hdp1	Hdp1-C4-AflR	24.02	22.96	0.85			
Hdp1-C5-Hdp1	Hdp1-C5-AflR	24.18	22.67	0.63			
Hdp1-C5-Hdp1	Hdp1-C5-AflR	24.24	22.61	0.59	0.62	0.74	1.00
Hdp1-C5-Hdp1	Hdp1-C5-AflR	24.19	22.66	0.63			
Hdp1-C6-Hdp1	Hdp1-C6-AflR	25.69	24.44	0.72			
Hdp1-C6-Hdp1	Hdp1-C6-AflR	25.71	24.32	0.66	0.70	0.84	1.00
Hdp1-C6-Hdp1	Hdp1-C6-AflR	25.62	24.34	0.71			

(A) Lane L is 1 kb+ ladder. Lane + is positive control with NZE10 WT gDNA as template for PCR. Lanes C2-C6-5 are from PCR screens of five independent complemented transformants for *DsHdp1*. All screened colonies showed PCR products of the expected size for complementation (387 bp) when screened using gene specific primers, as indicated by the black arrow. (B) PCR confirmed colonies C3-C6 were selected for real-time PCR to estimate gene copy number as shown. CT values of *DsHdp1* amplification ('Cp target') in the complemented strains were compared to those of the single copy reference gene *DsAflR* ('Cp reference') and the results normalized to WT. All four *DsHdp1* complemented strains (C3-C6) showed normalized ratios to WT of <1.5 which suggested an estimated copy of one for the target *DsHdp1* gene tested in these strains.

4.2.4 *D. septosporum ⊿DsHdp1* showed reduced colony surface hydrophobicity

The *D. septosporum DsHdp1* mutant (DsHdp1-T1 FJT145, DsHdp1-T2 FJT146) and complemented (DsHdp1-C4 FJT147) strains were used to study the function of *DsHdp1*. *⊿DsHdp1* showed no significant difference in growth rate, sporulation, germination,

spore adhesion or virulence compared to WT (Table 4.3A and B) (Materials and Methods section 2.9). However Δ*DsHdp1* did show reduced surface hydrophobicity (Material and methods section 2.9.4) compared to WT (Figure 4.5). The hydrophobicity was recovered in the complemented strain, indicating the loss of hydrophobicity was due to disruption of *DsHdp1*.

Table 4.3 Phenotypic analysis and virulence assay using *DsHdp1* mutant and complemented strains

(A) Phenotypic analysis

Name	Growth rate (mm/day); n=9	P (T-test)	Sporulation (spores/ml); n=3	P (T-test)	Germination (%); n=3	P (T-test)	Spore adhesion (%); n=3	P (T-test)
WT	0.51±0.03		6.74E+07±2.33E+07		27.92±6.85		72.13±7.33	
FJT145 (DsHdp1-T1)	0.51±0.04	0.15	9.68E+07±1.54E+07	0.14	25.63±1.36	0.74	76.73±9.85	0.55
FJT146 (DsHdp1-T4)	0.52±0.04	0.42	9.88E+07±1.42E+07	0.12	26.37±3.37	0.63	65.41±12.43	0.47
FJT147 (DsHdp1-C4)	0.48±0.02	0.05	4.53E+07±3.84E+07	0.18	25.84±1.19	0.72	66.98±3.13	0.33

Phenotypic analysis was done using WT, *⊿DsHdp1* (DsHdp1-T1 FJT145 and DsHdp1-T4 FJT146) and complemented (DsHdp1-C4 FJT147) strains. Three biological replicates were used for each strain. The average growth was calculated as mm/day. The sporulation was calculated as spores germinated/ml. The % of germination was calculated as % of germinated spores/total spores. Spore adhesion was calculated as: % of spores left on cytometer after wash / total spores applied to cytometer. Values shown are means ± standard deviation. The T-test value of ⩾0.05 indicates no significant difference between WT, *⊿DsHdp1* and complemented strains in all four tests. The full data are shown in Appendix 4.4

(B) Pathogenicity assay

Name	% Needles showing	P (T-test)	Lesion number/needle	P (T-test)	Lesion size (mm, mean ± SD for all lesions)	P (T-test)
WT	42.13±13.64		1.33±0.22		2.17±0.29	
FJT145 (DsHdp1-T1)	26.78±5.34	0.14	1.1±0.11	0.18	2.33±0.58	0.68

Three parameters (average lesion number, average lesion size and % of needles showing infection symptoms) were used to access if DsHdp1 is a virulence factor in pine needle blight. Three replicate clonal susceptible *P. radiata* seedlings were used for WT (FJT20) and *⊿DsHdp1* (DsHdp1-T1 FJT145) strains. Values shown are means ± standard deviation. The T-test value of ⩾0.05 indicates no significant difference between WT and *⊿DsHdp1*. The *⊿DsHdp1* (DsHdp1-T1 FJT145) showed no significant difference in any of the three virulence parameters tested; the results suggested that DsHpd1 is not a virulence factor when infecting *P. radiata*. The full data are shown in Appendix 4.4

Figure 4.5 Hydrophobicity assay

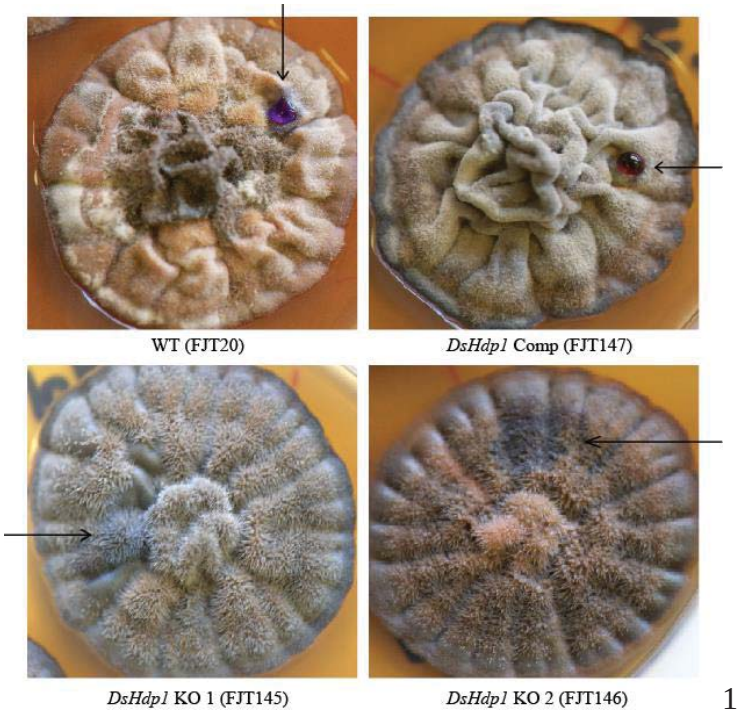

Black arrows indicate the positions of the dye droplet. In both *⊿DsHdp1* (FJT145 and FJT146) strains, the water droplets were dispersed immediately over the colony surface. However the water droplets stayed on top of the WT and *DsHdp1* complemented (FJT147) colony surfaces after 10 minutes incubation, indicative of surface hydrophobicity.

4.3 Discussion

Fungal species show variation in the copy number of hydrophobin genes (Grünbacher et al., 2014; Mgbeahuruike et al., 2013; Sevim et al., 2012). There is no correlation between hydrophobin copy number and genome size; however non-pathogenic fungi tend to have higher numbers of hydrophobin genes compared to pathogenic fungi (Mgbeahuruike et al., 2013). In basidiomycetes, small hydrophobin gene clusters are observed in the genome, which could be caused by gene duplication from a common ancestral hydrophobin gene (Mgbeahuruike et al., 2013). A difference in hydrophobin gene copy number is seen between *C. fulvum* and *D. septosporum*. Six hydrophobin genes (*CfHcf1-6*) were originally identified as abundantly transcribed genes during developmental processes in *C. fulvum* by screening cDNA libraries (Nielsen et al., 2001; Segers et al., 1999); Later, re-annotation of *C. fulvum* genome by InterPro Scan and Gene Ontology terms identified five additional hydrophobin genes. (de Wit et al., 2012). Only four hydrophobin genes were identified in the *D. septosporum* genome, which is

far less than *C. fulvum*. Amino acid alignment results (Figure 4.1B) showed that class I hydrophobins CfHcf1, CfHcf2, CfHcf3 and CfHcf4 have high amino acid identity to each other (61-75%) and form a distinct cluster in the phylogenetic tree. Class II hydrophobins CfHcf6 and Cf188363 showed a 99% amino acid identity with one amino acid difference between Cys6-7 (Figure 4.1A). On the other hand, *D. septosporum* hydrophobins showed low amino acid identity to each other (24-40%). Gene duplication in *C. fulvum* might be the cause of different hydrophobin gene copy numbers between *C. fulvum* and *D. septosporum*.

Hydrophobin genes are highly expressed at different stages during infection of host, which correlate with their function. The transcriptome data showed that in *D. septosporum* the expression of *DsHdp2* and *DsHdp3* were low both *in vitro* and *in planta*. The transcriptome only captures gene expression at the time points that samples were taken. The artificial infection process of *D. septosporum* on *P. radiata* was 12 weeks long; only 3 time points were selected to represent early (fungal network and host penetration), mid (initial lesions) and late (mature) stages of infection. It is possible that samples were missed where those hydrophobin genes were highly expressed. More time points should be included in future experiments to gain a complete expression profile of all *D. septosporum* hydrophobin genes.

The class II hydrophobin gene *DsHdp1* was highly expressed *in vitro* and *in planta*, particularly during necrotrophic stages (mid and late) therefore this gene was selected for targeted gene replacement and complementation to study its role. Previous studies in *Beauveria bassiana* showed that deletion of a class I hydrophobin gene *hyd1* led to reduced spore hydrophobicity and changes in surface carbohydrate epitopes compared to WT. Deletion of another class I hydrophobin gene *hyd2* led to disrupted rodlet structure on spore surface, decreased cell surface hydrophobicity and adhesion compared to WT. However only *hyd1* was required for virulence but not *hyd2* (Zhang et al., 2011). The *D. septosporum* class II Δ*DsHdp1* stain showed reduced surface hydrophobicity, however deletion of *DsHdp1* had no effect on growth rate, sporulation, germination or spore adhesion. Similar results were seen in *Botrytis cinerea* (Doss et al., 1997). The expression of class I hydrophobin *Bhp1* and class II hydrophobins *Bhp2* and *Bhp3* were relatively low in conidia and mycelium but high in infected tomato leaves and sclerotia. Single, double or triple mutations of these hydrophobin genes had no

effect on growth rate, sporulation, germination or adhesion. An electron microscopy study showed that *B. cinerea* does not have a rodlet surface on conidia (Doss et al., 1997). No electron microscopy was done with *D. septosporum* conidia, it will be interesting to know if *D. septosporum* has a similar conidial surface structure as *B. cinerea*. One interesting observation is that *DsHdp4* is highly expressed at early infection stage with a 262-fold increase in expression compared to *in vitro*. It's possible that *DsHdp4* may have a role in early infection stage such as spore adhesion. Targeted *DsHdp4* replacement should be investigated to confirm this hypothesis.

Some hydrophobins have a role in pathogenicity (Kershaw et al., 1998), whilst deletion of *DsHdp1* had no effect on the ability of *D. septosporum* to cause disease symptoms on radiata pine. One explanation could be that there is redundancy of function and several hydrophobins contribute to the full virulence of *D. septosporum*. One example is cerato-ulmin (CU) produced by *Ophiostoma novo-ulmi*. CU was first classified as a toxin because injection of CU causes wilting and electrolyte loss in elm (Brasier, 1991; Russo et al., 1982). A later study showed that CU is a class II hydrophobin (Temple et al., 1997). Deletion of *CU* did not reduce pathogenicity; however introduction of *CU* into a non-pathogenic strain of *O. quercus* led to pathogenicity of that strain (Sorbo et al., 2000). *O. novo-ulmi* produces several hydrophobins other than CU. It is suggested that each hydrophobin is dispensable and the full virulence is achieved by all hydrophobins together (Bowden et al., 1996). In the case of *D. septosporum* full virulence may be achieved by a combination of all four hydrophobins, and possibly the expression of the other hydrophobin genes might have increased to compensate for loss of *DsHdp1* in the mutant strain. Expression analysis of other hydrophobin genes (*DsHdp2*, *DsHdp3* and *DsHdp4*) in the *DsHdp1* mutant could be done to test if any of these hydrophobins compensated for loss of *DsHdp1*. Targeted replacement of single or multiple *D. septosporum* hydrophobin genes should be investigated to gain a whole picture of the roles of *D. septosporum* hydrophobin genes.

In summary, three class II hydrophobin genes (*DsHdp1*, *DsHdp3* and *DsHdp4*) and one class I hydrophobin gene (*DsHdp2*) were identified in the *D. septosporum* genome. Transcriptome analysis showed that only *DsHdp1* is highly expressed *in planta*. Targeted gene replacement of *DsHdp1* did not affect fungal growth rate, sporulation, germination or spore adhesion *in vitro*, but colony surface hydrophobicity was reduced

in *ΔDsHdp1* mutants. Pathogenicity assay results suggested that DsHdp1 is not a virulence factor. More experiments are required to gain a whole picture of the function of *D. septosporum* hydrophobin genes.

Chapter 5. Functional characterization of putative effectors in *Dothistroma septosporum* NZE10 strain

5.1 Introduction

Effectors are secreted pathogen proteins that facilitate infection and suppress host immunity in the absence of corresponding host resistance proteins. Effectors can function as virulence factors by targeting host proteins involved in defense responses, to allow pathogen invasion (for details see Chapter 1 section 1.3.1). Targeted gene replacement and complementation of putative *D. septosporum* effectors *DsAvr4*, *DsEcp2-1* and *DsEcp6* were used to test whether selected *D. septosporum* effector candidates are virulence factors when they infect *P. radiata*.

Identification of effectors involved in R protein recognition provides information to screen for new effector candidates, and ultimately to develop host genotypes that are more resistant to the pathogen. *Cladosporum fulvum* effector Avr4 is directly recognized by the tomato resistance protein Cf-4 (Joosten et al., 1994). *Cf-4* encodes an NB-LRR-CC receptor protein; the LRR domain is involved in effector recognition (Thomas et al., 1997; van der Hoorn et al., 2001). Homologues of CfAvr4 were identified in *Cercospora beticola, Cercospora apii* (Stergiopoulos et al., 2010), *Mycosphaerella fijiensis* and *D. septosporum* (de Wit et al., 2012) which showed 30%, 29.6%, 33.8% and 51% amino acid identities to CfAvr4 respectively (Chapter 3 section 3.3.2). DsAvr4 and MfAvr4 can also be recognized by the tomato resistance protein Cf-4 and trigger host HR in tomato (de Wit et al., 2012; Wulff et al., 2009). However CbAvr4 and CaAvr4 do not induce a Cf-4 mediated HR. A domain swap study between CfAvr4 and CaAvr4 identified that regions between CfAvr4 cysteine residues Cys6 to Cys7 are required for recognition by Cf-4 (Mesarich et al., data not published). Because of the importance of this knowledge for interpreting the results of polymorphism studies and their potential effects on R protein recognition, the DsAvr4 regions important for Cf-4 recognition were analysed using the same type of domain swap experiment between DsAvr4 and CbAvr4.

D. septosporum is the causal agent of DNB on pine species (details see Chapter 1 section 1.1.2). Some R proteins against fungal invasion were identified in *Pinus* species

(details see Chapter 1 section 1.2.2.3). However R proteins with specificity for *D. septosporum* have not been identified in *P. radiata* so far. To study the cellular function of *D. septosporum* effectors when infecting *P. radiata*, and to screen for necrosis inducing activity of selected *D. septosporum* effectors. DsAvr4, DsAvr4-CbCys6-Cys8, DsEcp2-1 and DsEcp2-3 were selected for protein expression based on the following findings. *DsAvr4* expression is low *in planta* compared to *CfAvr4* which is highly expressed *in planta* (van Esse et al., 2007). The down-regulation of *DsAvr4* expression could be a pathogen mechanism to avoid detection, as part of the evolutionary arms race adaption of pathogen to the host. Studies showed that Ecp2-1 may target a guardee which is protected by an R protein in the host. CfEcp2-1 is able to trigger non-host HR in *Nicotiana paniculata* through a single dominant gene which shows no homology to tomato Cf R proteins (de Kock et al., 2004). MfEcp2-1 which is also recognized by Cf-Ecp2 can target a guardee protected by Cf-Ecp2 and trigger necrosis in the absence of Cf-Ecp2 in tomato (de Wit et al., 2012; Stergiopoulos et al., 2010).

5.2 Results

5.2.1 Functional characterization of *D. septosporum* effectors

5.2.1.1 Targeted gene replacement and complementation of *D. septosporum* effectors *DsAvr4*, *DsEcp2-1* and *DsEcp6*

Avr4, Ecp2-1 and Ecp6 are core effectors that have conserved biological functions to facilitate the infection of various fungi on different host species (Stergiopoulos et al., 2010). Targeted gene knockouts of *D. septosporum* effector genes *DsAvr4*, *DsEcp2-1* and *DsEcp6* were created by protoplast mediated transformation (Materials and Methods section 2.8) to test whether they are virulence factors during *P. radiata* infection. Gene KO transformants were initially confirmed by PCR (Materials and Methods section 2.4.1); two positive transformants for each gene showed correct 5' and 3' bands (Figure 5.1).

Southern hybridization (Materials and Methods section 2.7) on single-spore purified colonies was then used to confirm the KO, using two restriction enzymes for gDNA digestion. From this, both *⊿DsAvr4* (DsAvr4-T1 FJT134, DsAvr4-T2 FJT135) and *⊿DsEcp2-1* (DsEcp2-1-T1 FJT141, DsEcp2-1-T2 FJT142) strains lost the wild-type (WT)

gene fragment as expected for gene replacement, and showed correct-sized *Sal*I or *Sca*I digestion products, indicating successful targeted *DsAvr4* and *DsEcp2-1* replacement. For *⊿DsEcp6*, only one KO strain (DsEcp6-T1 FJT138) lost the WT gene fragment and showed correct *Pst*I or *Hind*III digestion products, indicating successful targeted *DsEcp6* replacement; the second putative KO strain (DsEcp6-T2) showed both expected WT band and KO bands for *Pst*I or *Hind*III suggesting this is an ectopic strain that retains an intact copy of *DsEcp6*. There are extra bands shown on some KO lanes (*Sal*I or *Sca*I digested *DsAvr4* and *Sca*I digested *DsEcp2-1*). This could be due to nonspecific binding of high sensitivity DIG-labelled probe to regions of the genome or random insertion of the KO construct in the genome The WT band was lost in those KO strains indicating successful targeted replacement of *DsAvr4* and *DsEcp2-1* (Figure 5.2).

Figure 5.1 PCR screening of *D. septosporum* transformants for targeted gene replacement of *DsAvr4, DsEcp2-1* and *DsEcp6*

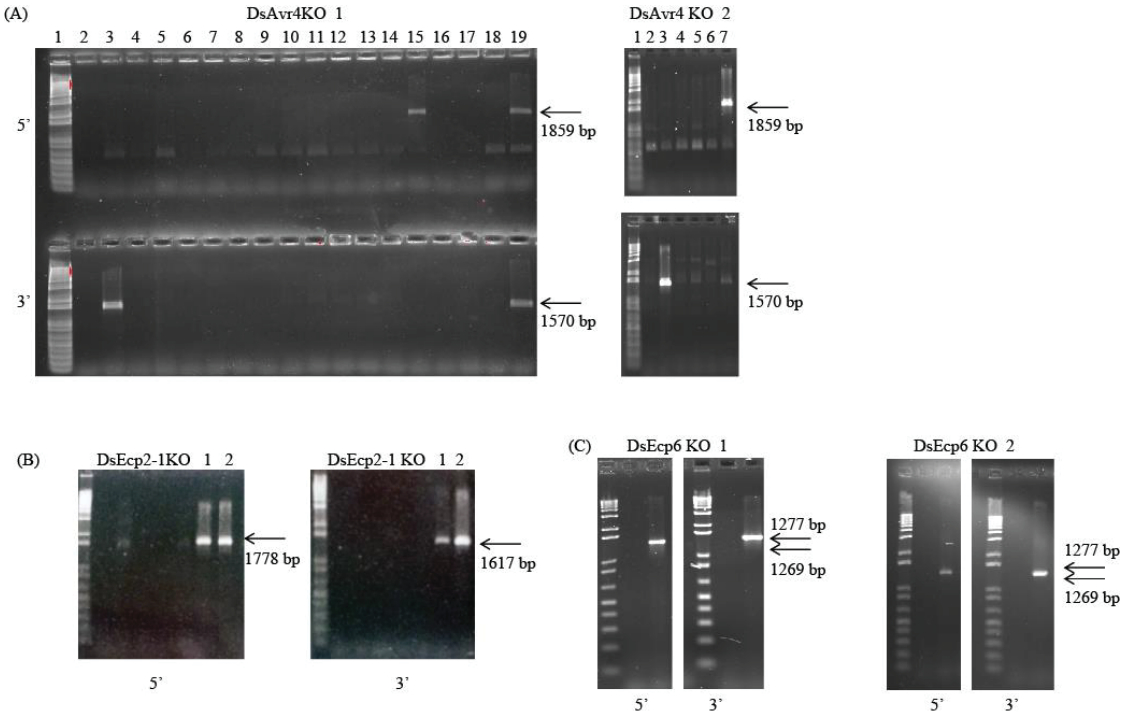

PCR was used to screen for positive *D. septosporum* transformants. The black arrows indicate the size of expected PCR products. Two colonies for *DsAvr4* (A), *DsEcp2-1* (B) and *Ds-Ecp6* (C) showed both correct sized bands for 5' and 3' integration on gel when screened using primers that bind outside of flanking regions of targeted genes and *hph* outward primers respectively.

Figure 5.2 Southern hybridization confirmation of targeted gene replacement of *DsAvr4*, *DsEcp2-1* and *DsEcp6* in *D. septosporum*

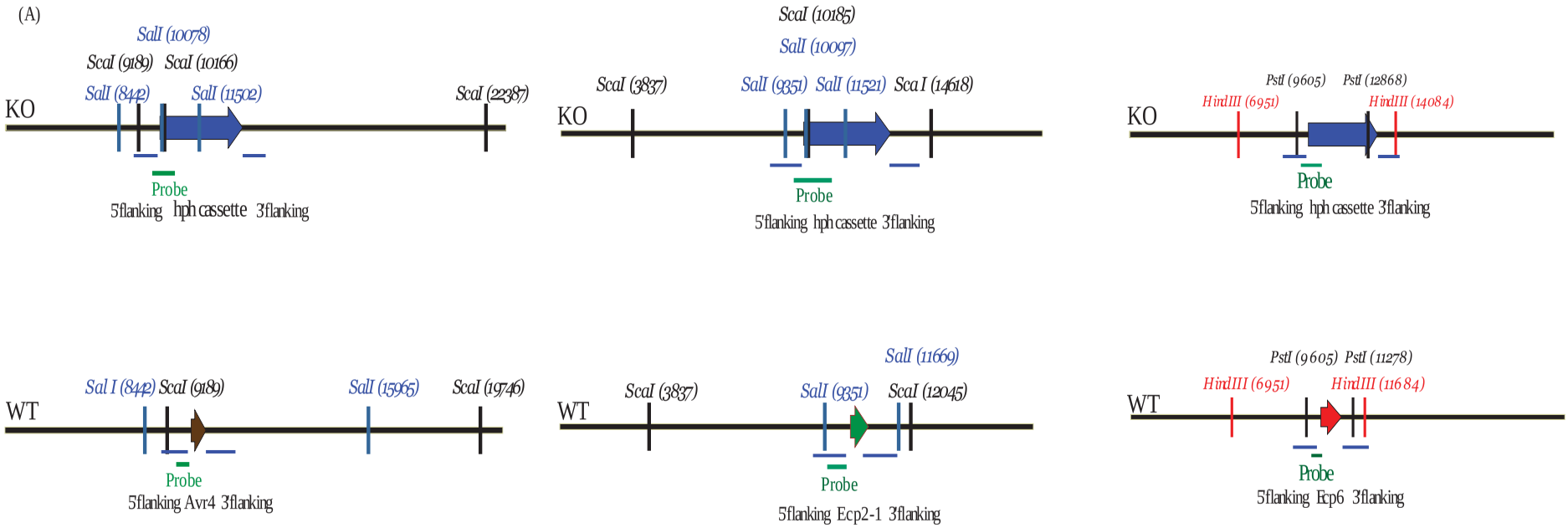

(A) Schematic diagrams of enzyme cutting sites and probe binding sites for WT, *ΔDsAvr4*, *ΔDsEcp2-1* and *ΔDsEcp6* used in Southern hybridization. The blue, black and red vertical lines show enzyme cutting sites. The horizontal green lines show the probe binding sites. The horizontal blue lines show 5' and 3' flanking regions. The brown, green and red big arrows show *DsAvr4*, *DsEcp2-1* and *DsEcp6* coding regions. The big blue arrow shows the hygromycin replacement cassette in KO strains.

(B)

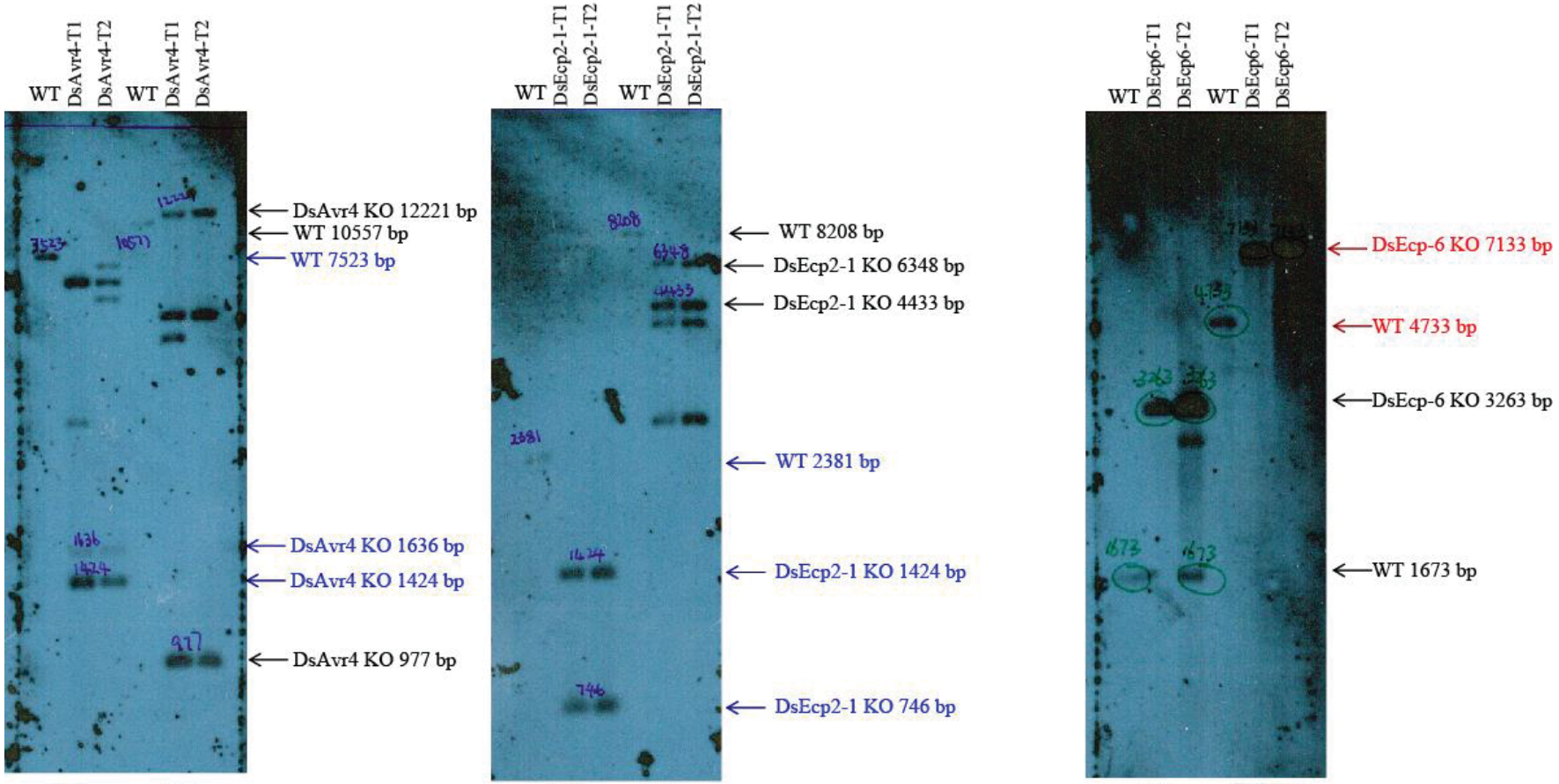

Name	Enzyme	WT (bp)	KO (bp)
DsAvr4	*Sca* I	10557	12221+977
	Sal I	7523	1424+1636

Name	Enzyme	WT (bp)	KO (bp)
DsEcp2-1	*Sca* I	8082	4433+6348
	Sal I	2381	1424+746

Name	Enzyme	WT (bp)	KO (bp)
DsEcp6	*Hind* III	4733	7133
	Pst I	1673	3263

(B) The blue, black and red arrows (which correspond to the colours used for each restriction enzymes in (A) show the expected restriction band sizes for WT, *⊿DsAvr4*, *⊿DsEcp2-1* and *⊿DsEcp6* strains in Southern hybridization. The table shows the expected band sizes for Southern hybridization. Both *⊿DsAvr4*

transformants (DsAvr4-T1 FJT134 and DsAvr4-T2 FJT135) lost the WT bands when digested by *Sca*I or *Sal*I (10557 bp or 7523 bp respectively) and showed expected *Sca*I or *Sal*I digestion bands (12221 bp + 977 bp or 1424 bp + 1636 bp respectively). Similarly for *DsEcp2-1*, both KO transformants (DsEcp2-1-T1 FJT 141 and DsEcp2-1-T2 FJT142) lost the WT bands when digested by *Sca*I or *Sal*I (8208 bp or 2381 bp respectively) and showed expected *Sca*I or *Sal*I digestion bands (4433 bp +6348 bp or 1424 bp + 746 bp respectively). Those results indicate successful targeted *DsAvr4* and *DsEcp2-1* replacement. Only one *ΔDsEcp6* transformant (DsEcp6-T1 FJT138) lost the *Pst*I and *Hind*III WT fragments (1673 bp and 4733 bp respectively) and showed correct *Pst*I and *Hind*III digestion products (3263 bp and 7133 bp), indicating successful targeted *DsEcp6* replacement. The second *ΔDsEcp6* transformant (DsEcp6-T2) showed both expected WT band and KO bands for *Pst*I and *Hind*III suggesting this is an ectopic strain that retains an intact copy of *DsEcp6*. The extra bands in *Sal*I cut DsAvr4-T1 (FJT134) and DsAvr4-T2 (FJT135) and the extra bands in *Sca*I cut DsAvr4-T1 (FJT134), DsAvr4-T2 (FJT135), DsEcp2-1-T1 (FJT141) and DsEcp2-1-T2 (FJT142) are due to non-specific binding of DIG-labelled probe or random insertion of the KO construct in the genome.

To confirm that mutant phenotypes were due to the specific gene deletion but not to other non-specific effects of the transformation process, one KO strain of each gene, i.e. *DsAvr4*-T1 (FJT134), *DsEcp2-1*-T1 (FJT141) and *DsEcp6*-T1 (FJT138) was selected for complementation by protoplast mediated transformation (Materials and Methods section 2.8). The complemented transformants were screened using gene specific primers (Materials and Methods section 2.4.1). Five complemented transformants for each gene showed expected sized PCR products on a gel and were selected for two rounds of purification on selective plates (Figure 5.3).

Figure 5.3 PCR screening for *DsAvr4*, *DsEcp2-1* and *DsEcp6* complementation strains

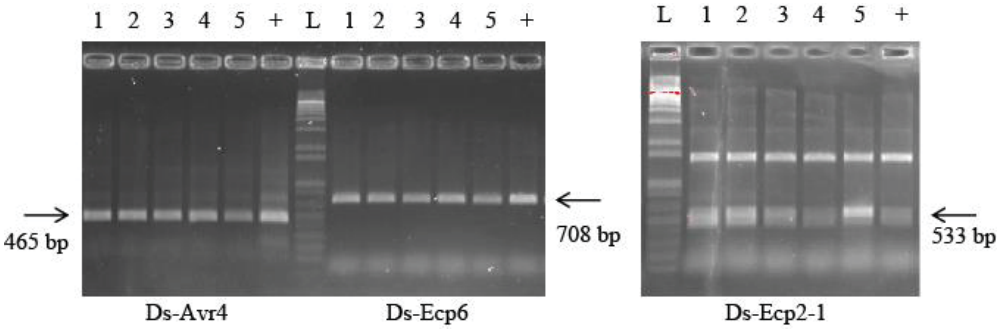

Lane L is 1 kb+ ladder. Lane + is positive control using NZE10 WT gDNA as template for PCR. The black arrows indicate the size of expected PCR products. Lanes 1-5 are from PCR screens of five independent complemented transformants for *DsAvr4*, *DsEcp6* and *DsEcp2-1*. All screened colonies for *DsAvr4* and *DsEcp6* showed bands of the expected size for complementation when screened using gene specific primers. For *DsEcp2-1*, all the colonies showed bands of expected size (533 bp) gene specific primers. However an extra band was seen in all the *DsEcp2-1* complemented strains, suggesting that the primers used for *DsEcp2-1* PCR had low specificity compared to *DsAvr4* and *DsEcp6* gene specific primers.

By protoplast mediated transformation, WT genes can integrate randomly into the genome. Traditionally, the number of intact WT genes in complemented strain is confirmed using Southern hybridization. However, this method is time consuming, not very accurate at high copy numbers, and requires a lot of high molecular weight gDNA. More recently, quantitative real-time PCR (qPCR) has been widely used to determine transgene copy numbers (Bubner and Baldwin, 2004; Zhu et al., 2014). Four complemented transformants for each of *DsAvr4*, *DsEcp6* and *DsEcp2-1* were selected and the number of copies of intact genes in the complementation strains was estimated using qPCR (Materials and Methods section 2.5.3). The gDNA samples extracted from

complemented strains were checked on a gel and found to be of high molecular weight indicating good quality gDNA. The high molecular weight gDNA ensures full DNA amplicon length for the target and reference genes, and also reduces the chance of small DNA fragments competing with primers binding to the target sequence (Appendix figure 3.4). A normalized target/reference ratio of <1.5 indicated a copy number of one for the targeted genes tested (Weng et al., 2004). Three complemented strains of *DsAvr4* (C1, C3 and C4) and two complemented strains of each of *DsEcp2-1* (C2 and C4) and *DsEcp6* (C2 and C3) showed estimated copy numbers of one for the targeted gene tested. One complemented strain of *DsAvr4* (C2) and two complemented strains of *DsEcp2-1* (C3 and C5) and *DsEcp6* (C4 and C5) showed estimated copy numbers of two for the targeted genes tested (Appendix table 4.1). The KO and complemented strains were renamed as shown in table 2.2.

5.2.1.2. Virulence testing of DsAvr4, DsEcp2-1 and DsEcp6 *in planta*

Deletion of *CfAvr4*, *CfEcp2-1* and *CfEcp6* does not affect fungal physiology *in vitro* (Bolton et al., 2008; Lauge et al., 1997; van Esse et al., 2007). The *ΔDsAvr4*, *ΔDsEcp2-1* and *ΔDsEcp6* and single copy complemented strains were tested for *in vitro* growth rate, sporulation and germination compared to WT with a two tailed T-test (Materials and Methods section 2.9). None of these mutants showed any significant difference ($P < 0.05$) in these parameters compared to WT (Table 5.1A).

In *C. fulvum*, CfAvr4, CfEcp2-1 and CfEcp6 are virulence factors (Bolton et al., 2008; Lauge et al., 1997; van Esse et al., 2007). A pathogenicity assay (Materials and Methods section 2.9.6) was performed comparing *ΔDsAvr4*, *ΔDsEcp2-1* and *ΔDsEcp6* and single complemented strains to WT. Parameters measured included the percentage of needles showing symptoms, lesion size and lesion number per needle. The *ΔDsAvr4* strain (DsAvr4-T1 FJT134) showed no significant difference in any of these three parameters compared to WT. However the single complemented strain of *DsAvr4* (DsAvr4-C4 FJT136) showed a significant reduction in % of infection (Table 5.1B). The *ΔDsEcp2-1* strain (DsEcp2-1-T1 FJT141) showed no significant difference in % of infection and average lesion number compared to WT, but a significant difference in

lesion size compared to WT (P= 0.00003). The *⊿DsEcp2-1* strain infected needles had larger lesions compared to WT infected needles. The *DsEcp2-1* complemented strain (DsEcp2-1-C2 FJT143) showed no significant difference in all three measurements compared to WT, indicating the larger lesion seen in *⊿DsEcp2-1* strain is due to deletion of *DsEcp2-1* (Table 5.1B). The *⊿DsEcp6* strain (DsEcp6-T1 FJT138) showed no significant difference in average lesion number or lesion size compared to WT, but a significant difference (P= 0.03) in % of infection compared to WT. However the *DsEcp6* complemented strain (DsEcp6-C2 FJT139) also showed a significant difference in % of infection compared to WT suggesting the phenotype in *⊿DsEcp6* strain is not a genuine KO effect (Table 5.1 B).

Table 5.1 Phenotypic and pathogenicity assay

Gene	Name	Growth rate (mm/day); n=9	P (T-test)	Sporulation (spores/ml); n=3	P (T-test)	Germination (%); n=3	P (T-test)
	WT	0.52±0.03		6.74E+07±2.33E+07		27.92±6.85	
DsAvr4	**FJT134 (DsAvr4-T1)**	0.51±0.02	0.41	8.22E+07±2.99E+07	0.54	21.62±0.27	0.19
	FJT135 (DsAvr4-T2)	0.51±0.06	0.65	4.51E+07±6.56E+05	0.17	22.70±1.98	0.27
	FJT136 (DsAvr4-C4)	0.53±0.02	0.80	9.07E+07±1.42E+07	0.21	23.05±1.68	0.30
DsEcp6	**FJT138 (DsEcp6-T1)**	0.52±0.05	0.96	8.56E+07±1.54E+07	0.32	22.44±2.81	0.27
	FJT139 (DsEcp6-C2)	0.52±0.03	0.70	9.73E+07±2.26E+07	0.19	21.32±1.67	0.18
DsEcp2-1	**FJT141 (DsEcp2-1-T1)**	0.51±0.02	0.34	8.95E+07±1.67E+07	0.25	25.19±3.06	0.56
	FJT142 (DsEcp2-1-T2)	0.50±0.01	0.05	7.17E+07±1.27E+07	0.79	20.91±3.96	0.20
	FJT143 (DsEcp2-1-C2)	0.51±0.05	0.67	6.93E+07±1.58E+07	0.91	19.22±2.23	0.10

(A) Phenotypic analysis was done using WT, *ΔDsAvr4* (DsAvr4-T1 FJT134 and DsAvr4 T2 FJT135) and complemented (DsAvr4-C4 FJT136) strains, *ΔDsEcp6* (DsEcp6-T1 FJT138) and complemented (DsEcp6-C2 FJT139) strains and *ΔDsEcp2-1* (DsEcp2-1-T1 FJT141 and DsEcp2-1-T2 FJT142) and complemented (DsEcp2-1-C2 FJT143) strains. The results are shown as mean±standard deviation. Three biological replicates were used for each strain. The average growth was calculated as mm/day. The sporulation was calculated as spores germinated/ml. The % of germination was calculated as % of germinated spores/total spores. The T-test value of ⩾0.05 indicates no significant difference between WT, *ΔDsAvr4*, *ΔDsEcp2-1*, *ΔDsEcp6* and complemented strains in all three tests. The full data are shown in Appendix 4.4

Gene	Name	% Needles showing symptoms (%)	P (T-test)	Lesion number/needle	P (T-test)	Lesion size (mm, mean ± SD for all lesions)	P (T-test)
	WT	42.13±13.64		1.33±0.22		2.68±0.11	
DsAvr4	**FJT134 (DsAvr4-T1)**	19.36±7.81	0.07	1.12±0.1	0.21	2.33±0.14	0.05
	FJT136 (DsAvr4-C4)	10.83±11.4	0.04	1.05±0.48	0.11	2.57±1.33	0.23
DsEcp6	**FJT138 (DsEcp6-T1)**	12.99±5.69	0.03	1.18±0.2	0.44	2.76±0.55	0.25
	FJT139 (DsEcp6-C2)	11.98±11.39	0.04	1.13±0.44	0.31	2.42±1.1	0.33
DsEcp2-1	**FJT141 (DsEcp2-1-T1)**	26.55±7.32	0.16	1.11±0.1	0.19	3.6±0.04	0.00003
	FJT143 (DsEcp2-1-C2)	24.05±21.27	0.29	1.25±0.35	0.57	2.66±1	0.73

(B) Pathogenicity assay using WT, *ΔDsAvr4*, *ΔDsEcp6*, *ΔDsEcp2-1* and single complemented strains. Three replicates of *P. radiata* clonal susceptible seedlings were used to test the virulence of each strain. The pathogenicity assay was assessed in three aspects. The % of needles showing symptoms was calculated as needles showing necrotic lesions/total needles. The lesion number/needle was calculated as number of total lesions/number of needles showing symptoms. The lesion size was calculated by average lesion size. Values are means ± standard deviation. A two-tailed T-test was used to test the hypothesis of no significance different between WT, KO and complemented strains at the 95% confidence level. Red color shows a T-test with P value <0.05, indicating significant difference when compared to WT. The *ΔDsAvr4* strain (DsAvr4-T1, FJT134) showed no significant difference in all three measurements compared to WT. The single complemented *DsAvr4* strain showed a significant reduction in % of needles showing infection compared to WT. The *ΔDsEcp2-1* strain induced significantly larger lesions compared to WT and the single *DsEcp2-1* complemented strain showed no significant difference in lesion size compared to WT, indicating the phenotype is due to deletion of *DsEcp2-1*. The *ΔDsEcp6* strain (FJT138) showed a significant difference in % of infection, however the phenotype was not complemented by complementation of *ΔDsEcp6*. The full data are shown in Appendix 4.4

5.2.2 One or more amino acid residues in the conserved chitin binding domain of DsAvr4 is required for Cf-4 mediated hypersensitive response

As mentioned in the introduction, the region between Cys6-Cys7 in CfAvr4 is a chitin binding domain and is involved in Cf-4 recognition. To compare DsAvr4 with CfAvr4 and other homologs in this region, an amino acid alignment of mature Avr4 polypeptides was performed (Figure 5.4). The region between Cys6-Cys7 has the highest number of amino acid residues that are conserved between CfAvr4, DsAvr4 and MfAvr4 but are different from those of CaAvr4 and CbAvr4. A domain swap experiment between CbAvr4 (not recognized by Cf-4) and DsAvr4 (recognized by Cf-4) was used to detect whether the Cys6-Cys7 region of DsAvr4 is involved in Cf-4 recognition.

Figure 5.4 Amino acid alignment of mature Avr4

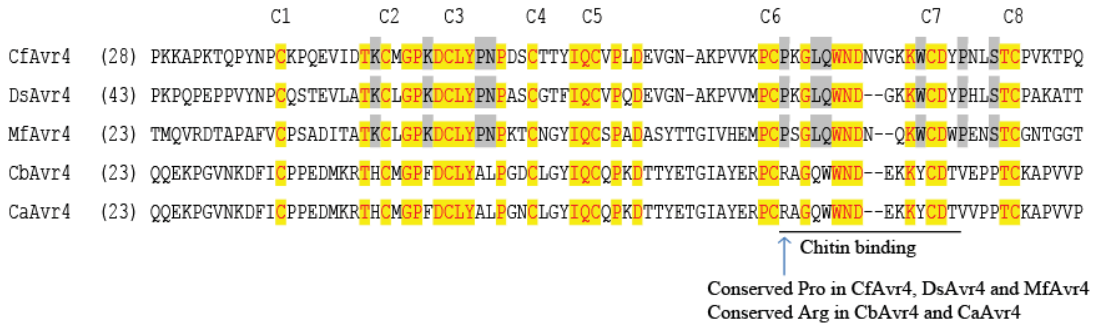

Amino acid alignment of mature Avr4 from *C. fulvum* (CfAvr4 JGI: 189855), *D. septosporum* (DsAvr4 JGI: 36707), *M. fijiensis* (MfAvr4 JGI: 87167), *C. apii* (CaAvr4 NCBI:ADE28521.1) and *C. beticola* (CbAvr4 NCBI: ADE28519.1). Identical amino acids are highlighted in yellow. Amino acids conserved between CfAvr4, DsAvr4 and MfAvr4 but not shared in CaAvr4 and CbAvr4 are highlighted in grey. The eight conserved cysteine residues are indicated on top of the alignment. The chitin binding domain is located between Cys6-Cys7. The blue arrow indicates the conserved Pro residue in CfAvr4, DsAvr4 and MfAvr4. CbAvr4 and CaAvr4 have an Arg residue at the same position.

Avr4 chimeric plasmids were constructed using PCR and the Gateway system (Materials and Methods sections 2.4.1 and 2.3.8.2) then transformed into Agrobacterium strain GV3101 (Materials and Methods section 2.10.1). PCR was used to screen for positive Agrobacteria transformants carrying different Avr4 chimeric plasmids (Materials and Methods section 2.4.2). Several colonies showed expected sized PCR products on a gel (Figure 5.5). One colony was selected for each chimeric for

plasmid extraction and the sequence of each chimeric was confirmed by sequencing (Materials and Methods sections 2.3.10).

Figure 5.5 PCR screening for positive Agrobacterium colonies having Avr4 chimeras

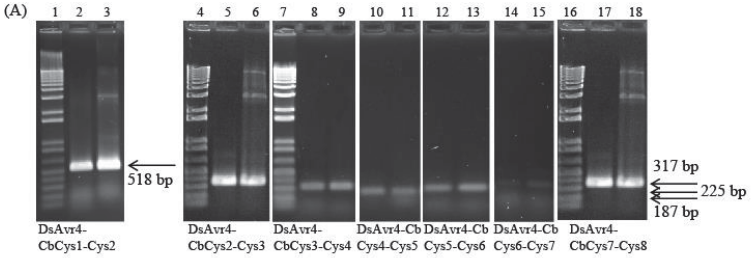

Name	Lane	Size (bp)
1 kb+ ladder	1,4,7 and 16	
DsAvr4-CbCys1-Cys2	2-3	518
DsAvr4-CbCys2-Cys3	5-6	317
DsAvr4-CbCys3-Cys4	8-9	225
DsAvr4-CbCys4-Cys5	10-11	187
DsAvr4-CbCys5-Cys6	12-13	225
DsAvr4-CbCys6-Cys7	14-15	317
DsAvr4-CbCys7-Cys8	17-18	317

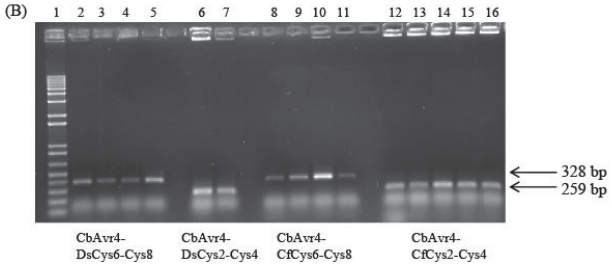

Name	Lane	Size (bp)
1 kb+ ladder	1	
CbAvr4-DsCys6-Cys8	2-5	328
CbAvr4-DsCys2-Cys4	6-7	259
CbAvr4-CfCys6-Cys8	8-11	328
CbAvr4-CfCys2-Cys4	12-16	259

(A) PCR screening for positive Agrobacterium colonies having DsAvr4 chimeras. (B) PCR screening for positive colonies for CbAvr4 chimeras. The expected molecular sizes of DNA bands are indicated as black arrows in the gel picture and are shown in the table. The expected sequences of one positive transformant (the first +ve colony for each strain) of each Avr4 chimeras were confirmed and used for further experiments.

The DsAvr4 chimeras with some sections replaced with CbAvr4 segments, were tested for the recognition by the tomato resistance protein Cf-4. Agrobacterium culture filtrates carrying plasmids harboring different DsAvr4 chimeras were co-infiltrated with Agrobacterium culture filtrates carrying an additional plasmid harboring the tomato Cf-4 resistant gene (kindly provided by Prof de Wit, Wageningen University). The mixture was co-infiltrated on the lower sides of 6 month old *N. tabacum* leaves at an OD600 of 1.0 (Materials and Methods section 2.10.2). Infiltration of negative controls: WT DsAvr4, WT CbAvr4 or Cf-4 only did not trigger any HR response, indicating the infiltration method did not induce any necrosis response. Co-infiltration of Cf-4 with WT DsAvr4 or CfAvr4 induced necrosis responses as expected based on previous work, and served as positive controls. Co-infiltration of Cf-4 with WT CbAvr4 did not induce a necrosis response. These results confirmed recognition of WT DsAvr4 and CfAvr4 but not CbAvr4 by Cf-4 (Figure 5.6A).

DsAvr4 chimeras carrying various blocks of sequence from CbAvr4 were tested first. Co-infiltration of DsAvr4 chimeras carrying CbAvr4 sequence between cysteine residues Cys1 to Cys4 (DsAvr4-CbCys1-Cys4), Cys4 to Cys6 (DsAvr4-CbCys4-Cys6) and Cys6 to Cys8 (DsAvr4-CbCys6-Cys8) showed that only the DsAvr4-CbCys6-Cys8 chimeric could not trigger Cf-4 mediated HR, indicating that regions between cysteine residues Cys6 to Cys8 are involved in Cf-4 recognition (Figure 5.6B).

Next, DsAvr4 chimeras carrying more defined regions between adjacent pairs of cysteine residues from CbAvr4 were tested (DsAvr4-CbCys1-Cys2, DsAvr4-CbCys2-Cys3, DsAvr4-CbCys3-Cys4, DsAvr4-CbCys4-Cys5, DsAvr4-CbCys5-Cys6, DsAvr4-CbCys6-Cys7 and DsAvr4-CbCys7-Cys8). When co-infiltrated with Cf-4, only DsAvr4-CbCys6-Cys7 did not trigger any necrosis whilst all the other DsAvr4 chimeras triggered Cf-4 mediated necrosis response on *N. tabacum* leaf at same level as the positive control. The results suggested that amino acid residues between Cys6 and Cys7 in DsAvr4 are involved in Cf-4 recognition (Figure 5.6B). A western blot was used to confirm that the loss of HR in DsAvr4-CbCys6-Cys7 is not due to unstable protein (Materials and Methods section 2.12). Apoplastic fluid was extracted from infiltrated *N. tabacum* leaves; however antibody against DsAvr4 failed to detect chimeric proteins in apoplast fluid. This could be due to low protein concentration in the apoplastic fluid.

To further confirm that DsAvr4 amino acid residues between Cys6 to Cys7 are involved in recognition by Cf-4, a reciprocal 'gain of recognition' test was done. In a CbAvr4 background, regions between CbAvr4 Cys6-Cys8 were exchanged with the corresponding regions from DsAvr4 or CfAvr4 (CbAvr4-DsCys6-Cys8 and CbAvr4-CfCys6-Cys8). CbAvr4 regions between Cys2-Cys4 were also exchanged with the corresponding regions from DsAvr4 or CfAvr4 (CbAvr4-DsCys2-Cys4 and CbAvr4-CfCys2-Cys4) as a control. Co-infiltration of CbAvr4 chimeras with Cf-4 on *N. tabacum* leaves showed that CbAvr4-DsCys6-Cys8 and CbAvr4-CfCys6-Cys8 were able to trigger Cf-4 mediated HR at the same level as DsAvr4 or CfAvr4 WT control, while CbAvr4-DsCys2-Cys4 and CbAvr4-CfCys2-Cys4 could not trigger any Cf-4 mediated HR (Figure 5.6C). These results suggested that one or more amino acid residues between DsAvr4 Cys6 to Cys7 are sufficient for Cf-4 recognition.

Figure 5.6 Co-infiltration of Cf-4 with Avr4 chimeras on *N. tabacum* leaves

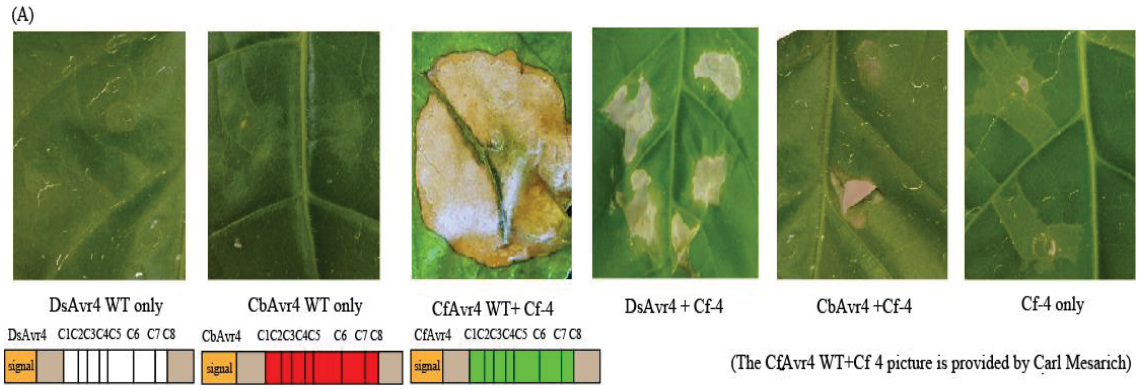

The lower sides of *N. tabacum* leaves were co-infiltrated with a mixture of Cf-4 and Avr4 chimeric cultures at OD_{600} = 1.0. The schematic diagrams of Avr4 chimeras are indicated below the pictures. (A) Infiltration of WT DsAvr4, CbAvr4 and Cf-4 alone did not trigger an HR. Co-infiltration of Cf-4 with WT DsAvr4 and CfAvr4 induced an HR, but CbAvr4 failed to do so.

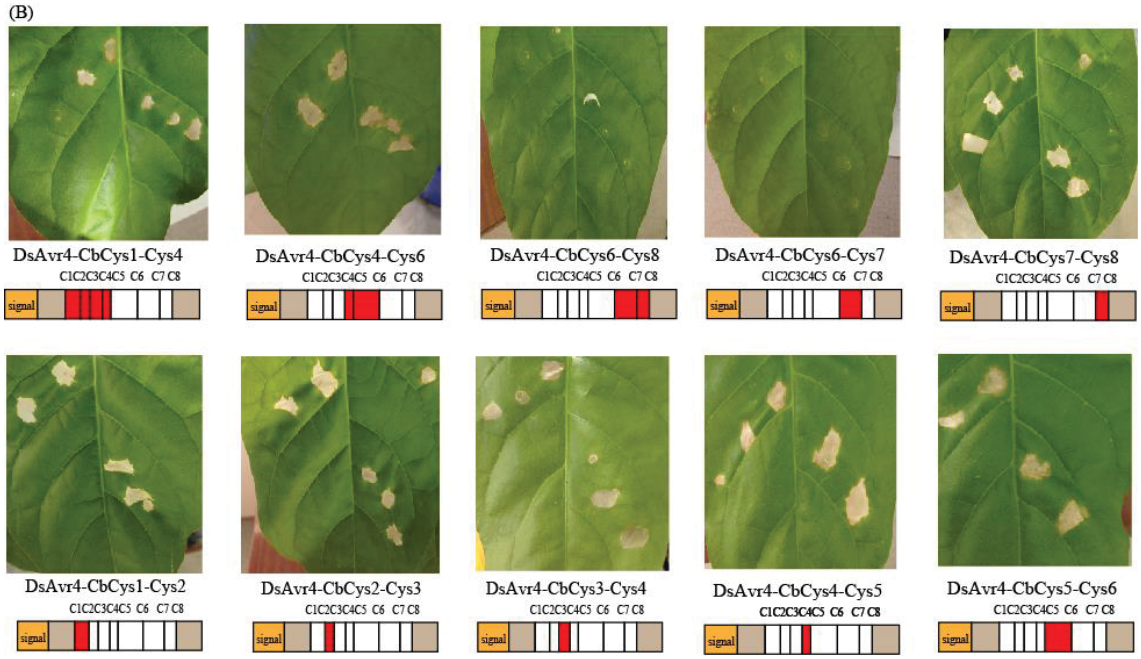

(B) Co-infiltration of Cf-4 with DsAvr4-CbCys1-Cys4, DsAvr4-CbCys4-Cys6, DsAvr4-CbCys1-Cys2, DsAvr4-CbCys2-Cys3, DsAvr4-CbCys3-Cys4, DsAvr4-CbCys4-Cys5, DsAvr4-CbCys5-Cys6 and DsAvr4-CbCys7-Cys8 triggers HR same as WT. While Co-infiltration of Cf-4 with DsAvr4-CbCys6-Cys8, DsAvr4-CbCys6-Cys7 cannot trigger Cf-4 mediated HR.

(C)

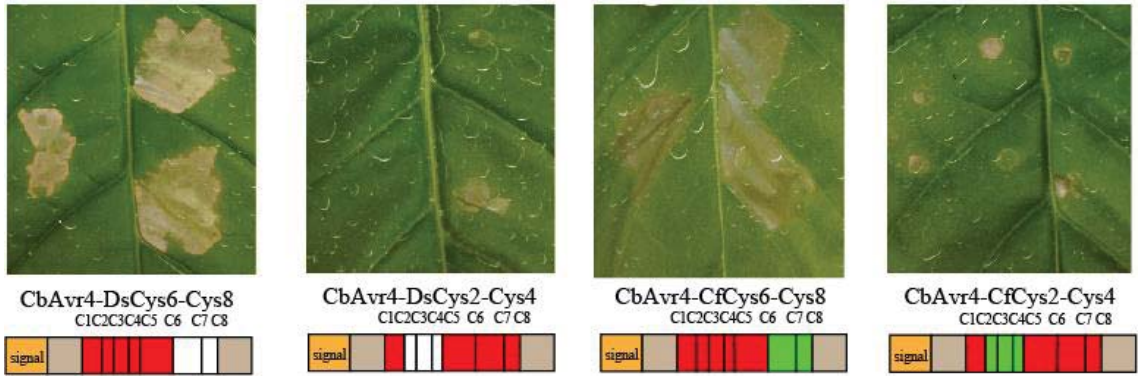

(C) When co-infiltrated with Cf-4, CbAvr4 chimeras carrying the region between Cys6 to Cys8 from DsAvr4 or CfAvr4 were able to trigger Cf-4 mediated HR at the same level as WT control, while CbAvr4-DsCys2-Cys4 and CbAvr4-CfCys2-Cys4 did not trigger any Cf-4 mediated HR.

5.2.3 Screening for necrosis inducing activity of *D. septosporum* effectors in *P. radiata*

5.2.3.1 *P. pastoris* heterologous protein production

In order to understand the cellular functions of DsAvr4, DsEcp2-1 and DsEcp2-3, heterologous protein expression in *P. pastoris* was used. Heterologously expressed *D. septosporum* effector proteins are used in infiltration assays. A necrosis and ethylene-inducing like protein (NLP), which is able to cause necrosis response in a non-host plant (*N. tabacum*) (Feng et al., 2014) was selected as a positive control in infiltration assays. However the gene model prediction of *D. septosporum NLP* (JGI protein ID 114624) showed it has an internal stop codon and is predicted to encode a pseudogene. Thus the *C. fulvum NLP* (CfNLP JGI: 194232) was trialed as a positive control for infiltration assays. cDNA of selected *D. septosporum* effectors and *CfNLP* were amplified by PCR using primers with restriction enzyme digestion sites (Materials and Methods section 2.4.1). The PCR products and expression vector were digested by restriction enzymes and the PCR products were inserted into *P. pastoris* expression vector by ligation (Materials and Methods section 2.3.8.1). The *P. pastoris* expression plasmids were constructed and transformed into *P. pastoris* strain GS115 (Materials and Methods section and 2.11.1). Transformants with the phenotypes His+ and Mut+ (able to grow on histidine deficient medium and to utilize methanol, indicating presence of recombinant plasmid) were selected for protein production.

In the *P. pastoris* system, the expressed protein has a yeast α-factor signal peptide and is secreted into the growth medium by the yeast cells. Culture filtrates were tested for the presence of secreted proteins using SDS-PAGE gels with Coomassie blue staining (Materials and Methods section 2.12.1). *P. pastoris* transformants were obtained that secreted DsAvr4, DsAvr4-CbCys6-Cys8, DsEcp2-1 or CfNLP into the culture filtrate and showed expected sized bands when checked on SDS-PAGE gels with Coomassie blue staining. One *P. pastoris* transformant (lane 4 in Figure 5.7) contained *DsEcp2-3* secreted protein of a smaller size than expected (23 kD instead of 29 kD). Apart from the 23kD bands, several other smaller bands were also shown on SDS-PAGE for DsEcp2-3, indicating more than one DsEcp2-3 truncated forms were produced (Figure 5.7). The expressed proteins each had a His-FLAG tag at the C-terminus; antibody against FLAG-tag was used in western blots to confirm the presence of the recombinant secreted proteins in the culture filtrate (Materials and Methods section 2.12.2). The FLAG-tagged DsAvr4, DsAvr4-CbCys6-Cys8, DsEcp2-1 and CfNLP were confirmed by western blotting. However none of the smaller bands produced by DsEcp2-3 could be detected, since the primary antibody used for western blot recognizes the FLAG-tag; the result suggested that the FLAG-tag was missing from all truncated DsEcp2-3 produced by *P. pastoris* (Figure 5.7).

Figure 5.7 Western blot confirmation of heterologous *D. septosporum* effector protein production

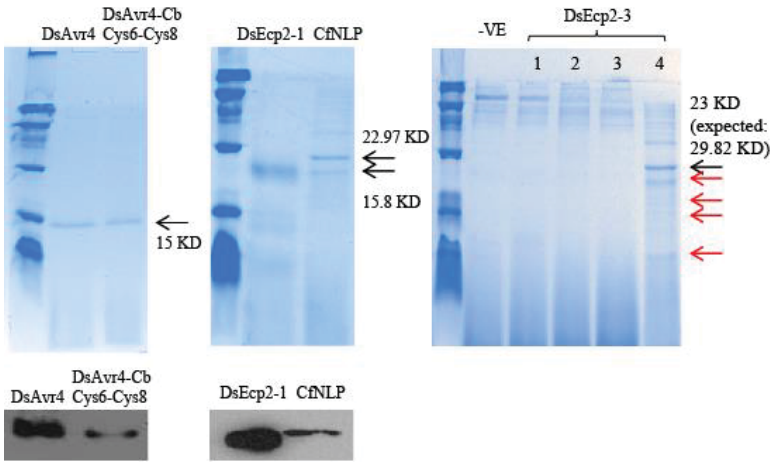

Heterologous expressed proteins were checked by SDS-PAGE Coomassie blue stained gels (top) and western blots (bottom). *P. pastoris* transformant carrying the empty expression vector was used as –ve control. The black arrows indicate the expected sizes of expressed proteins. Secreted DsAvr4 (15 KD), DsAvr4-CbCys6-Cys8 (15 KD), DsEcp2-1 (15.8 KD) and CfNLP (22.97 KD) proteins were confirmed by both methods. Three DsEcp2-3 transformants (1-3) showed no expression of DsEcp2-3 on SDS-PAGE gel, only one transformant (lane 4) showed a smaller sized band (23 kD instead of expected 29 kD) and several other smaller bands on the SDS-PAGE gel compared to the –ve control. None of the DsEcp2-3 bands could be detected by anti-FLAG tag antibody in western blot.

5.2.3.2 DsEcp2-1 and DsEcp2-3 are able to trigger a necrosis response in *N. tabacum*

CfEcp2-1 is able to trigger non-host necrosis in *Nicotiana* species (de Kock et al., 2004). To test whether selected *D. septosporum* effector proteins are able to trigger non-host necrosis, protein culture filtrates expressed by *P. pastoris* were tested by infiltration on *N. tabacum* leaves (Materials and Methods section 2.10). The CfNLP protein that was being trialed as a positive control caused necrosis seven days after infiltration on *N. tabacum*, but infiltration of culture filtrate from a *P. pastoris* transformant carrying empty expression vector (negative control) did not cause necrosis (Figure 5.8). Infiltration of DsAvr4 or DsAvr4-CbCys6-Cys8 did not trigger any necrosis response on *N. tabacum* leaves but DsEcp2-1 and DsEcp2-3 did cause necrosis (Figure 5.8). Two possibilities are suggested by the results: DsEcp2-1 and DsEcp2-3 target different non-host proteins or a common region shared by DsEcp2-1 and DsEcp2-3 is involved in interaction with the same non-host target. The experiment was repeated once and the same result was obtained on *N. tabacum* leaves.

Figure 5.8 Infiltration of expressed protein culture filtrates on *N. tabacum* leaves

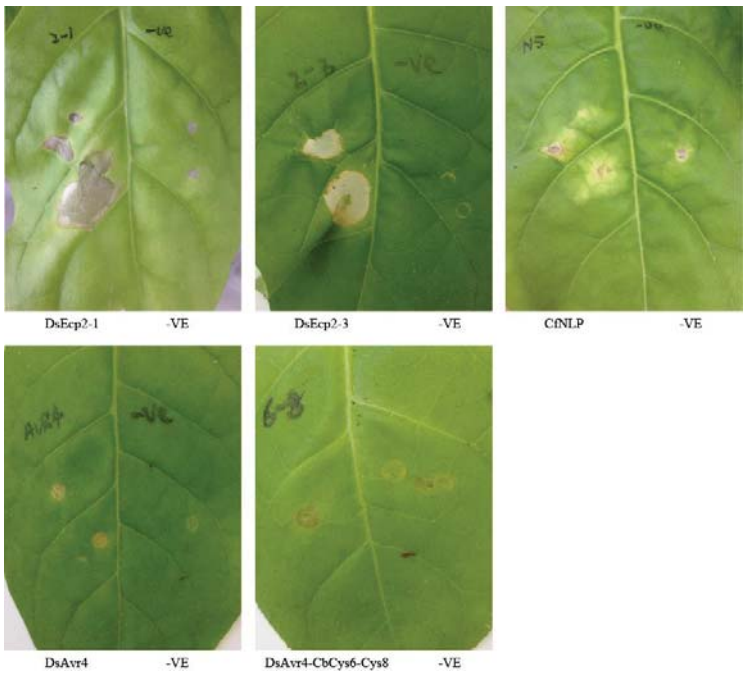

Expressed protein culture filtrates were infiltrated on three month old *N. tabacum* leaves. Pictures were taken seven days post-infiltration. CfNLP, known to trigger necrosis on *N. tabacum* was used as positive control. *P. pastoris* transformant carrying empty expressed vector was used as negative control. Both positive and negative controls showed expected necrosis and no-necrosis responses when infiltrated on *N. tabacum* leaves respectively. DsAvr4, DsAvr4-CbCys6-Cys8, DsEcp2-1 and DsEcp2-3 culture filtrates were infiltrated on *N. tabacum* leaves, of these, only DsEcp2-1 and DsEcp2-3 were able to cause necrosis. The experiment was repeated once and the same results were observed.

5.2.3.3 Screening for necrosis-inducing activity of *D. septosporum* effectors in *P. radiata*

Vacuum infiltration assays have been used to test interactions between *C. fulvum* effector proteins and the corresponding resistance proteins on tomato leaves (Bolton et al., 2008). To test whether vacuum infiltration could also be used on pine needles, the water soluble dye neutral red was used. Both younger and older needles collected from 6 month old seedlings were tested. Whole needles or cross sections of pine needles were observed (Figure 5.9). The neutral red solution was able to penetrate through stomata and stain the mesophyll cells under vacuum infiltration. No difference was observed between younger and older needles for neutral red solution penetration under the same vacuum conditions (data not shown). However not all of the stomata were stained, this could be due to some stomata being closed when the vacuum infiltration was performed as the neutral red was only able to penetrate through opening stomata. This result showed that vacuum infiltration assay was successful in allowing penetration of solution into intercellular spaces of pine needles and the assay could be used to test whether *D. septosporum* effectors are able to trigger necrosis on pine needles.

Figure 5.9 Vacuum infiltration of pine needles using 0.1% neutral red dye

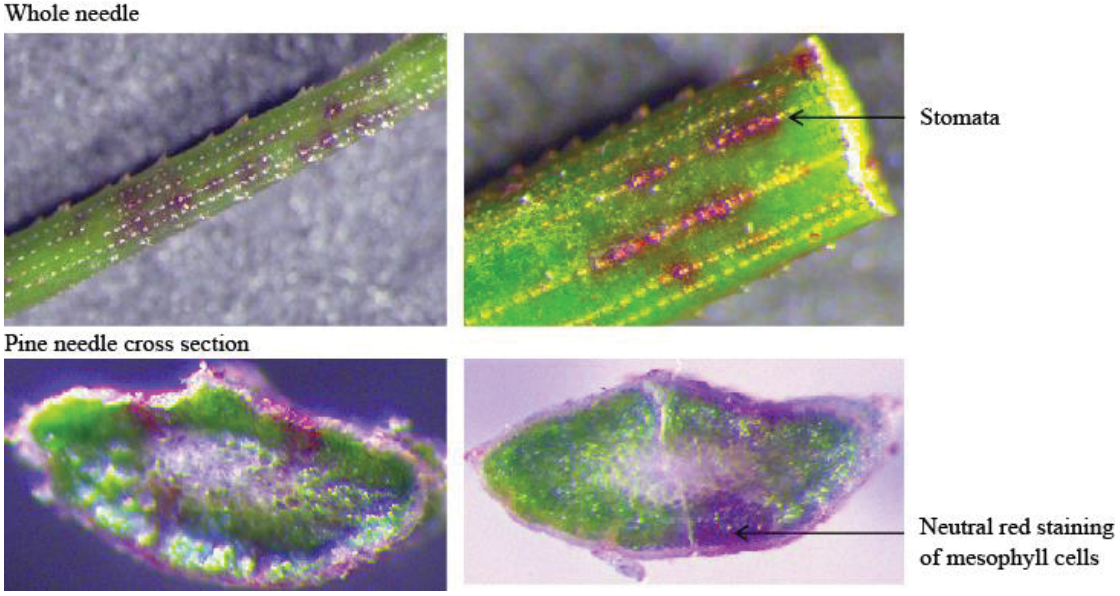

Vacuum infiltration of pine needles using 0.1% neutral red. On whole needle, some stomata were stained red. Pine needle cross section showed that neutral red was able to penetrate through stomata and stain the mesophyll cells.

To test whether infiltration of DsAvr4, DsEcp2-1 and DsEcp2-3 is able to cause necrosis on *P. radiata* needles, *P. pastoris* heterologous protein expression culture filtrates were used to screen detached *P. radiata* needles collected from 6 month old susceptible seedlings by infiltration. Three needles were tested for each *P. pastoris* culture filtrate and the experiment was repeated twice (Materials and Method section 2.10). Seven days post-infiltration, negative control *P. pastoris* (empty vector culture filtrate) did not cause any necrosis on all the needles tested. Positive control CfNLP caused necrosis on four out of six detached needles, indicating successful entry of culture filtrates through stomata into the apoplast of pine needles. However as shown in the neutral red infiltration result, penetration of culture filtrate does not happen on every needle tested; the number of open stomatal pores might affect penetration of culture filtrate. The preliminary infiltration showed that culture filtrates with DsAvr4 (4 out of 6 needles), DsAvr4-CbCys6-Cys7 (3 out of six needles) and DsEcp2-1 (5 out of six needles) triggered necrosis on pine needles (Figure 5.10). Infiltration of DsEcp2-3 failed to trigger any necrosis on all the pine needles tested (data not shown). The results indicate that DsAvr4 and DsEcp2-1 are able to induce necrosis on *P. radiata* needles. One interesting finding is when repeating the experiment, the freeze and thawed culture filtrates caused decreased number of lesions (total of 1-2 lesions/3 infiltrated needles) compared to freshly collected culture filtrate (total of 3-5 lesions/3 infiltrated needles). The freeze and thawed cycle could led to degradation of *D. septosporum* effector proteins in the filtrate; suggesting that correct protein folding of *D. septosporum* effectors is important for necrosis inducing activity on *P. radiata* needles.

Figure 5.10 Infiltration of *P. pastoris* culture filtrates on detached susceptible *P. radiata* needles

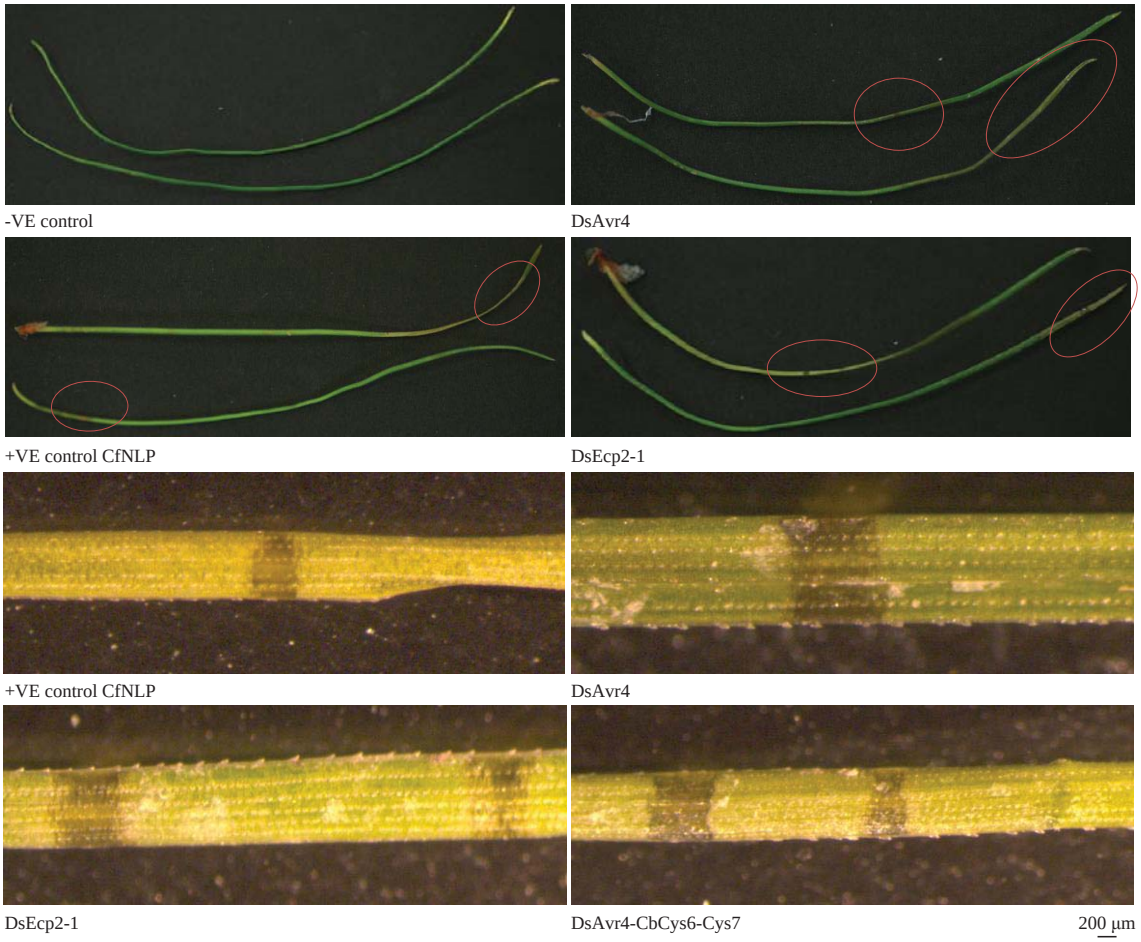

Infiltration of *P. pastoris* culture filtrates on susceptible *P. radiata* detached needles. Three detached susceptible needles were used for each culture filtrate. Pictures were taken seven days post-infiltration. The top pictures are whole needles; the red circles indicate the positions of necrosis. The bottom pictures are microscope images of lesions on detached needles. Infiltration of *P. pastoris* transformant carrying empty vector culture filtrate (-VE control) did not cause any necrosis while CfNLP (+VE control) caused necrosis on detached needles. Infiltration of DsAvr4, DsAvr4-CbCys6-Cys7 and DsEcp2-1 culture filtrates triggered necrosis on susceptible needles. The experiment was repeated once using frozen and thawed culture filtrates. A decreased number of lesions (total of 1-2 lesions/3 infiltrated needles) compared to when using freshly collected culture filtrate (total of 3-5 lesions/3 infiltrated needles) was observed.

5.3 Discussion

5.3.1 *DsEcp2-1* mutants showed increased lesion size compared to wild-type

D. septosporum is a hemibiotrophic fungus which has a symptomless biotrophic phase (Kabir et al., 2015). Deletion of *DsEcp2-1* led to bigger necrotic lesions compared to WT. The result suggested that DsEcp2-1 may act to inhibit a host target which is

involved in triggering necrosis during the biotrophic infection stage. Inhibition of HR by effectors is also seen in other biotrophic pathogens. Deletion of type III effector *AvrXacE2* secreted by *Xanthomonas axonopodis* pv. *citri*, which causes citrus canker, leads to bigger lesions compared to WT. A yeast two-hybrid assay showed that AvrXacE2 directly interacts with host protein LSD1, which is a transcription factor involved in regulating cell death. AvrXacE2 inhibits necrosis by disrupting LSD1 mediated cell death which benefits pathogen growth (Dunger et al., 2012). The role of DsEcp2-1 is discussed in more details in section 5.3.3.4.

Pathogenicity assays using a *DsAvr4* mutant suggested that DsAvr4 is not a virulence factor when *D. septosporum* infects *P. radiata*. This result was expected since, from the transcriptome time-course analysis, *DsAvr4* expression is very low both *in vitro* and *in planta*. Pine needle infiltration with DsAvr4 expressed in *P. pastoris* showed a necrotic response. It is possible that the *P. radiata* susceptible genotype may carry an R protein that recognizes DsAvr4. To avoid recognition, *D. septosporum* may suppress *DsAvr4* expression *in planta*. Gain of virulence in some *P. infestans* strains is achieved by effector gene silencing, such as the effector PiAVR2 that is recognized by resistance protein R2 in the host. Expression analysis by rt-PCR showed that the avirulent strain of *P. infestans* expresses *PiAVR2*, but the virulent strain suppresses *PiAVR*2 expression when infecting the R2 host genotype (Gilroy et al., 2011).

Orthologues of Ecp6 have been identified in several fungal species (Bolton et al., 2008). Targeted gene KO studies suggested that *CfEcp6* is required for virulence when infecting tomato (Bolton et al., 2008). Mutation of *CfEcp6* orthologues in rice pathogen *Magnaporthe oryzae Slp1* and maize pathogen *Setosphaeria turcica StEcp6* led to reduced colonization and smaller lesions respectively when infecting the hosts (Mentlak et al., 2012; Xue et al., 2013). Although the *⊿DsEcp6* showed a significant reduction in percentage infection compared to the WT, suggesting a possible role for *DsEcp6* as a virulence factor, the same phenotype was shown in the complemented *DsEcp6* strain. It cannot be ruled out that the reduction in infection levels was caused by other factors involved in the artificial infection process such as uneven spraying of fungal spores on the seedlings.

One interesting observation is that the single complemented *DsAvr4* strain showed a significant difference in percentage of infection compared to WT. Also the *DsEcp6* single complement strain did not 100% complement the mutant phenotype as mentioned above. One possible explanation is that the positions of *DsAvr4* and *DsEcp6* in the genome are important for their regulation. Protoplast mediated complementation can led to random insertion of the complementing gene into the genome (Turgeon et al., 2010), and position effects can alter levels of expression of complementing genes compared to that of the original gene in its wild type position. Some effectors are under chromatin mediated regulation. Deletion of histone H3 lysine 9 methyltransferase, which is involved in heterochromatin formation, results in up-regulation of effectors in *Leptosphaeria maculans* (Soyer et al., 2014). LaeA is a global regulator involved in chromatin mediated regulation of secondary metabolite biosynthesis in *Aspergillus* species. It regulates transcription in a similar mechanism to histone methyltransferases (Bok and Keller, 2004). In *D. septosporum*, dothistromin biosynthesis genes are regulated by DsLaeA (Chettri., et al data not published). Real-time PCR results showed that *DsAvr4* is up-regulated and *DsEcp6* is down regulated in a *DsLaeA* deletion strain compared to WT (Appendix table 4.2). The results support the hypothesis that *DsAvr4* and *DsEcp6* are under chromatin-mediated regulation.

The pathogenicity assay was repeated once with WT, *ΔDsAvr4*, *ΔDsEcp2-1*, *ΔDsEcp6* and single complemented strains using clonal *P. radiata* susceptible seedlings. However the overall infection rate was very low (less than 10% infection) for all the strains tested, and the result was not considered. The low infection rate could be due to the increased age of clonal cuttings, as aged cuttings have a higher level of resistance to *D. septosporum* (Bulman et al., 2013) compared to young cuttings which were used for the first pathogenicity assay. To confirm the larger lesion caused by *ΔDsEcp*2-1 and the possible reduced percentage of infection caused by *ΔDsEcp6*, the pathogenicity assays should be repeated using younger *P. radiata* clonal susceptible cuttings.

5.3.2 One or more amino acid residues in the conserved chitin binding domain of DsAvr4 are required for Cf-4 mediated hypersensitive response

Several Avr4 homologues have been identified: in the pine pathogen *D. septosporum* (DsAvr4), banana pathogen *M. fijiensis* (MfAvr4), sugar beet pathogen *C. beticola*

(CbAvr4) and celery pathogen *C.apii* (CaAvr4) (de Wit et al., 2012; Stergiopoulos et al., 2010). Domain swap experiments in this study showed that swap of the region between Cys6-Cys7 caused loss of recognition of DsAvr4 (DsAvr4 with CbAvr4 Cys6-Cys7) and gain of recognition of CbAv4 (CbAvr4 with DsAvr4 or CfAvr4 Cys6-Cys7) by Cf-4 indicating one or more amino acids in the DsAvr4 Cys6-Cys7 region is required for Cf-4 recognition. My findings support the previous domain swap result between CfAvr4 and CaAvr4 that CfAvr4-CaCys6-Cys7 chimeric is not recognized by Cf-4 while CaAvr4-CfAvr4Cys6-Cys7 is recognized by Cf-4 (Mesarich et al., 2015). Further experiments were carried out in Wageningen University with the aim of detecting the specific amino acid residues between Cys6-Cys7 that are involved in Cf-4 recognition. Point mutation of four conserved amino acids shared between CfAvr4, DsAvr4 and MfAvr4 showed that a Pro residue between Cys6-Cys7 is required for Cf-4 mediated HR (CfAvr4 Pro87, DsAvr4 Pro102 and MfAvr4 Pro83). Co-infiltration of CfAvr4, DsAvr4 and MfAvr4 chimeras carrying a Pro to Arg substitution with Cf-4 did not trigger any HR. CbAvr4 and CaAvr4 have an Arg residue (CbAvr4 Pro83 and CaAvr4 Pro83) which occupy the same position relative to Cys6-Cys7 as the Pro residue in CfAvr4, DsAvr4 and MfAvr4 (Figure 5.4). Co-infiltration of CbAvr4 and CaAvr4 carrying a Arg59 to Pro substitution with Cf-4 led to HR (Mesarich et al., 2015). Although only CfAvr4, DsAvr4 and MfAvr4 are able to trigger Cf-4 mediated HR (de Wit et al., 2012; Stergiopoulos et al., 2010), all WT and mutant forms of Avr4 can bind chitin (Mesarich et al., 2015).

It is not known if Cf-4 directly interacts with Avr4, however a gene-for gene model is predicted since CfAvr4 and MfAvr4 are shown to protect fungal cell chitin from degradation, suggesting that Avr4 probably lacks a virulence guardee monitored by Cf-4 (Stergiopoulos et al., 2010; van den Burg et al., 2006). Polymorphism analysis of CfAvr4 isoforms showed that CfAvr4 is under diversifying selection which is commonly associated with effectors involved in gene-for-gene interactions (Stergiopoulos et al., 2007). The loss of R protein mediated HR by a single amino acid mutation is also seen in other fungal effectors. For example, a Phe24 to Ser amino acid mutation in *M. oryzae* effector AvrPita leads to loss of direct recognition by R protein RGA5-A (Cesari et al., 2013). Even though the gene-for-gene model is considered most likely for the interaction between Cf-4 and Avr4, it has not been confirmed by experimental results.

Substitution of amino acid residues involved in Avr4 stability were shown to affect R protein triggered HR in the host. Studies of CfAvr4 isoforms showed that CfAvr4 with amino acid substitutions in Cys11 and Cys35 to Thr can still bind chitin, but those isoforms are more susceptible to plant proteases. CfAvr4 Cys mutant isoforms retained their role to protect fungi cell wall chitin from host protease, while the excess secreted CfAvr4 proteins were degraded by plant proteases from triggering Cf-4 mediated HR (Joosten et al., 1997; van den Burg et al., 2003). The Pro residue is located in the chitin binding domain which is predicted to be surface exposed (van den Burg et al., 2004). Polymorphism analysis of CfAvr4 isoforms showed that no naturally occurring mutations in Pro were identified so far, suggesting that Pro may have a role in CfAvr4 chitin-binding activity during infection (Stergiopoulos et al., 2007). However this is in conflict with the result that CfAvr4, and DsAvr4 with a Pro to Arg substitution can still bind chitin (Mesarich et al., 2015). It is possible that the Pro residue is involved in Avr4 stability *in planta*, and that the loss of recognition of mutant Avr4 Pro to Arg proteins by Cf-4 is due to protein instability in the apoplastic fluid in *N. tabacum*. A western blot was performed using apoplast fluid extracted from *N. tabacum* leaves and no mutant Avr4 protein could be detected, but no WT Avr4 could be detected either (Mesarich et al., 2015). As mentioned before, antibody against DsAvr4 failed to detect DsAvr4 chimeras from apoplastic fluid as well (Section 5.2.2). This could be due to low protein concentration in the apoplastic fluid.

Amino acid alignments of Avr4 (Figure 5.4) showed that, apart from Pro, several other amino acid residues are conserved between CfAvr4, DsAvr4 and DsAvr4 but not in CaAvr4 and CbAvr4. It is possible that one or more of these amino acid residues are also required for Cf-4 recognition. A natural isoform of MfAvr4 that carries a Thr109 to Ile substitution which is outside of the chitin binding domain is not recognized by Cf-4. But as mentioned before, the stability of this MfAvr4 isoform *in planta* is not clear (Stergiopoulos et al., 2014). Future experiments should be carried out to determine the stability of Avr4 mutant chimeras *in planta* to confirm the role of Pro in Cf-4 recognition.

5.3.3 Screening for necrosis inducing activity of *D. septosporum* effectors

5.3.3.1 *D. septosporum* contains a *DsNLP* pseudogene

The necrosis and ethylene-inducing peptide 1 (Nep1)-like proteins (NLP) that are found in many fungal and oomycete pathogens have broad spectrum toxicity against dicotyledonous plants (Qutob et al., 2006). The finding that *C. fulvum*, a biotroph, has a functional *CfNLP* gene, while *D. septosporum*, a hemibiotroph, contains a non-functional *DsNLP* pseudogene is interesting, because expression of NLP is thought to be related to the switch from biotrophy to necrotrophy in some oomycete pathogens (Qutob et al., 2002). It is possible that *C. fulvum* does not express its *CfNLP* gene (JGI: 194232) when infecting tomato plants. Interestingly, another biotrophic pathogen, *Hyaloperonospora arabidopsidis*, produces NLP protein (HaNLP) that doesn't trigger necrosis on tobacco or *Arabidopsis* plants. In this case a domain swap experiment between HaNLP and a functional NLP from *P. infestans* identified an exposed domain involved in inhibiting necrosis, indicating a different role of biotrophic NLP during infection (Cabral et al., 2012). Given that CfNLP causes necrosis on tobacco a similar type of inhibitory role in *C. fulvum* seems unlikely.

The wheat pathogen *Zymoseptoria tritici* (previously called *M. graminicola*) contains a single copy of *MgNLP*, which is highly expressed at the end of the symptomless stage before early lesion formation during infection (Motteram et al., 2009). However whilst MgNLP is able to trigger necrosis on *Arabidopsis* it does not on wheat leaves. A mutation study showed that MgNLP is dispensable during infection of susceptible wheat; the mutant strain showed no difference in infection compared to WT. The authors hypothesized that NLP may play a role in competing with other microorganisms when infecting the host, since the host cell death caused by *Z. tritici* leads to release of nutrients that could benefit other microorganisms on wheat leaves. The expression pattern of *MgNLP* is consistent with MgNLP acting before host cell death to inhibit other microorganisms competing when the nutrients are released (Motteram et al., 2009). Lack of functional NLP in *D. septosporum* shows that the function of DsNLP is also dispensable during infection of pine. *D. septosporum* produces a broad range toxin dothistromin which is a virulence factor (Kabir et al., 2015). Unlike most other secondary metabolite biosynthesis which occurs during late exponential phase, dothistromin is produced during the onset of exponential growth and may also have a

role in competing with other microorganisms during infection of pine (Schwelm et al., 2008; Zhang et al., 2010).

5.3.3.2 *Pichia pastoris* heterologous protein production

P. pastoris was used for heterologous expression of *D. septosporum* effectors in this study. This eukaryotic expression system allows post-translational modification such as disulfide bond formation and glycosylation (Daly and Hearn, 2005). The recombinant *D. septosporum* effectors carried a His-FLAG tag at the C-terminus for western blot detection and were fused to *P. pastoris* α-signal peptide in the expression vector for secretion. From *P. pastoris* culture filtrates, DsEcp2-3 showed a smaller sized band than expected and on SDS-PAGE but could not be detected by western blotting. This suggested that DsEcp2-3 is secreted into the growing culture by *P. pastoris*, but that proteolytic degradation of DsEcp2-3 may have occurred after secretion. A study by Sinha et. al. (2005) showed that *P. pastoris* protease activity was not detected during the glycerol growing phase; however the protease activity increased during the methanol induction stage, which is the time at which Ds-effectors were secreted in the current study. The online protease cleavage site prediction tool PeptideCutter (http://web.expasy.org/peptide_cutter/) showed that DsEcp2-3 carries several putative protease cleavage sites which may have led to production of a truncated protein (data not shown). For future experiments, protease inhibitors could be used during the *P. pastori*s growth to avoid protein degradation, or a protease deficient *P. pastoris* strain could be used for DsEcp2-3 expression.

5.3.3.3 DsEcp2-1 and DsEcp2-3 are able to trigger necrosis in *N. tabacum*

Infiltration of effector proteins on *N. tabacum* leaves showed that DsEcp2-1 and DsEcp2-3 are able to trigger necrosis in non-host species. Non-host resistance (NHR) can be classified into two types. Type I NHR does not produce any visible symptoms; the resistance is activated by genes involved in primary plant immunity such as PAMP receptors. Type II NHR is associated with rapid localized necrotic HR (Uma et al., 2011). *C. fulvum* Ecp2-1 is able to trigger a type II NHR in *Nicotiana* species (de Kock et al., 2004; Laugé et al., 2000). Recognition of CfEcp2-1 is mediated by a single dominant *Nicotiana* gene, but PCR and hybridization assays showed that this gene has no homology to any known Cf R proteins. It is possible that DsEcp2-1 and DsEcp2-3 are recognized by the same dominant gene in *N. tabacum*. A common region shared by

DsEcp2-1 and DsEcp2-3 may be required for recognition by the dominant gene in *N. tabacum*.

DsAvr4 and DsAvr4-CbAvr4Cys6-Cys7 did not trigger any necrosis on *N. tabacum* leaves. One possibility could be due to low level of DsAvr4 and DsAvr4-CbAvr4Cys6-Cys7 protein in the culture filtrate. The incorporation of expression vector sequence into the *P. pastoris* genome is random. *P. pastoris* transformants carrying multiple copies of expression vector sequence in the *P. pastoris* genome could led to higher levels of protein production in the culture filtrate compared to *P. pastoris* transformants carrying a single copy of expression vector sequence. The same result was obtained from the domain swap experiments; agroinfiltration of DsAvr4 on *N. tabacum* did not trigger any necrosis, while co-agroinfiltration of DsAvr4 with Cf-4 led to necrosis. Together those results suggested that DsAvr4 lacks a target in *N. tabacum*.

To gain a more complete picture of non-host necrosis inducing activity by DsAvr4, DsEcp2-1 and DsEcp2-3, the experiment should be repeated using serial dilutions of purified *D. septosporum* effector protein from *P. pastoris* culture filtrates.

5.3.3.4 Screening for necrosis inducing activity on *P. radiata*

Infiltration of DsAvr4 triggered necrosis on dothistroma-susceptible *P. radiata* needles. One hypothesis is that Cf-4 like R proteins may be present in *P. radiata* that can recognize DsAvr4. The finding that the expression of *DsAvr4* was low *in planta* also supported this hypothesis. One interesting finding is that the DsAvr4 chimeric that carried the Cys6-Cys7 region from CbAvr4 also triggered HR on pine needles, despite the lack of necrosis induction by this chimeric protein on tobacco leaves. As mentioned in the Avr4 domain swap discussion (section 5.3.2), other amino acid residues apart from Pro may be required for R protein recognition. Alternatively a Cf-4 like R protein in *P. radiata* may carry functional polymorphisms that allow recognition of Avr4 isoforms.

Infiltration of DsEcp2-1, but not DsEcp2-3, also triggered necrosis on susceptible *P. radiata* needles. This suggests that Cf-Ecp2 like R proteins that can recognize DsEcp2-1 but not DsEcp2-3 may be present in the genome of the *P. radiata* cultivar used. A

different R protein may be involved in DsEcp2-3 recognition. Similar loss of recognition by Cf-Ecp2 was also seen in *M. fijiensi*s MfEcp2-3. The tomato Cf-Ecp2 R protein is only able to recognize MfEcp2-1 but not MfEcp2-2 and MfEcp2-3 (Stergiopoulos et al., 2010). Or from SDS-PAGE gel result, *P. pastoris* produced a truncated form of DsEcp2-3 which could led to non-functional protein product that abolished R protein recognition.

Ecp2-1 is shown to have different virulence functions in biotrophic and hemibiotrophic fungi (Lauge et al., 1997; Stergiopoulos et al., 2010). In *C. fulvum*, deletion of *CfEcp2-1* led to reduced colonization of tomato leaves. A microscopy study showed that the mutant strain produced short hyphae that showed restricted entry through stomata. In cases when the hyphae did penetrate, abnormal mycelium structure with short and twisted internodes occurred (Lauge et al., 1997). Furthermore, tomato plants inoculated with the *CfEcp2-1* mutant stain showed faster pathogen-induced HR responses such as leaf desiccation compares to WT-inoculated tomato. Apoplast fluid extraction analysis from tomato with the *CfEcp2-1* mutant stain showed that more pathogenesis-related proteins were produced compared to WT-inoculated tomato (Lauge et al., 1997). All those results suggested that CfEcp2-1 is involved in suppressing host defense responses during infection of tomato, in accordance with the biotrophic lifestyle of *C. fulvum* which requires living host cells for nutrients (de Wit et al., 2012; Lauge et al., 1997). MfEcp2-1 from the hemibiotroph *M. fijiensis* is recognized by the tomato R protein Cf-Ecp2 and is able to trigger Cf-Ecp2 mediated HR in tomato. However in the absence of Cf-Ecp2, a weaker HR is induced by MfEcp2-1 in tomato plants, suggesting that MfEcp2-1 has a host target which is protected by Cf-Ecp2 and triggers host-target mediated necrosis. This could benefit the fungus in later infection stages when *M. fijiensis* is in the necrotrophic phase of its life cycle. On the other hand CfEcp2-1 does not trigger HR in the absence of Cf-Ecp2; in this case the CfEcp2-1 might have mutated to avoid recognition of the host target protected by Cf-Ecp2, since *C. fulvum* is a biotroph (Stergiopoulos et al., 2010).

Because *D. septosporum* is a hemibiotrophic fungus, it is expected that DsEcp2-1 will act like MfEcp2-1, however DsEcp2-1 did not trigger HR in the absence of Cf-Ecp2 in tomato plants, suggesting that DsEcp2-1 may have a different role in virulence compared to MfEcp2-1 (de Wit et al., 2012). As discussed in section 5.3.1, deletion of

DsEcp2-1 caused larger lesions on needles compared to WT, suggesting that DsEcp2-1 acts in a similar way to CfEcp2-1 in inhibiting necrosis. In this case DsEcp2-1 might inhibit a host target which is involved in triggering necrosis during the biotrophic stage. A model of interaction between DsEcp2-1, the host target and putative Cf-Ecp2 like R protein in *P. radiata* is shown in Figure 5.11. However two observations raise questions about this model. First transcriptome analysis (Chapter 3 section 3.2.2) showed that *DsEcp2-1* expression was low in early infection stage. *DsEcp2-1* expression was up-regulated approximately 30-fold at mid infection stage, which is when necrosis occurred, so does not support the role of DsEcp2-1 as a necrosis inhibitor at early biotrophic stage. In contrast expression of *CfEcp2-1* was already highly induced at early stage (4 days post-inoculation) (Lauge et al., 1997; van den Ackerveken et al., 1993) and reached peak expression at mid infection stage (8 days post-inoculation) (de Wit et al., *unpublished*), consistent with a role of CfEcp2-1 in suppressing host defense response at an early infection stage. Further work is required to determine whether DsEcp2-1 is highly expressed at an even earlier stage than that sampled for the 'early' transcriptome data, which were taken 3 weeks post inoculation. The second observation that raises questions about the model is that the pine needles used for infiltration study were collected from susceptible *P. radiata* seedlings; the presence of R proteins with major effects on resistance is not expected.

To understand the role of DsEcp2-1 during infection of *P. radiata*. Needles with different levels of resistance to *D. septosporum* should be tested in the infiltration assay to test for the presence of R proteins against DsEcp2-1. The pathogenicity assay should be repeated to confirm the phenotype caused by Δ*DsEcp2-1*. More aspects such as time of lesion appearance and fungal biomass during infection should be considered to compare the pathogenicity assay results between Δ*DsEcp2-1* and WT strains. The host defense responses such as expression of pathogenesis-related proteins should be assessed comparing Δ *DsEcp2-1* inoculated and WT inoculated pine seedlings. Microscopy work comparing Δ*DsEcp2-1* and WT hyphae morphology during infection of pine should also be included.

In summary, the domain swap experiments in this study showed that swap of the region between Cys6-Cys7 caused loss of Cf-4 recognition of DsAvr4 (when swapped with CbAvr4) and gain of Cf-4 recognition of CbAv4 (when swapped with DsAvr4 or CfAvr4). Those findings support the previous domain swap results in CfAvr4 that the region between Cys6-Cys7 is involved in Cf-4 recognition. Further experiments carried out at Wageningen University showed that a Pro residue located in the chitin binding domain between Cys6-Cys7 in DsAvr4 is important for Cf-4 recognition, and may have a role in DsAvr4 stability. Deletion of the *DsAvr4* gene did not affect fungal physiology *in vitro* or alter virulence. Likewise deletion of *DsEcp6* did not affect virulence. In contrast, deletion of *DsEcp2-1* led to enlarged lesions compared to WT, suggesting that DsEcp2-1 may suppress a host target and inhibit necrosis during the biotrophic infection stage. But curiously DsEcp2-1, and also DsEcp2-3, was able to trigger a non-host necrosis response in *N. tabacum* suggesting interaction with a host protein in that species. Infiltration of DsAvr4, DsEcp2-1 and DsEcp6 *P. pastoris* expression culture filtrate also triggered necrosis in *P. radiata* needles, suggesting that R proteins that recognise *D. septosporum* effectors may be present in *P. radiata*.

Figure 5.11 Proposed function of DsEcp2-1 when infecting *P. radiata*

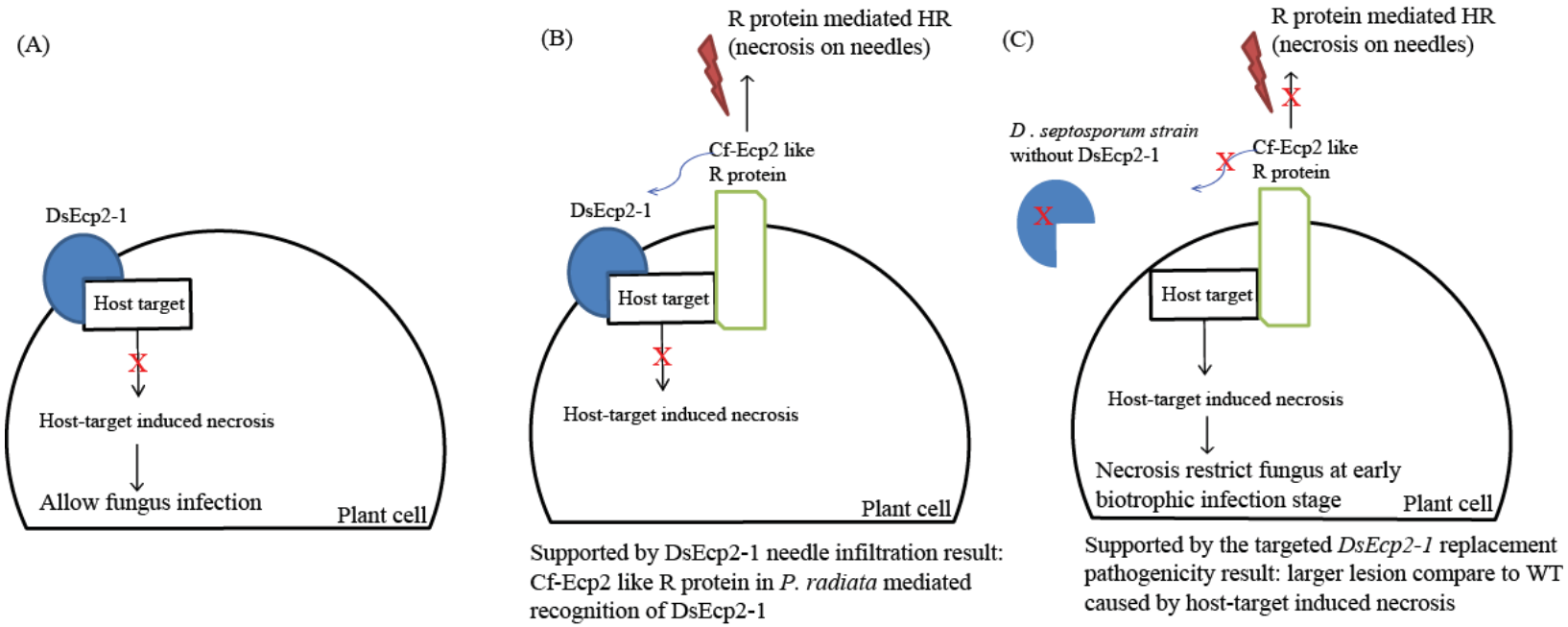

The model suggests: (A) DsEcp2-1 is able to interact with a host protein which is involved in necrosis induction in the host. Interaction of DsEcp2-1 with the host target inhibits host-protein mediated necrosis and allows infection of *D. septosporum* during early biotrophic phase. (B) In the presence of a Cf-Ecp2 like R protein, DsEcp2-1 is recognized and triggers R protein mediated necrosis in the host. This is supported by the needle infiltration result that DsEcp2-1 is able to cause necrosis on *P. radiata* needles. (C) In the case of *D. septosporum* KO strains without *DsEcp2-1*, the host target is able to induce necrosis and restrict fungal growth in early biotrophic infection stage. This is supported by targeted *DsEcp2-1* replacement pathogenicity result that *⊿DsEcp2-1* causes larger lesion compare to WT.

Chapter 6. Allelic variation of candidate effector genes in *Dothistroma septosporum*

6.1 Introduction

There is a constant evolutionary arms race between pathogen effectors and host R proteins. Genes under positive selection pressure evolve rapidly and show high variability and adaptability. Effectors that have an important role in pathogen virulence are often under positive selection to avoid R protein recognition (Oliva et al., 2011; Sperschneider et al., 2014; Stergiopoulos et al., 2013).

Gain of virulence can be achieved by sequence diversification, deletion of recognized effector genes or silencing of effector genes (Anderson et al., 2010; Ma and Guttman, 2008; Stukenbrock and McDonald, 2009). For example *Melampsora lini* effector *AvrP123* is recognized by flax proteins P1, P2 and P3. *AvrP123* isoforms sequenced from several field-collected *M. lini* showed a high level of polymorphisms. Agrobacterium-mediated transient expression of *AvrP123* isoforms on flax lines carrying P1, P2 or P3 showed that several *AvrP123* isoforms are no longer recognized by the R protein (Barrett et al., 2009). The *C. fulvum* effectors also showed a high level of allelic variation (for detailed discussion see section 1.4.3).

Understanding the evolution of effectors can provide information to help screen for new effector candidates. Studies show that effectors that have a role in pathogen virulence are often under positive selection (Aguileta et al., 2012; Pedersen et al., 2012; Win and Kamoun, 2008). For example in wheat stem rust *Puccinia graminis* f. sp. *Tritici*, *in planta* up-regulated pathogen-associated genes are under positive selection (Sperschneider et al., 2014). Understanding the genetic diversity of pathogen effectors also provides important information to screen for more durable resistant host genotypes in the field. Resistance that depends on a single dominant resistance protein can be easily overcome by deletion or mutation of pathogen effectors (Ma and Guttman, 2008; Stukenbrock and McDonald, 2009). However if the recognized effector domain is important for virulence function, mutations in the recognized effector domain could led to loss of virulence function of the effector. For example *Pseudomonas syringae* pv. *glycinea* effector AvrB is recognized by soybean R protein Rpg1-b. AvrB is able to

promote *P. syringae* pv. *glycinea* growth on susceptible soybean plants. Mutations in *AvrB* led to loss of R protein recognition; however the mutant strain also lost its ability to promote bacteria growth on susceptible soybean plants (Ong and Innes, 2006).

A global collection of *D. septosporum* strains from various pine species was used to study the allelic variation of *D. septosporum* effector candidates. Nucleotide substitutions in gene coding regions can leads to synonymous (do not change amino acid) or non-synonymous (change amino acid) changes. The number of synonymous or non-synonymous changes can be used to assess the selection pressure on a particular gene. dN/dS ratios which calculate the nonsynonymous to synonymous substitution rates (Aguileta et al., 2009; Hurst, 2002) were used to estimate whether *D. septosporum* effector genes are under positive selection. DNA from this global collection was provided by Dr Irene Barnes from University of Pretoria, South Africa and is listed in Table 6.1

Table 6.1 Global collection of *D. septosporum* strains and sequencing results

Continent	Strain Name	Country	Avr4	Ecp2-1	Ecp2-3	Ecp4	Ecp5	Ecp6	Ecp13	Ecp14	Ds69335
Asia	BHU1	Bhutan							x		
Oceania	NZE2	New Zealand									
	NZE10	New Zealand									
	AUST6	Australia								**x**	
North America	ORE12	USA							**x**		
	USA-MON8	USA							**x**		
	CAN3	Canada							**x**		
Africa	SAF1625	South Africa									
	SAF4	South Africa									
	KEN4	Kenya									**x**
South America	GUA1	Guatemala									
	GUA-N1	Guatemala						**x**			
	COL-N	Colombia									
	COL-C	Colombia									
	BRZ1	Brazil							**x**		
	CHI17	Chile							x		**x**
	ECU 13	Ecuador							**x**		**x**
Europe	GRED1	Greece								**x**	
	ROM11	Romania			**x**			**x**			
	SLV1	Slovakia									
	POL4	Poland									
	CZE1	Czech Republic									
	ATRA4-2	Austria						**x**		**x**	
	Hun2-53	Hungary									
	ALP3	Germany									
	DPAR1	Denmark			**x**						
	FRA1	France									
	SP2	Spain									
	UK402	England							**x**		
	SCO484	Scotland			**x**				**x**	**x**	
	FIN3.2	Finland									

The global collection of *D. septosporum* strains is organized by continent, along with date of collection and *Pinus* host species, where known, are listed in the table. Black x indicates sequence data not available for that *D. septosporum* stain (see text). Primers used for PCR were listed in Appendix 5.6

6.2 Results

6.2.1 Presence/absence of effectors in a global collection of *D. septosporum* strains

Nine *D. septosporum* effector gene candidates (*DsAvr4*, *DsEcp2-1*, *DsEcp2-3*, *DsEcp4*, *DsEcp5*, *DsEcp6*, *DsEcp13*, *DsEcp14* and *Ds69335*) were amplified by PCR (Materials and Methods section 2.4.1) using primers that bound to the 5' or 3' flanking regions. For genes that could not be amplified using the first set of flanking primers, combinations of different primers that bind to the 5' or 3' UTR and gene coding regions were used to repeat the PCR. *DsAvr4*, *DsEcp2-1*, *DsEcp4* and *DsEcp5* were amplified from all the thirty-one *D. septosporum* strains tested. On the basis of lack of amplification, *DsEcp2-3* appears to be absent from three European strains (ROM11, DPAR1 and SCO484). *DsEcp6* appears to be absent from two European strains (ROM11 and ATRA4-2) and a Guatemala strain (GUA-N1). *DsEcp14* appears to be absent from AUST6, GRED1 and ATRA4-2 strains. *Ds69335* appears to be absent from three strains collected in the Southern hemisphere (KEN4, CHI17 and ECU13). *DsEcp13* appears to be absent from nine strains tested (BHU1, ORE12, CAN3, BRZ1, CHI17, ECU13, UK402, USA-MON8 and SCO484) suggesting that R proteins that recognize DsEcp13 may be present in pine species, that *DsEcp13* may not be required for full virulence in *D. septosporum*, and the gene is dispensable without affecting fungal fitness. However although more than one primer set was used in PCR amplification in each of these cases, the presence of those effectors cannot be completely excluded by a negative PCR test due to low sequence similarities of some fungal effectors (Stergiopoulos and de Wit, 2009), or highly divergent effector flanking regions.

As mentioned in Chapter 3, BlastP analysis using *C. fulvum CfAvr2*, *CfAvr9* and *CfAvr4E* amino acid sequences against the entire set of predicted proteins from the New Zealand *D. septosporum* genome (NZE10) suggested this strain does not contain homologues of these effector genes. From a previous study the Guatemalan strain (GUA1 collected in 1983) is known to have many genetic differences compared to NZE10 and is thought to belong to an ancestral grouping of *D. septosporum* (Bradshaw et al., 2013). Therefore the GUA1 strain was screened for the presence of *CfAvr2*, *CfAvr9* and *CfAvr4E* by gradient PCR (45 to 55 ℃ primer annealing temperature)

using primers designed according to *C. fulvum* sequences. Homologues of *CfAvr2*, *CfAvr9* and *CfAvr4E* were not detected in *D. septosporum* GUA1 strains by PCR (data not shown). However, due to the same reasons as mentioned above, the presence of *CfAvr2*, *CfAvr9* and *CfAvr4E* in *D. septosporum* GUA1 cannot be completely excluded.

6.2.2 Allelic variation of candidate effector genes

The PCR products were sequenced by Macrogen (Materials and Methods section 2.3.10). For all the effectors tested the amino acid sequences were compared to the New Zealand (NZE10) strain. The percentages of amino acid identity for each of the nine effectors amongst the thirty-one *D. septosporum* strains are shown in Appendix table 4.3. The allelic variations of the nine *D. septosporum* effectors are summarised in Table 6.2. The dN/dS ratio was calculated using MEGA6.0 (Kumar et al., 2008) (Table 6.2). *DsEcp2-3* and *DsEcp13* showed the highest and lowest total number of nucleotide differences and non-synonymous amino acid changes respectively. Out of nine effectors tested, only *DsEcp4* and *DsEcp5* showed a dN/dS ratio greater than one, suggesting these two genes are under positive selection. An alternative way to determine evidence of positive selection, a Codon based Z-test (Nei and Gojobori, 1986) was also calculated using MEGA6.0 (Kumar et al., 2008). Using this method, DsEcp4 and DsEcp5 showed *P* values greater than 0.05, thus the Codon based Z-test result suggested that the hypothesis of dN/dS>1 (positive selection) was not significant (Table 6.2).

D. septosporum strains collected from Southern hemisphere countries (New Zealand, Australia, South Africa, Kenya, Brazil, Ecuador and Chile) showed fewer non-synonymous amino acid variations compared to *D. septosporum* collected from the Northern hemisphere, in all nine effectors tested. All three strains from Oceania (NZE2, NZE10 and AUST6) have identical amino acid sequences for all effectors tested, although for DsEcp14 the AUST6 sequence was not available, possibly due to variations at the primer binding site for PCR amplification. Strains from Brazil (BRZ1), Chile (CHI17) and Ecuador (ECU13) showed 100% amino acid identity to the Oceania strains for all the effectors tested except for DsEcp2-1, DsEcp2-3 and DsEcp14. Two strains from Guatemala (GUA1 and GUA-N1) and two strains from Colombia (COL-N, and COL-S) showed the highest number of amino acid variants for DsAvr4, DsEcp2-3, DsEcp4, DsEcp5 and Ds69335.

Table 6.2 Summary of allelic variations of *D. septosporum* effectors

Gene	nt/aa	Intron	dN	dS	dN/dS	Codon based Z-test (*P* value)
DsAvr4	33/19	1	0.01	0.02	0.50	1
DsEcp2-1	28/12	2	0.01	0.02	0.50	1
DsEcp2-3	67/41	4	0.011	0.025	0.44	1
DsEcp4	65/39	8	0.017	0.013	1.31	0.20
DsEcp5	23/14	0	0.005	0.003	1.67	0.12
DsEcp6	26/5	4	0.001	0.018	0.06	1
DsEcp13	12/3	3	0.002	0.019	0.11	1
DsEcp14	26/11	4	0.004	0.017	0.24	1
Ds69335	18/6	2	0.002	0.01	0.20	1

nt/aa: number of total nucleotide variation/ number of total non-synonymous amino acid changes

Intron: number of nucleotide variation at intron position

dN: number of non-synonymous differences per non-synonymous site from averaging over all sequence pairs

dS: number of synonymous differences per synonymous site from averaging over all sequence pairs

dN/dS: dN/dS>1 indicate positive/diversifying selection. dN/dS<1 indicate negative/purifying selection. dN/dS=1 indicate neutral selection

Codon based Z-test: An alternative test used to determine the probability of rejecting the null hypothesis (dN/dS=1, neutrality) and in favour of the alternative hypothesis (dN/dS>1, positive selection). A *P* value <0.05 is considered significant at the 5% level. DsEcp4 and DsEcp5 have *P* values greater than 0.05 and the result did not support the alternative hypothesis (dN/dS>1, positive selection).

The amino acid substitutions for DsAvr4 are shown in Figure 6.1. For *DsAvr4* 33 DNA polymorphisms were identified resulting in 19 amino acid substitutions. One DNA polymorphism was present inside the intron. Two amino acid substitutions were present in the signal peptide (ORE12 has Gly to Ala substitution; both Colombia strains have Gln to His substitution). However neither mutations affected the signal cleavage site (predicted using SignalP 4.0 (Petersen et al., 2011)). The Guatemala and Colombia strains contain a high number of amino acid substitutions compared to the New Zealand NZE10 strain. No amino acid substitutions were present between Cys6-Cys7 (Figure 6.1) which contains the chitin binding domain and was previously shown to be involved in Cf-4 recognition (Chapter 5 section 5.2.2).

The amino acid substitutions for DsEcp2-1 are shown in Figure 6.2. For *DsEcp2-1*, 28 DNA polymorphisms were identified which resulted in 12 amino acid substitutions. Two DNA polymorphisms were present inside the intron. Both Colombia strains carried an amino acid substitution in the signal peptide of His to Gln, but this mutation does not affect the signal cleavage site in DsEcp2-1 (predicted using SignalP 4.0 (Petersen et al.,

2011)). Out of thirty-one *D. septosporum* strains used, two strains from each of New Zealand, South Africa, USA and Guatemala were collected at different time points. (NZE2 collected in 1965, NZE10 collected in 2005; SAF1625 collected in 1984, SAF4 collected in 2002; ORE12 collected in 1983, USA-MON8 collected in 2006; GUA1 collected in 1983, GUA-N1 collected in 2012). Amino acid alignments of DsEcp2-1 showed that the old and new strains from the same country had 100% amino acid identity. The USA strains (ORE12 and USA-MON8), South Africa strains (SAF1625 AND SAF4) and Guatemala strains (GUA1 and GUA-N1) showed four,four and six amino acid substitutions compared to the New Zealand strains (NZE2 and NZE10) respectively, and accounted for eight out of the twelve amino acid substitutions found in DsEcp2-1. Compared to other highly polymorphic *D. septosporum* effectors (DsAvr4, DsEcp2-3, DsEcp4 and DsEcp5), DsEcp2-1 had relatively few amino acid changes. Especially in Guatemala and Colombia strains where DsAvr4, DsEcp2-3, DsEcp4 and DsEcp5 showed a high level of unique amino acid variations compared to other *D. septosporum* strains. In keeping with the results that suggest DsEcp2-1 may have a role in *D. septosporum* during infection of pine (Chapter 5 Figure 5.11), the polymorphism results further suggest that *DsEcp2-1* may be under purifying selection.

Figure 6.1 DsAvr4 amino acid changes summary

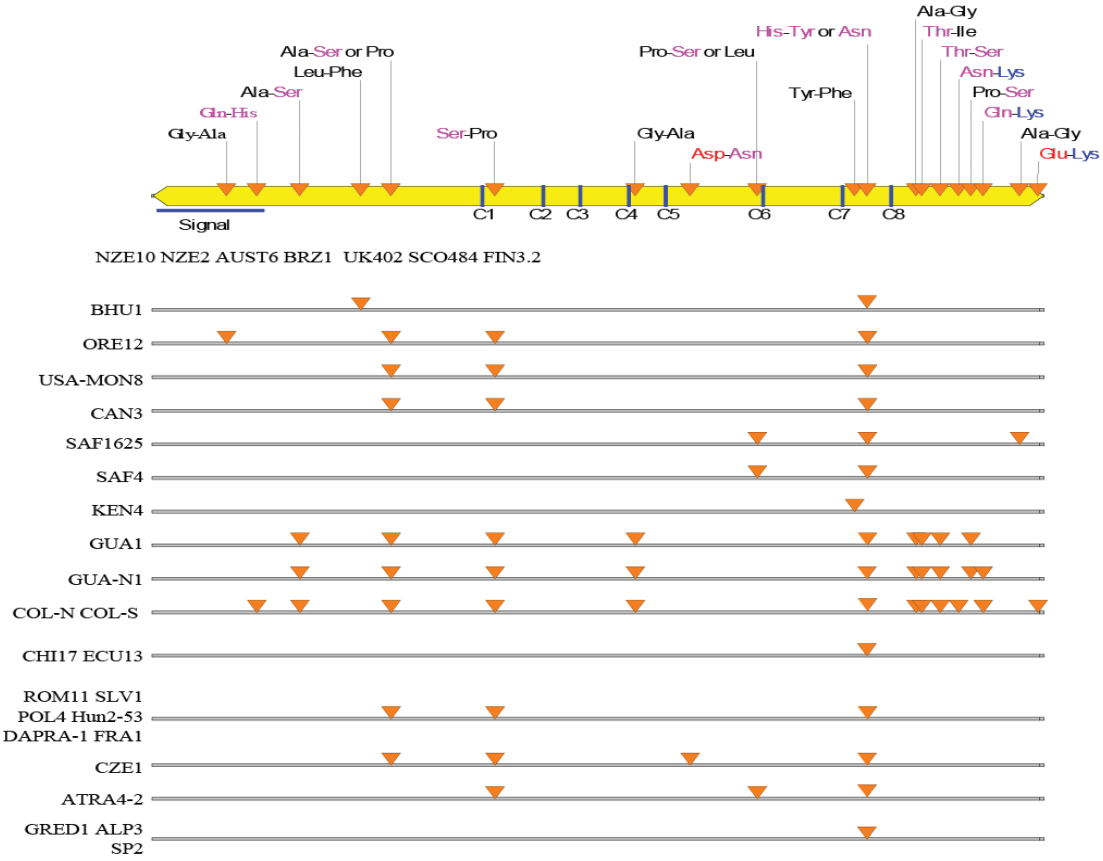

The schematic diagram at the top shows approximate positions of non-synonymous mutations as orange triangles and the amino acid changes compared to NZE10 are labelled on top with colour coding (NZE10 sequence is the amino acid on the left in each case) (Colour black: hydrophobic, pink: hydrophilic, red: negatively charged, blue: positively charged). The blue vertical lines indicate cysteine residues. The blue horizontal line indicates the signal peptide. Strains showing no amino acid difference to NZE10 are written under the schematic diagram. Each line under the schematic diagram indicates amino acid changes in the strains indicated on the left.

Figure 6.2 DsEcp2-1 amino acid changes summary

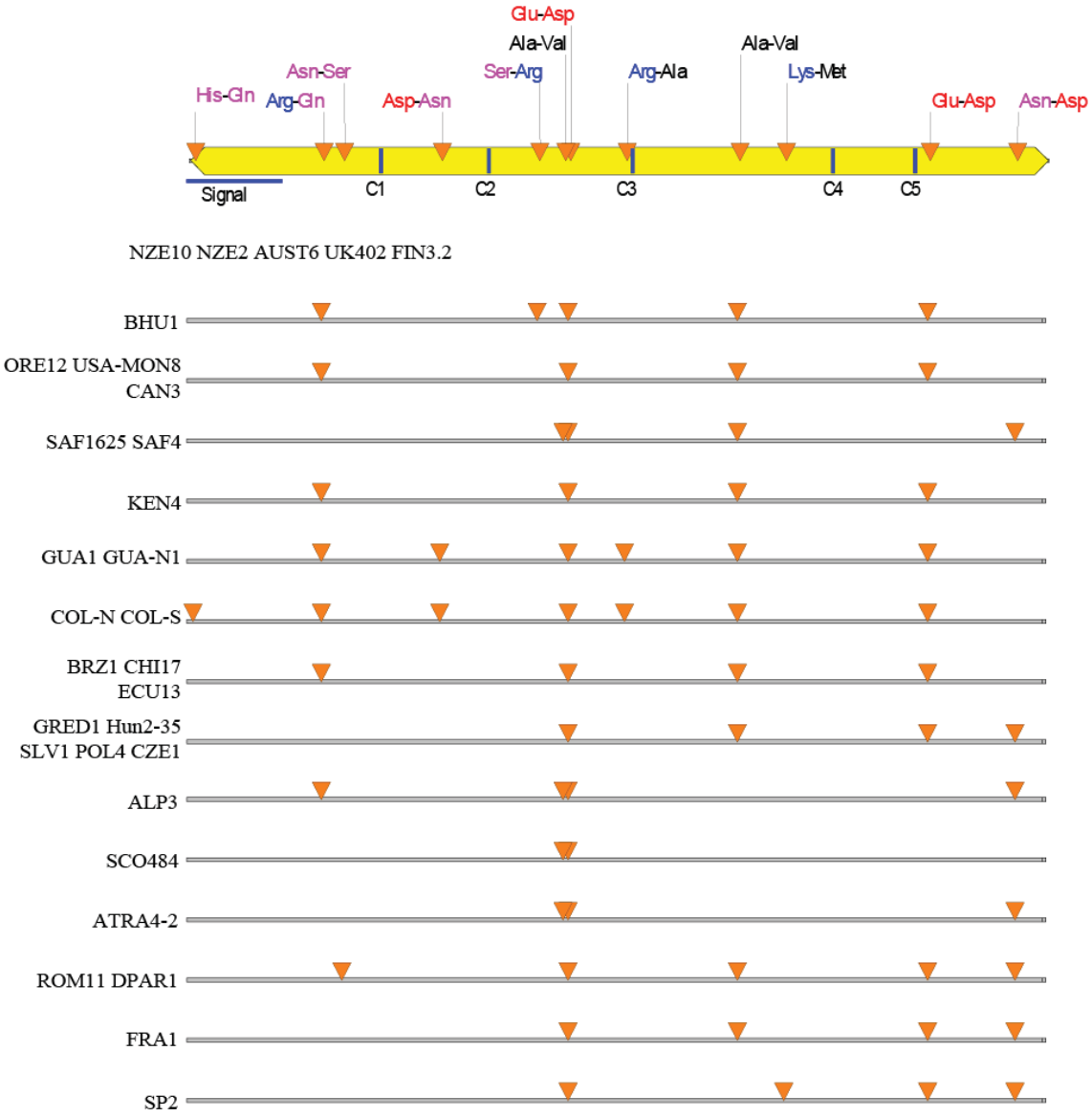

The schematic diagram at the top shows approximate positions of non-synonymous mutations as orange triangles and the amino acid changes compared to NZE10 are labelled on top with colour coding (NZE10 sequence is the amino acid on the left in each case) (Colour black: hydrophobic, pink: hydrophilic, red: negatively charged, blue: positively charged). The blue vertical lines indicate cysteine residues. The blue horizontal line indicates the signal peptide. Strains showing no amino acid difference to NZE10 are written under the schematic diagram. Each line under the schematic diagram indicates amino acid changes in the strains indicated on the left.

The amino acid substitutions for DsEcp2-3 are shown in Figure 6.3. *DsEcp2-3* showed the highest number of DNA polymorphisms (67) across all nine effectors tested. Four DNA polymorphisms were present inside the intron. One amino acid substitution was present in the signal peptide (ORE12, USA-MON8, CAN3, SAF4, BRZ1 and CHI17

have Phe to Leu substitution), but this mutation does not affect the signal cleavage site in DsEcp2-3 (predicted using SignalP 4.0 (Petersen et al., 2011)). The DNA polymorphisms resulted in 41 amino acid substitutions; however 24 of these were only found in the Guatemala (GUA1 and GUA-N1) and Colombia (COL-N and COL-S) strains. The two Guatemala strains (GUA1 and GUA-N1) had identical amino acid sequences to each other and both had a three nucleotide deletion which resulted in deletion of a Ser residue compared to the other strains tested. The two Colombia strains (COL-N and COL-S) also had identical sequences to each other and both had a 15 nucleotide deletion at the second exon of *DsEcp2-3* which resulted in deletion of five amino acid residues. The Colombia strains also contain eight extra amino acid residues at the end of the C-terminus. Two regions at the C-terminus of DsEcp2-3 in Guatemala and Colombia strains showed higher numbers of amino acid substitutions (7 and 15 respectively) compared to the rest of isolates (Figure 6.3). DsEcp2-3 is able to trigger non-host necrosis in *N. tabacum* and is thought to be able to interact with a host target in *N. tabacum* (Chapter 5 Figure 5.8 and section 5.3.3.3). The high variation of amino acid sequence at the C-terminus suggests that these two regions may be involved in host target interaction.

Figure 6.3 DsEcp2-3 amino acid changes summary

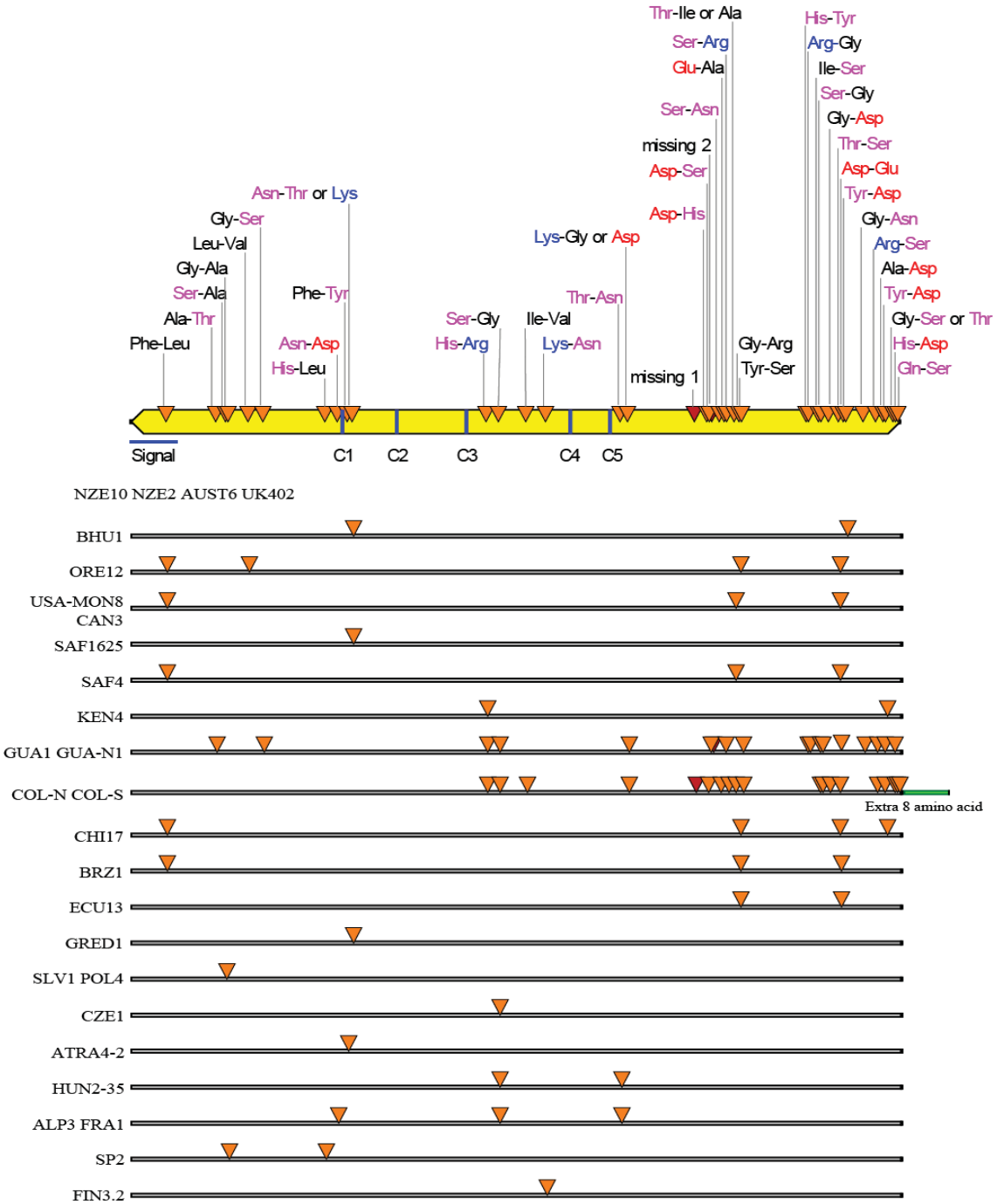

The schematic diagram at the top shows approximate positions of non-synonymous mutations as orange triangles and the amino acid changes compared to NZE10 are labelled on top with colour coding (NZE10 sequence is the amino acid on the left in each case) (Colour black: hydrophobic, pink: hydrophilic, red: negatively charged, blue: positively charged). The red triangles indicate positions of deletions in Guatemalan and Colombia strains. The green vertical line indicates extra eight amino acid residues in Colombia strains. The blue vertical lines indicate cysteine residues. The blue horizontal line indicates the signal peptide. Strains showing no amino acid difference to NZE10 are written under the schematic diagram. Each line under the schematic diagram indicates amino acid changes in the strains indicated on the left.

The amino acid substitutions for DsEcp4 are shown in Figure 6.4. Sixty-five DNA polymorphisms were identified in *DsEcp4*, resulting in 39 amino acid substitutions. Eight DNA polymorphisms were present inside the intron. Three amino acid substitutions were present in the signal peptide (GUA1 has His to Thr and Asn to Ser substitutions, BHU1 has Gly to Glu substitution), however these mutations do not affect the signal cleavage site (predicted using SignalP 4.0 (Petersen et al., 2011)). The GUA1 strain showed amino acid substitutions of Cys3 and Cys4 to Arg and the Fin3.2 strain showed amino acid substitution of Cys5 to Tyr. Cysteine residues have an important role in protein stability, thus mutations in Cys residues may leads to unstable proteins in the apoplast of the host. DsEcp4 had one internal stop codon in all strains tested except for both Guatemalan and both Colombian strains in which a serine is present. The CfEcp4 also had a Ser at this position. All four DsEcp4 from both Guatemalan and Colombian strains are predicted to be functional forms. The presence of more than one type of nonsense mutation in *DsEcp4* genes in the population suggests that DsEcp4 does not have an important function and that there may be some selection for strains that no longer make this protein.

The amino acid substitutions for DsEcp5 are shown in Figure 6.5. Twenty-three DNA polymorphisms were identified in *DsEcp5*, resulting in 14 amino acid substitutions. All strains tested contain a Thr to Pro amino acid substitution in the signal peptide except for NZE10, NZE2, AUST6, BRZ1, CHI17, ECU13, ATRA4-2 and SCO484, but this mutation does not affect the signal cleavage site (predicted using SignalP 4.0 (Petersen et al., 2011)). The USA-MON8 and CAN3 strains both showed both amino acid substitutions of Cys3 and Cys6 to Tyr which may leads to unstable proteins. Three strains, USA-MON8, GUA1 and GUA-N1, showed amino acid substitution of the initiator Met. One nucleotide deletion in Colombia (COL-N and COL-S) strains and one nucleotide insertion in Guatemala (GUA1 and GUA-N1) strains led to frame shifts in translation. All strains tested contain internal stop codons suggesting that DsEcp5 is not functional in any of them (Figure 6.5).

Figure 6.4 DsEcp4 amino acid changes summary

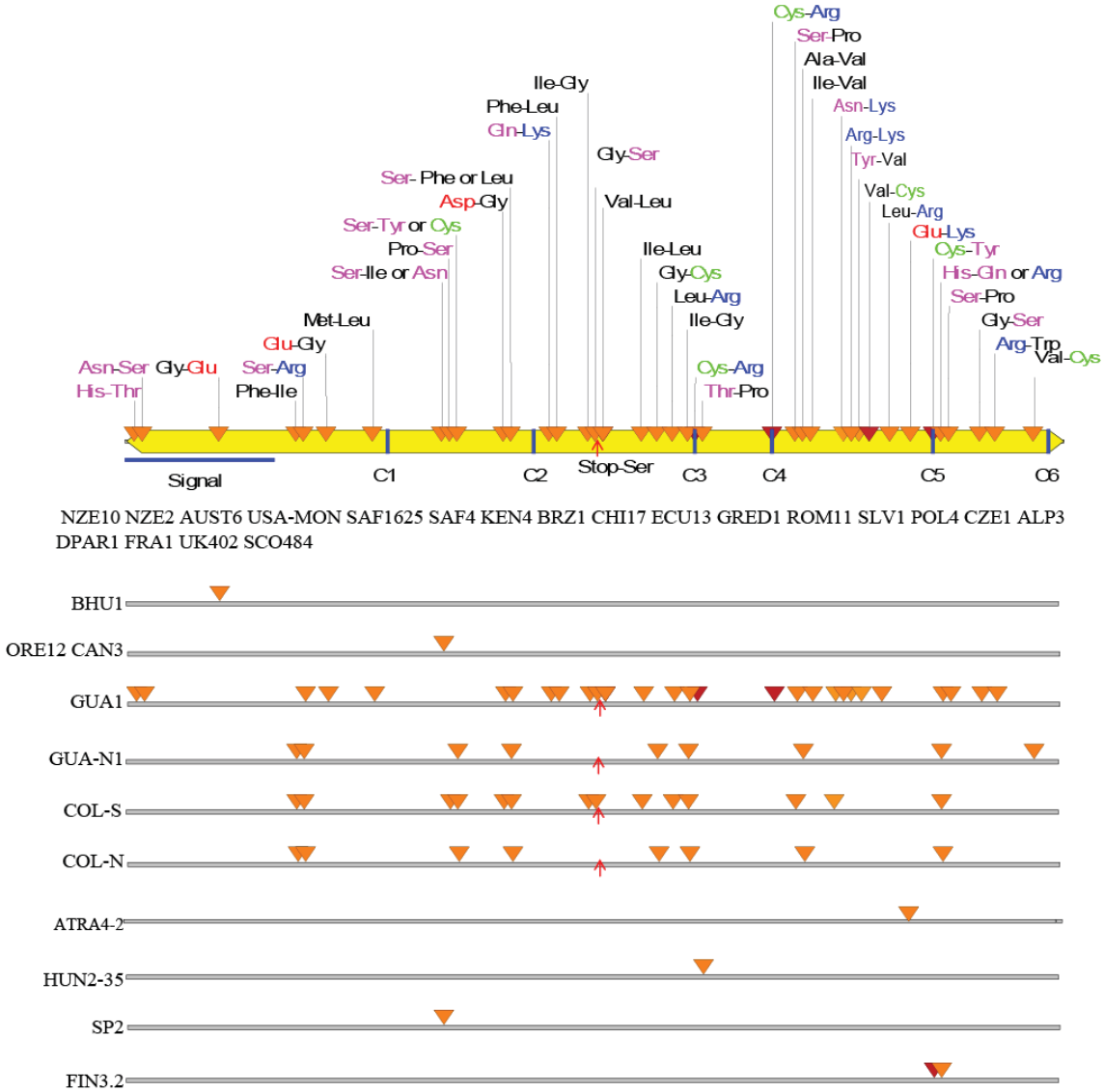

The schematic diagram at the top shows approximate positions of non-synonymous mutations as orange triangles and the amino acid changes compared to NZE10 are labelled on top with colour coding (NZE10 sequence is the amino acid on the left in each case) (Colour black: hydrophobic, pink: hydrophilic, red: negatively charged, blue: positively charged, green: cysteine). The red triangles indicate cysteine residue substitution in GUA1 and Fin3.2 compare to NZE10 strain. The blue vertical lines indicate cysteine residues. The blue horizontal line indicates signal peptide. The red arrows indicate positions of internal stop codons to Serine substitution in Guatemala and Colombian strains. Strains showing no amino acid difference to NZE10 are written under the schematic diagram. Each line under the schematic diagram indicates amino acid changes in the strains indicated on the left.

Figure 6.5 DsEcp5 amino acid changes summary

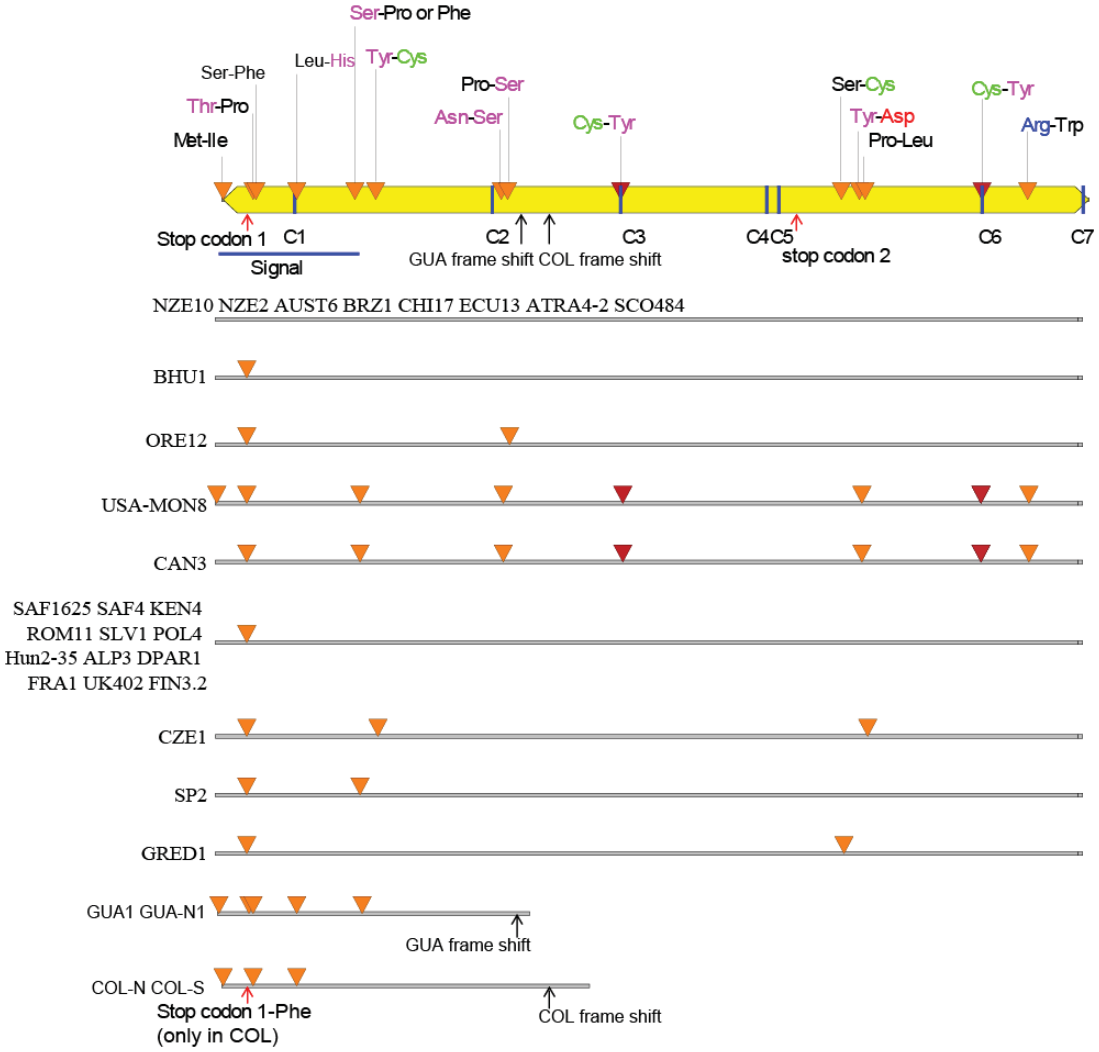

The schematic diagram at the top shows approximate positions of non-synonymous mutations as orange triangles and the amino acid changes compared to NZE10 are labelled on top with colour coding (NZE10 sequence is the amino acid on the left in each case) (Colour black: hydrophobic, pink: hydrophilic, red: negatively charged, blue: positively charged, green: cysteine). The red triangles indicate cysteine residue substitution in USA-MON8 and CAN3 compare to NZE10 strain. The red arrows indicate positions of internal stop codons. Only the Colombia strains have the first stop codon to Phe substitution. The blue vertical lines indicate cysteine residues. The blue horizontal line indicates the signal peptide. The black arrows indicate the positions of one nucleotide deletion in Colombia strains and one nucleotide insertion in Guatemala strains which led to frame shifts and result in truncated protein. Strains showing no amino acid difference to NZE10 are written under the schematic diagram. Each line under the schematic diagram indicates amino acid changes in the strains indicated on the left.

DsEcp6, DsEcp13, DsEcp14 and Ds69335 are the most conserved effectors. *DsEcp6* contained 26 DNA polymorphisms resulting in five amino acid substitutions. Four DNA polymorphisms were present inside the intron. One amino acid substitution was present in the LysM1 domain and three amino acid substitutions were present in the LysM2

domain (Figure 6.6A). *DsEcp13* contained 12 DNA polymorphisms resulting in 3 amino acid substitutions. Three DNA polymorphisms were present inside the intron. The KEN4 strain showed amino acid substitutions of Cys4 to Ser which may affect DsEcp13 stability (Figure 6.6B). *Ds69335* contains 18 DNA polymorphisms resulting in six amino acid substitutions. Two DNA polymorphisms were present inside the intron. As described in Chapter 3 section 3.2.4, Ds69335 contains a SCP/TAPS domain. Structure analysis identified four conserved amino acid residues (two Lys and two Glu) in the catalytic site of the SCP/TAPS domain (Teixeira et al., 2012). No variation was observed in Ds69335 in those four conserved amino acid residues in all *D. septosporum* strains tested, suggesting that those four amino acid residues are important for Ds69335 function (Figure 6.6C). *DsEcp14* contains 26 DNA polymorphisms of which 4 were present in the intron. A total of 11 amino acid substitutions were present, however of these eight amino acid substitutions were found only in the Guatemala and Colombia strains. Two amino acids substitutions were present in the signal peptide (SLV1 has Leu to Ser substitution, COL-N, COL-S have Ala to Ser substitution) but do not affect the signal cleavage site (Figure 6.6D).

Figure 6.6 Amino acid changes summary for DsEcp6, DsEcp13, Ds69335 and DsEcp14

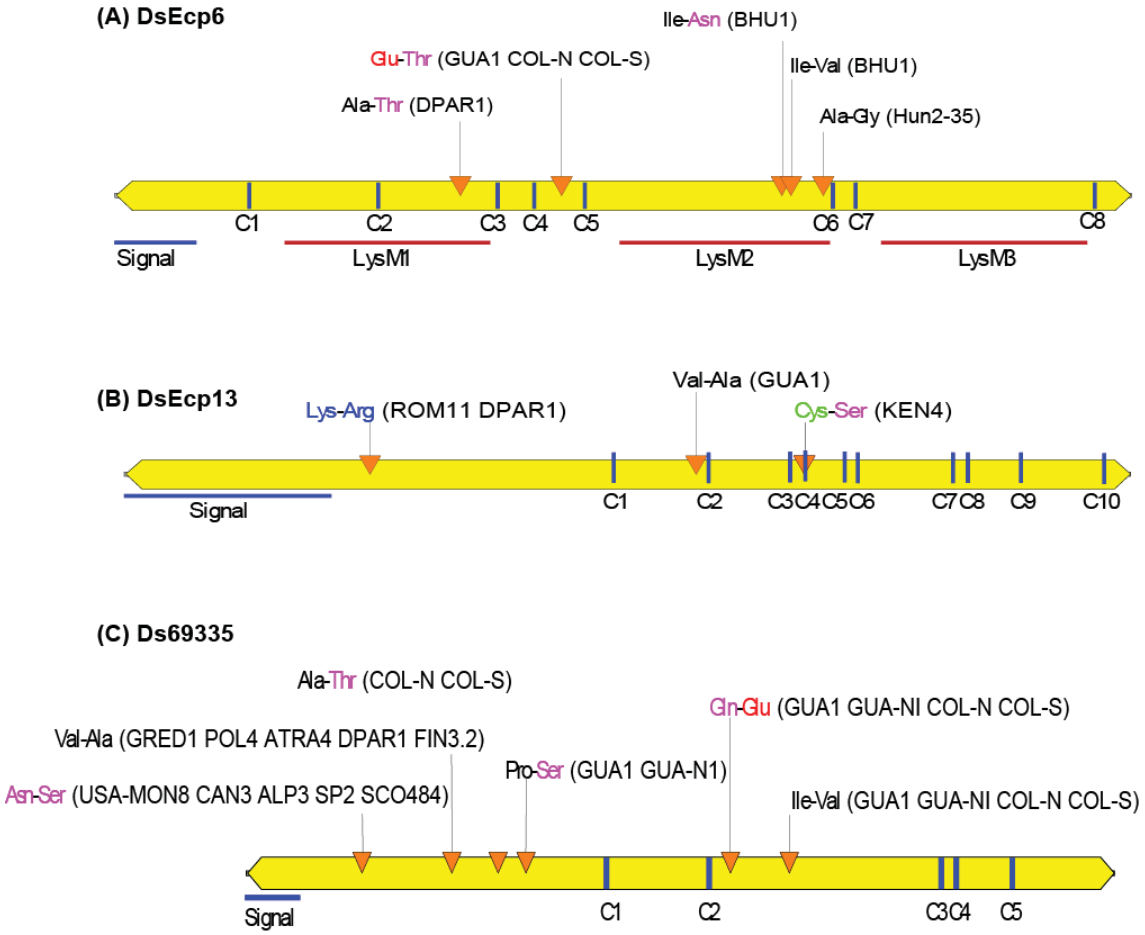

(A-C) The schematic diagram at the top shows approximate positions of non-synonymous mutations as orange triangles and the amino acid changes compared to NZE10 are labelled on top with colour coding (NZE10 sequence is the amino acid on the left in each case) (Colour black: hydrophobic, pink: hydrophilic, red: negatively charged, blue: positively charged, green: cysteine). Strains collected from countries carrying the amino acid substitution are listed after the amino acid substitution. The blue vertical lines indicate cysteine residues. The blue horizontal line indicates the signal peptide. The red horizontal lines indicate positions of three LysM domains in DsEcp6.

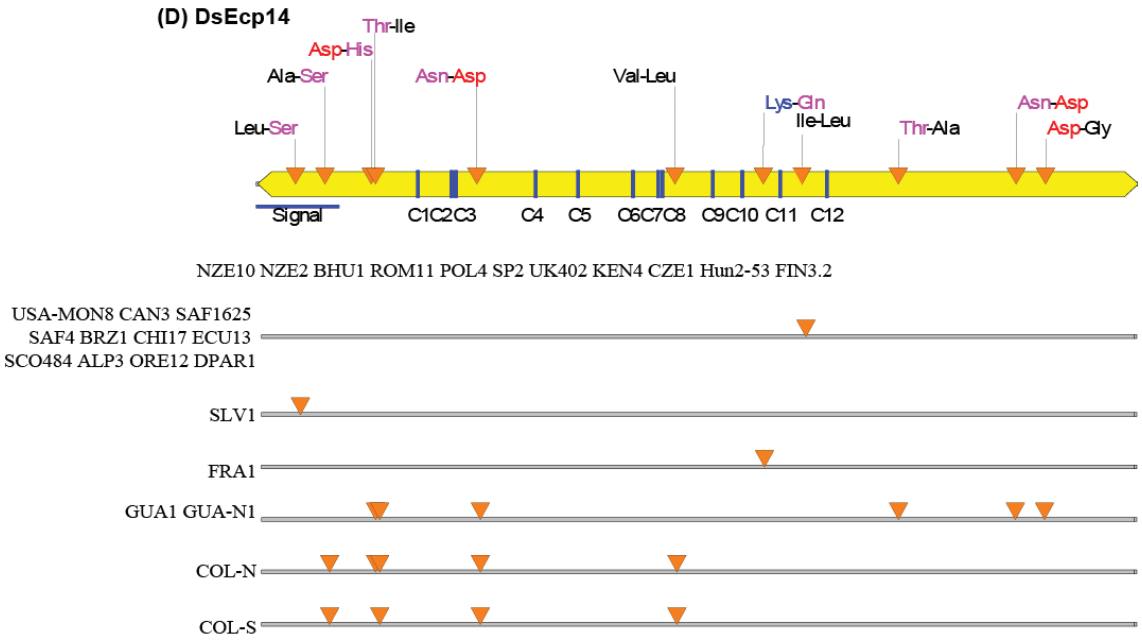

(D) The schematic diagram at the top shows approximate positions of non-synonymous mutations as orange triangles and the amino acid changes compared to NZE10 are labelled on top with colour coding (NZE10 sequence is the amino acid on the left in each case) (Colour black: hydrophobic, pink: hydrophilic, red: negatively charged, blue: positively charged, green: cysteine). The blue vertical lines indicate cysteine residues. The blue horizontal line indicates the signal peptide. Strains showing no amino acid difference to NZE10 are written under the schematic diagram. Each line under the schematic diagram indicates amino acid changes in the strains indicated on the left.

6.3 Discussion

6.3.1 The geographic distribution of *D. septosporum* strains is related to the number of amino acid variations in *D. septosporum* effectors.

Two Guatemala strains and two Colombia strains showed high levels of amino acid variation in *D. septosporum* effectors. One hypothesis is that *D. septosporum* originated in Central America (Barnes et al., 2014). Construction of gene genealogy tree using 17 dothistromin gene sequences from intergenic and flanking regions showed that the Guatemala (GUA1) strain was the most divergent of those tested and is thought to belong to an ancestral grouping of *D. septosporum*, although Columbian strains were not available for testing at that time (Bradshaw et al., 2013). In Colombia, the first epidemic of *D. septosporum* was identified in 2008 on *P. tecunumanii*. A population study, using 12 microsatellite markers on 160 Colombia isolates showed that isolates from the central and northern zones of Colombia (COL-S and COL-N) have mating type MAT-2.

More than half of the alleles found in Colombian strains were not seen in strains from Europe and the Southern hemisphere. Both Colombian strains were thought to have been imported from the Guatemala region (Barnes, I., oral presentation 10th International Mycological Congress Bangkok Thailand).

Within the Southern hemisphere *D. septosporum* strains from New Zealand (NZE2 and NZE10), Australia (AUST6), Brazil (BRZ1), Chile (CHI17) and Ecuador (ECU13) strains have identical effector amino acid sequences, while strains from South Africa (SAF1625 and SAF4) and Kenya (KEN4) showed high numbers of amino acid substitutions compared to NZE10 strain. In the case of New Zealand, Australia, Brazil, Chile and Ecuador, population structure analysis (Barnes et al., 2014) showed that strains from those countries have low levels of diversity and form a cluster. The same analysis further suggested that *D. septosporum* has been introduced into South Africa and Kenya more than once from Europe, hence strains from those countries have higher levels of genetic variation than seen in the other Southern hemisphere countries examined (Barnes et al., 2014).

D. septosporum strains collected from the Southern hemisphere and equatorial regions (New Zealand, Australia, Brazil, South Africa, Kenya, Ecuador and Chile) showed fewer amino acid variations compared to *D. septosporum* collected from the Northern hemisphere for all nine effectors tested. Both mating types MAT-1 and MAT-2 were found in Northern hemisphere isolates. Sexual forms of *D. septosporum* (*Mycosphaerella pini*) were identified in Europe. All the Southern hemisphere isolates have mating type MAT-2, except for South Africa and Kenya, where both mating types were found. No sexual forms of *D. septosporum* were identified in Southern hemisphere countries (Groenewald et al., 2007). Sexual recombination could contribute to higher genetic variability in the Northern hemisphere isolates. Sexual recombination plays an important role in the genetic structure of *Z. tritici* (Chen and McDonald, 1996; Schulze-Lefert, 2014). Genome analysis of twelve *Z. tritici* strains showed that 40% of non-synonymous substitutions are under positive selection which corresponds to a high level of effector amino acid changes in different isoforms (Stukenbrock et al., 2011).

6.3.2 Mutations in *D. septosporum* effector protein domains

Amino acid substitutions were identified in predicted protein domains in several *D. septosporum* effectors. Various *D. septosporum* strains contain non-synonymous mutations in the signal peptide of DsAvr4, DsEcp2-1, DsEcp2-3, DsEcp4, DsEcp5 and DsEcp14. However none of the mutations abolished the predicted cleavage site for the signal peptide. Since only the mature effector proteins are required for function those mutations in the signal peptide are likely not to affect effector function.

One and three amino acid substitutions were identified in DsEcp6 LysM1 and LysM2 motifs respectively. Other studies showed that LysM motifs in *C. fulvum* CfEcp6 are involved in chitin binding and help to avoid chitin triggered immunity in tomato (de Jonge et al., 2011). In *CfEcp6*, sequence analysis identified five DNA polymorphisms but only one non-synonymous amino acid change that occurred outside the three LysM motifs (Bolton et al., 2008). Crystal structure of CfEcp6 suggested that when it binds to chitin, a chitin tetramer is buried in a groove formed by LysM1 and LysM3, where it is protected from recognition by the host chitin receptor. Several amino acid residues in LysM 1 and LysM3 are involved in forming non-covalent bonds with chitin. In DsEcp6, only one amino acid change was identified in LysM1, and the corresponding amino acid residue in CfEcp6 LysM1 is not involved in forming non-covalent bond with chitin. So this amino acid change in DsEcp6 may not affect chitin binding affinity. However, new non-covalent bonds such as hydrogen bonds may be possible for the Ala to Thr variant. Three amino acid changes were identified in DsEcp6 LysM2. In CfEcp6, LysM2 showed lower chitin binding affinity and is not involved in chitin protection, but might instead prevent host chitin receptor activation (Sanchez-Vallet et al., 2013). The role of LysM2 in DsEcp6 is not known, it would be interesting to test whether DsEcp6 WT and LysM2 mutant forms have same role when infecting pine. Another possibility is that there is an R protein in pine that recognizes DsEcp6; the DsEcp6 mutant may be able to avoid triggering R protein mediated HR when infecting pine.

Amino acid substitution of cysteine residues was identified in DsEcp4 (GUA1, Fin3.2), DsEcp5 (USA-MON8, CAN3) and DsEcp13 (KEN4). Cysteine residues are involved in disulphide bond formation which is important for protein stability and function. In *C. fulvum*, all eight cysteine residues are involved in disulphide bond formation in CfAvr4 (van den Burg et al., 2001) and three of the four disulphide bonds are involved in

maintaining protein stability. In *C. fulvum*, cysteine substitutions led to mutant CfAvr4 protein which is more susceptible to host proteases. However the mutant CfAvr4 could still bind chitin and protect fungal hyphae from protease degradation, and excess mutant CfAvr4 protein secreted by the fungus was digested by host protease before being able to be recognized by resistance protein Cf-4 (van den Burg et al., 2003).

One interesting observation is that no amino acid changes were found in DsAvr4 between the Cys6-Cys7 that contain the chitin binding domain. The domain swap experiment suggests that DsAvr4 Cys6-Cys7 is involved in recognition by Cf-4 (Chapter 5 section 5.2.2). However due to the importance of the chitin binding domain to DsAvr4 function, together with these polymorphism results, this region may be under purifying selection to maintain DsAvr4 function.

6.3.3 *D. septosporum* effectors under positive selection

To test whether *D. septosporum* effectors are under positive selection, two methods (dN/dS value and Codon based Z-test) were used. Both methods are based on calculating nonsynonymous/synonymous differences between a pair of homologous sequences. Several factors may affect the result (Nei and Gojobori, 1986). For example if positive selection happens only on certain sites of the protein (regions involved in R protein recognition), the dN/dS ratio is less sensitive in estimating positive selection (Aguileta et al., 2009). Moreover two types of DNA substitutions, transitions (A-G T-C) and transversions (A-T A-C G-T G-C) can occur in the genome. The dN/dS ratio method assumes that transitions and transversions occur at same frequency which will affect estimation of the number of synonymous or nonsynonymous sites and can led to inaccurate results. Several other methods such as a modified Nei-Gojobori method which takes transition and transversion ratios into account could be used to confirm the result (Zhang et al., 1998).

The dN/dS ratio method suggested that *DsEcp4* and *DsEcp5* are under positive selection. Both genes contain internal stop codons and are predicted to encode pseudogenes in NZE10 and most other strains tested, except for Guatemala and Colombia strains which are thought to have a functional copy of the DsEcp4 gene. It is highly possible that R proteins that recognize DsEcp4 and DsEcp5 are present in pine species and that

non-functional *D. septosporum* DsEcp4 and DsEcp5 were produced to avoid triggering R protein mediated HR. An example of producing a non-functional effector to avoid R protein recognition is seen in *C. fulvum* Avr2 which targets the host cysteine protease Rcr3 and can trigger Cf-2 mediated immunity (Dixon et al., 2000). Sequence analysis showed that CfAvr2 mutant isoforms contain a transposon insertion which leads to truncated protein that avoids Cf-2 mediated HR (Luderer et al., 2002). It will be interesting to test whether DsEcp4 isoforms from Guatemala and Colombia strains can trigger R protein mediated HR in pine.

DsEcp2-3 from Guatemala and Colombia strains showed a high level of amino acid differences compared to DsEcp2-3 from other *D. septosporum* isolates tested. In particular, the high number of amino acid differences in two regions near the C-terminus suggests that those regions may be involved in DsEcp2-3 recognition by R proteins. However dN/dS values suggested that the DsEcp2-3 protein as a whole is not under positive selection. Two possibilities may explain the result. First, the dN/dS value is not very sensitive in estimating positive selection that happens in particular regions of the protein (in this case, the C-terminus). Second, except for Guatemala and Colombia strains, which are thought to belong to an ancestral grouping of *D. septosporum* (Bradshaw et al., 2013), other strains showed low levels of amino acid substitution. It is possible that DsEcp2-3 is required for a virulence function of *D. septosporum* and that purifying selection maintains the sequence of DsEcp2-3 required for its function.

DsEcp6 and DsEcp13 are highly conserved with only four and three amino acid substitutions in 21 *D. septosporum* strains tested respectively. However *DsEcp13* appears to be absent from nine *D. septosporum* strains and *DsEcp6* is the only core effector that appears to be absent from 3 *D. septosporum* strains. Variability in effector genes between strains may have been influenced by the fact that the *D. septosporum* gDNAs were collected from 14 different pine species and that the pine hosts differed between different samples from the different countries (Table 2.1). The different host species may also influence the presence/absence of *D. septosporum* effectors, since one host may contain a specific R protein that recognizes the corresponding effector. Pathogens can avoid recognition by deleting recognized effectors. For example, *Phytophthora sojae* effector Avr1d is recognized by soybean Rps1d. Sequence comparisons of avirulent and virulent strains of *P. sojae* showed that a 1.5 kb deletion

which removes *Avr1d* occurs in the virulent strain of *P. sojae*, whilst all avirulent strains carry the *Avr1d* gene (Na et al., 2013). Similarly in the tomato pathogen *C. fulvum*, effectors Avr4E and Avr9, which are recognized by R proteins Cf-4E and Cf-9 respectively, are absent from several natural strains (Stergiopoulos et al., 2007). From the pathogenicity test, DsEcp6 does not appear to be a virulence factor and may be dispensable. However it cannot be ruled out that the absence of *DsEcp6* and *DsEcp13* is due to highly divergent flanking regions. The presence or absence of *DsEcp6* and *DsEcp13* should be tested with gene specific primers that bind to the conserved regions of *DsEcp6* and *DsEcp13* in future experiments.

In summary, allelic variations were observed for all nine *D. septosporum* effector candidates tested. The geographic distribution of *D. septosporum* strains is related to the number of amino acid variations in *D. septosporum* effectors. Northern hemisphere countries with both mating types present have more allelic variations in *D. septosporum* effector sequences. Regions in which *D. septosporum* has been introduced as a pathogen (Oceania, South Africa) have fewer allelic variations in *D. septosporum* effectors than Northern hemisphere strains. Out of nine *D. septosporum* effectors tested, only the pseudogenes *DsEcp4* and *DsEcp5* showed evidence of positive selection, leading to the suggestion that R proteins that recognise DsEcp4 and DsEcp5 may be present in pine species. *DsEcp13* appears to be absent from ten *D. septosporum* strains, suggesting that DsEcp13 is not important for virulence and can also be deleted to avoid R protein mediated HR.

Chapter 7. General conclusions and future work

7.1 General conclusions

This PhD thesis focused on identification and characterization of *D. septosporum* effectors and their role in the infection of pine. The hemibiotrophic fungus *D. septosporum* and the biotrophic fungus *C. fulvum*, in which the study of fungal effectors was pioneered, are phylogenetically closely related (de Wit et al., 2012). A comparative approach to analyse these genomes, together with analysis of *D. septosporum in planta* transcriptome data, identified nine *D. septosporum* effector candidates which are homologous to *C. fulvum* effectors and additional new effector candidates in *D. septosporum*.

The well-characterized *C. fulvum* effector CfAvr4 is able to bind chitin and protect fungal hyphae from host chitinase degradation (van den Burg et al., 2006). DsAvr4 can also bind chitin and trigger Cf-4 mediated HR in tomato. The domain swap experiments showed that the region between Cys6-Cys7 (chitin binding domain) is required for Cf-4 recognition. Polymorphism results showed that no amino acid substitutions were identified between Cys6-Cys7, suggesting the importance of this region for DsAvr4 function. However DsAvr4 showed very low expression *in vitro* and *in planta* and is not required for virulence. Infiltration of DsAvr4 culture filtrate caused necrosis on pine needles, suggesting that an R protein that recognizes DsAvr4 may present in pine. Gene silencing of DsAvr4 may thus avoid R protein recognition.

DsEcp2-1 is able to trigger a non-host response in *N. tabacum* suggesting that DsEcp2-1 can interact with a host target in *N. tabacum*. Deletion of *DsEcp2-1* did not affect fungal physiology *in vitro*, however significantly larger lesions were observed in *P. radiata* seedlings infected with the *DsEcp2-1* mutant strain compared to the WT. The result suggests that DsEcp2-1 may act to suppress a host target which is involved in inducing necrosis during the biotrophic infection stage. The observation that DsEcp2-1 has relatively few amino acid substitutions even when comparing the Guatemala strain (which belongs to the ancestral grouping of *D. septosporum*) to other *D. septosporum* strains, and has a low dN/dS ratio, suggested that DsEcp2-1 is under purifying selection. The polymorphism results support the finding that DsEcp2-1 has an important role

when infecting *D. septosporu*m. However the transcriptome pattern of DsEcp2-1 *in planta* does not support the proposed role of DsEcp2-1. *DsEcp2-1* is highly expressed in mid necrotrophic (early lesion formation) stage, while the role of DsEcp2-1 is suggested to be at early biotrophic (fungal network formation) stage. Infiltration of DsEcp2-1 caused necrosis in *P. radiata* needles suggesting that an R protein that recognizes DsEcp2-1 may present.

CfEcp6 contains three LysM motifs and is able to bind chitin and avoid chitin triggered immunity (de Jonge et al., 2011). DsEcp6 also contains three LysM motifs. Deletion of DsEcp6 does not affect fungal physiology *in vitro*. The mutant *DsEcp6* strain led to reduced infection rate on *P. radiata* seedlings, suggesting that DsEcp6 may be required for virulence. However the complemented strain did not complement the mutant phenotype, leading to doubt about the virulence role of DsEcp6. The polymorphism study showed that DsEcp6 is highly conserved for all the strains tested. Studies in *Z. triciti* showed that a CfEcp6 homologous effector Mg3LysM is able to bind chitin. Mg3LysM has multiple roles when infecting wheat in which it not only protects fungal hyphae from host chitinase degradation but also avoids chitin triggered immunity in the host, a role done by CfAvr4 in *C. fulvum*. No homologues of Avr4 were identified in *Z. triciti* (Marshall et al., 2010). Since DsAvr4 is not expressed during infection, it will be interesting to test if DsEcp6 has dual roles as seen for Mg3LysM. Infiltration of DsEcp6 caused necrosis in *P. radiata* needles suggesting that R proteins that recognize DsEcp6 may present.

The allelic variations of *D. septosporum* were analysed. Nonsynonymous amino acid changes were observed for all nine *D. septosporum* effectors tested. Out of nine *D. septosporum* effectors tested, only the pseudogenes DsEcp4 and DsEcp5 showed evidence of positive selection. DsEcp4 and DsEcp5 are shown to contain internal stop codons and are pseudogenes in all strains tested except for DsEcp4 that has a functional gene in GUA-N1 and COL-S strains. The polymorphism results led to the suggestion that R proteins that recognise DsEcp4 and DsEcp5 may be present in pines. *DsEcp13* appears to be absent from ten *D. septosporum* strains, suggesting that DsEcp13 is not important for virulence and can also be deleted to avoid R protein mediated HR.

DsHdp1 encodes a class II hydrophobin. Target gene replacement of *DsHdp1* led to reduced colony surface hydrophobicity, however deletion of *DsHdp1* did not affect fungal growth rate, sporulation, germination, spore adhesion or virulence. Re-annotation of the *D. septosporum* genome identified three other hydrophobin genes (class I: *DsHdp2* and class II: *DsHdp*3, *DsHdp4*). However in contrast to the highly expressed *DsHdp1*, none of these other three hydrophobins are highly expressed *in planta* and the role of hydrophobins in the infection biology of *D. septosporum* is not clear.

The findings of this study provide basic knowledge of molecular cross-talk between *D. septosporum* and pine. Functional studies and infiltration assays of *D. septosporum* effectors led to knowledge of possible roles of *D. septosporum* effectors during disease progression, and prediction of resistance proteins in pine. The polymorphism study provided important information to screen for durable R proteins in the field. Eventually the results could lead to identification of plant susceptibility and/or resistance genes that could be exploited in pine breeding programmes.

7.2 Future work

The comparative genome analysis and transcriptome analysis provided important tools to identify effector candidates in *D. septosporum*. The results supported the hypothesis that homologues of *C. fulvum* effectors are present in the *D. septosporum* genome. However the present transcriptome data were limited in that only three time points during the disease progression stage were included. In the future more time points representing different stages during disease progression, particularly for early time points, should be analysed in a transcriptome study to reveal information for screening new effector candidates and to provide further insight into expression patterns of known effectors during disease progression.

Pathogenicity assays using targeted effector gene replacement strains provide important information about virulence functions of *D. septosporum* effectors. However factors such as the age of clonal seedlings can affect the infection rate, which could led to inaccurate results, and some contradictory results were obtained, For example the *DsEcp6* complemented strain did not complement the *DsEcp6* mutant phenotype. Moreover, a contradictory result was observed for deletion of *DsEcp2-1* which caused a

larger lesion compare to WT, suggesting a necrosis inhibition role for DsEcp2-1 in early biotrophic stage; this hypothesis was not supported by *DsEcp2-1 in planta* expression data or by the necrosis produced by DsEcp2-1 protein when delivered to pine needles. To confirm the mutant *DsEcp2-1* and *DsEcp6* phenotype, the pathogenicity assay should be repeated using young susceptible *P. radiata* clonal seedlings. Also to investigate the role of hydrophobin genes in *D. septosporum*, single or multiple targeted replacement of hydrophobin genes should be performed.

The polymorphism data provide important information to understand the evolutionary arms race between *D. septosporum* effectors and R proteins. To confirm the presence/absence of *D. septosporum* effectors, primers designed to conserved regions using polymorphism results as guidelines should be used. More *D. septosporum* strains collected from different regions or strains collected from same region but different time points should be included. *D. pini* is another causal agent of dothistroma needle blight. A global collection of *D. pini* strains is also available; it will be interesting to investigate the presence or absence of *D. septosporum* effectors in *D. pini* and, if the effectors are present, polymorphism analysis of homologues of *D. pini* effectors will provide more information about effector evolution.

The pine needle infiltration assay is a useful and fast screening method to screen for pine genotypes that may carry R proteins, which provides a base to identify plant susceptibility and/or resistance genes that could be exploited in future breeding programmes. Preliminary results were obtained using DsAvr4, DsEcp2-1 and DsEcp6 culture filtrates. However in order to develop an improved screening system, several factors need to be considered in the future. First pine needles collected from *P. radiata* seedlings with different resistance level to *D. septosporum* should be included. Purified effector proteins with the same concentrations should be used in order to assess necrosis inducing ability such as time of necrosis, lesion appearance and lesion size.

Appendix 1. Media, buffers and solutions

All media used in this study were prepared in MilliQ water and autoclaved at 121°C for 15 minutes, then allowed to cool by standing in a water bath maintained at 50°C before adding any antibiotics.

Appendix 1.1 Growth media

Luria B broth (LB)

20 g/L lennox L broth base (Invitrogen).

Luria B agar (LA)

20 g/L lennox L broth base (Invitrogen) and 15 g/L bacteriological agar (Oxoid).

Potato Dextrose Agar (PDA)

39 g/L potato dextrose agar (Merck).

***D. septosporum* Medium (DM)**

15 g/L bacteriological agar (Oxoid), 50 g/L malt extract (Oxoid) and 23 g/L nutrient broth (Oxoid).

***D. septosporum* Sporulating Medium (DSM)**

15 g/L malt extract (Oxoid) and 15 g/L yeast extract (BD)

Pine Needle Minimal Media with glucose (PMMG)

Water for this media was prepared by soaking fresh pine needles (10% w/v) in 1 L MilliQ water for 24 hours at room temperature and pH adjusted to 6.2 using HCl

0.2 g/L magnesium sulphate heptahydrate (Merk, Darmstadt, Germany)

0.9 g/L di potassium hydrogen orthophosphate (BDH, Poole, England)

0.2 g/L potassium chloride (Sigma, Louis, Germany)

1.0 g/L ammonium nitrate (Sigma Aldrich, Steinheim, Germany)

0.002 g/L iron sulfate (APS Chem.Ltd. NSW, Australia)

0.002 g/L zinc sulfate heptahydrate (BDH, Poole, England)

0.002 g/L manganese chloride (BDH, Poole, England)

2 g/L asparagine (Sigma Life Science, St.Louis, USA)

3 g/L glucose (APS Chem.Ltd. NSW, Australia)

15 g/L bacteriological agar (Oxoid)

Appendix 1.2 Buffers and reagents for DNA extraction, quantification and analysis

Hexadecyltrimethylammonium bromide (CTAB) extraction buffer

2% CTAB (Sigma), 1% PVP 40 (Sigma), 1.4 M NaCl (Merk), 20 mM EDTA (ethylenediaminetetraacetic acid, disodium salt) (Sigma) and 0.1M Tris/HCl pH8 (Invitrogen). Volume was made up to 40 ml with MilliQ water. Heated to 60°C to dissolve the CTAB and PVP.

1 x TE buffer

10 mM Tris (Invitrogen) and 1 mM EDTA (ethylenediaminetetraacetic acid, disodium salt) (Sigma) pH8.5

Fluorometer working solution

Hoechst dye stock solution: 10 mg of Hoechst H33258 (Amersham Biosciences) was added to 10 ml of MilliQ water.

10 x TNE buffer: 12.11 g/L Tris (Invitrogen), 3.72 g/L EDTA (ethylenediaminetetraacetic acid, disodium salt) (Sigma) and 116.89 g/L NaCl (Merck), dissolved in 800 ml MilliQ water, adjusted to pH to 7.4 using concentrated HCl (BDH), then volume made up to 100 ml with MilliQ water.

Fluorometer working solution: 5 µl Hoechst H33258 stock solution, 5 ml 10 x TNE and 45 ml MilliQ water

10 x TBE buffer

108 g/L Tris (Invitrogen), 9.3 g/L EDTA (ethylenediaminetetraacetic acid, disodium salt (Sigma) and 55 g/L Boric acid (Univar). Dissolved in 800 ml MilliQ water, adjusted pH to 8.2 using concentrated HCl (BDH), then volume made up to 100 ml with MilliQ water.

Gel loading dye

20% (w/v) Sucrose (BDH), 5 mM EDTA $Na_2.H_2O$ (BDH), 1% (w/v) SDS (BDH), 0.2% (w/v) bromophenol blue (J.T. Baker Chemical Co) and 0.2% (w/v) xylene cyanol (Sigma)

Ethidium bromide staining solution

1 μg/mL ethidium bromide in MilliQ water

1 x TE buffer

10 mM Tris (Invitrogen) and 1 mM EDTA (ethylenediaminetetraacetic acid disodium salt) (Sigma) pH8.5

Proteinase K solution

Dissolved at the concentration of 20 mg/ml in sterile 50 mM Tris (pH 8.0) and 1.5 mM calcium acetate.

Appendix 1.3 RNA extraction and manipulation solutions

10× MOPS buffer

41.9 g Morphilinepropanesulfonic acid (MOPS) (Sigma), 6.8 g $NaAc \cdot 3H_2O$ (Univar) and 40 ml of 250 mM EDTA (ethylenediaminetetraacetic acid, disodium salt) (Sigma), dissolved in 1 litre MilliQ water.

5x RNA loading dye

4 µl of saturated aqueous bromophenol blue solution, 20 µl of 500 mM EDTA (ethylenediaminetetraacetic acid disodium salt) pH 8, 180 µl 37% formaldehyde, 500 µl 100% glycerol, 771 µl of formamide and volume made up to 2.5 ml with 10x MOPS buffer.

Appendix 1.4 Southern blotting and hybridization solutions

0.25 M HCl acid treatment:
21 ml of concentrated HCl and 979 ml of water.

Denaturation buffer 500 mM NaOH (BDH) and 500 mM NaCl (BDH)

Neutralization Buffer

500 mM Tris HCl pH 7.4 and 0.5M NaCl (BDH)

20 x SSC Solution

3 M NaCl (BDH) and 0.3 mM Na citrate

Low stringency Washing Solution I

2 x SSC with 1% (w/v) SDS (Sigma)

High stringency Washing Solution II

0.5 x SSC with 1% (w/v) SDS (Sigma)

Buffer I

100 mM Tris pH7.5 and 150 mM NaCl (BDH)

Buffer II

buffer I + 1% blocking reagent (Roche)

Buffer III

100 mM Tris-HCl pH9.5 and 100 mM NaCl (BDH)

Stripping Solution

200 mM NaOH (BDH) with 0.1% (w/v) SDS (Sigma)

Appendix 1.5 Transformation of *D. septosporum*

OM buffer
1.4 M $MgSO_4$ (Ajax), 10 mM Na_2HPO_4 (BDH), dissolved in 100 mL Milli-Q water, adjust pH with 100 mM $NaH_2PO_4.2H_2O$ (BDH) to pH 5.8. Add MilliQ water to a final volume of 300 mL.

Glucanex (Novozymes) digestion buffer
10 mg /ml Glucanex (Novozymes) in OM buffer

ST buffer
0.6 M sorbitol (Sigma) and 100 mM Tris (Carl Roth) pH 8.0

STC buffer
1 M sorbitol (Sigma), 50 mM Tris pH 8.0 (Carl Roth) and 50 mM $CaCl_2$ (Merck).

40% Polyethylene Glycol (PEG) solution
40% (w/v) PEG 4000 (BDH), 50 mM $CaCl_2$ (Merck), 50 mM Tris pH 8.0 (Carl Roth) and 1 M sorbitol (Sigma)

Regeneration Media (RG)
15 g/L bacteriological agar (Oxoid), 50 g/L malt extract (Oxoid), 23 g/L nutrient broth (Oxoid) and 273.8 g/L sucrose (BDH).

0.8% Regeneration Media overlay
8 g/L bacteriological agar (Oxoid), 50 g/L malt extract (Oxoid), 23 g/L nutrient broth (Oxoid) and 273.8 g/L Sucrose (BDH).

For selection media:
Hygromycin B 50 mg/ml (Roche): Used at 70 μg/ml
Phleomycin 21mg/ml (Invitrogen): Used at 7 μg/ml

Appendix 1.6 Agro-infiltration on *Nicotiana tabacum* Plant

0.5 M MES buffer

Dissolve 24.4 g of MES (2-(N-morpholino) ethanesulfonic acid) in 200 mL Milli-Q water

MMA broth

20 g/L sucrose (BDH), 5 g/L Basal salt mixture without vitamins (Sigma) and 1.95 g/L MES (USB), pH 5.6

Appendix 1.7 Heterologous production of *D. septosporum* effector protein by *P. pastoris*

1 M sorbitol solution

Dissolove 182 g of sorbitol in 1 litre of MilliQ water.

10X YNB

Dissolve 134 g of yeast nitrogen base (YNB) with ammonium sulfate and without amino acids (Invitrogen) in 1 litre of MilliQ water and filter sterilize.

0.02% Biotin

Dissolve 20 mg biotin in 100 ml of MilliQ water and filter sterilize.

0.4% Histidine

Dissolve 400 mg of L-histidine in 100 ml of MilliQ water and filter sterilize.

20% Dextrose

Dissolve 200 g of D-glucose in 1 litre of MilliQ water and filter sterilize.

5% Methanol

Mix 5 ml of methanol with 95 ml of MilliQ water and filter sterilize.

10% Glycerol

Mix 100 ml of glycerol with 900 ml of MilliQ water.

1 M potassium phosphate buffer, pH 6.0:

Mix 132 ml of 1 M K_2HPO_4 and 868 ml of 1 M KH_2PO_4 pH 6.0 and filter sterilize

Yeast extract peptone dextrose agar (YPD)

Dissolve 10 g yeast extract (BD), 20 g peptone and 20 g bacteriological agar (Oxoid) in 900 ml MilliQ water, autoclave for 20 minutes on liquid cycle then add 100 ml of 20% dextrose.

Minimal dextrose (MD)

Dissolve 15 g bacteriological agar (Oxoid) in 800 ml of MilliQ water, autoclave for 20 minutes on liquid cycle, cool to 50°C and then add 100 ml of 10X YNB, 2 ml of 0.02% Biotin and 100 ml of 20% dextrose

Minimal Methanol (MM)

Dissolve 15 g bacteriological agar (Oxoid) in 800 ml of MilliQ water, autoclave for 20 minutes on liquid cycle, cool to 50°C and then add 100 ml of 10X YNB, 2 ml of 0.02% Biotin and 100 ml of 5% methanol

Glycerol-complex agar (BMGY)

Dissolve 10 g of yeast extract (BD), 20 g peptone and 15 g bacteriological agar (Oxoid) in 700 ml MilliQ water. Cool to 50℃, then add 100 ml 1 M potassium phosphate buffer, pH 6.0, 100 ml 10X YNB, 2 ml of 0.02% Biotin and 100 ml of 5% Methanol.

Methanol-complex (BMMY) agar

Dissolve 10 g of yeast extract (BD), 20 g peptone and 15 g bacteriological agar (Oxoid) in 700 ml MilliQ water. Cool to 50℃, then add 100 ml 1 M potassium phosphate buffer, pH 6.0, 100 ml 10X YNB, 2 ml of 0.02% Biotin and 100 ml of 10% of glycerol.

Appendix 1.8 Western blotting

5x SDS-PAGE loading dye

5% β-Mercaptoethanol (Sigma), 0.02% bromophenol blue (Sigma), 30% (v/v) glycerol (Univar), 10% sodium dodecyl sulfate (BDH) and 250 mM Tris-HCl (Pure Science) pH6.8

Coomassie blue staining solution

Dissolve 1 g of Coomassie Brilliant Blue R-250 (Bio-Rad) in 500 ml methanol, 100 ml glacial acetic acid (Merck) and 400 ml MilliQ water. Stir the solution for 3 hours and store at room temperature.

Destaining solution

Mix 100 ml methanol, 50 ml glacial acetic acid and 350 ml MilliQ water.

10x blotting buffer

30.3 g/L Tris and 144 g/L glycine pH8.1 to 8.4.

For 1 litre 1x buffer, mix 100 ml of 10x buffer with 700 ml MilliQ water and 200 ml methanol, cool the buffer in cold room before use.

10x TBST

100 mM Tris, pH8.0, 1.5 M NaCL and 0.5% (v/v) Tween-20

Appendix 2. Schematic diagrams for materials and methods

Appendix 2.1 Schematic diagram of primer positions for *DsAvr4* used in this study

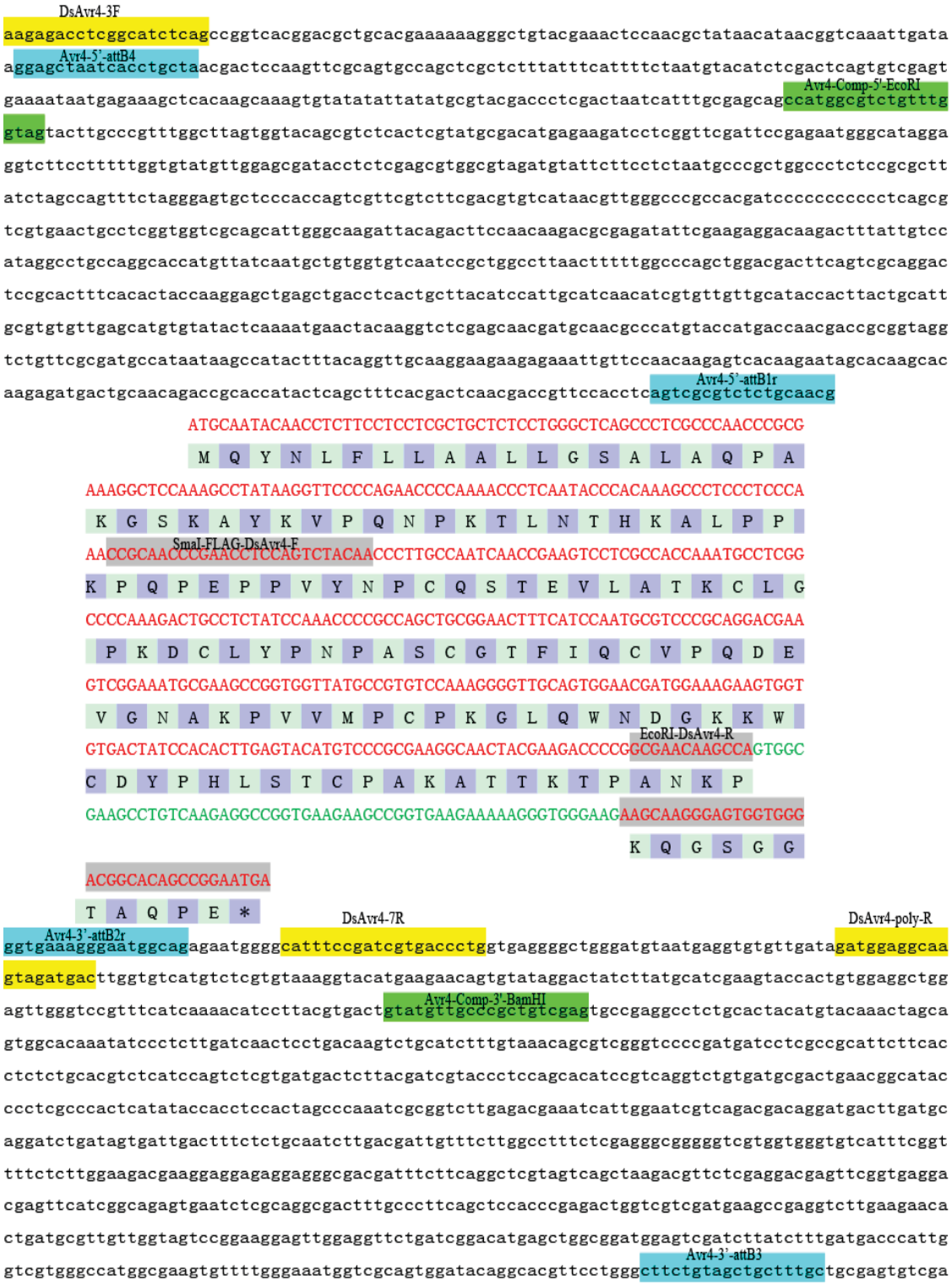

Primer name	Sequences
Polymorphism	
Avr4-3F	AAGAGACCTCGGCATCTCAG
Avr4-poly-R	GTCATCTACTTGCCTCCATC
Avr4-7R	CAGGGTCACGATCGGAAATG
Targeted *DsAvr4* replacement	
Avr4-5'-attB4	GGGGACAACTTTGTATAGAAAAGTTGCTGGAGCTAATCACCTGCTA
Avr4-5'-attB1r	GGGGACTGCTTTTTTGTACAAACTTGCCGTTGCAGAGACGCGACT
Avr4-3'-attB2r	GGGGACAGCTTTCTTGTACAAAGTGGCTGGTGAAAGGGAATGGCAG
Avr4-3'-attB3	GGGGACAACTTTGTATAATAAAGTTGCGCAAAGCAGCTACAGAAG
***DsAvr4* complementation**	
Avr4-Comp-5'-EcoRI	ATGCATGAATTCCCATGGCGTCTGTTTGGTAG
Avr4-Comp-3'-BamHI	ATGCATGGATCCCTCGACAGCGGGCAACATAC
DsAvr4 expression using *P. pastoris*	
SmaI-FLAG-DsAvr4_F	ATCGCCCGGGGACTACAAGGACGACGATGACAAGCCGCAACCCGAACCTCCAGTCTACAA
EcoRI-DsAvr4_R	ATCGGAATTCTCATTCCGGCTGTGCCGTCCCACCACTCCCTTGCTTTGGCTTGTTCGC

The red nucleotides indicate *DsAvr4* coding region sequences, the green nucleotides indicate *DsAvr4* intron sequences. The black nucleotides indicate *DsAvr4* 5' and 3' flanking sequences. The positions of primers are highlighted using different colors as indicated in the table. The primer name is written on top of the primer sequences.

Appendix 2.2 *DsAvr4* WT and chimeric nucleotide sequences

The colour codes for sequences are shown below:

Red: PR1A (signal peptide)

Black: *D. septosporum* Avr4 (Ds-Avr4)

Blue: *C. beticola* Avr4 (Cb-Avr4)

Green: Gateway recombination sequences (*attB1* and *attB2*)

Orange underlined: *Spe*I and *Sac*II restriction sites

Pink: Cys residue

Intron sequences

WT *DsAvr4* nucleotide sequences

GGGGACAAGTTTGTACAAAAAAGCAGGCTACTAGTATGGGATTTGTTCTCTT
TTCACAATTGCCTTCATTTCTTCTTGTCTCTACACTTCTCTTATTCCTAGTAAT
ATCCCACTCTTGCCGTGCCCAAAATccgcaacccgaacctccagtctacaacccttgccaatcaaccg
aagtcctcgccaccaaatgcctcggccccaaagactgcctctatccaaaccccgccagctgcggaactttcatccaatgcgtc
ccgcaggacgaagtcggaaatgcgaagccggtggttatgccgtgtccaaaggggttgcagtggaacgatggaaagaagtg
gtgtgactatccacacttgagtacatgtcccgcgaaggcaactacgaagaccccggcgaacaagccagtggcgaagcctgt
caagaggccggtgaagaagccggtgaagaaaaagggtgggaagaagcaagggagtggtgggacggcacagccggaat
gaCCGCGG ACCCAGCTTTCTTGTACAAAGTGGTCCCC

DsAvr4-CbCys1-Cys4 chimeric nucleotide

GGGGACAAGTTTGTACAAAAAAGCAGGCTACTAGTATGGGATTTGTTCTCTT
TTCACAATTGCCTTCATTTCTTCTTGTCTCTACACTTCTCTTATTCCTAGTAAT
ATCCCACTCTTGCCGTGCCCAAAATccgcaacccgaacctccagtctacaacccttgccccgcccgaa
gacatgaaacgaacacactgcatgggacccttcgactgcctgtacgcactaccaggagactgcggaactttcatccaatgcgt
cccgcaggacgaagtcggaaatgcgaagccggtggttatgccgtgtccaaaggggttgcagtggaacgatggaaagaagt
ggtgtgactatccacacttgagtacatgtcccgcgaaggcaactacgaagaccccggcgaacaagccagtggcgaagcctg
tcaagaggccggtgaagaagccggtgaagaaaaagggtgggaagaagcaagggagtggtgggacggcacagccggaat
gaCCGCGGACCCAGCTTTCTTGTACAAAGTGGTCCCC

DsAvr4-CbCys4-Cys6 chimeric nucleotide

GGGGACAAGTTTGTACAAAAAAGCAGGCTACTAGTATGGGATTTGTTCTCTT
TTCACAATTGCCTTCATTTCTTCTTGTCTCTACACTTCTCTTATTCCTAGTAAT
ATCCCACTCTTGCCGTGCCCAAAATccgcaacccgaacctccagtctacaacccttgccaatcaaccg
aagtcctcgccaccaaatgcctcggccccaaagactgcctctatccaaaccccgccagctgcctcggatacattcaatgccag
cccaaagacacgacgtacgagaccggtatcgcgtatgaaaggtcatgtccaaaggggttgcagtggaacgatggaaagaag
tggtgtgactatccacacttgagtacatgtcccgcgaaggcaactacgaagaccccggcgaacaagccagtggcgaagcct
gtcaagaggccggtgaagaagccggtgaagaaaaagggtgggaagaagcaagggagtggtgggacggcacagccggaa
atgaCCGCGG ACCCAGCTTTCTTGTACAAAGTGGTCCCC

***DsAvr4-CbCys6-Cys8* chimeric nucleotide**

GGGGACAAGTTTGTACAAAAAAGCAGGCTACTAGTATGGGATTTGTTCTCTT
TTCACAATTGCCTTCATTTCTTCTTGTCTCTACACTTCTCTTATTCCTAGTAAT
ATCCCACTCTTGCCGTGCCCAAAATccgcaacccgaacctccagtctacaacccttgccaatcaaccg
aagtcctcgccaccaaatgcctcggccccaaagactgcctctatccaaaccccgccagctgcggaactttcatccaatgcgtc
ccgcaggacgaagtcggaaatgcgaagccggtggttatgccgtgtcgtgcgggtcaatggtggaacgatgagaagaagtat
tgtgacacggtggaacctccaacatgtcccgcgaaggcaactacgaagaccccggcgaacaagccagtggcgaagcctgt
caagaggccggtgaagaagccggtgaagaaaaagggtgggaagaagcaagggagtggtgggacggcacagccggaat
gaCCGCGG ACCCAGCTTTCTTGTACAAAGTGGTCCCC

Appendix 2.3 *P. pastoris* heterologous protein expression plasmid

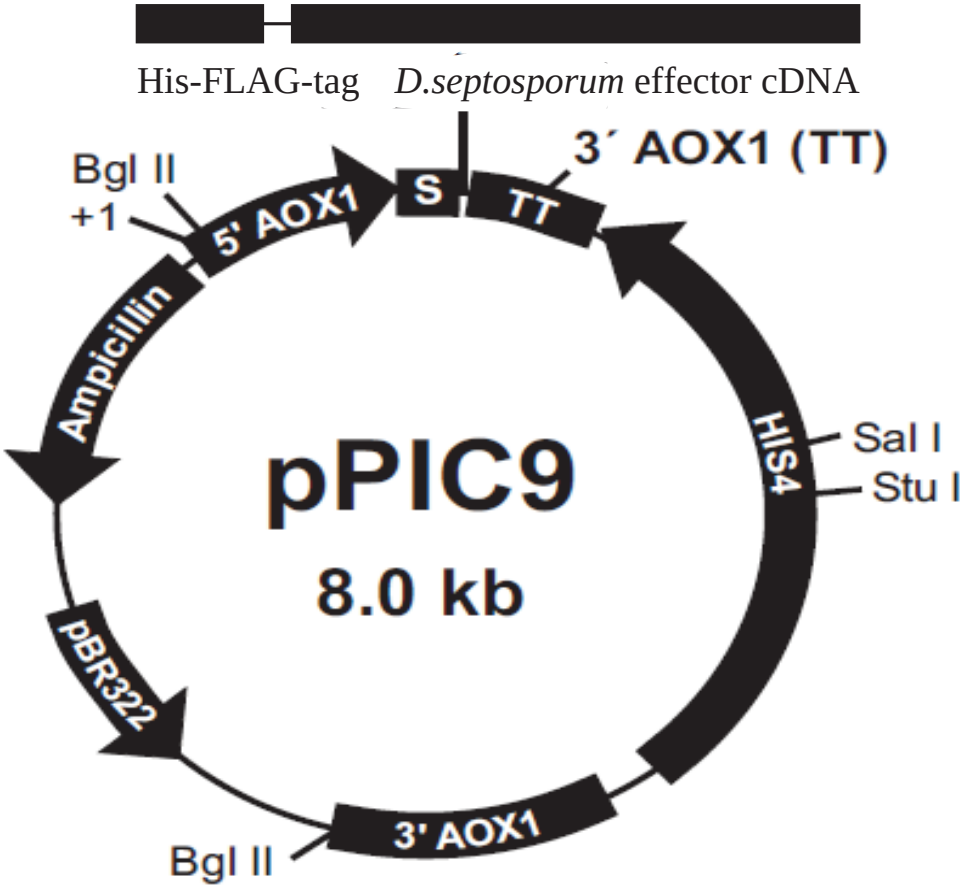

Schematic diagram of *P. pastoris* heterologous protein expression plasmid (Invitrogen, Carlsbad, CA, USA). The D. septosporum effector gene was under the control of the P. *pastoris* alcohol oxidase *AOX1* promoter. A His-FLAG-tag was fused to the N-terminus of the *D. septosporum* effector for western blot analysis.

Appendix 3. Figures

Appendix figure 3.1 Predicted translation of core *D. septosporum* effectors

DsAvr4 (JGI: 36707)

```
     M  Q  Y  N  L  F  L  L  A  A  L  L  G  S  A  L  A  Q  P  A
   1 atgcaatacaacctcttcctcctcgctgctctcctgggctcagccctcgcccaacccgcg 60
     K  G  S  K  A  Y  K  V  P  Q  N  P  K  T  L  N  T  H  K  A
  61 aaaggctccaaagcctataaggttccccagaaccccaaaaccctcaatacccacaaagcc 120
     L  P  P  K  P  Q  P  E  P  P  V  Y  N  P  C  Q  S  T  E  V
 121 ctccctcccaaaccgcaacccgaacctccagtctacaacccttgccaatcaaccgaagtc 180
     L  A  T  K  C  L  G  P  K  D  C  L  Y  P  N  P  A  S  C  G
 181 ctcgccaccaaatgcctcggccccaaagactgcctctatccaaaccccgccagctgcgga 240
     T  F  I  Q  C  V  P  Q  D  E  V  G  N  A  K  P  V  V  M  P
 241 actttcatccaatgcgtcccgcaggacgaagtcggaaatgcgaagccggtggttatgccg 300
     C  P  K  G  L  Q  W  N  D  G  K  K  W  C  D  Y  P  H  L  S
 301 tgtccaaaggggttgcagtggaacgatggaaagaagtggtgtgactatccacacttgagt 360
     T  C  P  A  K  A  T  T  K  T  P  A  N  K  P
 361 acatgtcccgcgaaggcaactacgaagaccccggcgaacaagccagtggcgaagcctgtc 420
                                                 K  Q  G  S  G  G
 421 aagaggccggtgaagaagccggtgaagaaaaagggtgggaagaagcaagggagtggtggg 480
     T  A  Q  P  E  *
 481 acggcacagccggaatga                                           498
```

The predicted intron position is highlighted in yellow.

DsEcp2-1 (JGI: 158381)

```
     M  H  F  N  A  A  A  V  L  A  L  L  P  A  L  S  L  A  A  V
   1 atgcacttcaacgccgccgctgtcttggccctcttgccagctctgtctctcgcggcagtc 60
     L  S  P  R  F  P  R  N  A  G  N  T  P  G  S  N  M  C  D  A
  61 ctcagcccgaggttccctcgaaacgctggaaatactccgggctcgaacatgtgcgacgcc 120
     S  T  F  N  D  G  T  T  Y  D  I  P  Q  A  P  V  A  D  C  R
 121 tcgaccttcaacgatggaacgacctacgacatccctcaggcaccagtcgccgactgtcgc 180
     N  L  V  N  S  I  D  T  S  Q  T  F  T  A  E  H  S  W  S  R
 181 aacctcgttaacagcatcgacacgagccagaccttcactgcagagcacagctggtcccga 240
     P  W  T  Y  G  R  C
 241 ccatggacctatggcagatgtgagtgacagaaatcttgatctcctccaaaggctatttcc 300
                           A  F  N  V  R  V  I  A  G  S  D  A
 301 actgacttgtttcccttcgcaggcgctttcaacgttcgtgtcatcgctggctccgacgct 360
     G  L  V  G  G  A  D  A  A  D  L  L  N  D  S  S  R  K  F  G
 361 ggattggtcggcggtgctgatgcggctgatctgttgaacgattcctctcgcaagttcggg 420
     E  S  G  S  Y  S  C  R  G  S  Y  G  Q  V  V  S  A  E  G  E
 421 gagagtggttcttactcttgcagaggcagttacggccaggtggtgtcggctgagggcgaa 480
     V  D  C  N  A  E  N  G  G  R  V  R  V  E  W  V  V  A  D  S
 481 gtcgattgcaacgctgaaaatggtgggagggtcagggtcgaatgggtcgtggctgactcg 540
     S  Y  N  P  R  N  D  E  *
 541 tcgtataacccgaggaacgacgagtga                                   566
```

The intron position, as verified by cDNA sequencing, is highlighted in yellow. The third cysteine residue is highlighted in pink.

DsEcp2-2 (JGI: 23431)

```
      M  F  V  S  H  I  Q  H  *  P  R  F  S  T
    1 atgttcgtgagccatatacaacactgaccgcggttctcgagttgccagcatctcaatccc 60
   61 gagtagccttagcgaatcgtaccacagaggtcggcgtccaacaagaccactgacgagccg 120
                           V  A  S  V  P  A  F  V  V  A  V  S
  121 tgaaccatgcacttccgccacagccgtcgccagcgtcccagctttcgtagtagcagtcag 180
       D  S  C  D  A  H  T  F  G  A  I  T  S  S  P  G  K  N  L  L
  181 cgacagctgtgatgctcatactttcggtgcgatcacctccagccctggtaaaaatctact 240
       L  S  D  V  E  A  L  V  A  H  W  A  G  D  Q  D  W  P  V  T
  241 cctcagcgacgtcgaggctctcgttgcccactgggctggcgaccaggactggccagtcac 300
       T  A  G  G  T  I  T  G  H  I
  301 cactgcgggcggcacaatcactgggcacatgtaagctagagactgggtgagtcatacgct 360
                                    P  G  A  F  N  G  V  A  A  A
  361 ggcggcgtaagtgtaggccaaccacgcagcccaggcgccttcaacggcgtggctgcggcc 420
       D  G  A  I  I  G  H  Q  D  F  I  D  L  L  K  E  Y  I  S  R
  421 gacggagcgatcatcggccaccaggattttattgacctgttgaaggaatacatctccagg 480
       F  A  K  G  E  T  V  A  G  D  G  R  V  A  I  G  A  A  G  E
  481 ttcgcaaagggagagactgttgctggtgatggaagagttgccatcggtgccgcaggagaa 540
       V  L  C  G  T  E  P  G  S  V  K  I  N  V  G  G  T  I  A  S
  541 gtgctatgtgggactgaacccggcagcgtcaagatcaatgtcggcgggactattgcctct 600
       T  *
  601 acatag                                                      606
```

The predicted intron position is highlighted in yellow. The internal stop codon is highlighted in green.

DsEcp2-3 (JGI: 127671)

```
      M  L  Y  S  T  A  V  V  V  A  L  L  P  T  F  G  V  A  T  R
    1 atgctttacagcacagcagtcgttgtcgccctgttgcccacctttggagtggcaaccaga 60
      F  L  Q  G  S  G  H  S  K  A  I  S  P  Q  A  L  Q  Q  S  G
   61 tttctccaagggagcggtcattctaaggcaatctctccacaggccttgcaacagtctggc 120
      G  Q  V  G  Q  P  D  L  A  T  S  L  K  G  D  G  G  L  P  S
  121 ggtcaagttggacagcccgacctggcaaccagcctcaaaggcgatggtggcctgccatct 180
      S  V  Q  D  F  A  E  G  D  S  P  Q  G  N  G  N  A  G  H  A
  181 agtgttcaggatttcgccgagggtgacagcccacaaggcaacggtaacgctggccatgct 240
      S  G  V  N  D  C  G  F  S  N  F  V  Q  L  K  E  D  Q  G  Y
  241 tctggcgtcaacgactgtggcttctccaattttgtgcagctgaaggaggaccaaggctac 300
      S  Q  A  S  V  Q  D  C  Y  Y  L  I  W  S  I  Q  A  D  E  E
  301 tcgcaggcttcggtgcaagactgctactacttgatttggtctattcaggctgatgaagag 360
      W  I  I  T  Q  E  L  Q  T  I  V  E  N  G  T  C
  361 tggatcatcactcaggaactgcaaaccatcgttgagaacggaacttgtaagttgtcaatg 420
                                                    A  F  Q  A
  421 catgcgtatccaaggcgttgcccatggtacctgactgacctcacgtaggcgccttccaag 480
        V  V  S  H  G  Q  G  N  S  L  V  A  A  L  G  N  A  D  I  I
  481 ccgtcgtttcccacggtcaaggaaatagccttgtcgcagcactgggcaacgccgatatca 540
        D  L  V  T  D  S  I  K  Q  F  G  A  D  G  Y  V  G  C  H  G
  541 tcgacctcgtcaccgactccatcaaacagttcggtgcggacggctacgttggctgccacg 600
        G  F  G  M  Y  T  S  A  A  G  A  M  P  C  D  S  P  T  L  D
  601 gtggctttggcatgtacacatccgcagctggtgccatgccctgcgacagccccaccctcg 660
        K  G  E  Q  V  F  V  D  W  F  L  T  T  P  E  G  I  S  G  S
  661 ataaaggcgagcaagtcttcgtcgactggttcctcactaccccggagggcatctctggca 720
        V  S  G  S  S  G  D  D  G  S  G  D  D  D  S  E  G  S  D  E
  721 gtgttagtggctcgtccggtgatgacggctcgggcgacgacgactcggaaggcagtgacg 780
        S  V  G  T  D  G  Y  S  H  S  Q  G  A  G  G  G  S  D  W  V
  781 aaagcgtcggtactgatgggtactcgcactctcagggcgctggaggtggctccgactggg 840
        Q  A  N  Q  K  Q  Q  Y  G  S  G  D  H  R  S  S  G  I  S  D
  841 tccaagccaaccagaagcagcagtatggcagtggtgatcataggagcagtggcatcagcg 900
        Y  G  S  S  G  T  G  D  Y  D  S  T  G  S  G  G  Y  G  S  T
  901 actatggtagcagtggtaccggggattatgatagtactggcagcggtggttatggtagca 960
        R  S  S  A  Y  G  S  G  H  Q  *
  961 ctaggagcagtgcgtatggcagcggccatcagtag                         995
```

The predicted intron position is highlighted in yellow.

DsEcp6 (JGI: 46236)

```
      M  Q  S  I  L  F  A  A  A  L  M  S  A  A  V  N  G  F  V  L
    1 atgcagtccattcttttcgctgccgctcttatgagcgccgcagttaacggcttcgttctc  60
      P  R  T  D  D  P  D  C
   61 ccacgtactgatgacccggattgtatcatcaatcctcacgagctgcatcagaatccgact 120
                        E  T  T  S  T  A  V  C  G  S  T  S  F  T
  121 aacgtttcgtctctcaggtgagaccacgagcaccgcagtctgcggctcgaccagcttcac  18
       N  Y  T  V  A  H  G  D  T  L  T  T  I  A  Q  K  F  N  S  G
  181 caactacaccgtcgcccacggggacaccctcaccaccatcgctcaaaagttcaactccgg 240
       I  C  D  I  A  S  V  N  D  I  T  N  P  N  F  I  E  T  G  A
  241 tatctgcgacattgcctcggtcaacgacatcaccaaccccaacttcatcgaaacaggcgc 300
       V  L  S  I  P  T  N  C  V  T  P  D  N  T  T  C  L  P  P  A
  301 cgtcctctcaatcccgaccaactgcgtcacgcccgacaacacgacctgtctcccaccagc 360
       T  E  V  T  E  T  C  V  A  G  L  P  G  T  Y  S  V  V  S  G
  361 gactgaggtcaccgagacctgcgttgcaggtcttccaggcacttactccgtcgtcagcgg 420
       D  T  L  S  A  I  A  K  D  F  N  I  T  L  A  A  L  E  G  A
  421 cgacactctctccgccatcgccaaggacttcaacatcaccctcgccgctctcgaaggcgc 480
       N  T  Q  I  A  N  P  D  V  I  S  I  G  E  L  I  N  I  P  I
  481 caacacacagatcgccaacccagatgtcattagtatcggcgaactcatcaacattccaat 540
       C  P  N  S  Q  C  A  T  V  G  T  Y  I  I  V  S  G  D  L  F
  541 ctgtcccaactctcagtgcgctactgttggaacttacatcatcgtgtctggcgatctttt 600
       V  D  L  A  T  T  H  H  T  T  I  G  Q  I  K  A  L  N  N  N
  601 cgttgatttggcgacgactcaccacactactatcggccagatcaaggctcttaacaacaa 660
       V  D  P  E  S  L  A  I  G  Q  Q  I  V  L  P  Q  N  C  M  N
  661 tgtcgatccagaatcgttggcgattggtcagcagattgttctgccacagaattgcatgaa 720
       I  T  A  V  A  *
  721 cattactgctgtggcgtaa                                         739
```

The intron position, as verified by cDNA sequencing, is highlighted in yellow.

Appendix figure 3.2 Phylogenetic analysis and amino acid alignment of Ecp6 homologues

(A)

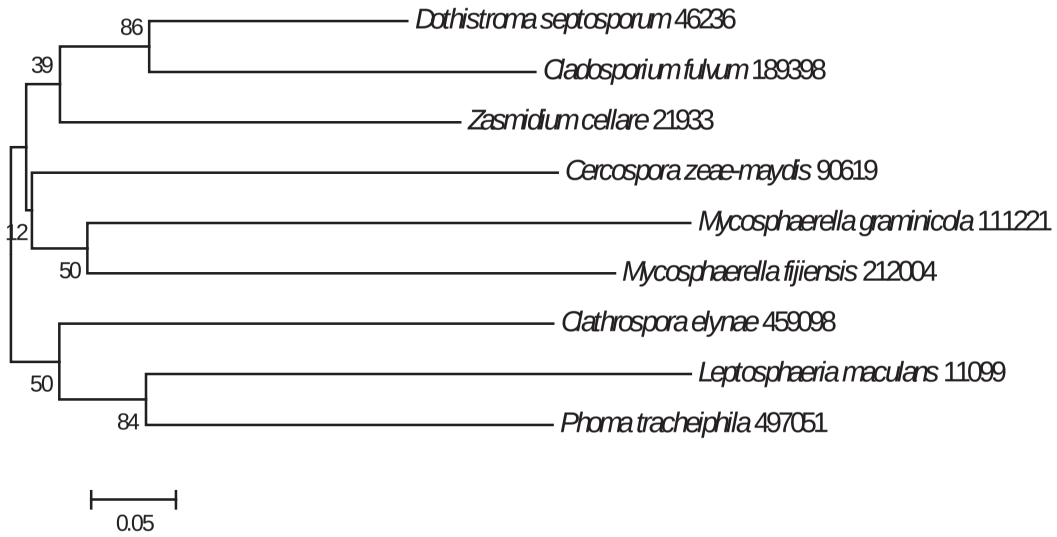

(A) A neighbor-joining tree of Ecp6 homologues from Dothideomycete fungi. The bootstrap values are shown at the nodes as percentages. *C. fulvum* Ecp6 (CfEcp JGI:6189398) and *D. septosporum* Ecp6 (DsEcp6, JGI:46236) are clustered together. Other numbers alongside the species names refer to JGI protein ID numbers.

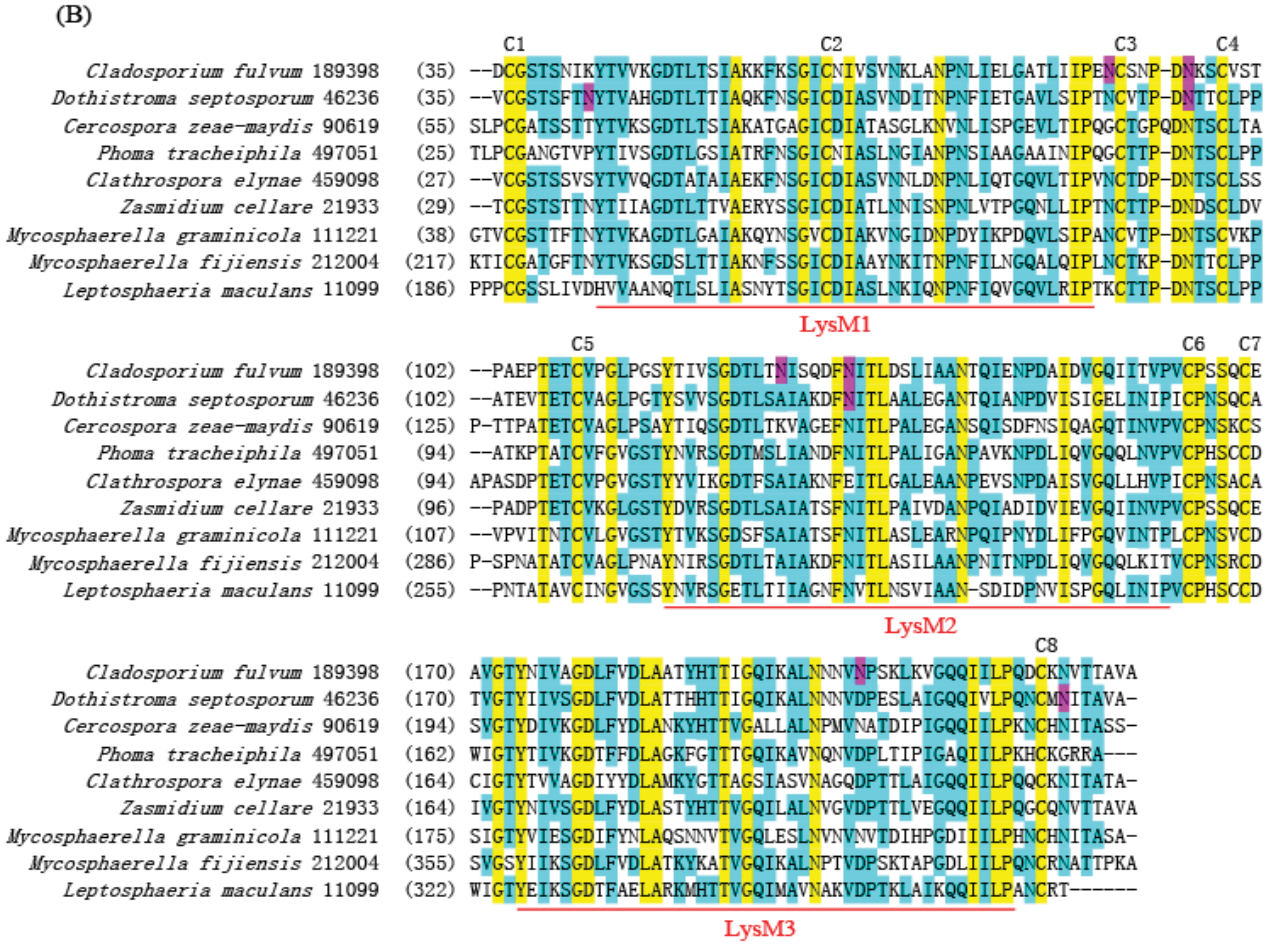

(B) Amino acid alignment of Ecp6 proteins from fungal species. Identical amino acids are highlighted in yellow and similar amino acids are highlighted in blue. Eight conserved cysteine residues are indicated on top of the alignment. The red lines indicate the positions of three predicted extracellular lysin motifs based on CfEcp6 predicted LysM motif sequences (Sanchez-Vallet et al., 2013). The predicted N-glycosylation sites of CfEcp6 and DsEcp6 are highlighted in pink.

Appendix figure 3.3 Predicted translation of *DsEcp4*, *DsEcp5*, *DsEcp13*, *DsEcp14* and hydrophobin genes

DsEcp4 (JGI: 192200)

```
      M  H  N  S  I  P  F  L  A  V  L  S  G  A  T  F  A  V  A  D
    1 atgcacaattccatcccatttctcgcagttctgtcaggagctaccttcgccgtcgctgat 60
      P  L  F  S  F  S  E  Y  G  Y  G  D  M  E  C  R  G  V  H  L
   61 ccactcttcagttttagtgaatacggctacggtgacatggaatgtcgcggggtgcatctc 120
      I  S  P  S  V  S  V  N  D  D  S  G  G  C  H  Q  F  P  V  G
  121 atcagcccatccgtcagcgtcaacgatgattccggcggctgtcaccaattccccgtcggt 180
      I  G  *  V  Q  Y  K  L  I  E  G  S  L  Q  I  C  T  V  E  L
  181 atcggctgagtgcaatacaagctcattgagggctcgctgcaaatatgcaccgtggagctg 240
      F  T  N  D  A  C  D  G  S  A  I  K  K  R  A  Y
  241 ttcacgaacgatgcttgtgatggatcagctatcaagaagcgagcatagtcctagaattga 300
                                 R  Y  V  L  K  V  G  E  T  K  C
  301 gcgcaactctcaggcactgatcttgaagtaggtatgtcctcaaggtcggcgagacaaagt 360
        H  S  P  I  G  G  G  R  Q  S  V  Q  V  T  C  P  *
  361 gccattctcctatcggtggcgggcggcagagtgtgcaggtcacttgtccataa         413
```

The predicted intron position is highlighted in yellow. The internal stop codon is highlighted in green.

DsEcp5 (JGI: 69490)

```
      M  V  V  G  G  *  T  V  S  N  A  L  R  C  L  T  G  T  L  T
    1 atggttgtgggcgggtaaaccgtctccaatgcgctacgttgtctcacgggaaccctcacc 60
      Q  I  I  A  E  S  L  L  Y  P  S  P  P  N  F  I  V  H  T  H
   61 cagatcatcgcggaatccctgctttacccttcgccccccaaatttcatcgtccacactcac 120
      T  G  N  P  T  Q  C  T  N  N  P  Y  D  E  A  G  V  D  R  W
  121 actggtaaccccacacagtgcacaaacaaccccctacgacgaggccggcgtcgaccgctgg 180
      L  Q  Q  A  R  G  G  I  G  C  S  T  L  I  E  H  G  A  W  Y
  181 ctccagcaagcgcgtggaggcatcggttgctcaacacttatagagcacggcgcgtggtac 240
      T  S  T  G  E  I  V  N  G  H  A  I  C  S  C  A  R  G  *  T
  241 acctcgacgggggagattgtcaacgggcatgcgatttgctcgtgtgcgcgcggctagacg 300
      K  A  H  N  Y  V  I  S  G  D  Y  P  A  G  T  A  K  L  T  F
  301 aaggcgcacaattatgtgattagcggggattatccggccgggacggccaagttgacgttt 360
      S  G  D  A  P  Q  E  V  S  G  C  G  S  K  R  A  W  K  R  G
  361 agtggagatgcgcctcaagaagtgtcagggtgtgggtcaaagagagcatggaaaagggga 420
      E  E  A  G  R  G  C  *
  421 gaggaagcagggagaggttgttga                                     444
```

The internal stop codons are highlighted in green.

DsEcp13 (JGI: 90760)

```
      M  R  F  F  A  L  A  I  F  A  T  A  A  K  A  A  V  F  K  G
    1 atgcgcttctttgctctcgccatctttgccaccgccgcgaaagcggctgtcttcaagggc 60
      L  D  S  R  S  D  A  M  S  I  F  E  R  R  S  S  C  N  S  D
   61 ctcgactcccgaagcgatgccatgagcatcttcgaacggcgatctagctgtaattcggac 120
      P  P
  121 cctcgtgagtggtctttccccacatcgcattcactcctgtctccctcgctgactaatggc 180
                  V  C  Y  Q  N  G  D  C  C  N  G  C  C  D  K  N
  181 ccgtctcaagccgtctgctatcagaatggcgactgttgcaacggttgctgcgacaagaat 240
      T  G  K  C  C  P  N  G  C  D  N  F  N  T  C  R  *
  241 acgggaaagtgttgccccaatggctgcgataatttcaacacctgcagatga           291
```

The predicted intron position is highlighted in yellow.

DsEcp14 (JGI: 71428)

```
      M  I  T  I  R  F  L  A  R  L  S  L  V  V  G  L  A  K  A  S
    1 atgatcacaatacgattcctggcccggttaagccttgtcgtaggtcttgcaaaagcctca 60
      P  Q  W  G  G  G  H  D  T  S  R  H  E  D  G  L  P  T  C  T
   61 ccacaatggggaggcggccacgacacatcgagacacgaagatggtctcccaacctgtacc 120
      D  G  G  Q  L  R  C  C  G  A  V  F  N  G  D  N  A  P  T  E
  121 gacggcggtcaattgcgctgctgtggagcagtcttcaatggcgacaatgcgccgacggaa 180
      L  L  T  S  L  S  C  Y  D  L  T  P  A  T  T  N  C  L  L  T
  181 ctgctcacctctctttcgtgctacgatctcacgccagcgacgaccaattgccttctcacc 240
      A  T  S  P  D  S  D  G  S  C  P  G  Y  W  Q  C  C  Q  I  V
  241 gcaacatcgccggatagcgacggcagctgcccgggctactggcagtgctgccaaatcgtc 300
      L  D  P  I  I  G  I  Y  C  G  P  P  P  G  P
  301 ttagacccaatcattggaatatactgtggaccgccacctgggcgtgggtatactcaacgt 360
                                              C  Q  G  P  E  K
  361 tacagcatgcgttgaagctttgctgacaagttcttttgtagcttgccagggccccgagaa 420
       S  P  R  C  L  D  I  I  S  G  R  F  G  V  C  P  A  S  S  P
  421 gtcgcctcgatgtctcgatataatcagtggaagatttggagtctgtcccgcgagcagccc 480
       L  K  G  L  L  D  T  D  G  E  Y  T  P  G  S  G  R  F  V  A
  481 gctgaagggacttttggacaccgacggagagtacacgccaggcagcggacgttttgtggc 540
       S  K  V  A  G  P  G  R  G  G  E  D  A  T  T  G  L  G  L  N
  541 gagcaaggtggcggggccaggcagaggcggcgaagatgccacgactggattgggtctaaa 600
       G  L  L  P  G  V  D  G  L  L  D  G  R  D  L  S  S  L  A  G
  601 tggtttactgccgggtgtcgatgggcttctcgatggaagagatctgtcgtcattggcagg 660
       H  L  A  E  A  P  S  T  *
  661 gcacctggcagaagcaccaagcacgtga                                  688
```

The predicted intron position is highlighted in yellow.

DsHdp1 (JGI 75009)

```
     M  Q  F  A  A  F  F  F  A  G  L  A  A  I  S  T  A  T  P  I
   1 atgcaattcgcagccttcttctttgccggccttgccgcgatctctaccgccaccccaatc 60
     A  G  E  E  P  G  I  S  G  A  G  T  Y  G  P  G  Q  V  S  D
  61 gctggcgaagagccgggcatttcgggtgctggaacatacggccccggccaagtctctgac 120
     G  D  A  A  G  I  C  T  A  L  Y  T  P  Q  C  C  E  T  S  V
 121 ggcgatgcagcgggcatctgtactgctctctacacccctcagtgctgcgagaccagcgtt 180
     L  G  V  A  D  L  A  C  N  T  P
 181 ctcggcgttgccgatcttgcttgcaacactcgtcagtagcgtcgagccaactgcatnggt 240
                          S  V  S  V  D  S  E  Q  S  L  I  N
 241 ataagactgacaatacttcctagcatctgtctccgtcgactccgagcagtctctcatcaa 300
      D  C  A  K  T  G  A  T  A  E  C  C  V  L  P  V
 301 tgactgtgccaagactggtgccacagctgagtgctgtgtccttccagttgtaagtacttc 360
                                      A  G  Q  A  L  L  C
 361 aagaagtccagaagtggactccatagctgatttgtcccaggctggccaagctcttctctg 420
      Y  D  L  *
 421 ctacgacctctaa                                             433
```

The intron position, as verified by cDNA sequencing, is highlighted in yellow.

DsHdp2 (JGI 67650)

```
     M  Q  F  T  T  L  F  A  A  A  L  S  A  C  L  V  A  A  I  P
   1 atgcaattcaccacacttttcgctgccgccttgagcgcctgcctcgtcgccgctatccct 60
     S  P  S  Y  L  P  E  G  G  D  G  S  M  D  S  F  C  G  N  Q
  61 tccccgtcttacctcccggaggggggtgacggttccatggactccttctgtggcaatcag 120
     Q  K  A  A  C  C  D  G  S  N  E  G  G  L  G  G  I  F  G  G
 121 cagaaggctgcctgctgcgatggctccaacgagggtggtctaggtggtatcttcggcggg 180
     I  L  G  G  V  L  G  G  D  C  A  L  T  V  V
 181 attttgggtggtgtcctgggtggcgactgtgctcttaccgttggtatgtctcaacattca 240
                                                  S  G  E  C  S
 241 ctggtttctctcccccaaagtaaagctgctaacgttcctctagtcagcggagagtgctcc 300
     Q  G  S  V  A  C  C  P  T  T  N  V  G  S  S
 301 cagggctctgtcgcatgttgcccaaccaccaacgtcggctcgtcggtttgtccttctttt 360
                                        S  L  V  S  L  G  S  I
 361 gccacgctatcttcgttcagcactaacgccatcgcagagcctcgtctccctcggatccat 420
      C  A  P  I  T  L  *
 421 ctgcgccccaatcaccttgtga                                    442
```

The predicted intron positionis highlighted in yellow.

DsHdp3 (JGI 37242)

```
      M  R  T  F  I  L  A  S  L  A  L  G  A  S  L  V  A  A  M  P
    1 atgcgtactttcatcctcgcatccttggctctcggcgccagtttggttgccgcaatgccc 60
      Q  D  G  L  Q  A  D  S  N  Q  V  D  R  R  W  N  D  E  I  Y
   61 caggacgggctccaggccgactccaaccaagttgaccgtcgctggaacgacgagatctac 120
      R  G  S  D  Y  R  G  T  G  Y  R  G  W  R  G  N  D  N  R  G
  121 cgtggcagtgattaccgcggcactggataccgtggctggcgtggcaatgacaaccgcggc 180
      N  R  Y  N  T  N  G  Y  H  G  Y  D  N  C  G  D  D  E  D  C
  181 aatcggtacaacaccaacggctaccacggttatgacaactgcggcgatgatgaggactgc 240
      Q  R  N  G  P  S  P  Q  G  Y  G  E  D  D  Y  N  D  N  Y  N
  241 caacgtaatggtcctagtccacagggttatggagaagatgactacaatgacaactacaac 300
      D  A  K  L  R  R  R  T  W  D  N  N  Y  D  G  D  R  P  Q  Q
  301 gacgcgaagctccgccgtcgtacctgggacaacaattatgatggagaccgcccccagcaa 360
      Y  G  N  S  R  Y  G  D  N  G  Y  S  G  D  G  Y  S  R  N  G
  361 tatggcaacagccgttacggtgacaatggctacagcggcgatggctacagccgcaatggc 420
      Y  N  G  D  C  E  D  G  N  C  D  S  R  D  G  D  Y  G  G  N
  421 tacaacggcgactgcgaggatggcaattgtgatagccgcgatggcgattacggaggcaac 480
      F  R  C  P  G  L  A  A  V  P  Q  C  C  E  L  N  A  A  G  V
  481 tttaggtgccctggactggcggctgtgccacaatgctgtgagctgaacgcagctggtgtt 540
      V  S  A  T  C  K  N
  541 gtgtctgccacttgcaagaaccgtgagtaccgttcagatgtgtaatatgattctcagtgc 600
                     P  S  R  T  P  D  S  K  G  E  F  Q  E  D  C  A
  601 tgatcgcgttcacagcttcccgcaccccggacagcaagggcgagttccaggaggactgtg 660
        Q  S  G  K  S  A  Q  C  C  V  L  P  L  G
  661 cccagagcggcaaatcggcgcagtgctgtgtgttgccacttggcgtgagtcgaccgttct 720
                                          I  G  I  S  V  A  C
  721 acctttcggcctggacgatcgtactgacatgtgtatcagatcggcattagcgtggcttgc 780
      N  N  V  *
  781 aacaacgtttag                                               792
```

The predicted intron position is highlighted in yellow.

DsHdp4 (JGI 120918)

```
      M  P  F  N  L  L  T  L  A  L  A  A  S  A  A  A  A  P  G  S     F1
    1 atgcctttcaatctccttaccctggctctcgcggcatctgccgcagcagcacctggttca 60
      S  R  L  S  E  R  Q  T  I  D  V  C  T  S  G  Y  S  A  Q  C     F1
   61 tctcgattgtcggaaaggcagaccatcgacgtttgcacgagcggatatagcgctcagtgc 120
      C  A  T  D  V  L  N  L  A  S  L  D  C  A  N
  121 tgcgcaacagacgttctcaacttggcgtctctggactgcgcaaatggtttgcattattgt 180
                                          V  P  I  T  P  T  S     F1
  181 tcactgcttccaagtccagagggctgacatgatcacacagtgcccataactcccacatcc 240
      K  E  D  F  T  E  Q  C  S  A  T  G  Q  Q  A  L  C  C  L  L     F1
  241 aaggaagactttactgagcagtgcagtgctactggacagcaagccttgtgctgtctcttg 300
      P  I
                                                            L  E     F2
  301 ccgattgtaagtgacagttggtgatcgttggaaatgcatggctaacaacttgtagcttga 360
       Q  G  L  I  C  Q  N  P  *                                     F2
  361 gcaaggtctgatctgccagaacccctga                                  388
```

The predicted intron position is highlighted in yellow.

Ds69335 (JGI: 69335)

```
      M  R  S  T  L  A  I  A  A  F  A  A  G  A  L  A  V  P  Y  N
    1 atgcgctccactcttgcaattgccgccttcgcggctggcgcgctcgccgtcccgtacaac 60
      K  E  Q  K  R  D  V  V  T  D  I  D  Y  V  T  A  Y  N  V  V
   61 aaggagcagaagcgcgacgttgtcaccgacatcgactatgtcactgcctacaatgtagtc 120
      T  V  T  A  G  Q  P  A  A  T  P  E  A  P  K  H  Y  G  H  H
  121 accgtcaccgccggccagccagccgcaactccagaggcgccaaagcactacggccaccac 180
      N  N  Y  N  N  P  V  A  Y  T  T  V  V  T  T  S  S  A  A  P
  181 aacaactacaacaatccagtggcgtacaccactgtcgtcaccacctcatctgccgctcca 240
      A  A  Y  S  P  P  A  V  E  Q  P  A  T  T  S  S  A  P  A  Y
  241 gcagcctacagcccaccagcggtggagcagccggcaaccacttcgtcggcaccagcttac 300
      S  A  S  S  A  S  G  P  E  P  T  D  Y  A  G  K  C  V  Y  H
  301 agcgcctcatcggcgagcggccctgaaccgactgactacgccggcaaatgcgtctaccac 360
      H  N  L  H  R  A  N  H  S  V  S  D  I  A  W  D  D  G  L  A
  361 cacaacttgcaccgtgccaatcactccgtctctgacatcgcgtgggacgacggtctcgcc 420
      S  I  A  Q  T  I  A  E  S  C  V  Y  A  H  N  V
  421 tccattgctcagaccattgctgagagctgcgtctacgcacacaacgtgtgagtggtgtcc 480
                                                Q  E  G  G  G  G  Y
  481 aatattctcaatgcaaagcgtgtgctaacatatcacagtcaagagggtggaggcggctac 540
      G  Q  N  I  A  A  G  V  D  A  A  N  I  S  A  I  I  T  D  L
  541 ggtcagaacattgcagctggtgttgacgctgccaacatttctgccatcatcaccgacctt 600
      F  Y  N  G  E  E  P  Y  F  A  D  Q  Y  G  K  D  D  P  D  M
  601 ttctacaacggcgaggagccatactttgccgatcagtacggcaaggacgacccagacatg 660
      T  N  F  E  L  F  G  H  F  T  Q  I  V  W  K  D  T  I  S  V
  661 accaactttgagcttttcggtcacttcacgcagatcgtctggaaggacaccatttccgtc 720
      G  C  A  T  V  Q  C  P  N  G  L  A  N  T  G  D  G  V  E  P
  721 gggtgcgccactgtccagtgtcccaacggtttggccaacactggtgatggtgttgagcca 780
      V  F  T  V  C  N  Y  K  N  P  G  N  Y  A  G  E  Y  G  A  N
  781 gtcttcaccgtctgcaactacaagaacccaggcaattacgctggcgaatacggcgccaac 840
      V  L  Q  P  L  G  H  P  T  A  N  W  N  T  G  S  S  *
  841 gtgctccagccacttgggcacccgaccgcgaattggaacaccggctcatcgtag       894
```

The predicted intron position is highlighted in yellow.

Appendix figure 3.4 gDNA of complemented *DsAvr4*, *DsEcp2-1* and *DsEcp6* mutants

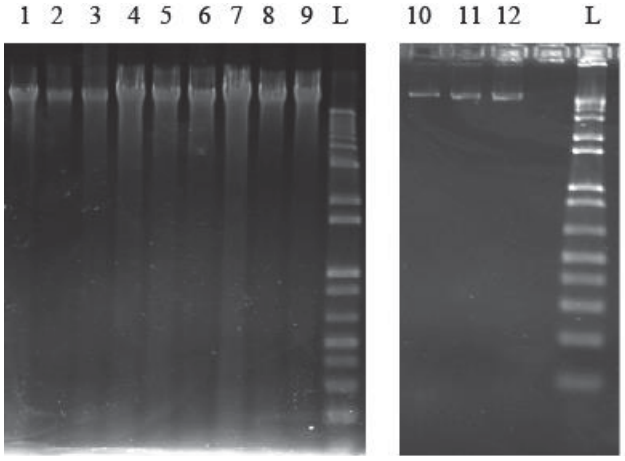

1	Avr4 comp-1	7	Ecp2-1 comp-1
2	Avr4 comp-2	8	Ecp2-1 comp-2
3	Avr4 comp-3	9	Ecp2-1 comp-3
4	Ecp6 comp-1	10	Avr4 comp-4
5	Ecp6 comp-2	11	Ecp6 comp-4
6	Ecp6 comp-3	12	Ecp2-1 comp-4
L	1 kb+ ladder		

Lane L is 1 kb+ ladder. LaneS 1-12 are gDNA extracted from complemented strains. All the complemented strains showed a high molecular weight gDNA band on the gel.

Appendix 4. Tables

Appendix table 4.1 Copy number estimation in *DsAvr4*, *DsEcp2-1* and *DsEcp6* complementation strains by real-time PCR

DsAvr4

Targets	References	Mean Cp	Mean Cp	Target/Ref	Average	Normalised	Copy number
WT-Avr4	WT-AflR	23.89	23.70	0.57	0.59	1.00	
WT-Avr4	WT-AflR	23.92	23.71	0.56			
WT-Avr4	WT-AflR	23.78	23.76	0.63			
Avr4-C1-Avr4	Avr4-C1-AflR	21.72	21.79	0.76	0.78	1.33	1
Avr4-C1-Avr4	Avr4-C1-AflR	21.83	22.01	0.82			
Avr4-C1-Avr4	Avr4-C1-AflR	21.90	21.96	0.75			
Avr4-C2-Avr4	Avr4-C2-AflR	21.60	21.98	0.94	0.96	1.65	2
Avr4-C2-Avr4	Avr4-C2-AflR	21.63	21.97	0.91			
Avr4-C2-Avr4	Avr4-C2-AflR	21.57	22.12	1.05			
Avr4-C3-Avr4	Avr4-C3-AflR	22.33	22.28	0.68	0.77	1.31	1
Avr4-C3-Avr4	Avr4-C3-AflR	22.32	22.45	0.77			
Avr4-C3-Avr4	Avr4-C3-AflR	22.26	22.55	0.85			
Avr4-C4-Avr4	Avr4-C4-AflR	22.55	22.54	0.69	0.71	1.21	1
Avr4-C4-Avr4	Avr4-C4-AflR	22.60	22.66	0.72			
Avr4-C4-Avr4	Avr4-C4-AflR	22.52	22.57	0.72			

DsEcp2-1

Targets	References	Mean Cp	Mean Cp	Target/Ref	Average	Normalised	Copy number
WT-Ecp2-1	WT-AflR	23.37	23.61	0.99	1.01	1.00	
WT-Ecp2-1	WT-AflR	23.46	23.47	0.86			
WT-Ecp2-1	WT-AflR	23.28	23.82	1.19			
Ecp2-1-C2-Ecp2-1	Ecp2-1-C2-AflR	24.66	24.55	0.77	0.81	0.80	1
Ecp2-1-C2-Ecp2-1	Ecp2-1-C2-AflR	24.62	24.65	0.84			
Ecp2-1-C2-Ecp2-1	Ecp2-1-C2-AflR	24.63	24.64	0.83			
Ecp2-1-C3-Ecp2-1	Ecp2-1-C3-AflR	21.92	23.54	2.43	2.49	2.46	2
Ecp2-1-C3-Ecp2-1	Ecp2-1-C3-AflR	21.89	23.58	2.55			
Ecp2-1-C3-Ecp2-1	Ecp2-1-C3-AflR	21.93	23.58	2.49			
Ecp2-1-C4-Ecp2-1	Ecp2-1-C4-AflR	23.74	23.26	0.62	0.66	0.65	1
Ecp2-1-C4-Ecp2-1	Ecp2-1-C4-AflR	23.69	23.35	0.68			
Ecp2-1-C4-Ecp2-1	Ecp2-1-C4-AflR	23.70	23.35	0.68			
Ecp2-1-C5-Ecp2-1	Ecp2-1-C5-AflR	21.83	23.46	2.46	2.41	2.38	2
Ecp2-1-C5-Ecp2-1	Ecp2-1-C5-AflR	21.86	23.62	2.67			
Ecp2-1-C5-Ecp2-1	Ecp2-1-C5-AflR	21.88	23.26	2.11			

DsEcp6

Targets	References	Mean Cp	Mean Cp	Target/Ref	Average	Normalised	Copy number
WT-Ecp6	WT-AflR	23.56	23.78	0.79	0.77	1.00	
WT-Ecp6	WT-AflR	23.56	23.78	0.79			
WT-Ecp6	WT-AflR	23.51	23.63	0.74			
Ecp6-C2-Ecp6	Ecp6-C2-AflR	22.14	22.25	0.80	0.89	1.14	1
Ecp6-C2-Ecp6	Ecp6-C2-AflR	22.09	22.47	0.96			
Ecp6-C2-Ecp6	Ecp6-C2-AflR	22.22	22.52	0.90			
Ecp6-C3-Ecp6	Ecp6-C3-AflR	22.91	22.51	0.56	0.54	0.69	1
Ecp6-C3-Ecp6	Ecp6-C3-AflR	22.95	22.55	0.56			
Ecp6-C3-Ecp6	Ecp6-C3-AflR	23.05	22.47	0.49			
Ecp6-C4-Ecp6	Ecp6-C4-AflR	21.72	22.78	1.50	1.34	1.74	2
Ecp6-C4-Ecp6	Ecp6-C4-AflR	21.91	22.70	1.25			
Ecp6-C4-Ecp6	Ecp6-C4-AflR	21.94	22.77	1.28			
Ecp6-C5-Ecp6	Ecp6-C5-AflR	21.61	22.71	1.54	1.72	2.22	2
Ecp6-C5-Ecp6	Ecp6-C5-AflR	21.57	22.93	1.82			
Ecp6-C5-Ecp6	Ecp6-C5-AflR	21.60	22.95	1.79			

The CT values of the target gene (*DsAvr4*, *DsEcp2-1* or *DsEcp6*) were compared to the reference gene *DsAflR* and the result normalized to WT (Materials and Methods section 2.5.2). Three *DsAvr4* complemented strains (1, 3 and 4), two *DsEcp2-1* complemented strains (2,4) and two *DsEcp6* complemented strains (2 and 3) showed a normalized ratio to WT of <1.5 and suggested an estimated copy number of 1 for the target gene tested in these strains.

Appendix table 4.2 *DsAvr4* and *DsEcp6* expression in *DsLaeA* mutant strain

(A) DsAvr4

Targets	References	Mean Cp (Ref)	Mean Cp (Tar)	Target/Ref Cp	Ratio	T-test
WT-Avr4	WT-tub	33.33	20.03	9.92E-05	1.00	0.004
WT-Avr4	WT-tub	33.21	20.08	1.12E-04	1.00	
WT-Avr4	WT-tub	33.14	20.08	1.17E-04	1.00	
LaeAKO1-Avr4	LaeAko1-Tub	30.23	20.38	1.08E-03	10.89	
LaeAKO1-Avr4	LaeAko1-Tub	30.83	20.37	7.09E-04	6.33	
LaeAKO1-Avr4	LaeAko1-Tub	30.87	20.45	7.30E-04	6.24	

(B) DsEcp6

Targets	References	Mean Cp (Ref)	Mean Cp (Tar)	Target/Ref Cp	Ratio	T-test
WT-Ecp6	WT-tub	21.87	20.03	0.2778	1.00	2.24E-07
WT-Ecp6	WT-tub	21.88	20.08	0.2871	1.00	
WT-Ecp6	WT-tub	21.86	20.08	0.2896	1.00	
LaeAKO1-Ecp6	LaeAko1-Tub	25.62	20.38	0.026	0.10	
LaeAKO1-Ecp6	LaeAko1-Tub	25.60	20.37	0.027	0.09	
LaeAKO1-Ecp6	LaeAko1-Tub	25.72	20.45	0.026	0.09	

RNA was extracted from *DsLaeA* mutant and WT strain mycelium growing in PMMG nine days post-inoculation. The expression of *Ds-Avr4* and *Ds-Ecp6* in *DsLaeA* mutant strain was compared to WT. Tubulin was used as reference, expression of *DsAvr4* and *DsEcp6* in the *DsLaeA* mutant strain was normalized to WT (WT=1). The changes in gene expression in the *DsLaeA* mutant strain compared to the WT strain were significant (T-test with $P<0.05$) for *Ds-Avr4* and *Ds-Ecp6*. *Ds-Avr4* was up-regulated in *DsLaeA* mutant strain compare to WT. *Ds-Ecp6* was down-regulated in the *DsLaeA* mutant strain compared to WT.

Appendix table 4.3 Percentage of amino acid identities of nine effectors from *D. septosporum* strains

DsAvr4

BHU1	NZE2	NZE10	AUST6	ORE12	USA-MON8	CAN3	SAF1625	SAF4	KEN4	GUA1	GUA-N1	COL-N	COL-S	BRZ1	CHI17	ECU13	GRED1	ROM11	SLV1	POL4	CZE1	ATRA4-2	Hun2-53	ALP3	DAPAR1	FRA1	SP2	UK402	SCO484	FIN3.2	Strain
	99	99	99	97	98	98	98	99	99	94	93	92	92	99	99	99	99	98	98	98	97	98	98	99	98	98	99	99	99	99	BHU1
		100	100	97	98	98	98	99	99	94	93	92	92	100	100	100	99	98	98	98	97	98	98	99	98	98	99	100	100	100	NZE2
			100	97	98	98	98	99	99	94	93	92	92	100	100	100	99	98	98	98	97	98	98	99	98	98	99	100	100	100	NZE10
				97	98	98	98	99	99	94	93	92	92	100	100	100	99	98	98	98	97	98	98	99	98	98	99	100	100	100	AUST6
					99	99	96	97	97	94	94	92	92	97	97	97	98	99	99	99	99	98	99	98	99	99	97	97	97	97	ORE12
						100	97	98	98	95	94	93	93	98	98	98	99	100	100	100	99	99	100	99	100	100	98	98	98	98	USA-MON8
							97	98	98	95	94	93	93	98	98	98	99	100	100	100	99	99	100	99	100	100	98	98	98	98	CAN3
								99	98	93	92	91	91	98	98	98	99	97	97	97	96	98	97	99	97	97	98	98	98	98	SAF1625
									99	94	93	92	92	99	99	99	99	98	98	98	97	99	98	99	98	98	99	99	99	99	SAF4
										94	93	92	92	99	99	99	99	98	98	98	97	98	98	99	98	98	99	99	99	99	KEN4
											99	96	96	94	94	94	94	95	95	95	94	94	95	94	95	95	94	94	94	94	GUA1
												97	97	93	93	93	94	94	94	94	94	94	94	94	94	94	93	93	93	93	GUA-N1
													100	92	92	92	92	93	93	93	92	92	93	92	93	93	92	92	92	92	COL-N
														92	92	92	92	93	93	93	92	92	93	92	93	93	92	92	92	92	COL-S
															100	100	99	98	98	98	97	98	98	99	98	98	99	100	100	100	BRZ1
																100	99	98	98	98	97	98	98	99	98	98	99	100	100	100	CHI17
																	99	98	98	98	97	98	98	99	98	98	99	100	100	100	ECU13
																		99	99	99	98	99	99	100	99	99	99	99	99	99	GRED1
																			100	100	99	99	100	99	100	100	98	98	98	98	ROM11
																				100	99	99	100	99	100	100	98	98	98	98	SLV1
																					99	99	100	99	100	100	98	98	98	98	POL4
																						98	99	98	99	99	97	97	97	97	CZE1
																							99	99	99	99	98	98	98	98	ATRA4-2
																								99	100	100	98	98	98	98	Hun2-53
																									99	99	99	99	99	99	ALP3
																										100	98	98	98	98	DAPAR1
																											98	98	98	98	FRA1
																												99	99	99	SP2
																													100	100	UK402
																														100	SCO484
																															FIN3.2

Amino acid identity comparing aa sequences of DsAvr4 from 31 *D. septosporum* strains. The color trends indicate high (darker) to low (lighter) % aa identity. Both Guatemala and Colombia strains showed low aa identity to other strains tested. COL-N showed 100% aa identity to COL-S.

DsEcp2-1

BHU1	NZE2	NZE10	AUST6	ORE12	USA-MON8	CAN3	SAF1625	SAF4	KEN4	GUA1	GUA-N1	COL-N	COL-C	BRZ1	CHI17	ECU13	GRED1	ROM11	SLV1	POL4	CZE1	ATRA4-2	Hun2-53	ALP3	DPAR1	FRA1	SP2	UK402	SCO484	FIN3.2	Strain
	97	97	97	99	99	99	96	96	99	98	98	98	98	99	99	99	98	98	98	98	98	96	98	97	98	98	97	97	97	97	BHU1
		100	100	98	98	98	98	98	98	96	96	96	96	98	98	98	98	97	98	98	98	98	98	98	97	98	98	100	99	100	NZE2
			100	98	98	98	98	98	98	96	96	96	96	98	98	98	98	97	98	98	98	98	98	98	97	98	98	100	99	100	NZE10
				98	98	98	98	98	98	96	96	96	96	98	98	98	98	97	98	98	98	98	98	98	97	98	98	100	99	100	AUST6
					100	100	97	97	100	99	99	98	98	100	100	100	99	98	99	99	99	97	99	98	98	99	98	98	98	98	ORE12
						100	97	97	100	99	99	98	98	100	100	100	99	98	99	99	99	97	99	98	98	99	98	98	98	98	USA-MON8
							97	97	100	99	99	98	98	100	100	100	99	98	99	99	99	97	99	98	98	99	98	98	98	98	CAN3
								100	97	96	96	95	95	97	97	97	98	98	98	98	98	100	98	99	98	98	98	98	99	98	SAF1625
									97	96	96	95	95	97	97	97	98	98	98	98	98	100	98	99	98	98	98	98	99	98	SAF4
										99	99	98	98	100	100	100	99	98	99	99	99	97	99	98	98	99	98	98	98	98	KEN4
											100	99	99	99	99	99	98	97	98	98	98	96	98	96	97	98	96	96	96	96	GUA1
												99	99	99	99	99	98	97	98	98	98	96	98	96	97	98	96	96	96	96	GUA-N1
													100	98	98	98	97	96	97	97	97	95	97	96	96	97	96	96	96	96	COL-N
														98	98	98	97	96	97	97	97	95	97	96	96	97	96	96	96	96	COL-C
															100	100	99	98	99	99	99	97	99	98	98	99	98	98	98	98	BRZ1
																100	99	98	99	99	99	97	99	98	98	99	98	98	98	98	CHI17
																	99	98	99	99	99	97	99	98	98	99	98	98	98	98	ECU13
																		99	100	100	100	98	100	98	99	100	99	98	98	98	GRED1
																			99	99	99	98	99	97	100	99	98	97	97	97	ROM11
																				100	100	98	100	98	99	100	99	98	98	98	SLV1
																					100	98	100	98	99	100	99	98	98	98	POL4
																						98	100	98	99	100	99	98	98	98	CZE1
																							98	99	98	98	98	98	99	98	ATRA4-2
																								98	99	100	99	98	98	98	Hun2-53
																									97	98	98	98	99	98	ALP3
																										99	98	97	97	97	DPAR1
																											99	98	98	98	FRA1
																												98	98	98	SP2
																													99	100	UK402
																														99	SCO484
																															FIN3.2

Amino acid identity comparing aa sequences of DsEcp2-1 from 31 *D. septosporum* strains. The color trends indicate high (darker) to low (lighter) % aa identity. Both Guatemala and Colombia strains showed low aa identity to other strains tested. COL-N showed 100% aa identity to COL-S.

DsEcp2-3

BHU1	NZE2	NZE10	AUST6	ORE12	USA-MON8	CAN3	SAF1625	SAF4	KEN4	GUA1	GUA-N1	COL-N	COL-C	BRZ1	CHI17	ECU13	GRED1	SLV1	POL4	CZE1	ATRA4-2	Hun2-53	ALP3	FRA1	SP2	UK402	Fin3.2	Strain
	99	99	99	98	98	98	99	98	99	94	94	93	93	98	98	99	99	99	99	99	99	99	98	98	99	99	99	BHU1
		100	100	99	99	99	100	99	99	94	94	94	94	99	99	99	100	100	100	100	100	99	99	99	99	100	100	NZE2
			100	99	99	99	100	99	99	94	94	94	94	99	99	99	100	100	100	100	100	99	99	99	99	100	100	NZE10
				99	99	99	100	99	99	94	94	94	94	99	99	99	100	100	100	100	100	99	99	99	99	100	100	AUST6
					99	99	98	99	98	94	94	93	93	99	99	99	98	98	98	98	98	98	98	98	98	99	98	ORE12
						100	99	100	98	94	94	94	94	100	100	100	99	99	99	99	99	98	98	98	98	99	99	USA-MON8
							99	100	98	94	94	94	94	100	100	100	99	99	99	99	99	98	98	98	98	99	99	CAN3
								99	99	94	94	93	93	99	98	99	100	99	99	99	99	99	99	99	99	100	99	SAF1625
									98	94	94	94	94	100	100	100	99	99	99	99	99	98	98	98	98	99	99	SAF4
										94	94	94	94	98	99	99	99	99	99	99	99	99	98	98	99	99	99	KEN4
											100	94	94	94	94	94	94	94	94	95	94	94	94	94	94	94	94	GUA1
												94	94	94	94	94	94	94	94	95	94	94	94	94	94	94	94	GUA-N1
													100	94	93	94	93	93	93	94	93	94	93	93	93	94	93	COL-N
														94	93	94	93	93	93	94	93	94	93	93	93	94	93	COL-C
															100	100	99	99	99	99	99	98	98	98	98	99	99	BRZ1
																99	98	98	98	98	98	98	98	98	98	99	98	CHI17
																	99	99	99	99	99	99	98	98	99	99	99	ECU13
																		99	99	99	99	99	99	99	99	100	99	GRED1
																			100	99	99	99	99	99	99	100	99	SLV1
																				99	99	99	99	99	99	100	99	POL4
																					99	100	99	99	99	100	99	CZE1
																						99	99	99	99	100	99	ATRA4-2
																							100	100	99	99	99	Hun2-53
																								100	98	99	99	ALP3
																									98	99	99	FRA1
																										99	99	SP2
																											100	UK402
																												Fin3.2

Amino acid identity comparing aa sequences of DsEcp2-3 from 28 *D. septosporum* strains. The color trends indicate high (darker) to low (lighter) % aa identity. Both Guatemala and Colombia strains showed low aa identity to other strains tested. GUA1 showed 100% aa identity to GUA-N1. COL-N showed 100% aa identity to COL-S.

DsEcp4

BHU1	NZE10	NZE2	AUST6	ORE12	USA-MON8	CAN3	SAF1625	SAF4	KEN4	GUA1	GUA-N1	COL-C	COL-N	BRZ1	CHI17	ECU13	GRED1	ROM11	SLV1	POL4	CZE1	ATRA4-2	Hun2-53	ALP3	DPAR1	FRA1	SP2	UK402	SCO484	Fin3.2	Strain
	99	99	99	98	99	98	99	99	99	78	92	88	93	99	99	99	99	99	99	99	99	98	98	99	99	99	98	99	98	98	BHU1
		100	100	99	100	99	100	100	100	79	93	89	93	100	100	100	100	100	100	100	100	99	99	100	100	100	99	100	99	98	NZE10
			100	99	100	99	100	100	100	79	93	89	93	100	100	100	100	100	100	100	100	99	99	100	100	100	99	100	99	98	NZE2
				99	100	99	100	100	100	79	93	89	93	100	100	100	100	100	100	100	100	99	99	100	100	100	99	100	99	98	AUST6
					99	100	99	99	99	78	92	88	93	99	99	99	99	99	99	99	99	98	98	99	99	99	99	99	98	98	ORE12
						99	100	100	100	79	93	89	93	100	100	100	100	100	100	100	100	99	99	100	100	100	99	100	99	98	USA-MON8
							99	99	99	78	92	88	93	99	99	99	99	99	99	99	99	98	98	99	99	99	99	99	98	98	CAN3
								100	100	79	93	89	93	100	100	100	100	100	100	100	100	99	99	100	100	100	99	100	99	98	SAF1625
									100	79	93	89	93	100	100	100	100	100	100	100	100	99	99	100	100	100	99	100	99	98	SAF4
										79	93	89	93	100	100	100	100	100	100	100	100	99	99	100	100	100	99	100	99	98	KEN4
											78	85	78	79	79	79	79	79	79	79	79	78	78	79	79	79	78	79	80	78	GUA1
												90	99	93	93	93	93	93	93	93	93	92	92	93	93	93	92	93	92	92	GUA-N1
													91	89	89	89	89	89	89	89	89	88	88	89	89	89	88	89	88	88	COL-C
														93	93	93	93	93	93	93	93	93	93	93	93	93	93	93	93	93	COL-N
															100	100	100	100	100	100	100	99	99	100	100	100	99	100	99	98	BRZ1
																100	100	100	100	100	100	99	99	100	100	100	99	100	99	98	CHI17
																	100	100	100	100	100	99	99	100	100	100	99	100	99	98	ECU13
																		100	100	100	100	99	99	100	100	100	99	100	99	98	GRED1
																			100	100	100	99	99	100	100	100	99	100	99	98	ROM11
																				100	100	99	99	100	100	100	99	100	99	98	SLV1
																					100	99	99	100	100	100	99	100	99	98	POL4
																						99	99	100	100	100	99	100	99	98	CZE1
																							98	99	99	99	98	99	98	98	ATRA4-2
																								99	99	99	98	99	98	98	Hun2-53
																									100	100	99	100	99	98	ALP3
																										100	99	100	99	98	DPAR1
																											99	100	99	98	FRA1
																												99	98	98	SP2
																													99	98	UK402
																														98	SCO484
																															Fin3.2

Amino acid identity comparing aa sequences of DsEcp4 from 31 *D. septosporum* strains. The color trends indicate high (darker) to low (lighter) % aa identity. Both Guatemala and Colombia strains showed low aa sequence identity to other strains tested, with GUA1 showing the lowest values.

DsEcp5

BHU1	NZE10	NZE2	AUST6	ORE12	USA-MON8	CAN3	SAF1625	SAF4	KEN4	BRZ1	CHI17	ECU13	GRED1	ROM11	SLV1	POL4	CZE1	ATRA4-2	Hun2-35	ALP3	DPAR1	FRA1	SP2	UK402	SCO484	Fin3.2	Strain
	99	99	99	99	95	96	100	100	100	99	99	99	99	100	100	100	99	99	100	100	100	100	99	100	99	100	BHU1
		100	100	99	94	95	99	99	99	100	100	100	99	99	99	99	98	100	99	99	99	99	99	99	100	99	NZE10
			100	99	94	95	99	99	99	100	100	100	99	99	99	99	98	100	99	99	99	99	99	99	100	99	NZE2
				99	94	95	99	99	99	100	100	100	99	99	99	99	98	100	99	99	99	99	99	99	100	99	AUST6
					94	95	99	99	99	99	99	99	99	99	99	99	98	99	99	99	99	99	99	99	99	99	ORE12
						99	95	95	95	94	94	94	94	95	95	95	94	94	95	95	95	95	95	95	94	95	USA-MON8
							96	96	96	95	95	95	95	96	96	96	94	95	96	96	96	96	96	96	95	96	CAN3
								100	100	99	99	99	99	100	100	100	99	99	100	100	100	100	99	100	99	100	SAF1625
									100	99	99	99	99	100	100	100	99	99	100	100	100	100	99	100	99	100	SAF4
										99	99	99	99	100	100	100	99	99	100	100	100	100	99	100	99	100	KEN4
											100	100	99	99	99	99	98	100	99	99	99	99	99	99	100	99	BRZ1
												100	99	99	99	99	98	100	99	99	99	99	99	99	100	99	CHI17
													99	99	99	99	98	100	99	99	99	99	99	99	100	99	ECU13
														99	99	99	98	99	99	99	99	99	99	99	99	99	GRED1
															100	100	99	99	100	100	100	100	99	100	99	100	ROM11
																100	99	99	100	100	100	100	99	100	99	100	SLV1
																	99	99	100	100	100	100	99	100	99	100	POL4
																		98	99	99	99	99	98	99	98	99	CZE1
																			99	99	99	99	99	99	100	99	ATRA4-2
																				100	100	100	99	100	99	100	Hun2-35
																					100	100	99	100	99	100	ALP3
																						100	99	100	99	100	DPAR1
																							99	100	99	100	FRA1
																								99	99	99	SP2
																									99	100	UK402
																										99	SCO484
																											Fin3.2

Amino acid identity comparing aa sequences of DsEcp5 from 27 D. septosporum strains. The color trends indicate high (darker) to low (lighter) % aa identity. USA-MON8 and CAN3 showed low aa identity to other strains tested. One nucleotide difference in GUA (extra) and COL (missing) strains led to frame shift of translation which led to truncated proteins. The Guatemala and Colombia strains are not included in the table.

DsEcp6

BHU1	NZE2	NZE10	AUST6	ORE12	USA-MON8	CAN3	SAF1625	SAF4	KEN4	GUA1	COL-N	COL-S	BRZ1	CHI17	ECU13	GRED1	SLV1	POL4	CZE1	Hun2-35	ALP3	DPAR1	FRA1	SP2	UK402	SCO484	Fin3.2	Strain
	99	99	99	99	99	99	99	99	99	99	99	99	99	99	99	99	99	99	99	99	99	99	99	99	99	99	99	BHU1
		100	100	100	100	100	100	100	100	100	100	100	100	100	100	100	100	100	100	100	100	100	100	100	100	100	100	NZE2
			100	100	100	100	100	100	100	100	100	100	100	100	100	100	100	100	100	100	100	100	100	100	100	100	100	NZE10
				100	100	100	100	100	100	100	100	100	100	100	100	100	100	100	100	100	100	100	100	100	100	100	100	AUST6
					100	100	100	100	100	100	100	100	100	100	100	100	100	100	100	100	100	100	100	100	100	100	100	ORE12
						100	100	100	100	100	100	100	100	100	100	100	100	100	100	100	100	100	100	100	100	100	100	USA-MON8
							100	100	100	100	100	100	100	100	100	100	100	100	100	100	100	100	100	100	100	100	100	CAN3
								100	100	100	100	100	100	100	100	100	100	100	100	100	100	100	100	100	100	100	100	SAF1625
									100	100	100	100	100	100	100	100	100	100	100	100	100	100	100	100	100	100	100	SAF4
										100	100	100	100	100	100	100	100	100	100	100	100	100	100	100	100	100	100	KEN4
											100	100	100	100	100	100	100	100	100	99	100	99	100	100	100	100	100	GUA1
												100	100	100	100	100	100	100	100	99	100	99	100	100	100	100	100	COL-N
													100	100	100	100	100	100	100	99	100	99	100	100	100	100	100	COL-S
														100	100	100	100	100	100	100	100	100	100	100	100	100	100	BRZ1
															100	100	100	100	100	100	100	100	100	100	100	100	100	CHI17
																100	100	100	100	100	100	100	100	100	100	100	100	ECU13
																	100	100	100	100	100	100	100	100	100	100	100	GRED1
																		100	100	100	100	100	100	100	100	100	100	SLV1
																			100	100	100	100	100	100	100	100	100	POL4
																				100	100	100	100	100	100	100	100	CZE1
																					100	99	100	100	100	100	100	Hun2-35
																						100	100	100	100	100	100	ALP3
																							100	100	100	100	100	DPAR1
																								100	100	100	100	FRA1
																									100	100	100	SP2
																										100	100	UK402
																											100	SCO484
																												Fin3.2

Amino acid identity comparing aa sequences of DsEcp6 from 28 D. septosporum strains. The color trends indicate high (darker) to low (lighter) % aa identity. DsEcp6 is completely conserved in all strains tested except for Hun2-35, BHU1, GUA1, COL-N and COL-S.

DsEcp13

NZE2	NZE10	AUST6	SAF1625	SAF4	KEN4	GUA1	GUA-N1	COL-N	COL-S	GRED1	ROM11	SLV1	POL4	CZE1	ATRA4-2	Hun2-35	ALP3	DPAR1	FRA1	SP2	Fin3.2	Strain
	100	100	100	100	99	99	100	100	100	100	99	100	100	100	100	100	100	99	100	100	100	NZE2
		100	100	100	99	99	100	100	100	100	99	100	100	100	100	100	100	99	100	100	100	NZE10
			100	100	99	99	100	100	100	100	99	100	100	100	100	100	100	99	100	100	100	AUST6
				100	99	99	100	100	100	100	99	100	100	100	100	100	100	99	100	100	100	SAF1625
					99	99	100	100	100	100	99	100	100	100	100	100	100	99	100	100	100	SAF4
						97	99	99	99	99	97	99	99	99	99	99	99	97	99	99	99	KEN4
							99	99	99	99	97	99	99	99	99	99	99	97	99	99	99	GUA1
								100	100	100	99	100	100	100	100	100	100	99	100	100	100	GUA-N1
									100	100	99	100	100	100	100	100	100	99	100	100	100	COL-N
										100	99	100	100	100	100	100	100	99	100	100	100	COL-S
											99	100	100	100	100	100	100	99	100	100	100	GRED1
												99	99	99	99	99	99	100	99	99	99	ROM11
													100	100	100	100	100	99	100	100	100	SLV1
														100	100	100	100	99	100	100	100	POL4
															100	100	100	99	100	100	100	CZE1
																100	100	99	100	100	100	ATRA4-2
																	100	99	100	100	100	Hun2-35
																		99	100	100	100	ALP3
																			99	99	99	DPAR1
																				100	100	FRA1
																					100	SP2
																						Fin3.2

Amino acid identity comparing aa sequences of DsEcp13 from 22 *D. septosporum* strains. The color trends indicate high (darker) to low (lighter) % aa identity. The GUA1 and KEN4 showed low aa identity to other strains tested.

DsEcp14

BHU1	NZE2	NZE10	ORE12	USA-MON8	CAN3	SAF1625	SAF4	KEN4	GUA1	GUA-N1	COL-N	COL-C	BRZ1	CHI17	ECU13	ROM11	SLV1	POL4	CZE1	Hun2-53	ALP3	DPAR1	FRA1	SP2	UK402	SCO484	Fin3.2	Strain
	100	100	100	100	100	100	100	100	97	97	98	98	100	100	100	100	100	100	100	100	100	100	100	100	100	100	100	BHU1
		100	100	100	100	100	100	100	97	97	98	98	100	100	100	100	100	100	100	100	100	100	100	100	100	100	100	NZE2
			100	100	100	100	100	100	97	97	98	98	100	100	100	100	100	100	100	100	100	100	100	100	100	100	100	NZE10
				100	100	100	100	100	97	97	97	98	100	100	100	100	99	100	100	100	100	100	99	100	100	100	100	ORE12
					100	100	100	100	97	97	97	98	100	100	100	100	99	100	100	100	100	100	99	100	100	100	100	USA-MON8
						100	100	100	97	97	97	98	100	100	100	100	99	100	100	100	100	100	99	100	100	100	100	CAN3
							100	100	97	97	97	98	100	100	100	100	99	100	100	100	100	100	99	100	100	100	100	SAF1625
								100	97	97	97	98	100	100	100	100	99	100	100	100	100	100	99	100	100	100	100	SAF4
									97	97	98	98	100	100	100	100	100	100	100	100	100	100	100	100	100	100	100	KEN4
										100	98	97	97	97	97	97	97	97	97	97	97	97	97	97	97	97	97	GUA1
											98	97	97	97	97	97	97	97	97	97	97	97	97	97	97	97	97	GUA-N1
												100	97	97	97	98	97	98	98	98	97	97	97	98	98	97	98	COL-N
													98	98	98	98	98	98	98	98	98	98	98	98	98	98	98	COL-C
														100	100	100	99	100	100	100	100	100	99	100	100	100	100	BRZ1
															100	100	99	100	100	100	100	100	99	100	100	100	100	CHI17
																100	99	100	100	100	100	100	99	100	100	100	100	ECU13
																	100	100	100	100	100	100	100	100	100	100	100	ROM11
																		100	100	100	99	99	99	100	100	99	100	SLV1
																			100	100	100	100	100	100	100	100	100	POL4
																				100	100	100	100	100	100	100	100	CZE1
																					100	100	100	100	100	100	100	Hun2-53
																						100	99	100	100	100	100	ALP3
																							99	100	100	100	100	DPAR1
																								100	100	99	100	FRA1
																									100	100	100	SP2
																										100	100	UK402
																											100	SCO484
																												Fin3.2

Amino acid identity comparing aa sequences of DsEcp14 from 28 *D. septosporum* strains. The color trends indicate high (darker) to low (lighter) % aa identity. Both Guatemala and Colombia strains showed low aa identity to other strains tested. GUA1 showed 100% aa identity to GUA-N1. COL-N showed 100% aa identity to COL-S.

Ds69335

BHU1	NZE10	NZE2	AUST6	ORE12	USA-MON8	CAN3	SAF1625	SAF4	GUA1	GUA-N1	COL-N	COL-C	BRZ1	GRED1	ROM11	SLV1	POL4	CZE1	ATRA4-2	Hun2-53	ALP3	DPAR1	FRA1	SP2	UK402	SCO484	FIN3.2	Strain
	100	100	100	100	99	99	100	100	98	98	98	98	100	100	100	100	100	100	100	100	99	100	100	99	100	99	100	BHU1
		100	100	100	100	100	100	100	99	99	99	99	100	100	100	100	100	100	100	100	100	100	100	100	100	100	100	NZE10
			100	100	100	100	100	100	99	99	99	99	100	100	100	100	100	100	100	100	100	100	100	100	100	100	100	NZE2
				100	100	100	100	100	99	99	99	99	100	100	100	100	100	100	100	100	100	100	100	100	100	100	100	AUST6
					100	100	100	100	99	99	99	99	100	100	100	100	100	100	100	100	100	100	100	100	100	100	100	ORE12
						100	100	100	98	98	98	98	100	99	100	100	99	100	99	100	100	99	100	100	100	100	99	USA-MON8
							100	100	98	98	98	98	100	99	100	100	99	100	99	100	100	99	100	100	100	100	99	CAN3
								100	99	99	99	99	100	100	100	100	100	100	100	100	100	100	100	100	100	100	100	SAF1625
									99	99	99	99	100	100	100	100	100	100	100	100	100	100	100	100	100	100	100	SAF4
										100	99	99	99	98	99	99	98	99	98	99	98	98	99	98	99	98	98	GUA1
											99	99	99	98	99	99	98	99	98	99	98	98	99	98	99	98	98	GUA-N1
												100	99	98	99	99	98	99	98	99	98	98	99	98	99	98	98	COL-N
													99	98	99	99	98	99	98	99	98	98	99	98	99	98	98	COL-C
														100	100	100	100	100	100	100	100	100	100	100	100	100	100	BRZ1
															100	100	100	100	100	100	99	100	100	99	100	99	100	GRED1
																100	100	100	100	100	100	100	100	100	100	100	100	ROM11
																	100	100	100	100	100	100	100	100	100	100	100	SLV1
																		100	100	100	99	100	100	99	100	99	100	POL4
																			100	100	100	100	100	100	100	100	100	CZE1
																				100	99	100	100	99	100	99	100	ATRA4-2
																					100	100	100	100	100	100	100	Hun2-53
																						99	100	100	100	100	99	ALP3
																							100	99	100	99	100	DPAR1
																								100	100	100	100	FRA1
																									100	100	99	SP2
																										100	100	UK402
																											99	SCO484
																												FIN3.2

Amino acid identity comparing aa sequences of Ds69335 from 28 *D. septosporum* strains. The color trends indicate high (darker) to low (lighter) % aa identity. Both Guatemala and Colombia strains showed low aa identity to other strains tested. GUA1 showed 100% aa identity to GUA-N1. COL-N showed 100% aa identity to COL-S.

Appendix 4.4 Phenotypic and pathogenicity assay

Growth rate

	Name	Plate 1 (mm/day)	Plate 2 (mm/day)	Plate 3 (mm/day)	P (T-Test)
WT	**WT (FJT20)**	0.50	0.52	0.47	
		0.51	0.54	0.49	
		0.53	0.57	0.57	
DsAvr4	**DsAvr4-T1 (FJT134)**	0.51	0.53	0.48	0.41
		0.54	0.55	0.50	
		0.49	0.52	0.50	
	DsAvr4-T2 (FJT135)	0.44	0.59	0.53	0.65
		0.45	0.55	0.54	
		0.48	0.59	0.45	
	DsAvr4-C4 (1FJT136)	0.53	0.53	0.49	0.80
		0.51	0.56	0.52	
		0.52	0.54	0.53	
DsEcp6	**DsEcp6-T1 (FJT138)**	0.57	0.50	0.50	0.96
		0.63	0.48	0.48	
		0.54	0.53	0.46	
	DsEcp6-C2 (FJT139)	0.51	0.54	0.51	0.70
		0.55	0.54	0.44	
		0.53	0.52	0.50	
DsEcp2-1	**DsEcp2-1-T1 (FJT141)**	0.54	0.50	0.50	0.34
		0.53	0.53	0.49	
		0.52	0.50	0.47	
	DsEcp2-1-T2 (FJT142)	0.50	0.49	0.50	0.05
		0.50	0.52	0.50	
		0.49	0.48	0.50	
	DsEcp2-1-C2 (FJT143)	0.56	0.54	0.45	0.67
		0.52	0.52	0.45	
		0.57	0.56	0.46	
DsHdp1	**DsHdp1-T1 (FJT145)**	0.58	0.62	0.52	0.11
		0.57	0.50	0.51	
		0.60	0.55	0.50	
	DsHdp1-T4 (FJT146)	0.51	0.53	0.53	0.80
		0.47	0.56	0.57	
		0.46	0.49	0.47	
	DsHdp1-C4 (FJT147)	0.51	0.53	0.48	0.31
		0.50	0.48	0.48	
		0.50	0.50	0.48	

Growth rate was calculated as mm/day for each replicate plate. Growth rate of 3 replicates were used in a two tailed T-test to test if there is a significant difference between KO or complement strains to WT strains. The P value (T-test) of $\geqslant 0.05$ indicates no significant difference between KO or complement strains to WT strains.

Sporulation

	Name	Plate	Count 1	Count 2	Average count	spores/ ml	P (T-Test)
WT	**WT (FJT20)**	1	184	191	187.5	9.38E+07	
		2	250	336	293	5.86E+07	
		3	236	261	248.5	4.97E+07	
DsAvr4	**DsAvr4-T1 (FJT134)**	1	257	265	261	5.22E+07	0.54
		2	404	420	412	8.24E+07	
		3	585	534	559.5	1.12E+08	
	DsAvr4-T2 (FJT135)	1	207	238	222.5	4.45E+07	0.17
		2	218	240	229	4.58E+07	
		3	220	230	225	4.50E+07	
	DsAvr4-C4 (1FJT136)	1	505	555	530	1.06E+08	0.21
		2	443	335	389	7.78E+07	
		3	419	465	442	8.84E+07	
DsEcp6	**DsEcp6-T1 (FJT138)**	1	532	444	488	9.76E+07	0.32
		2	409	500	454.5	9.09E+07	
		3	352	330	341	6.82E+07	
	DsEcp6-C2 (FJT139)	1	444	475	459.5	9.19E+07	0.19
		2	621	600	610.5	1.22E+08	
		3	339	440	389.5	7.79E+07	
DsEcp2-1	**DsEcp2-1-T1 (FJT141)**	1	210	190	200	1.00E+08	0.25
		2	156	125	140.5	7.03E+07	
		3	210	183	196.5	9.83E+07	
	DsEcp2-1-T2 (FJT142)	1	124	105	114.5	5.73E+07	0.79
		2	134	173	153.5	7.68E+07	
		3	182	142	162	8.10E+07	
	DsEcp2-1-C2 (FJT143)	1	142	129	135.5	6.78E+07	0.91
		2	109	108	108.5	5.43E+07	
		3	160	183	171.5	8.58E+07	
DsHdp1	**DsHdp1-T1 (FJT145)**	1	211	240	225.5	1.13E+08	0.10
		2	183	145	164	8.20E+07	
		3	180	203	191.5	9.58E+07	
	DsHdp1-T4 (FJT146)	1	177	199	188	9.40E+07	0.07
		2	216	243	229.5	1.15E+08	
		3	203	147	175	8.75E+07	
	DsHdp1-C4 (FJT147)	1	209	200	204.5	4.09E+07	0.06
		2	250	231	240.5	4.81E+07	
		3	223	245	234	4.68E+07	

The sporulation was calculated as spores/ml. The sporulation (spores/ml) of 3 replicates was used in a two tailed T-test to test if there is a significant difference between KO or complement strains compared to WT strains. The P value (T-test) of $\geqslant 0.05$ indicates no significant difference.

Number of germinated spores

	Name	Plate	Germinated spore				Total spore				% germinated	P (T-Test)
			Count 1	Count 2	Average	spore/ml	Count 1	Count 2	Average	spore/ml		
WT	WT (FJT20)	1	151	153	152	1.52E+06	465	415	440	4.40E+06	34.55	
		2	87	168	127.5	1.28E+06	370	530	450	4.50E+06	28.33	
		3	124	116	120	1.20E+06	555	595	575	5.75E+06	20.87	
DsAvr4	DsAvr4-T1 (FJT134)	1	68	78	73	7.30E+05	335	350	342.5	3.43E+06	21.31	0.19
		2	99	111	105	1.05E+06	425	540	482.5	4.83E+06	21.76	
		3	157	98	127.5	1.28E+06	685	485	585	5.85E+06	21.79	
	DsAvr4-T2 (FJT135)	1	55	48	51.5	5.15E+05	265	235	250	2.50E+06	20.60	0.27
		2	44	48	46	4.60E+05	170	205	187.5	1.88E+06	24.53	
		3	54	39	46.5	4.65E+05	200	205	202.5	2.03E+06	22.96	
	DsAvr4-C4 (1FJT136)	1	104	110	107	1.07E+06	405	480	442.5	4.43E+06	24.18	0.30
		2	135	94	114.5	1.15E+06	465	495	480	4.80E+06	23.85	
		3	110	135	122.5	1.23E+06	510	650	580	5.80E+06	21.12	
	DsAvr4 C2 (FJT137)	1	110	86	98	9.80E+05	395	400	397.5	3.98E+06	24.65	0.30
		2	84	98	91	9.10E+05	395	365	380	3.80E+06	23.95	
		3	94	100	97	9.70E+05	400	550	475	4.75E+06	20.42	
DsEcp6	DsEcp6-T1 (FJT138)	1	89	100	94.5	9.45E+05	380	415	397.5	3.98E+06	23.77	0.27
		2	74	72	73	7.30E+05	315	285	300	3.00E+06	24.33	
		3	120	99	109.5	1.10E+06	620	520	570	5.70E+06	19.21	
	DsEcp6-C2 (FJT139)	1	69	106	87.5	8.75E+05	440	440	440	4.40E+06	19.89	0.18
		2	93	99	96	9.60E+05	430	488	459	4.59E+06	20.92	
		3	85	84	84.5	8.45E+05	385	345	365	3.65E+06	23.15	
	DsEcp6-C5 (FJT140)	1	70	91	80.5	8.05E+05	360	435	397.5	3.98E+06	20.25	0.19
		2	121	109	115	1.15E+06	535	495	515	5.15E+06	22.33	
		3	117	80	98.5	9.85E+05	450	435	442.5	4.43E+06	22.26	
DsEcp2-1	DsEcp2-1-T1 (FJT141)	1	65	65	65	6.50E+05	260	260	260	2.60E+06	25.00	0.56
		2	65	85	75	7.50E+05	280	395	337.5	3.38E+06	22.22	
		3	68	85	76.5	7.65E+05	260	280	270	2.70E+06	28.33	
	DsEcp2-1-T2 (FJT142)	1	62	66	64	6.40E+05	240	290	265	2.65E+06	24.15	0.20
		2	44	62	53	5.30E+05	185	295	240	2.40E+06	22.08	
		3	45	40	42.5	4.25E+05	215	300	257.5	2.58E+06	16.50	
	DsEcp2-1-C2 (FJT143)	1	54	54	54	5.40E+05	335	170	252.5	2.53E+06	21.39	0.10
		2	55	55	55	5.50E+05	355	295	325	3.25E+06	16.92	
		3	68	52	60	6.00E+05	380	240	310	3.10E+06	19.35	
	DsEcp2-1-C3 (FJT144)	1	56	62	59	5.90E+05	301	298	299.5	3.00E+06	19.70	0.16
		2	63	60	61.5	6.15E+05	304	255	279.5	2.80E+06	22.00	
		3	71	50	60.5	6.05E+05	290	274	282	2.82E+06	21.45	
DsHdp1	DsHdp1-T1 (FJT145)	1	89	121	105	1.05E+06	350	420	385	3.85E+06	27.27	0.01
		2	127	120	123.5	1.24E+06	425	480	452.5	4.53E+06	27.29	
		3	138	115	126.5	1.27E+06	525	490	507.5	5.08E+06	24.93	
	DsHdp1-T4 (FJT146)	1	84	74	79	7.90E+05	260	375	317.5	3.18E+06	24.88	0.09
		2	91	57	74	7.40E+05	255	250	252.5	2.53E+06	29.31	
		3	77	41	59	5.90E+05	340	180	260	2.60E+06	22.69	
	DsHdp1-C4 (FJT147)	1	109	90	99.5	9.95E+05	410	360	385	3.85E+06	25.84	0.01
		2	119	114	116.5	1.17E+06	425	415	420	4.20E+06	27.74	
		3	130	110	120	1.20E+06	490	450	470	4.70E+06	25.53	

The % of germination was calculated as % of germinated spores/total spores. The % of germated spores of 3 replicates were used in a two tailed T-test to test if there is a significant difference between KO or complement strains compared to WT strains. The P value (T-test) of $\geqslant 0.05$ indicates no significant difference.

Pathogenicity test with mutant strains

Strain	WT (FJT20)			DsAvr4-T1 (FJT134)			P (T-Test)	DsAvr4-C4 (FJT136)			P (T-Test)
	Rep 1	Rep 2	Rep 3	Rep 1	Rep 2	Rep 3		Rep 1	Rep 2	Rep 3	
No. of uninfected needles	200	152	188	252	219	213		228	193	243	
No. of Infected needles	75	179	154	39	86	42		5	64	14	
Lesion No.	81	253	232	44	88	51		5	73	14	
Lesion size	2.7	2.78	2.57	2.3	2.48	2.21	0.05	3.4	2.45	1.86	0.23
Mean Lesion No.	1.08	1.41	1.51	1.13	1.02	1.21	0.21	1.00	1.14	1.00	0.11
% of needles with infection	27.27	54.08	45.03	13.40	28.20	16.47	0.07	2.15	24.90	5.45	0.04
Strain	WT (FJT20)			DsEcp6-T1 (FJT138)			P (T-Test)	DsEcp6-C2 (FJT139)			P (T-Test)
	Rep 1	Rep 2	Rep 3	Rep 1	Rep 2	Rep 3		Rep 1	Rep 2	Rep 3	
No. of uninfected needles	200	152	188	182	168	233		202	187	348	
No. of Infected needles	75	179	154	35	33	16		69	15	11	
Lesion No.	81	253	232	49	38	16		71	15	15	
Lesion size	2.7	2.78	2.57	3.07	3.08	2.13	0.25	1.98	2.47	2.8	0.33
Mean Lesion No.	1.08	1.41	1.51	1.40	1.15	1.00	0.44	1.03	1.00	1.36	0.31
% of needles with infection	27.27	54.08	45.03	16.13	16.42	6.43	0.03	25.46	7.43	3.06	0.04
Strain	WT (FJT20)			DsEcp2-1-T1 (FJT141)			P (T-Test)	DsEcp2-1-C2 (FJT143)			P (T-Test)
	Rep 1	Rep 2	Rep 3	Rep 1	Rep 2	Rep 3		Rep 1	Rep 2	Rep 3	
No. of uninfected needles	200	152	188	121	240	275		188	82	191	
No. of Infected needles	75	179	154	64	79	70		37	77	15	
Lesion No.	81	253	232	71	80	85		44	104	18	
Lesion size	2.7	2.78	2.57	3.56	3.59	3.64	0.00003	2.28	2.8	2.89	0.73
Mean Lesion No.	1.08	1.41	1.51	1.11	1.01	1.21	0.19	1.19	1.35	1.20	0.57
% of needles with infection	27.27	54.08	45.03	34.59	24.76	20.29	0.16	16.44	48.43	7.28	0.29
Strain	WT (FJT20)			DsHdp1-T1 (FJT145)			P (T-Test)				
	Rep 1	Rep 2	Rep 3	Rep 1	Rep 2	Rep 3					
No. of uninfected needles	200	152	188	77	104	112					
No. of Infected needles	75	179	154	36	28	42					
Lesion No.	81	253	232	44	30	42					
Lesion size	2.7	2.78	2.57	2.07±1.11	2.76±1.2	2.25±1.18	0.68				
Mean Lesion No.	1.08	1.41	1.51	1.22	1.07	1.00	0.18				
% of needles with infection	27.27	54.08	45.03	31.86	21.21	27.27	0.14				

The percentage of needles showing infection symptoms was calculated as infected needles/total needles. The numbers of lesions per needle was calculated by total number of lesions/ number of infected needles. The lesion size was measured with a ruler and the lesion size was calculated as average lesion size/number of lesions. Data of 3 replicates (Rep1, Rep2 and Rep3) were was used in a two tailed T-test to test if there is a significant difference between KO or complement strains compared to WT strains. The P value (T-test) of $\geqslant$0.05 indicates no significant difference.

DsHdp1 adhesion test

Name	Plate	Before wash				After wash				% of spore left on cytometer	T-test
		Count 1	Count 2	Average	spore/ml	Count 1	Count 2	Average	spore/ml		
WT (FJT20)	1	132	105	118.5	1.19E+06	83	85	84	8.40E+05	70.89	
	2	155	125	140	1.40E+06	101	123	112	1.12E+06	80	
	3	129	155	142	1.42E+06	102	84	93	9.30E+05	65.49	
DsHdp1-T1 (FJT145)	1	116	89	102.5	1.03E+06	102	33	67.5	6.75E+05	65.85	0.55
	2	112	82	97	9.70E+05	86	79	82.5	8.25E+05	85.05	
	3	138	118	128	1.28E+06	109	94	101.5	1.02E+06	79.3	
DsHdp1-T4 (FJT146)	1	123	106	114.5	1.15E+06	90	89	89.5	8.95E+05	78.17	0.47
	2	127	97	112	1.12E+06	98	47	72.5	7.25E+05	64.73	
	3	118	137	127.5	1.28E+06	72	64	68	6.80E+05	53.33	
DsHdp1-C4 (FJT147)	1	47	65	56	5.60E+05	26	51	38.5	3.85E+05	68.75	0.33
	2	58	43	50.5	5.05E+05	28	36	32	3.20E+05	63.37	
	3	82	72	77	7.70E+05	60	46	53	5.30E+05	68.83	

Spore adhesion was calculated as: % of spores left on cytometer after wash / total spores applied to cytometer. The % of spores left on cytometer from 3 replicated samples were used in a two tailed T-test to test if there is a significant difference between KO or complement strains compared to WT strains. The P value (T-test) of $\geqslant$0.05 indicates no significant difference.

Appendix 5. Primers used in this study

Appendix 5.1 Construction of gene replacement plasmids

Lab No.	Name	Sequence
1343	Avr4-5'-attB4	GGGGACAACTTTGTATAGAAAAGTTGCTGGAGCTAATCACCTGCTA
1344	Avr4-5'-attB1r	GGGGACTGCTTTTTTGTACAAACTTGCCGTTGCAGAGACGCGACT
1345	Avr4-3'-attB2r	GGGGACAGCTTTCTTGTACAAAGTGGCTGGTGAAAGGGAATGGCAG
1346	Avr4-3'-attB3	GGGGACAACTTTGTATAATAAAGTTGCGCAAAGCAGCTACAGAAG
1347	Ecp2-1-5'-attB4	GGGGACAACTTTGTATAGAAAAGTTGCTGCGTTGACGCATCTGCTG
1348	Ecp2-1-5'-attB1r	GGGGACTGCTTTTTTGTACAAACTTGCGGTCGATGTCGTTGTTGT
1349	Ecp2-1-3'-attB2r	GGGGACAGCTTTCTTGTACAAAGTGGCTAGCGCAGTGAAACTTGAG
1350	Ecp2-1-3'-attB3	GGGGACAACTTTGTATAATAAAGTTGCGCGCCATAGACTACCTCT
966	ecp6 5-attB4	GGGGACAACTTTGTATAGAAAAGTTGCTTCGCATGCGCTTGGAAGA
967	ecp6 5-attB1r	GGGGACTGCTTTTTTGTACAAACTTGCGTTGGAAACTGGGGCTTC
968	ecp6 3-attB2r	GGGGACAGCTTTCTTGTACAAAGTGGCTACGGTTATGAGTTTGATG
969	ecp6 3-attB3	GGGGACAACTTTGTATAATAAAGTTGCTCGCATCAGCTCCAAAAG
1319	Hyd_75009_KO_5F	GGGGACAACTTTGTATAGAAAAGTTGCTGCCCTCAAGACGGGATGAAA
1320	Hyd_75009_KO_5R	GGGGACTGCTTTTTTGTACAAACTTGCGAGCTGCGGTTGGTTGCATA
1321	Hyd_75009_KO_3F	GGGGACAGCTTTCTTGTACAAAGTGGCTTGGCAACCTTTCGAGACTGA
1322	Hyd_75009_KO_3R	GGGGACAACTTTGTATAATAAAGTTGCACTGGTGTTGGTATGGCTGT

Appendix 5.2 Construction of plasmids by restriction endonuclease digestion and ligation

Construction of complementation plasmid		
Lab No.	**Name**	**Sequence**
1335	Ecp6-5'-BamHI	ATGCATGGATCCTTCAGCTCCCGTCAGCGATG
1336	Ecp6-3'-EcoRI	ATGCATGAATTCTGAGGATGGCGACTTATCTG
1393	Avr4-Comp-5'-EcoRI	ATGCATGAATTCCCATGGCGTCTGTTTGGTAG
1394	Avr4-Comp-3'-BamHI	ATGCATGGATCCCTCGACAGCGGGCAACATAC
1395	Ecp2-1-Comp-5'-EcoRI	ATGCATGAATTCGGTTGAGGTGGTCGATCTTC
1396	Ecp2-1-Comp-3'-BamHI	ATGCATGGATCCAAGTTCTACGTGCTGCCTTG
1461	Hdp1-comp-EcoRI	ATGCATGAATTCGTCCTCTTGGCAAAGCACAG
1462	Hdp1-comp-ClaI	ACTGTATCGATGCCAGCCTCCTTGATATGTC

Screen for complement transformants by PCR		
Lab No.	**Name**	**Sequence**
1032	avr4-1F	TCTTCCTCCTCGCTGCTCTC
1033	avr4-2R	CACCACTCCCTTGCTTCTTC
1127	ecp2-1-1F	CCTCTTGCCAGCTCTGTCTC
1128	ecp2-1-2R	CGTCGTTCCTCGGGTTATAC
1025	ecp6-1F	TATGAGCGCCGCAGTTAACG
1026	ecp6-2R	ACGCCACAGCAGTAATGTTC
1369	Hyd75009-1F	CTGACGCAGACGAGCATGAC
1370	Hyd75009-2R	GTGGTGGAGAGGTACTGTTG

Construction of *D.septosporum* effector *P. pastoris* expression plasmid		
Lab No.	**Name**	**Sequence**
1470	5'-AOX1-primer	GACTGGTTCCAATTGACAAGC
1471	3'-AOX1-primer	GCAAATGGCATTCTGACATCC
1472	PPICZα-Factor	TACTATTGCCAGCATTGCTGC
1495	SmaI-FLAG-DsAvr4_F	ATCGCCCGGGGACTACAAGGACGACGATGACAAGCCGCAACCCGAACCTCCAGTCTACAA
1496	EcoRI-DsAvr4_R	ATCGGAATTCTCATTCCGGCTGTGCCGTCCCACCACTCCCTTGCTTTGGCTTGTTCGC
1497	SmaI-FLAG-DsEcp6_F	ATCGCCCGGGGACTACAAGGACGACGATGACAAGTTCGTTCTCCCACGTGAGAC
1498	EcoRI-DsEcp6_R	ATCGGAATTCTTACGCCACAGCAGTAATGT
1503	SmaI-FLAG-DsEcp2-1_F	ATCGCCCGGGGACTACAAGGACGACGATGACAAGGCAGTCCTCAGCCCGAGGTTCC
1504	DsEcp2-1_R	GAACGTTGAAAGCGCATCTGCCATAGGTCC
1505	DsEcp2-1_F	TATGGCAGATGCGCTTTCAACGTTCGTGTC
1506	EcoRI-DsEcp2-1_R	ATCGGAATTCTCACTCGTCGTTCCTCGGGTTATACG
1509	SmaI-FLAGEcp2-3_F	ATCGCCCGGGGACTACAAGGACGACGATGACAAGACCAGATTTCTCCAAGGGAG
1510	EcoRIEcp2-3_R	ATCGGAATTCCTACTGATGGCCGCTGCCAT
1511	DsEcp2-3_R	GCGCAAGTTCCGTTCTCAACGATGG
1512	DsEcp2-3_F	GAACGGAACTTGCGCCTTCCAAGC
1525	SmaI-FLAGCf-NLP_F	ATCGCCCGGGGACTACAAGGACGACGATGACAAGGCCGCCATCAATAGACG
1526	EcoRICf-NLP_R	ATCGGAATTCCTACAGAGCTGCCTTGCCCA

Appendix 5.3 Construction of *DsAvr4* and *CbAvr4* domain swap chimeras

Construction of DsAvr4 chimeras		
Lab No.	**Name**	**Sequence**
1203	pDONR-F	TCGCGTTAACGCTAGCATGGATCTC
1204	pDONR-R	GTAACATCAGAGATTTTGAGACAC
1205	pDONR207-F	TCGCGTTAACGCTAGCATGGATCTC
1206	pDONR207-R	GTAACATCAGAGATTTTGAGACAC
1199	ChimC1-C2-F	AAACGAACACACTGCCTCGG
1200	ChimC1-C2-R	CGAGGCAGTGTGTTCGTTTC
1263	chimC2-C4-F	CTCGCCACCAAATGCATGGG
1264	chimC2-C4-R	ATGCATTTGGTGGCGAGGAC
1265	chimC2-C3-F	CGACTGCCTCTATCCAAACC
1266	chimC2-C3-R	TGGATAGAGGCAGTCGAAGG
1267	chimC3-C4-F	GACTGCCTGTACGCACTACC
1268	chimC3-C4-R	TGCGTACAGGCAGTCTTTGG
1269	chimC4-C5-F	CATTCAATGCGTCCCGCAGG
1270	chimC4-C5-R	CGGGACGCATTGAATGTATC
1271	chimC5-C6-F	CATCCAATGCCAGCCCAAAG
1272	chimC5-C6-R	GGGCTGGCATTGGATGAAAG
1273	chimC6-C7-F	ATTGTGACTATCCACACTTG
1274	chimC6-C7-R	TGTGGATAGTCACAATACTT
1275	chimC7-C8-F	GTGGTGTGACACGGTGGAAC
1276	chimC7-C8-R	CGTGTCACACCACTTCTTTC
Construction of CbAvr4 chimeras		
1371	Cb-Avr4-attB2	GGGGACCACTTTGTACAAGAAAGCTGGGTACCGCGGTCAGCAAGGAGACGT
1372	Cb-Avr4-S6	CCCTTTGGGCATGGCCTTTC
1373	Cb-Avr4-S8	GTACATGCAAAGCTCCAGTG
1374	Ds-Avr4-S6	GCCATGCCCAAAGGGGTTGC
1375	Ds-Avr4-S8	GCTTTGCATGTACTCAAGTG
1376	Cb-Avr4-S2	CGAGACAGTGTGTTCGTTTC
1377	Cb-Avr4-S4	CAGCTGCCTCGGATACATTC
1378	Ds-Avr4-S2	ACACTGTCTCGGCCCCAAAG
1379	Ds-Avr4-S4	GAGGCAGCTGGCGGGGTTTG
1397	Cf-Avr4-S6	GAAAGGCCATGCCCAAAAGG
1398	Cf-Avr4-S8	GCTTTGCACGTACTCAGGTT
1399	Cb-Cf-Avr4-S6	TGGGCATGGCCTTTCATACG
1340	Cb-Cf-Avr4-S8	AACCTGAGTACGTGCAAAGC
1341	Cf-Avr4-S2	CACACTGTATGGGTCCCAAG
1342	Cf-Avr4-S4	TATCCGAGGCAACTGTCGGG
1343	Cb-Cf-Avr4-S2	CCATACAGTGTGTTCGTTTC
1344	Cb-Cf-Avr4-S4	CAGTTGCCTCGGATACATTC

Appendix 5.4 real-time PCR primer sequences

Lab No.	Name	Sequence
1013	AflR exF	GGAAGAGTAGTGTTACCATTGT
1022	AflR exR	CATCTATTCAACGACCTCACA
709	RtTUBfwI	CATGCGGTCTGGGAAC
710	RtTUBrevI	CATGCGGTCTGGGAAC
1255	Avr4-realtime-1F	GGTTATGCCGTGTCCAAA
1256	Avr4-realtim-2R	GGTCTTCGTAGTTGCCTTC
1487	Ecp2-1-real-5F	AACGATGGAACGACCTAC
1488	Ecp2-1-real-6R	CAGTGGAAATAGCCTTTGG
1463	Ecp6-real-3F	ACTCATCAACATTCCAATCTG
1464	Ecp6-real-4R	GAACAATCTGCTGACCAATC
1507	Hdp1-rt-3F	TGTGTCCTTCCAGTTGTAA
1508	Hdp1-rt-4R	TAGAGGTCGTAGCAGAGA

Appendix 5.5 DIG-labelling of the probes (PCR based)

Lab No.	Name	Sequence
1389	Avr4-GFP-KO-probe1F	CAAGGTCTCGAGCAACGATG
1390	Avr4-GFP-KO-probe2R	TTGACTGGAGCGAGGCGATG
1391	Ecp2-1-GFP-KO-probe1F	GACGGTGTAATGACTCTTCC
1392	Ecp2-1-GFP-KO-probe2R	TTATCGGCACTTTGCATCGG
1387	Ecp6-GFP-KO-probe1F	TCTCCGGAACGGCGACATAG
1388	Ecp6-GFP-KO-probe2R	ACCTCGTGCATGCGGATTTC
1371	Hyd75009-KO-probe-1F	ATCGCACAGCTAAGCGTGAG
1372	Hyd75009-KO-probe-2R	TCCGGAAGTGCTTGACATTG

Appendix 5.6 Primers used for polymorphism analysis

Lab No.	Name	Sequence	Lab No.	Name	Sequence
1032	avr4-1F	TCTTCCTCCTCGCTGCTCTC	1025	ecp6-1F	TATGAGCGCCGCAGTTAACG
1033	avr4-2R	CACCACTCCCTTGCTTCTTC	1026	ecp6-2R	ACGCCACAGCAGTAATGTTC
1155	avr4-3F	AAGAGACCTCGGCATCTCAG	1151	ecp6-3F	ACGCCGCTGGACACCAATTC
1198	avr4-7R	CAGGGTCACGATCGGAAATG	1197	ecp6-7R	GAGCTGTCGAATAGCTGATG
1311	avr4-8F	GCACCATACTCAGCTTTCAC	1307	Ecp6-8F	CTTTGTACCCTCGCCTTCTC
1536	avr4-poly-R	GTCATCTACTTGCCTCCATC	1541	ecp6-poly-R	AAGCGAACGCGAACGCGAAC
1127	ecp2-1-1F	CCTCTTGCCAGCTCTGTCTC	1527	ecp13-1F	CTGCAGCAACACGACATCAG
1128	ecp2-1-2R	CGTCGTTCCTCGGGTTATAC	1528	ecp13-2R	AATGAGCGTATCGCGTGGAC
1159	ecp2-1-5F	CGCAAGGACAGTGCGTTGAC	1529	ecp13-3R	ACGCACAAGCAACCAGACAC
1253	ecp2-1-9R	ATACCGCCCAGATGTTGTTG	1544	ecp13-4F	CAGACGCGAACTACCATTAC
1308	Ecp2-1-10F	CAGCACGCCTTCAAGATAAC	1549	ecp13-5F	ACGACAATGCGCTTCTTTGC
1537	Ecp2-1-poly-R	CAGATCCTCGATACGTACTG	1530	ecp14-1F	CGTCGCGGACAGGCTTAATC
1129	ecp2-3-1F	ACAGCACAGCAGTCGTTGTC	1531	ecp14-2R	TCGCAGTCGACCTCTACAAG
1130	ecp2-3-2R	ACTGATGGCCGCTGCCATAC	1532	ecp14-3R	TCAACGAGCGACTGTTGTTC
1163	ecp2-3-7F	TGTTGGCCAGGGAGGTCTTC	1545	ecp14-4F	GACAAGGAGCGATCAATGAG
1309	ecp2-3-12F	TTCCTACAGCCGGTCGTTTC	1548	ecp14-5F	GCGACCATGATCACAATACG
1310	ecp2-3-13R	CCCTAGCCATCTATGAAAGC	1533	Ds69335-1F	ACTACTACCACCACCACTAC
1538	ecp2-3-poly-R	GCGGTCGATTACGATATCTC	1534	Ds69335-2R	AAGAGCCACGTGAGCCATTG
1027	ecp4-1F	CATCCCATTTCTCGCAGTTC	1535	Ds69335-3R	TAGACCGTTGTCCGACTCAG
1028	ecp4-2R	GACAAGTGACCTGCACACTC	1546	Ds69335-4F	AACACCCGTTCAGCCATATC
1143	ecp4-5F	CCACTACCGTCGAGAAGATG	1547	Ds69335-5F	TCGCCGTCCCGTACAACAAG
1195	ecp4-9R	CCCAGACTGTCTTGCTTACC	1303	Avr2-1F	CTGCGTGCCGACGACAAAGA
1306	ecp4-10F	TCGAACCTCAGCATCGGTAG	1304	Avr2-2R	CCTTCTTAGCAGCCGTGATG
1539	ecp4-poly-R	TGACAACGATGCGACCACTC	1191	Avr9-1F	GCTACTACTCTCCCACTTTG
1029	ecp5-1F	TTCGACTGGCCGCACTCTTG	1192	Avr9-2R	GTCGAAGGCCCTAGTACAAC
1030	ecp5-2F	TTGTGGGCGGGTAAACCGTC	1193	Avr4E-1F	CTATCACAACCGCCGATTTC
1031	ecp5-3R	ACCTCTCCCTGCTTCCTCTC	1194	Avr4E-2R	CTCAATCTCCCACTCCTTAC
1147	ecp5-4F	ACAGGTGTTACGGAACAGAG			
1196	ecp5-9R	GTTTCCTCGTTGCTTGAGTC			
1540	ecp5-poly-R	GCTCGATTTGCTGGAGGAAG			

References

Abramovitch, R.B., Kim, Y.J., Chen, S.R., Dickman, M.B., and Martin, G.B. (2003). *Pseudomonas* type III effector AvrPtoB induces plant disease susceptibility by inhibition of host programmed cell death. The EMBO Journal *22*, 60-69.

Aguileta, G., Lengelle, J., Chiapello, H., Giraud, T., Viaud, M., Fournier, E., Rodolphe, F., Marthey, S., Ducasse, A., Gendrault, A., Poulain, J., Wincker, P., and Gout, L. (2012). Genes under positive selection in a model plant pathogenic fungus, *Botrytis*. Infection, Genetics and Evolution *12*, 987-996.

Aguileta, G., Refrégier, G., Yockteng, R., Fournier, E., and Giraud, T. (2009). Rapidly evolving genes in pathogens: Methods for detecting positive selection and examples among fungi, bacteria, viruses and protists. Infection, Genetics and Evolution *9*, 656-670.

Akcapinar, G.B., Kappel, L., Sezerman, O.U., and Seidl-Seiboth, V. (2015). Molecular diversity of LysM carbohydrate-binding motifs in fungi. Current Genetics.

Alfano, J.R., and Collmer, A. (2004). Type III secretion system effector proteins: Double agents in bacterial disease and plant defense. In Annual Review of Phytopathology, pp. 385-414.

Anderson, J.P., Gleason, C.A., Foley, R.C., Thrall, P.H., B., B.J., and Singh, K.B. (2010). Plants versus pathogens: an evolutionary arms race. Functional Plant Biology *37*, 499-512.

Barnes, I., Kirisits, T., Wingfield, M.J., and Wingfield, B.D. (2011). Needle blight of pine caused by two species of Dothistroma in Hungary. Forest Pathology *41*, 361-369.

Barnes, I., Wingfield, M.J., Carbone, I., Kirisits, T., and Wingfield, B.D. (2014). Population structure and diversity of an invasive pine needle pathogen reflects anthropogenic activity. Ecology and Evolution.ADD DETAILS

Barrett, L.G., Thrall, P.H., Dodds, P.N., van der Merwe, M., Linde, C.C., Lawrence, G.J., and Burdon, J.J. (2009). Diversity and evolution of effector loci in natural populations of the plant pathogen *Melampsora lini*. Molecular Biology and Evolution *26*, 2499-2513.

Bella, J., Hindle, K.L., McEwan, P.A., and Lovell, S.C. (2008). The leucine-rich repeat structure. Cellular and Molecular Life Sciences *65*, 2307-2333.

Bendahmane, A. (2003). Constitutive gain-of-function mutants in a nucleotide binding site-leucine rich repeat protein encoded at the *Rx* locus of potato. Plant Journal *33*, 603-603.

Bernard, P., and Couturier, M. (1992). Cell killing by the F plasmid CcdB protein involves poisoning of DNA-topoisomerase II complexes. Journal of Molecular Biology *226*, 735-745.

Birch, P.R.J., Boevink, P.C., Gilroy, E.M., Hein, I., Pritchard, L., and Whisson, S.C. (2008). Oomycete RXLR effectors: delivery, functional redundancy and durable disease resistance. Current Opinion in Plant Biology *11*, 373-379.

Bok, J.W., and Keller, N.P. (2004). LaeA, a regulator of secondary metabolism in *Aspergillus* spp. Eukaryotic Cell *3*, 527-535.

Bolton, M.D., van Esse, H.P., Vossen, J.H., de Jonge, R., Stergiopoulos, I., Stulemeijer, I.J.E., van den Berg, G.C.M., Borras-Hidalgo, O., Dekker, H.L., de Koster, C.G., de Wit, P.J.G.M., Joosten, M.H.A.J., and Thomma, B.P.H.J. (2008). The novel *Cladosporium fulvum* lysin motif effector Ecp6 is a virulence factor with orthologues in other fungal species. Molecular Microbiology *69*, 119-136.

Bos, J.I.B., Armstrong, M.R., Gilroy, E.M., Boevink, P.C., Hein, I., Taylor, R.M., Zhendong, T., Engelhardt, S., Vetukuri, R.R., Harrower, B., Dixelius, C., Bryan, G., Sadanandom, A., Whisson, S.C., Kamoun, S., and Birch, P.R.J. (2010). *Phytophthora infestans* effector AVR3a is essential for virulence and manipulates plant immunity by stabilizing host E3 ligase CMPG1. Proceedings of the National Academy of Sciences of the United States of America *107*, 9909-9914.

Bos, J.I.B., Kanneganti, T.D., Young, C., Cakir, C., Huitema, E., Win, J., Armstrong, M.R., Birch, P.R.J., and Kamoun, S. (2006). The C-terminal half of *Phytophthora infestans* RXLR effector AVR3a is sufficient to trigger R3a-mediated hypersensitivity and suppress INF1-induced cell death in *Nicotiana benthamiana*. Plant Journal *48*, 165-176.

Bowden, C.G., Smalley, E., Guries, R.P., Hubbes, M., Temple, B., and Horgen, P.A. (1996). Lack of association between cerato-ulmin production and virulence in *Ophiostoma novo-ulmi*. Molecular Plant-Microbe Interactions *9*, 556-564.

Bradshaw, R.E. (2004). Dothistroma (red-band) needle blight of pines and the dothistromin toxin: a review. Forest Pathology *34*, 163-185.

Bradshaw, R.E., Bhatnagar, D., Ganley, R.J., Gillman, C.J., Monahan, B.J., and Seconi, J.M. (2002). *Dothistroma pini*, a forest pathogen, contains homologs of aflatoxin biosynthetic pathway genes. Applied and Environmental Microbiology *68*, 2885-2892.

Bradshaw, R.E., Guo, Y., Sim, A., Kabir, M.S., Chettri, P., Ozturk, I.K., Hunziker, L., Ganley, R.L., and Cox, M.P. (2015). Genome-wide gene expression dynamics of the fungal pathogen *Dothistroma septosporum* throughout its infection cycle of the gymnosperm host *Pinus radiata*. Molecular Plant Pathology, doi: 10.1111/mpp.12273.

Bradshaw, R.E., Slot, J.C., Moore, G.G., Chettri, P., de Wit, P.J.G.M., Ehrlich, K.C., Ganley, A.R.D., Olson, M.A., Rokas, A., Carbone, I., and Cox, M.P. (2013). Fragmentation of an aflatoxin-like gene cluster in a forest pathogen. New Phytologist *198*, 525-535.

Bradshaw, R.E., and Zhang, S.G. (2006). Biosynthesis of dothistromin. Mycopathologia *162*, 201-213.

Brasier, C.M. (1991). *Ophiostoma novo-ulmi sp. nov.*, causative agent of current Dutch elm disease pandemics. Mycopathologia *115*, 151-161.

Bubner, B., and Baldwin, I.T. (2004). Use of real-time PCR for determining copy number and zygosity in transgenic plants. Plant Cell Reports *23*, 263-271.

Bulman, L.S., Dick, M.A., Ganley, R.J., McDougal, R.L., Schwelm, A., and Bradshaw, R.E. (2013). Dothistroma needle blight. In, pp. 436-457.

Cabral, A., Oome, S., Sander, N., Küfner, I., Nürnberger, T., and van den Ackerveken, G. (2012). Nontoxic nep1-like proteins of the downy mildew pathogen *Hyaloperonospora arabidopsidis*: Repression of necrosis-inducing activity by a surface-exposed region. Molecular Plant-Microbe Interactions *25*, 697-708.

Caicedo, A.L., and Schaal, B.A. (2004). Heterogeneous evolutionary processes affect R gene diversity in natural populations of *Solanum pimpinellifolium*. Proceedings of the National Academy of Sciences of the United States of America *101*, 17444-17449.

Cesari, S., Bernoux, M., Moncuquet, P., Kroj, T., and Dodds, P.N. (2014). A novel conserved mechanism for plant NLR protein pairs: The "integrated decoy" hypothesis. Frontiers in Plant Science *5*, 606. doi: 10.3389/fpls.2014.00606

Cesari, S., Thilliez, G., Ribot, C., Chalvon, V., Michel, C., Jauneau, A., Rivas, S., Alaux, L., Kanzaki, H., Okuyama, Y., Morel, J.B., Fournier, E., Tharreau, D., Terauchi, R., and Kroj, T. (2013). The rice resistance protein pair RGA4/RGA5 recognizes the *Magnaporthe oryzae* effectors AVR-Pia and AVR1-CO39 by direct binding. Plant Cell *25*, 1463-1481.

Chen, R.S., and McDonald, B.A. (1996). Sexual reproduction plays a major role in the genetic structure of populations of the fungus *Mycosphaerella graminicola*. Genetics *142*, 1119-1127.

Chen, S., Songkumarn, P., Venu, R.C., Gowda, M., Bellizzi, M., Hu, J., Liu, W., Ebbole, D., Meyers, B., Mitchel, T., and Wang, G.L. (2013). Identification and characterization of *in planta*-expressed secreted effector proteins from *Magnaporthe oryzae* that induce cell death in rice. Molecular Plant-Microbe Interactions *26*, 191-202.

Cheng, Y.T., and Li, X. (2012). Ubiquitination in NB-LRR-mediated immunity. Current Opinion in Plant Biology *15*, 392-399.

Chinchilla, D., Bauer, Z., Regenass, M., Boller, T., and Felix, G. (2006). The Arabidopsis receptor kinase FLS2 binds flg22 and determines the specificity of flagellin perception. Plant Cell *18*, 465-476.

Chomczynski, P., and Sacchi, N. (1987). Single-step method of RNA isolation by acid guanidinium thiocyanate-phenol-chloroform extraction. Analytical Biochemistry *162*, 156-159.

Ciuffetti, L.M., Manning, V.A., Pandelova, I., Betts, M.F., and Martinez, J.P. (2010). Host-selective toxins, Ptr ToxA and Ptr ToxB, as necrotrophic effectors in the *Pyrenophora tritici-repentis*-wheat interaction. New Phytologist *187*, 911-919.

Dagenais, T.R.T., Giles, S.S., Aimanianda, V., Latgé, J.P., Hull, C.M., and Keller, N.P. (2010). *Aspergillus fumigatus* LaeA-mediated phagocytosis is associated with a decreased hydrophobin layer. Infection and Immunity *78*, 823-829.

Daly, R., and Hearn, M.T.W. (2005). Expression of heterologous proteins in *Pichia pastoris*: A useful experimental tool in protein engineenring and production. Journal of Molecular Recognition *18*, 119-138.

Dangl, J.L., Horvath, D.M., and Staskawicz, B.J. (2013). Pivoting the plant immune system from dissection to deployment. Science *341*, 746-751.

de Jonge, R., and Thomma, B. (2009). Fungal LysM effectors: extinguishers of host immunity? Trends in Microbiology *17*, 151-157.

de Jonge, R., van Esse, H.P., Kombrink, A., Shinya, T., Desaki, Y., Bours, R., van der Krol, S., Shibuya, N., Joosten, M., and Thomma, B. (2011). Conserved fungal LysM effector Ecp6 prevents chitin-triggered immunity in plants. Science *329*, 953-955.

de Kock, M.J.D., Iskandar, H.M., Brandwagt, B.F., Laugé, R., De Wit, P.J.G.M., and Lindhout, P. (2004). Recognition of *Cladosporium fulvum* Ecp2 elicitor by non-host Nicotiana spp. is mediated by a single dominant gene that is not homologous to known Cf-genes. Molecular Plant Pathology *5*, 397-408.

de Vocht, M.L., Reviakine, I., Wosten, H.A.B., Brisson, A., Wessels, J.G.H., and Robillard, G.T. (2000). Structural and functional role of the disulfide bridges in the hydrophobin SC3. Journal of Biological Chemistry *275*, 28428-28432.

de Vries, O.M.H., Fekkes, M.P., Wösten, H.A.B., and Wessels, J.G.H. (1993). Insoluble hydrophobin complexes in the walls of *Schizophyllum commune* and other filamentous fungi. Archives of Microbiology *159*, 330-335.

de Wit, P. (2007). Visions & reflections (minireview) - How plants recognize pathogens and defend themselves. Cellular and Molecular Life Sciences *64*, 2726-2732.

de Wit, P.J.G.M., Joosten, M.A.J., Thomma, B.P.J., and Stergiopoulos, I. (2009). Gene for Gene Models and Beyond: the *Cladosporium fulvum*-Tomato Pathosystem. In Plant Relationships, H. Deising, ed. (Springer Berlin Heidelberg), pp. 135-156.

de Wit, P.J.G.M., van der Burgt, A., Ökmen, B., Stergiopoulos, I., Abd-Elsalam, K.A., Aerts, A.L., Bahkali, A.H., Beenen, H.G., Chettri, P., Cox, M.P., Datema, E., de Vries, R.P., Dhillon, B., Ganley, A.R., Griffiths, S.A., Guo, Y., Hamelin, R.C., Henrissat, B., Kabir, M.S., Jashni, M.K., Kema, G., Klaubauf, S., Lapidus, A., Levasseur, A., Lindquist, E., Mehrabi, R., Ohm, R.A., Owen, T.J., Salamov, A., Schwelm, A., Schijlen, E., Sun, H., van den Burg, H.A., van Ham, R.C.H.J., Zhang, S., Goodwin, S.B., Grigoriev, I.V., Collemare, J., and Bradshaw, R.E. (2012). The genomes of the fungal plant pathogens *Cladosporium fulvum* and *Dothistroma septosporum* reveal adaptation to different hosts and lifestyles but also signatures of common ancestry. PLoS Genetics *8*. e1003088.

Dempsey, G.P., and Beever, R.E. (1979). Electron microscopy of the rodlet layer of *Neurospora crassa* conidia. Journal of Bacteriology *140*, 1050-1062.

Diepold, A., and Wagner, S. (2014). Assembly of the bacterial type III secretion machinery. FEMS Microbiology Reviews *38*, 802-822.

Dixon, M.S., Golstein, C., Thomas, C.M., van der Biezen, E.A., and Jones, J.D.G. (2000). Genetic complexity of pathogen perception by plants: The example of *Rcr3*, a tomato gene required specifically by *Cf-2*. Proceedings of the National Academy of Sciences of the United States of America *97*, 8807-8814.

Dixon, M.S., Hatzixanthis, K., Jones, D.A., Harrison, K., and Jones, J.D.G. (1998). The tomato Cf-5 disease resistance gene and six homologs show pronounced allelic variation in leucine-rich repeat copy number. Plant Cell *10*, 1915-1925.

Dixon, M.S., Jones, D.A., Keddie, J.S., Thomas, C.M., Harrison, K., and Jones, J.D.G. (1996). The tomato Cf-2 disease resistance locus comprises two functional genes encoding leucine-rich repeat proteins. Cell *84*, 451-459.

Djamei, A., Schipper, K., Rabe, F., Ghosh, A., Vincon, V., Kahnt, J., Osorio, S., Tohge, T., Fernie, A.R., Feussner, I., Feussner, K., Meinicke, P., Stierhof, Y.D., Schwarz, H., MacEk, B., Mann, M., and Kahmann, R. (2011). Metabolic priming by a secreted fungal effector. Nature *478*, 395-398.

Dodds, P.N., Lawrence, G.J., Catanzariti, A.M., Teh, T., Wang, C.I.A., Ayliffe, M.A., Kobe, B., and Ellis, J.G. (2006). Direct protein interaction underlies gene-for-gene specificity and coevolution of the flax resistance genes and flax rust avirulence genes. Proceedings of the National Academy of Sciences of the United States of America *103*, 8888-8893.

Doss, R.P., Potter, S.W., Christian, J.K., Soeldner, A.H., and Chastagner, G.A. (1997). The conidial surface of *Botrytis cinerea* and several other *Botrytis* species. Canadian Journal of Botany *75*, 612-617.

Dou, D., Kale, S.D., Wang, X., Chen, Y., Wang, Q., Wang, X., Jiang, R.H.Y., Arredondo, F.D., Anderson, R.G., Thakur, P.B., McDowell, J.M., Wang, Y., and Tyler, B.M. (2008). Conserved C-terminal motifs required for

avirulence and suppression of cell death by *Phytophthora sojae* effector Avr1b. Plant Cell *20*, 1118-1133.

Dower, W.J., Miller, J.F., and Ragsdale, C.W. (1988). High efficiency transformation of *E. coli* by high voltage electroporation. Nucleic Acids Research *16*, 6127-6145.

Doyle, J.J., and Doyle, J.L. (1987). A rapid DNA isolation procedure for small quantities of fresh leaf tissue. Phytochemical Bulletin *19*, 11-15.

Dunger, G., Garofalo, C.G., Gottig, N., Garavaglia, B.S., Rosa, M.C.P., Farah, C.S., Orellano, E.G., and Ottado, J. (2012). Analysis of three *Xanthomonas axonopodis* pv. *citri* effector proteins in pathogenicity and their interactions with host plant proteins. Molecular Plant Pathology *13*, 865-876.

Ellis, J.G., Dodds, P.N., and Lawrence, G.J. (2007). Flax rust resistance gene specificity is based on direct resistance-avirulence protein interactions. In Annual Review of Phytopathology, pp. 289-306.

Ellis, S.B., Brust, P.F., Koutz, P.J., Waters, A.F., Harpold, M.M., and Gingeras, T.R. (1985). Isolation of alcohol oxidase and two other methanol regulatable genes from the yeast *Pichia pastoris*. Molecular and Cellular Biology *5*, 1111-1121.

Esse, H.P.v., Klooster, J.W.v.t., Bolton, M.D., Yadeta, K.A., Baarlen, P.v., Boeren, S., Vervoort, J., Wit, P.J.G.M.d., and Thomma, B.P.H.J. (2008). The *Cladosporium fulvum* virulence protein Avr2 inhibits host proteases required for basal defense. Plant Cell *20*, 1948-1963.

Fabre, B., Ioos, R., Piou, D., and Marçais, B. (2012). Is the emergence of Dothistroma needle blight of pine in France caused by the cryptic species *Dothistroma pini*? Phytopathology *102*, 47-54.

Fabre, B., Ioos, R., Piou, D., and Marcais, B. (2010). Is the emergence of dothistroma needle blight of pine in France caused by the cryptic species *Dothistroma pini*? Phytopathology *102*, 47-54.

Feau, N., Mottet, M.J., Périnet, P., Hamelin, R.C., and Bernier, L. (2010). Recent advances related to poplar leaf spot and canker caused by *Septoria musiva*. Canadian Journal of Plant Pathology *32*, 122-134.

Feng, B.Z., Zhu, X.P., Fu, L., Lv, R.F., Storey, D., Tooley, P., and Zhang, X.G. (2014). Characterization of necrosis-inducing NLP proteins in *Phytophthora capsici*. BMC Plant Biology *14*.126.

Fenton, A., Antonovics, J., and Brockhurst, M.A. (2009). Inverse-gene-for-gene infection genetics and coevolutionary dynamics. American Naturalist *174*, 230-242.

Flor, H.H. (1971). Current status of the gene-for-gene concept. Annual Review of Phytopathology *9*, 275-296.

Franich, R.A., Carson, M.J., and Carson, S.D. (1986). Synthesis and Accumulation of Benzoic-Acid in *Pinus. Radiata* Needles in Response to Tissue-Injury by Dothistromin, and Correlation with Resistance of *Pinus.Radiata* Families to *Dothistroma. Pini*. Physiological and Molecular Plant Pathology *26*, 267-286.

Galán, J.E., Lara-Tejero, M., Marlovits, T.C., and Wagner, S. (2014). Bacterial type III secretion systems: Specialized nanomachines for protein delivery into target cells. In Annual Review of Microbiology, pp. 415-438.

Gibson, I.A.S. (1972). Dothistroma blight of *pinus. radiata*. Annual Review of Phytopathology *10*, 51-72.

Gilroy, E.M., Breen, S., Whisson, S.C., Squires, J., Hein, I., Kaczmarek, M., Turnbull, D., Boevink, P.C., Lokossou, A., Cano, L.M., Morales, J., Avrova, A.O., Pritchard, L., Randall, E., Lees, A., Govers, F., van West, P., Kamoun, S., Vleeshouwers, V.G.A.A., Cooke, D.E.L., and Birch, P.R.J. (2011). Presence/absence, differential expression and sequence polymorphisms between PiAVR2 and PiAVR2-like in *Phytophthora infestans* determine virulence on R2 plants. New Phytologist *191*, 763-776.

Giraldo, M.C., Dagdas, Y.F., Gupta, Y.K., Mentlak, T.A., Yi, M., Martinez-Rocha, A.L., Saitoh, H., Terauchi, R., Talbot, N.J., and Valent, B. (2013). Two distinct secretion systems facilitate tissue invasion by the rice blast fungus *Magnaporthe oryzae*. Nature Communications *4*. doi:10.1038/ncomms2996

Giraldo, M.C., and Valent, B. (2013). Filamentous plant pathogen effectors in action. Nature Reviews Microbiology *11*, 800-814.

Glazebrook, J. (2005). Contrasting mechanisms of defense against biotrophic and necrotrophic pathogens. In Annual Review of Phytopathology *43*, pp. 205-227.

Glowacki, S., Macioszek, V.K., and Kononowicz, A.K. (2011). R proteins as fundamentalss of plant innate immunity. Cellular and Molecular Biology Letters *16*, 1-24.

Grünbacher, A., Throm, T., Seidel, C., Gutt, B., Röhrig, J., Strunk, T., Vincze, P., Walheim, S., Schimmel, T., Wenzel, W., and Fischer, R. (2014). Six hydrophobins are involved in hydrophobin rodlet formation in *Aspergillus nidulans* and contribute to hydrophobicity of the spore surface. Plos One *9*, e94546.

Groenewald, M., Barnes, I., Bradshaw, R.E., Brown, A.V., Dale, A., Groenewald, J.Z., Lewis, K.J., Wingfield, B.D., Wingfield, M.J., and Crous, P.W. (2007). Characterization and distribution of mating type genes in the Dothistroma needle blight pathogens. Phytopathology *97*, 825-834.

Hakanpää, J., Paananen, A., Askolin, S., Nakari-Setälä, T., Parkkinen, T., Penttilä, M., Linder, M.B., and Rouvinen, J. (2004). Atomic Resolution Structure of the HFBII Hydrophobin, a Self-assembling Amphiphile. Journal of Biological Chemistry *279*, 534-539.

Hakanpää, J., Szilvay, G.R., Kaljunen, H., Maksimainen, M., Linder, M., and Rouvinen, J. (2006). Two crystal structures of *Trichoderma reesei* hydrophobin HFBI - The structure of a protein amphiphile with and without detergent interaction. Protein Science *15*, 2129-2140.

Hektor, H.J., and Scholtmeijer, K. (2005). Hydrophobins: Proteins with potential. Current Opinion in Biotechnology *16*, 434-439.

Hellens, R., Mullineaux, P., and Klee, H. (2000). A guide to Agrobacterium binary Ti vectors. Trends in Plant Science *5*, 446-451.

Hemetsberger, C., Herrberger, C., Zechmann, B., Hillmer, M., and Doehlemann, G. (2012). The *Ustilago maydis* effector Pep1 suppresses plant immunity by inhibition of host peroxidase activity. Plos Pathogens *8*, e1002684.

Holsters, M., Silva, B., Van Vliet, F., Genetello, C., De Block, M., Dhaese, P., Depicker, A., Inzé, D., Engler, G., Villarroel, R., Van Montagu, M., and Schell, J. (1980). The functional organization of the nopaline *A. tumefaciens* plasmid pTiC58. Plasmid *3*, 212-230.

Hurst, L.D. (2002). The Ka/Ks ratio: Diagnosing the form of sequence evolution. Trends in Genetics *18*, 486-487.

Johal, G.S., and Briggs, S.P. (1992). Reductase activity encoded by the *HM1* disease resistance gene in maize. Science *258*, 985-987.

Jones, D.A., Thomas, C.M., Hammond-Kosack, K.E., Balint-Kurti, P.J., and Jonest, J.D.G. (1994). Isolation of the tomato Cf-9 gene for resistance to *Cladosporium fulvum* by transposon tagging. Science *266*, 789-793.

Jones, J.D.G., and Dangl, J.L. (2006). The plant immune system. Nature *444*, 323-329.

Joosten, M., Cozijnsen, T.J., and Dewit, P. (1994). Host resistance to a fungal tomato pathogen lost by a single base-pair change in an avirulence gene. Nature *367*, 384-386.

Joosten, M.H.A.J., Vogelsang, R., Cozijnsen, T.J., Verberne, M.C., and De Wit, P.J.G.M. (1997). The biotrophic fungus *Cladosporium fulvum* circumvents Cf-4-mediated resistance by producing unstable AVR4 elicitors. Plant Cell *9*, 367-379.

Kabir, M.S., Ganley, R.J., and Bradshaw, R.E. (2013). An improved artificial pathogenicity assay for Dothistroma needle blight on *Pinus radiata*. Australasian Plant Pathology *42*, 503-510.

Kabir, M.S., Ganley, R.J., and Bradshaw, R.E. (2015). Dothistromin toxin is a virulence factor in dothistroma needle blight of pines. Plant Pathology. doi: 10.1111/ppa.12229

Kale, S.D., Gu, B., Capelluto, D.G.S., Dou, D., Feldman, E., Rumore, A., Arredondo, F.D., Hanlon, R., Fudal, I., Rouxel, T., Lawrence, C.B., Shan, W., and Tyler, B.M. (2010). External Lipid PI3P mediates entry of eukaryotic pathogen effectors into plant and animal host cells. Cell *142*, 981-981.

Kankanala, P., Czymmek, K., and Valent, B. (2007). Roles for rice membrane dynamics and plasmodesmata during biotrophic invasion by the blast fungus. Plant Cell *19*, 706-724.

Kanneganti, T.D., Huitema, E., Cakir, C., and Kamoun, S. (2006). Synergistic interactions of the plant cell death pathways induced by *Phytophthora infestans* Nep1-like protein PiNPP1.1 and INF1 elicitin. Molecular Plant-Microbe Interactions *19*, 854-863.

Kelley, L.A., and Sternberg, M.J. (2009). Protein structure prediction on the Web: a case study using the Phyre server. Nature Protocols *4*, 363-371.

Kennedy, S.G., Yanchuk, A.D., Stackpole, D.J., and Jefferson, P.A. (2014). Incorporating non-key traits in selecting the *Pinus radiata* production population. New Zealand Journal of Forestry Science *44*, doi:10.1186

Kershaw, M.J., Wakley, G., and Talbot, N.J. (1998). Complementation of the Mpg1 mutant phenotype in *Magnaporthe grisea* reveals functional relationships between fungal hydrophobins. Embo Journal *17*, 3838-3849.

Khang, C.H., Berruyer, R., Giraldo, M.C., Kankanala, P., Park, S.Y., Czymmek, K., Kang, S., and Valent, B. (2010). Translocation of *Magnaporthe oryzae* effectors into rice cells and their subsequent cell-to-cell movement. Plant Cell *22*, 1388-1403.

Kim, S., Ahn, I.P., Rho, H.S., and Lee, Y.H. (2005). MHP1, a *Magnaporthe grisea* hydrophobin gene, is required for fungal development and plant colonization. Molecular Microbiology *57*, 1224-1237.

Kinloch, B.B., and Dupper, G.E. (2002). Genetic specificity in the white pine-blister rust pathosystem. Phytopathology *92*, 278-280.

Kinloch, B.B., Jr., and Littlefield, J.L. (1977). White pine blister rust: hypersensitive resistance in sugar pine. Canadian Journal of Botany *55*, 1148-1155.

Kinloch, B.B., Jr., Sniezko, R.A., Barnes, G.D., and Greathouse, T.E. (1999). A major gene for resistance to white pine blister rust in western white pine from the Western Cascade Range. Phytopathology *89*, 861-867.

Kleemann, J., Rincon-Rivera, L.J., Takahara, H., Neumann, U., van Themaat, E.V.L., van der Does, H.C., Hacquard, S., Stüber, K., Will, I., Schmalenbach, W., Schmelzer, E., and O'Connell, R.J. (2012). Sequential delivery of host-induced virulence effectors by appressoria and intracellular hyphae of the phytopathogen *colletotrichum higginsianum*. Plos Pathogens *8*, e1002643.

Kumar, S., Nei, M., Dudley, J., and Tamura, K. (2008). MEGA: A biologist-centric software for evolutionary analysis of DNA and protein sequences. Briefings in Bioinformatics *9*, 299-306.

Kwan, A.H.Y., Winefield, R.D., Sunde, M., Matthews, J.M., Haverkamp, R.G., Templeton, M.D., and Mackay, J.P. (2006). Structural basis for rodlet assembly in fungal hydrophobins. Proceedings of the National Academy of Sciences of the United States of America *103*, 3621-3626.

Lacroix, H., Whiteford, J.R., and Spanu, P.D. (2008). Localization of *Cladosporium fulvum* hydrophobins reveals a role for HCf-6 in adhesion. Fems Microbiology Letters *286*, 136-144.

Laugé, R., Goodwin, P.H., De Wit, P.J.G.M., and Joosten, M.H.A.J. (2000). Specific HR-associated recognition of secreted proteins from *Cladosporium fulvum* occurs in both host and non-host plants. Plant Journal *23*, 735-745.

Lauge, R., Goodwin, P.H., de Wit, P., and Joosten, M. (2000). Specific HR-associated recognition of secreted proteins from *Cladosporium fulvum* occurs in both host and non-host plants. Plant Journal *23*, 735-745.

Lauge, R., Joosten, M., Vanden Ackerveken, G.F.J.M., Vanden Broek, H.W.J., and De Wit, P.J.G.M. (1997). The *in planta*-produced extracellular proteins ECP1 and ECP2 of *Cladosporium fulvum* are virulence factors. Molecular Plant-Microbe Interactions *10*, 725-734.

Li, B., Lu, D., and Shan, L. (2014). Ubiquitination of pattern recognition receptors in plant innate immunity. Molecular Plant Pathology *15*, 737-746.

Linder, M.B., Szilvay, G.R., Nakari-Setälä, T., and Penttilä, M.E. (2005). Hydrophobins: The protein-amphiphiles of filamentous fungi. FEMS Microbiology Reviews *29*, 877-896.

Liu, J.-J., and Ekramoddoullah, A.K.M. (2011). Genomic organization, induced expression and promoter activity of a resistance gene analog (PmTNL1) in western white pine (*Pinus monticola*). Planta *233*, 1041-1053.

Liu, J.J., and Ekramoddoullah, A.K.M. (2004). Isolation, genetic variation and expression of TIR-NBS-LRR resistance gene analogs from western white pine (*Pinus monticola*). Molecular Genetics and Genomics *270*, 432-441.

Liu, J.J., and Ekramoddoullah, A.K.M. (2007). The CC-NBS-LRR subfamily in *Pinus monticola*: Targeted identification, gene expression, and genetic linkage with resistance to *Cronartium ribicola*. Phytopathology *97*, 728-736.

Liu, J.J., Hunt, R.S., and Ekramoddoullah, A.K.M. (2004). Recent insights into western white pine genetic resistance to white pine blister rust. In Recent Research Developments in Biotechnology and Bioengineering, pp. 65-76.

Liu, Z., Faris, J.D., Oliver, R.P., Tan, K.C., Solomon, P.S., McDonald, M.C., McDonald, B.A., Nunez, A., Lu, S., Rasmussen, J.B., and Friesen, T.L. (2009). SnTox3 acts in effector triggered susceptibility to induce disease on wheat carrying the *Snn3* gene. Plos Pathogens *5*, e1000581.

Luck, J.E., Lawrence, G.J., Dodds, P.N., Shepherd, K.W., and Ellis, J.G. (2000). Regions outside of the leucine-rich repeats of flax rust resistance proteins play a role in specificity determination. Plant Cell *12*, 1367-1377.

Luderer, R., Takken, F.L.W., de Wit, P., and Joosten, M. (2002). Cladosporium fulvum overcomes Cf-2-mediated resistance by producing truncated AVR2 elicitor proteins. Molecular Microbiology *45*, 875-884.

Ma, L.J. (2014). Horizontal chromosome transfer and rational strategies to manage *Fusarium vascular* wilt diseases. Molecular Plant Pathology *15*, 763-766.

Ma, W., and Guttman, D.S. (2008). Evolution of prokaryotic and eukaryotic virulence effectors. Current Opinion in Plant Biology *11*, 412-419.

Manning, V.A., Hardison, L.K., and Ciuffetti, L.M. (2007). Ptr ToxA interacts with a chloroplast-localized protein. Molecular Plant-Microbe Interactions *20*, 168-177.

Marshall, R., Kombrink, A., Motteram, J., Loza-Reyes, E., Lucas, J., Hammond-Kosack, K.E., Thomma, B.P.H.J., and Rudd, J.J. (2011). Analysis of two *in planta* expressed LysM effector homologs from the fungus *mycosphaerella graminicola* reveals novel functional properties and varying contributions to virulence on wheat. Plant Physiology *156*, 756-769.

Marshall, R., Konbrink, A., Motteram, J., Loza-Reyes, E., Lucas, J., Hammond-Kosack, K.E., Thomma, B.P.H.J., and Rudd, J.J. (2010). Analysis of two in planta expressed LysM effector homologues from the fungus *Mycosphaerella graminicola* reveals novel functional properties and varying contributions to virulence on wheat. Plant Physiology *156*, 756-769.

Mentlak, T.A., Kombrink, A., Shinya, T., Ryder, L.S., Otomo, I., Saitoh, H., Terauchi, R., Nishizawa, Y., Shibuya, N., Thomma, B.P.H.J., and Talbot, N.J. (2012). Effector-mediated suppression of chitin-triggered immunity by *Magnaporthe oryzae* is necessary for rice blast disease. Plant Cell *24*, 322-335.

Mesarich, C.H., Griffiths, S.A., van der Burgt, A., Ökmen, B., Beenen, H.G., Etalo, D.W., Joosten, M.H.A.J., and De Wit, P.J.G.M. (2014). Transcriptome sequencing uncovers the Avr5 avirulence gene of the tomato leaf mould pathogen *Cladosporium fulvum*. Molecular Plant-Microbe Interactions. *8*, 846-57. doi: 10.1094/MPMI-02-14-0050-R.

Mesarich, C.H., Stergiopoulos, I., beenen, H.G., Cordovez, V., Guo, Y., Jashni, M.K., Bradshaw, R.E., and de Wit, P.J. (2015). A conserved proline residue within Dothideomycete Avr4 effector proteins is required to trigger a Cf-4-dependent hypersensitive response. doi: 10.1111/mpp.12265

Mgbeahuruike, A.C., Kovalchuk, A., Chen, H., Ubhayasekera, W., and Asiegbu, F.O. (2013). Evolutionary analysis of hydrophobin gene family in two wood-degrading basidiomycetes, *Phlebia brevispora* and *Heterobasidion annosum s.l.* BMC Evolutionary Biology *13*, doi:10.1186/1471-2148-13-240

Motteram, J., Küfner, I., Deller, S., Brunner, F., Hammond-Kosack, K.E., Nürnberger, T., and Rudd, J.J. (2009). Molecular characterization and functional analysis of MgNLP, the sole NPP1 domain-containing protein, from the fungal wheat leaf pathogen *Mycosphaerella graminicola*. Molecular Plant-Microbe Interactions *22*, 790-799.

Na, R., Yu, D., Chapman, B.P., Zhang, Y., Kuflu, K., Austin, R., Qutob, D., Zhao, J., Wang, Y., and Gijzen, M. (2014). Genome re-sequencing and functional

analysis places the *Phytophthora sojae* avirulence genes Avr1c and Avr1a in a tandem repeat at a single locus. Plos One *9*, e89738

Na, R., Yu, D., Qutob, D., Zhao, J., and Gijzen, M. (2013). Deletion of the *Phytophthora sojae* avirulence gene Avr1d causes gain of virulence on Rps1d. Molecular Plant-Microbe Interactions *26*, 969-976.

Nakari-Setälä, T., Aro, N., Ilmén, M., Muñoz, G., Kalkkinen, N., and Penttilä, M. (1997). Differential expression of the vegetative and spore-bound hydrophobins of *Trichoderma reesei*: Cloning and characterization of hfb2 gene. European Journal of Biochemistry *248*, 415-423.

Nei, M., and Gojobori, T. (1986). Simple methods for estimating the numbers of synonymous and nonsynonymous nucleotide substitutions. Molecular Biology and Evolution *3*, 418-426.

Nielsen, P.S., Clark, A.J., Oliver, R.P., Huber, M., and Spanu, P.D. (2001). HCf-6, a novel class II hydrophobin from *Cladosporium fulvum*. Microbiological Research *156*, 59-63.

Niu, B., Gong, Y., Gao, X., Xu, H., Qiao, M., and Li, W. (2014). The functional role of Cys3–Cys4 loop in hydrophobin HGFI. Amino Acids *46*, 2615-2625.

Ökmen, B., Etalo, D.W., Joosten, M.H.A.J., Bouwmeester, H.J., de Vos, R.C.H., Collemare, J., and De Wit, P.J.G.M. (2013). Detoxification of α-tomatine by *Cladosporium fulvum* is required for full virulence on tomato. New Phytologist. *4*, 1203-14. doi: 10.1111/nph.12208.

Oliva, R., Win, J., Raffaele, S., Boutemy, L., Bozkurt, T.O., Chaparro-Garcia, A., Segretin, M.E., Stam, R., Schornack, S., Cano, L.M., van Damme, M., Huitema, E., Thines, M., Banfield, M.J., and Kamoun, S. (2011). Recent developments in effector biology of filamentous plant pathogens. Cellular Microbiology *12*, 705-715.

Oliveira-Garcia, E., and Valent, B. (2015). How eukaryotic filamentous pathogens evade plant recognition. Current Opinion in Microbiology *26*, 92-101.

Ong, L.E., and Innes, R.W. (2006). AvrB mutants lose both virulence and avirulence activities on soybean and Arabidopsis. Molecular Microbiology *60*, 951-962.

Park, C.H., Chen, S., Shirsekar, G., Zhou, B., Khang, C.H., Songkumarn, P., Afzal, A.J., Ning, Y., Wang, R., Bellizzi, M., Valent, B., and Wang, G.L. (2012). The *magnaporthe oryzae* effector avrpiz-t targets the RING E3 ubiquitin ligase APIP6 to suppress pathogen-associated molecular pattern-triggered immunity in rices. Plant Cell *24*, 4748-4762.

Parniske, M., HammondKosack, K.E., Golstein, C., Thomas, C.M., Jones, D.A., Harrison, K., Wulff, B.B.H., and Jones, J.D.G. (1997). Novel disease resistance specificities result from sequence exchange between tandemly repeated genes at the *Cf-4/9* locus of tomato. Cell *91*, 821-832.

Pedersen, C., van Themaat, E.V.L., McGuffin, L.J., Abbott, J.C., Burgis, T.A., Barton, G., Bindschedler, L.V., Lu, X., Maekawa, T., Weßling, R., Cramer, R., Thordal-Christensen, H., Panstruga, R., and Spanu, P.D. (2012). Structure and evolution of barley powdery mildew effector candidates. BMC Genomics *13*, doi:10.1186/1471-2164-13-694.

Petersen, T.N., Brunak, S., Von Heijne, G., and Nielsen, H. (2011). SignalP 4.0: Discriminating signal peptides from transmembrane regions. Nature Methods *8*, 785-786.

Pfaffl, M.W. (2001). A new mathematical model for relative quantification in real-time RT-PCR. Nucleic Acids Research *29*, e45.

Piou, D., and Ioos, R. (2014). First report of *Dothistroma pini*, a recent agent of the dothistroma needle blight, on *pinus radiata* in France. Plant Disease *98*, 841.

Piškur, B., Hauptman, T., and Jurc, D. (2013). Dothistroma needle blight in Slovenia is caused by two cryptic species: *Dothistroma pini* and *Dothistroma septosporum*. Forest Pathology *43*, 518-521.

Queloz, V., Wey, T., and Holdenrieder, O. (2014). First record of *Dothistroma pini* on *Pinus nigra* in Switzerland. Plant Disease *98*, 1744.

Qutob, D., Kamoun, S., and Gijzen, M. (2002). Expression of a *Phytophthora sojae* necrosis-inducing protein occurs during transition from biotrophy to necrotrophy. Plant Journal *32*, 361-373.

Qutob, D., Kemmerling, B., Brunner, F., Küfner, I., Engelhardt, S., Gust, A.A., Luberacki, B., Seitz, H.U., Stahl, D., Rauhut, T., Glawischnig, E., Schween, G., Lacombe, B., Watanabe, N., Lam, E., Schlichting, R., Scheel, D., Nau, K., Dodt, G., Hubert, D., Gijzen, M., and Nürnberger, T. (2006). Phytotoxicity and innate immune responses induced by Nep1-like proteins. Plant Cell *18*, 3721-3744.

Qutob, D., Patrick Chapman, B., and Gijzen, M. (2013). Transgenerational gene silencing causes gain of virulence in a plant pathogen. Nature Communications *4*, doi:10.1038/ncomms2354.

Rafiqi, M., Bernoux, M., Ellis, J.G., and Dodds, P.N. (2009). In the trenches of plant pathogen recognition: Role of NB-LRR proteins. Seminars in Cell & Developmental Biology *20*, 1017-1024.

Rairdan, G.J., and Moffett, P. (2006). Distinct domains in the ARC region of the potato resistance protein Rx mediate LRR binding and inhibition of activation. Plant Cell *18*, 2082-2093.

Rasmussen, M.W., Roux, M., Petersen, M., and Mundy, J. (2012). MAP kinase cascades in Arabidopsis innate immunity. Frontiers in Plant Science *3*, doi: 10.3389/fpls.2012.00169.

Rooney, H.C.E. (2005). *Cladosporium* Avr2 inhibits tomato Rcr3 protease required for Cf-2-dependent disease resistance. Science *310*, 54-54.

Russo, P.S., Blum, F.D., Ipsen, J.D., Abul-Hajj, Y.J., and Miller, W.G. (1982). The surface activity of the phytotoxin cerato-ulmin. Canadian Journal of Botany *60*, 1414-1422.

Sanchez-Vallet, A., Saleem-Batcha, R., Kombrink, A., Hansen, G., Valkenburg, D.J., Thomma, B., and Mesters, J.R. (2013). Fungal effector Ecp6 outcompetes host immune receptor for chitin binding through intrachain LysM dimerization. eLife *2*, e00790

Schoettle, A.W., Sniezko, R.A., Kegley, A., and Burns, K.S. (2014). White pine blister rust resistance in limber pine: Evidence for a major gene. Phytopathology *104*, 163-173.

Schornack, S., van Damme, M., Bozkurt, T.O., Cano, L.M., Smoker, M., Thines, M., Gaulin, E., Kamoun, S., and Huitema, E. (2010). Ancient class of translocated oomycete effectors targets the host nucleus. Proceedings of the National Academy of Sciences of the United States of America *107*, 17421-17426.

Schulze-Lefert, P. (2014). Microbial genome-enabled insights into plant-microorganism interactions. Nature reviews Genetics *15*, 797-813.

Schwelm, A., Barron, N.J., Zhang, S., and Bradshaw, R.E. (2008). Early expression of aflatoxin-like dothistromin genes in the forest pathogen *Dothistroma septosporum*. Mycological Research *112*, 138-146.

Segers, G.C., Hamada, W., Oliver, R.P., and Spanu, P.D. (1999). Isolation and characterisation of five different hydrophobin-encoding cDNAs from the fungal tomato pathogen *Cladosporium fulvum*. Molecular and General Genetics *261*, 644-652.

Sevim, A., Donzelli, B.G.G., Wu, D., Demirbag, Z., Gibson, D.M., and Turgeon, B.G. (2012). Hydrophobin genes of the entomopathogenic fungus, *Metarhizium brunneum*, are diVerentially expressed and corresponding mutants are decreased in virulence. Current Genetics *58*, 79-92.

Shabab, M., Shindo, T., Gu, C., Kaschani, F., Pansuriya, T., Chintha, R., Harzen, A., Colby, T., Kamoun, S., and van der Hoorn, R.A.L. (2008). Fungal effector protein AVR2 targets diversifying defense-related Cys proteases of tomato. Plant Cell *20*, 1169-1183.

Shain, L., and Franich, R.A. (1981). Induction of Dothistroma blight symptoms with dothistromin. Physiological Plant Pathology *19*, 49

Sharma, T.R., Das, A., Thakur, S., and Jalali, B.L. (2014). Recent understanding on structure, function and evolution of plant disease resistance genes. Proceedings of the Indian National Science Academy *80*, 83-93.

Shimizu, T., Nakano, T., Takamizawa, D., Desaki, Y., Ishii-Minami, N., Nishizawa, Y., Minami, E., Okada, K., Yamane, H., Kaku, H., and Shibuya, N. (2010). Two LysM receptor molecules, CEBiP and OsCERK1, cooperatively regulate chitin elicitor signaling in rice. Plant Journal *64*, 204-214.

Song, J., Win, J., Tian, M.Y., Schornack, S., Kaschani, F., Ilyas, M., van der Hoorn, R.A.L., and Kamoun, S. (2009). Apoplastic effectors secreted by two unrelated eukaryotic plant pathogens target the tomato defense protease Rcr3. Proceedings of the National Academy of Sciences of the United States of America *106*, 1654-1659.

Sorbo, G.D., Scala, F., Parrella, G., Lorito, M., Comparini, C., Ruocco, M., and Scala, A. (2000). Functional expression of the gene cu, encoding the phytotoxic hydrophobin cerato-ulmin, enables *Ophiostoma quercus*, a nonpathogen on elm, to cause symptoms of Dutch elm disease. Molecular Plant-Microbe Interactions *13*, 43-53.

Soyer, J.L., El Ghalid, M., Glaser, N., Ollivier, B., Linglin, J., Grandaubert, J., Balesdent, M.H., Connolly, L.R., Freitag, M., Rouxel, T., and Fudal, I. (2014). Epigenetic control of effector gene expression in the plant pathogenic fungus *Leptosphaeria maculans*. PLoS Genetics *10*, doi: 10.1371/journal.pgen.1004227.

Sperschneider, J., Ying, H., Dodds, P.N., Gardiner, D.M., Upadhyaya, N.M., Singh, K.B., Manners, J.M., and Taylor, J.M. (2014). Diversifying selection in the wheat stem rust fungus acts predominantly on pathogen-associated gene families and reveals candidate effectors. Frontiers in Plant Science *5*, doi: 10.3389/fpls.2014.00372.

Stergiopoulos, I., Cordovez, V., Ökmen, B., Beenen, H.G., Kema, G.H.J., and de Wit, P.J.G.M. (2014). Positive selection and intragenic recombination contribute to high allelic diversity in effector genes of *Mycosphaerella fijiensis*, causal agent of the black leaf streak disease of banana. Molecular Plant Pathology *15*, 447-460.

Stergiopoulos, I., de Kock, M.J.D., Lindhout, P., and De Wit, P. (2007). Allelic variation in the effector genes of the tomato pathogen *Cladosporium fulvum* reveals different modes of adaptive evolution. Molecular Plant-Microbe Interactions *20*, 1271-1283.

Stergiopoulos, I., and de Wit, P.J.G.M. (2009). Fungal effector proteins. Annual Review of Phytopathology *47*, 233-263.

Stergiopoulos, I., Kourmpetis, Y.A.I., Slot, J.C., Bakker, F.T., De Wit, P.J.G.M., and Rokas, A. (2012). In silico characterization and molecular evolutionary analysis of a novel superfamily of fungal effector proteins. Molecular Biology and Evolution *29*, 3371-3384.

Stergiopoulos, I., van den Burg, H.A., Okmen, B., Beenen, H.G., van Liere, S., Kema, G.H.J., and de Wit, P.J.G.M. (2010). Tomato Cf resistance proteins mediate recognition of cognate homologous effectors from fungi pathogenic on dicots and monocots. Proceedings of the National Academy of Sciences of the United States of America *107*, 7610-7615.

Stotz, H.U., Mitrousia, G.K., de Wit, P.J.G.M., and Fitt, B.D.L. (2014). Effector-triggered defence against apoplastic fungal pathogens. Trends in Plant Science *19*, 491-500.

Stukenbrock, E.H., Bataillon, T., Dutheil, J.Y., Hansen, T.T., Li, R., Zala, M., McDonald, B.A., Wang, J., and Schierup, M.H. (2011). The making of a new pathogen: Insights from comparative population genomics of the domesticated wheat pathogen *Mycosphaerella graminicola* and its wild sister species. Genome Research *21*, 2157-2166.

Stukenbrock, E.H., and McDonald, B.A. (2009). Population genetics of fungal and oomycete effectors involved in gene-for-gene interactions. Molecular Plant-Microbe Interactions *22*, 371-380.

Sunde, M., Kwan, A.H.Y., Templeton, M.D., Beever, R.E., and Mackay, J.P. (2008). Structural analysis of hydrophobins. Micron *39*, 773-784.

Tameling, W.I.L., Elzinga, S.D.J., Darmin, P.S., Vossen, J.H., Takken, F.L.W., Haring, M.A., and Cornelissen, B.J.C. (2002). The tomato R gene products I-2 and Mi-1 are functional ATP binding proteins with ATPase activity. Plant Cell *14*, 2929-2939.

Teixeira, P.J.P.L., Thomazella, D.P.T., Vidal, R.O., do Prado, P.F.V., Reis, O., Baroni, R.M., Franco, S.F., Mieczkowski, P., Pereira, G.A.G., and Mondego, J.M.C. (2012). The fungal pathogen *Moniliophthora perniciosa* has genes similar to plant PR-1 that are highly expressed during its interaction with cacao. Plos One *7*, e45929

Temple, B., Horgen, P.A., Bernier, L., and Hintz, W.E. (1997). Cerato-ulmin, a hydrophobin secreted by the causal agents of Dutch elm disease, is a parasitic fitness factor. Fungal Genetics and Biology *22*, 39-53.

Thomas, C.M., Jones, D.A., Parniske, M., Harrison, K., Balint-Kurti, P.J., Hatzixanthis, K., and Jones, J.D.G. (1997). Characterization of the tomato *Cf-4* gene for resistance to *Cladosporium fulvum* identifies sequences that determine recognitional specificity in Cf-4 and Cf-9. Plant Cell *9*, 2209-2224.

Thomma, B., Nurnberger, T., and Joosten, M. (2011). Of PAMPs and effectors: the blurred PTI-ETI dichotomy. Plant Cell *23*, 4-15.

Tian, M.Y., Win, J., Song, J., van der Hoorn, R., van der Knaap, E., and Kamoun, S. (2007). A *Phytophthora infestans* cystatin-like protein targets a novel tomato papain-like apoplastic protease. Plant Physiology *143*, 364-377.

Trujillo, M., and Shirasu, K. (2010). Ubiquitination in plant immunity. Current Opinion in Plant Biology *13*, 402-408.

Tschopp, J.F., Brust, P.F., Cregg, J.M., Stillman, C.A., and Gingeras, T.R. (1987). Expression of the *lacZ* gene from two methanol-regulated promoters in *Pichia pastoris*. Nucleic Acids Research *15*, 3859-3876.

Turgeon, B.G., Condon, B., Liu, J., and Zhang, N. (2010). Protoplast transformation of filamentous fungi. Methods in molecular biology *638*, 3-19.

Uma, B., Swaroopa Rani, T., and Podile, A.R. (2011). Warriors at the gate that never sleep: Non-host resistance in plants. Journal of Plant Physiology *168*, 2141-2152.

van den Ackerveken, G.F., Van Kan, J.A., Joosten, M.H., Muisers, J.M., Verbakel, H.M., and De Wit, P.J. (1993). Characterization of two putative pathogenicity genes of the fungal tomato pathogen *Cladosporium fulvum*. Molecular plant-microbe interactions : MPMI *6*, 210-215.

van den Ackerveken, G.F.J.M., Van Kan, J.A.L., and De Wit, P.J.G.M. (1992). Molecular analysis of the avirulence gene avr9 of the fungal tomato pathogen *Cladosporium fulvum* fully supports the gene-for-gene hypothesis. Plant Journal *2*, 359-366.

van den Burg, H.A., de Wit, P.J.G.M., and Vervoorta, J. (2001). Efficient 13C/15N double labeling of the avirulence protein AVR4 in a methanol-utilizing strain (Mut+) of *Pichia pastoris*. Journal of Biomolecular NMR *20*, 251-261.

van den Burg, H.A., Harrison, S.J., Joosten, M., Vervoort, J., and de Wit, P. (2006). *Cladosporium fulvum* Avr4 protects fungal cell walls against hydrolysis by plant chitinases accumulating during infection. Molecular Plant-Microbe Interactions *19*, 1420-1430.

van den Burg, H.A., Spronk, C., Boeren, S., Kennedy, M.A., Vissers, J.P.C., Vuister, G.W., de Wit, P., and Vervoort, J. (2004). Binding of the AVR4 elicitor of *Cladosporium fulvum* to chitotriose units is facilitated by positive allosteric protein-protein interactions - The chitin-binding site of AVR4 represents a novel binding site on the folding scaffold shared between the invertebrate and the plant chitin-binding domain. Journal of Biological Chemistry *279*, 16786-16796.

van den Burg, H.A., Westerink, N., Francoijs, K.J., Roth, R., Woestenenk, E., Boeren, S., de Wit, P., Joosten, M., and Vervoort, J. (2003). Natural disulfide bond-disrupted mutants of AVR4 of the tomato pathogen *Cladosporium fulvum* are sensitive to proteolysis, circumvent Cf-4-mediated resistance, but retain their chitin binding ability. Journal of Biological Chemistry *278*, 27340-27346.

van der Hoorn, R.A.L., and Kamoun, S. (2008). From Guard to Decoy: A new model for perception of plant pathogen effectors. Plant Cell *20*, 2009-2017.

van der Hoorn, R.A.L., Roth, R., and De Wit, P.J.G.M. (2001). Identification of distinct specificity determinants in resistance protein Cf-4 allows construction of a Cf-9 mutant that confers recognition of avirulence protein AVR4. Plant Cell *13*, 273-285.

van Esse, H.P., Bolton, M.D., Stergiopoulos, L., de Wit, P., and Thomma, B. (2007). The chitin-binding *Cladosporium fulvum* effector protein Avr4 is a virulence factor. Molecular Plant-Microbe Interactions *20*, 1092-1101.

van Loon, L.C., Rep, M., and Pieterse, C.M.J. (2006). Significance of inducible defense-related proteins in infected plants. In Annual Review of Phytopathology, pp. 135-162.

Vankan, J.A.L., Vandenackerveken, G., and Dewit, P. (1991). Cloning and characterization of cDNA of avirulence gene *avr9* of the fungal pathogen *Cladosporium fulvum*, causal agent of tomato leaf mold. Molecular Plant-Microbe Interactions *4*, 52-59.

Vleeshouwers, V.G.A.A., and Oliver, R.P. (2014). Effectors as tools in disease resistance breeding against biotrophic, hemibiotrophic, and necrotrophic plant pathogens. Molecular Plant-Microbe Interactions *27*, 196-206.

Wösten, H.A.B. (2001). Hydrophobins: Multipurpose proteins. In Annual Review of Microbiology, pp. 625-646.

Wösten, H.A.B., Van Wetter, M.A., Lugones, L.G., van der Mei, H.C., Busscher, H.J., and Wessels, J.G.H. (1999). How a fungus escapes the water to grow into the air. Current Biology *9*, 85-88.

Wan, J., Zhang, S., and Stacey, G. (2004). Activation of a mitogen-activated protein kinase pathway in Arabidopsis by chitin. Molecular Plant Pathology *5*, 125-135.

Wan, J., Zhang, X.C., and Stacey, G. (2008). Chitin signaling and plant disease resistance. Plant Signaling and Behavior *3*, 831-833.

Wang, X., Jiang, N., Liu, J., Liu, W., and Wang, G.L. (2014). The role of effectors and host immunity in plant–necrotrophic fungal interactions. Virulence *5*, 722-732.

Wang, X., Permentier, H.P., Rink, R., Kruijtzer, J.A.W., Liskamp, R.M.J., Wösten, H.A.B., Poolman, B., and Robillard, G.T. (2004). Probing the self-assembly and the accompanying structural changes of hydrophobin SC3 on a hydrophobic surface by spectrometry. Biophysical Journal *87*, 1919-1928.

Wang, X., Shi, F., Wösten, H.A.B., Hektor, H., Poolman, B., and Robillard, G.T. (2005). The SC3 hydrophobin self-assembles into a membrane with distinct mass transfer properties. Biophysical Journal *88*, 3434-3443.

War, A.R., Paulraj, M.G., War, M.Y., and Ignacimuthu, S. (2011). Role of salicylic acid in induction of plant defense system in chickpea (cicer arietinum l). Plant Signaling and Behavior *6*, 1787-1792.

Watt, M.S., Ganley, R.J., Kriticos, D.J., and Manning, L.K. (2011). Dothistroma needle blight and pitch canker: the current and future potential distribution of two important diseases of Pinus species. Canadian Journal of Forest Research-Revue Canadienne De Recherche Forestiere *41*, 412-424.

Watt, M.S., Kriticos, D.J., Alcaraz, S., Brown, A.V., and Leriche, A. (2009). The hosts and potential geographic range of Dothistroma needle blight. Forest Ecology and Management *257*, 1505-1519.

Welsh, C., Lewis, K.J., and Woods, A.J. (2014). Regional outbreak dynamics of Dothistroma needle blight linked to weather patterns in British Columbia,Canada. Canadian Journal of Forest Research *44*, 212-219.

Weng, H., Pan, A., Yang, L., Zhang, C., Liu, Z., and Zhang, D. (2004). Estimating number of transgene copies in transgenic rapeseed by real-time PCR assay with HMG I/Y as an endogenous reference gene. Plant Molecular Biology Reporter *22*, 289-300.

Wessels, J.G.H. (1994). Developmental regulation of fungal cell wall formation. Annual Review of Phytopathology *32*, 413-437.

Westerink, N., Brandwagt, B.F., de Wit, P., and Joosten, M. (2004). *Cladosporium fulvum* circumvents the second functional resistance gene homologue at the *Cf-4 locus* (*Hcr9-4E*) by secretion of a stable avr4E isoform. Molecular Microbiology *54*, 533-545.

Whisson, S.C., Boevink, P.C., Moleleki, L., Avrova, A.O., Morales, J.G., Gilroy, E.M., Armstrong, M.R., Grouffaud, S., van West, P., Chapman, S., Hein, I., Toth, I.K., Pritchard, L., and Birch, P.R.J. (2007). A translocation signal for delivery of oomycete effector proteins into host plant cells. Nature *450*, 115.

Whiteford, J.R., Lacroix, H., Talbot, N.J., and Spanu, P.D. (2004). Stage-specific cellular localisation of two hydrophobins during plant infection by the pathogenic fungus *Cladosporium fulvum*. Fungal Genetics and Biology *41*, 624-634.

Whiteford, J.R., and Spanu, P.D. (2001). The hydrophobin HCf-1 of *Cladosporium fulvum* is required for efficient water-mediated dispersal of conidia. Fungal Genetics and Biology *32*, 159-168.

Win, J., and Kamoun, S. (2008). Adaptive evolution has targeted the C-terminal domain of the RXLR effectors of plant pathogenic oomycetes. Plant Signaling and Behavior *3*, 251-253.

Wosten, H.A.B., Schuren, F.H.J., and Wessels, J.G.H. (1994). Interfacial self-assembly of a hydrophobin into an amphipathic protein membrane mediates fungal attachment to hydrophobic surfaces. The EMBO Journal *13*, 5848-5854.

Wu, C.H., Krasileva, K.V., Banfield, M.J., Terauchi, R., and Kamoun, S. (2015). The"sensor domains"of plant NLR proteins: More than decoys? Frontiers in Plant Science *6*, doi:10.3389/fpls.2015.00134.

Wulff, B.B.H., Chakrabarti, A., and Jones, D.A. (2009). Recognitional specificity and evolution in the tomato - Cladosporium fulvum pathosystem. Molecular Plant-Microbe Interactions *22*, 1191-1202.

Xue, C., Wu, D., Condon, B.J., Bi, Q., Wang, W., and Turgeon, B.G. (2013). Efficient gene knockout in the maize pathogen *Setosphaeria turcica* using *Agrobacterium tumefaciens*-mediated transformation. Phytopathology *103*, 641-647.

Yaeno, T., Li, H., Chaparro-Garcia, A., Schornack, S., Koshiba, S., Watanabe, S., Kigawa, T., Kamoun, S., and Shirasu, K. (2011). Phosphatidylinositol monophosphate-binding interface in the oomycete RXLR effector AVR3a is required for its stability in host cells to modulate plant immunity. Proceedings of the National Academy of Sciences of the United States of America *108*, 14682-14687.

Yelton, M.M., Hamer, J.E., and Timberlake, W.E. (1984). Transformation of *Aspergillus nidulans* by using a trpC plasmid. Isotopenpraxis *20*, 1470-1474.

Yuan, Y., Haanstra, J., Lindhout, P., and Bonnema, G. (2002). The *Cladosporium fulvum* resistance gene Cf-ECP3 is part of the Orion cluster on the short arm of tomato Chromosome 1. Molecular Breeding *10*, 45-50.

Zhang, J., Rosenberg, H.F., and Nei, M. (1998). Positive Darwinian selection after gene duplication in primate ribonuclease genes. Proceedings of the National Academy of Sciences of the United States of America *95*, 3708-3713.

Zhang, S., Guo, Y., and Bradshaw, R.E. (2010). Genetics of dothistromin biosynthesis in the peanut pathogen *Passalora arachidicola*. Toxins *2*, 2738-2753.

Zhang, S., Xia, Y.X., Kim, B., and Keyhani, N.O. (2011). Two hydrophobins are involved in fungal spore coat rodlet layer assembly and each play distinct roles in surface interactions, development and pathogenesis in the entomopathogenic fungus, *Beauveria bassiana*. Molecular Microbiology *80*, 811-826.

Zhang, S.G., Schwelm, A., Jin, H.P., Collins, L.J., and Bradshaw, R.E. (2007). A fragmented aflatoxin-like gene cluster in the forest pathogen *Dothistroma septosporum*. Fungal Genetics and Biology *44*, 1342-1354.

Zhu, H., Wen, F., Li, P., Liu, X., Cao, J., Jiang, M., Ming, F., and Chu, Z. (2014). Validation of a reference gene (BdFIM) for quantifying transgene copy

numbers in *Brachypodium distachyon* by Real-Time PCR. Applied Biochemistry and Biotechnology, 1-13.